GEOLOGIC AND GEOTECHNICAL CONTROLS ON THE STABILITY OF COAL MINE ENTRIES

by

William Francis Kane

Dissertation submitted to the Graduate Faculty of the
Virginia Polytechnic Institute and State University
in partial fulfillment of the requirements for the degree of

DOCTOR OF PHILOSOPHY

in

Civil Engineering

APPROVED:

M. Karmis, Chairman

T. Kuppusamy, Co-Chairman

R. C. Milici

N. N. Moebs

G. V. Faulkner

January, 1985

Blacksburg, Virginia

ACKNOWLEDGEMENTS

The author would especially like to thank his parents, and , for their tremendous support and encouragement in this endeavor. He also extends his appreciation to his wife for typing and drafting, but, most of all for her patience and aid.

On the more technical side, my committee chairman, must be thanked for the many productive discussions of which this is the result. Special thanks are also due to of the Virginia Division of Mineral Resources for the patience he exhibited in teaching the author geologic mapping and the geology of the southwestern Virginia coal fields. I would also like to acknowledge the help of my committee co-chairman who assisted with the analytical portion of this research as well as the valuable input of and , the remaining committee members.

There are also a good many people in the coal industry of southwestern Virginia without whom this work would have been impossible. Although all their names are not known to me, they include , , , and of the Clinchfield Coal Company; and of the Paramont Coal Company; of the Sue Lee Coal Co.; Chief Mine Inspector of the Commonwealth of Virginia; of the

the Virginia Division of Mineral Resources; and A. Grenoble and M. L. Orth of Virginia Tech.

Thanks are also due to my colleagues and for the stimulating discussions over morning coffee.

This work is based, in part, upon work supported by the Generic Mineral Technology Center, Mine Systems Design and Control, Bureau of Mines, United States Department of the Interior. Any opinions, findings, conclusions, or recommendations expressed in this thesis are those of the author and do not necessarily reflect the views of the sponsor.

TABLE OF CONTENTS

LIST OF FIGURES

LIST OF TABLES

CHAPTER 1

INTRODUCTION

1.1 OBJECTIVES

Roof and rib failures in underground coal mines are one of the major safety problems facing the industry today. In addition to the substantial number of fatalities caused by such failures, their economic impact can be considerable. Uncovering or replacing buried equipment and clearing entries can account for a very large expenditure in lost man-hours and equipment.

The unstable ground conditions in some coal mines are the results of a complex geologic history promoting unstable ground conditions during mining. This is especially true along the southeastern edge of the Appalachian coal fields where a great deal of faulting and movement has occurred.

If the different geologic features which give rise to instability could, perhaps, be identified, the most efficient means of support could be provided to deal with the troublesome areas. This research is an attempt to determine which geologic factors contribute to roof instability in Virginia mines.

1.2 DESCRIPTION OF APPROACH

After reviewing the literature pertaining to the causes of roof falls in different sectors of the Appalachians, a list was made of those factors which might be detrimental to

roof stability in Virginia. Four mines were selected and mapped for the different parameters. Statistical analysis was carried out in order to determine which factors led to roof instability and which were associated with good roof conditions. As a result of this effort, a simplified roof classification was developed so that all data were discriminated into certain categories, which became apparent during the course of the work. Finite element analysis was used to model the behavior of certain conditions which resisted analysis by statistical means. A code accounting for non-linear elastic-plastic deformation was employed to model these cases.

1.3 OUTLINE OF CHAPTERS

The research consisted of four distinct parts: (i) delineation of the selected variables for mapping, (ii) mapping, (iii) modeling data analysis, and (iv) determination of significant parameters for roof control.

Chapter 1 introduces the problem while Chapter 2 contains a literature review which highlights previous work in the field of roof control, and presents different approaches to the problem which have been used in the past. Chapter 3 describes the mapping program as well as the numerical finite element techniques which were utilized. The results of the statistical analysis are contained in Chapter 4 and the results of the finite element analysis are in Chapter 5.

Chapter 6 is a discussion of the various results and how they might be implemented by mining engineers in helping to reduce the incidence of unexpected roof failures. Because work of this nature is never conclusive and always leads to the need for more research, Chapter 7 is a suggestion for further work and a brief summary of the conclusions derived from the preceding chapters.

CHAPTER 2

LITERATURE REVIEW

2.1 GEOLOGY

2.1.1 Introduction

The Pine Mountain thrust block is of interest because it not only comprises the major part of the southern Appalachian coal field in Virginia, but it is also within the Appalachian thrust belt. Bounded by the Pine Mountain fault on the northwest, the Russell Fork fault on the northeast, the Jacksboro fault on the southwest, and the Clinchport fault on the southeast, the thrust plate is 200 kilometers long, 40 kilometers wide and comprises parts of Tennessee and Kentucky as well as part of Virginia (Figure 2.1). In Virginia, the counties of Buchanan, Dickenson, Russell, Wise, Scott, and Lee are either wholly or partially contained within the block. Campbell (1893), Giles (1921, 1925), Wentworth (1922), and Eby (1923) contributed detailed accounts of the geology of this area in Virginia and parts of Kentucky while Glenn (1925) and Stearns (1954, 1955) have written concerning the block in Tennessee. Harris (1970) and Harris and Milici (1977) have synthesized the earlier papers, and recent stratigraphic summaries of the coal field region of the block have been provided by R. L. Miller (1969), M. S. Miller (1974), and Englund (1979).

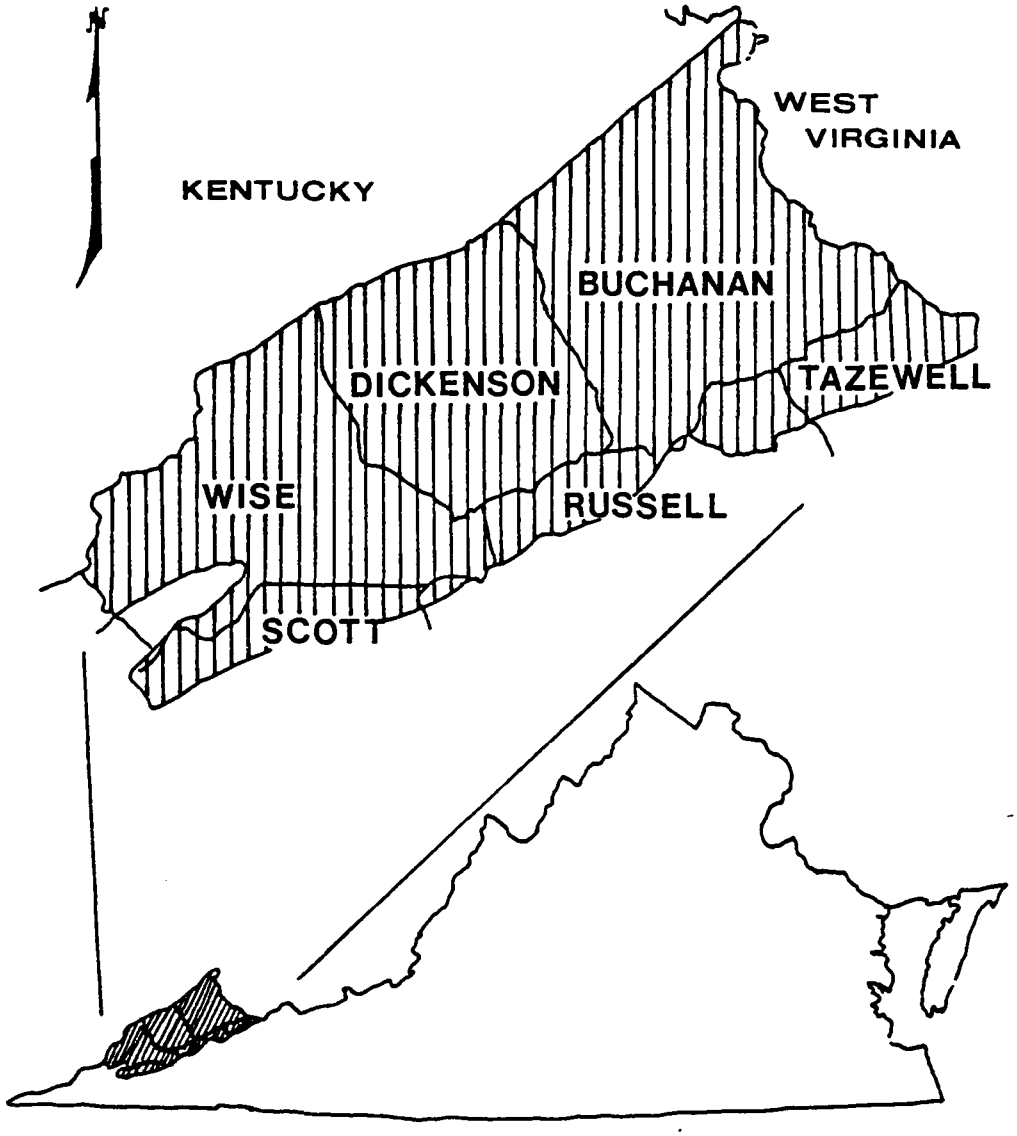

Figure 2.1: Location map of study area in southwestern Virginia.

2.1.2 Stratigraphy

Although the Pine Mountain sheet contains rocks of Cambrian through Pennsylvanian age, the coal-bearing formations are classified almost entirely within the Pennsylvanian System (Table 2.1). Campbell (1893) has divided these rocks into the Lee, Norton, Gladeville, Wise, and Harlan Formations, and, with some modifications, this is the nomenclature that is presently used. Though this study concerns itself with only two coal beds, the Jawbone and Upper Banner, both within the Norton formation, in the interest of completeness, brief descriptions of the other formations are provided.

Lee Formation

Named for Lee County, Virginia by Campbell (1893) who described its type section at Big Stone Gap, the Lee Formation contains the lowest of the Pennsylvanian System in southwest Virginia. Englund (1964) has further divided the Lee into seven members which are, in ascending order, the Pinnacle Overlook, Chadwell, White Rocks Sandstone, Dark Ridge, Middlesboro, Hensley, and Bee Rock Sandstone Members. The Pinnacle Overlook, Chadwell, and White Rocks Sandstone Members are all of Upper Mississippian age. Disconformably overlying the Dark Ridge Member are the Middlesboro, Hensley, and White Rocks Sandstone Members. Eby (1923) also named another resistant unit the Bald Rock Conglomerate

TABLE 2.1

Pennsylvanian rocks of Pine Mountain thrust plate study area (After R. L. Miller, 1969 and M. S. Miller, 1974)

AGE	NAME	CHARACTER	APPROX-IMATE THICKNESS (METERS)
MIDDLE	Harlan Formation	Massive, quartzose sandstone, pebbly or coarse-grained to fine-grained. Contains shale and coal beds.	?-182
	Wise Formation	Intertongueing units of sandstone, siltstone, and shale. Sandstone is medium-grained, feldspathic, friable, massively-bedded or cross-bedded. Locally argillaceous and some units may contain abundant silvery mica flakes. Named units are the Robbins Chapel, Keokee, Clover Fork, and Marcum Hollow Members. Shales and siltstones are similar to the Norton Formation except the Kendrick Shale, a dark-gray to nearly black, locally silty, calcareous and fossiliferous shale. Magoffin Beds: limestone, dense, hard, nearly black, and fossiliferous; Magoffin Beds; 0.5 meters thick. Includes Dorchester, Imboden, Marker, Taggart, Low Splint, and High Splint coal seams.	?-744
LOWER	Norton Formation	Impure, fine-grained sandstone, dark shale and siltstone, and coal beds; includes the Norton, Hagy, Splash Dam, Upper Banner, Lower Banner, and Kennedy coal beds in the northwestern areas, and with the tonguing out of the Bee Rock Sandstone to the southeast includes the Aily, Raven, Jawbone, and Tiller coal	

TABLE 2.1 (continued)

AGE	NAME		CHARACTER	APPROXIMATE THICKNESS (METERS)
			beds. The top of the Norton is taken to be the Gladeville Sandstone; a very strongly cross-bedded, massive, medium-grained quartz sandstone.	
LOWER	Lee Formation	Upper quartz arenite member	Referred to as Bee Rock Sandstone Member in some areas; a massive quartzose sandstone, more than 90 percent quartz, strongly consolidated with lenses of well-rounded quartz pebbles; a few interbeds of silty sandstone and shale.	0-76
			Shale, sandstone, and coal: shale is gray, silty, and commonly carbonaceous; sandstone is gray, fine to coarse grained, and micaceous; includes the Aily, Raven Jawbone, and Tiller coal beds.	55-168
		Middle quartz arenite member	Predominantly quartzose sandstone; over 90 percent quartz; fine to coarse grained, locally conglomeratic; strongly consolidated; thin interbeds of silty sandstone and sandy shale; tongues out to the southest into finer textured sediments; includes the Upper, Middle, and Lower Seaboard coal beds.	0-183
			Shale, sandstone, and coal: shale is dark, silty, and interbedded with siltstone; sandstone is gray, fine to medium grained, micaceous, and silty; includes all the Horsepen, War Creek, Pocahontas No. 9 and No. 8 coal beds; includes the Seaboard coal beds in southeastern areas with the tonguing out of	24-244

TABLE 2.1 (continued)

AGE	NAME		CHARACTER	APPROXIMATE THICKNESS (METERS)
LOWER	Lee Formation		the middle quartz arenite member.	
		Lower quartz arenite member	Almost all quartzose sandstone with over 90 percent quartz; fine to coarse grained; basal intervals commonly conglomeratic; includes a few thin lenticular coals and shales	0-152

Member which he placed in the middle of the Lee but, R. L. Miller (1969) has shown this bed to be at the base of the Lee in some places.

According to Englund (1979), the Mississippian members consist of 135 meters of quartzose sandstone and conglomeratic sandstone lobes while the Pennsylvanian Dark Ridge Member is dark-gray shale, and fine-grained sandstone, and coal. The Middlesboro Member is made up of coalescing sandstone tongues that total up to 150 meters thick. The lower and upper ones are the lower and middle quartz arenite members of M. S. Miller (1974). The Hensley Member contains non-resistant sandstone, siltstone, shale, and coal with a total thickness of 122 meters and is overlain by the resistant Bee Rock Sandstone Member. The Bee Rock is a quartzose conglomeratic sandstone which becomes as thick as 90 meters.

In places, coal within the Lee Formation itself is thin and badly sheared (R. L. Miller, 1969). The sandstone and conglomeratic beds thin and then grade laterally to the northeast into the coal-bearing Pocahontas, Norton, and New River Formations; Englund and Delaney, (1966) have correlated the Dark Ridge Member with the Pocahontas Formation. However, in western Wise county and northwestern Dickenson and Buchanan Counties, M. S. Miller (1974) has placed the Tiller, Jawbone, Raven, Aily, and Kennedy coal beds within the Lee Formation. This occurs where the base of the overlying Norton Formation is defined by the top of the Bee Rock

Sandstone Member instead of the top of the Middlesboro Sandstone Member (Table 2.1).

Norton Formation

Campbell (1893) named the sequence of siltstone, shale, sandstone, and coal beds between the Lee Formation below and the Gladeville Sandstone above the Norton Formation for a type area near the largest town in Wise County, Virginia. Due to the fact that the base of the Norton depends on the position and presence of the quartz arenite members of the Lee Formation, its thickness ranges from 168 to 365 meters (M. S. Miller, 1974).

According to R. L. Miller (1969), the Norton Formation contains proportionally much more shale and siltstone than the Lee. The sandstone is darker, finer-grained, and more impure than that of the Lee Formation. The shales and siltstone of the two formations, however, are quite similar. Coal beds contained within the Norton Formation are the Norton, Hagy, Splash Dam, Upper and Lower Banner, and Kennedy. In those areas, where the Bee Rock Sandstone Member is missing and the base of the Norton is defined by the middle quartz arenite member of the Lee, the Norton contains the Middlesboro Sandstone Member, the Aily, Raven, Jawbone, and Tiller coals. These coal beds have been mined to a large degree east of the town of Norton (Harnsberger, 1919, Giles, 1921, Wentworth, 1922, Eby, 1923), but west of

Norton little mining has occurred because of steep dips associated with the Powell Valley Anticline.

The top of the Norton Formation is defined as the base of the Gladeville Sandstone. As R. L. Miller (1969) points out, it is difficult to map the Gladeville Sandstone everywhere along its trend. For example Campbell (1893) had misidentified another sandstone southwest of Norton as being the Gladeville. The Gladeville is a very strongly cross-bedded, massive, quartz sandstone. It is medium-grained and, where mapped by R. L. Miller (1969), ranges between 10 and 17 meters thick.

Wise Formation

Conformably overlying the Gladeville Sandstone is the Wise Formation (Campbell, 1893). This formation varies in thickness but averages about 580 meters and stratigraphically lies between the Gladeville and Harlan Sandstones. The top of the Wise is defined as being at the top of the High Splint coal seam (R. L. Miller, 1969). It consists chiefly of thick sequences of sandstone, siltstone, and shale. Many coal beds are found within the Wise Formation and economically, it is the most important formation in Lee and western Wise Counties (R. L. Miller, 1969).

R. L. Miller (1969) has delineated approximately twelve sandstone units more than 7.5 meters thick within the Wise. These units are medium-grained, friable, and feldspathic.

They are usually either massively bedded or cross-bedded and sometimes are both. Some units contain profuse amounts of silvery mica flakes while others are completely lacking in mica. R. L. Miller (1969) assigned names to four of the more conspicuous sandstone units: the Robbins Chapel, Keokee, Clover Fork, and Marcum Hollow Sandstone Members. Ashley and Glenn (1906) named the uppermost sand stone unit the Reynolds Sandstone Member.

The Robbins Chapel Sandstone Member is a massively-bedded, medium-to-fine grained, quartzose sandstone about 9 to 24 meters thick. The Keokee Sandstone is similar to the Clover Fork Sandstone Member in that it is a medium-grained, feldspathic, and slightly micaceous sandstone. Average thicknesses range from 9 meters for the Keokee to 15 meters for the Clover Fork. The Marcum Hollow Sandstone Member is the most prominent sandstone unit of the Wise Formation and is often greater than 30 meters thick. It is a massively-bedded, medium-grained moderately quartzose sandstone which lies either near or on top of the Taggart coal bed. The Reynolds Sandstone Member is difficult to map but consists in outcrop of fine-grained, moderately quartzose sandstone. It is approximately 30 meters thick.

Two extensive marine marker beds are distinguishable within the Wise Formation. These are the Kendrick Shale of Jillson (1919) and the Magoffin Beds of Morse (1931). Ac-

cording to R. L. Miller (1969), the Kendrick Shale is 1.5 to 3 meters of dark gray to black, locally silty, shale with small brachiopods common in a calcareous and fossiliferous unit. Large, oval limestone concretions exhibiting cone-in-cone structure can be found within the shale in some areas of Lee County. The Magoffin beds of Morse (1931) are important in that they, too, comprise a well-defined marker bed. The most distinctive and prevalent unit is a nearly black, dense limestone containing white brachiopod fossils. This unit is usually 0.3 to 0.6 meters thick but locally may be as much as 6 meters thick (R. L. Miller, 1969).

Eby (1923) shows coal beds contained within the Wise Formation to be the Dorchester, Lyons, Blair, Clintwood, Addington, Rocky Fork, Imboden, Kelly, Pinehook, Lower Standiford (L. Wilson), Upper Standiford (Upper Wilson), Taggart Marker, Taggart, Low Splint, Phillips, Pardee, Morris, and High Splint.

Harlan Formation

The Harlan Formation (Campbell, 1893) consists of the youngest Carboniferous rocks in Virginia. A basal sandstone is highly resistant, massive, and cliff-forming. It ranges from 5 to 9 meters thick and grades upward from pebbly or coarse-grained sandstone to fine-grained sandstone (R. L. Miller, 1969). Campbell (1893) found this basal unit to be 12 to 30 meters thick. Less resistant beds comprise the

rest of the 120 to 180 meters of the formation and are composed of a mixture of sandstone, siltstone, shale and coal. R. L. Miller (1969) mapped 22 distinct coal beds above the basal sandstone but most were only a few inches thick with the thickest of these being 0.6 meters.

2.1.3 Structural Geology

The Pine Mountain thrust plate in Virginia is the westernmost of a series of thrust sheets along, and containing, what Price (1931) termed the Appalachian structural front and Rodgers (1964) renamed the Allegheny front. The structural geology of the block has been described in detail by Safford (1869), Wentworth (1921, 1922), Eby (1923), and Butts (1927) among early investigators and, more recently, by Harris (1965, 1967, 1970), Harris and Milici (1977), Froelich (1973), and R. L. Miller (1973). Essentially, the block is a large quadrilateral bounded, as noted earlier, by the Clinchport, Russell Fork, Jacksboro, and Pine Mountain faults (Figure 2.2). The Powell Valley anticline, exposing rocks as old in age as Cambrian to Ordovician, is the most striking structural feature (Figures 2.2 and 2.3). The limbs of this large anticline contain resistant sandstones which hold up Cumberland, Powell, and Stone Mountains while the axial portion of the anticline itself is underlain by a carbonate lowland. The complementary syncline, the Middlesboro syncline, contains rocks as young as the Pennsylvanian

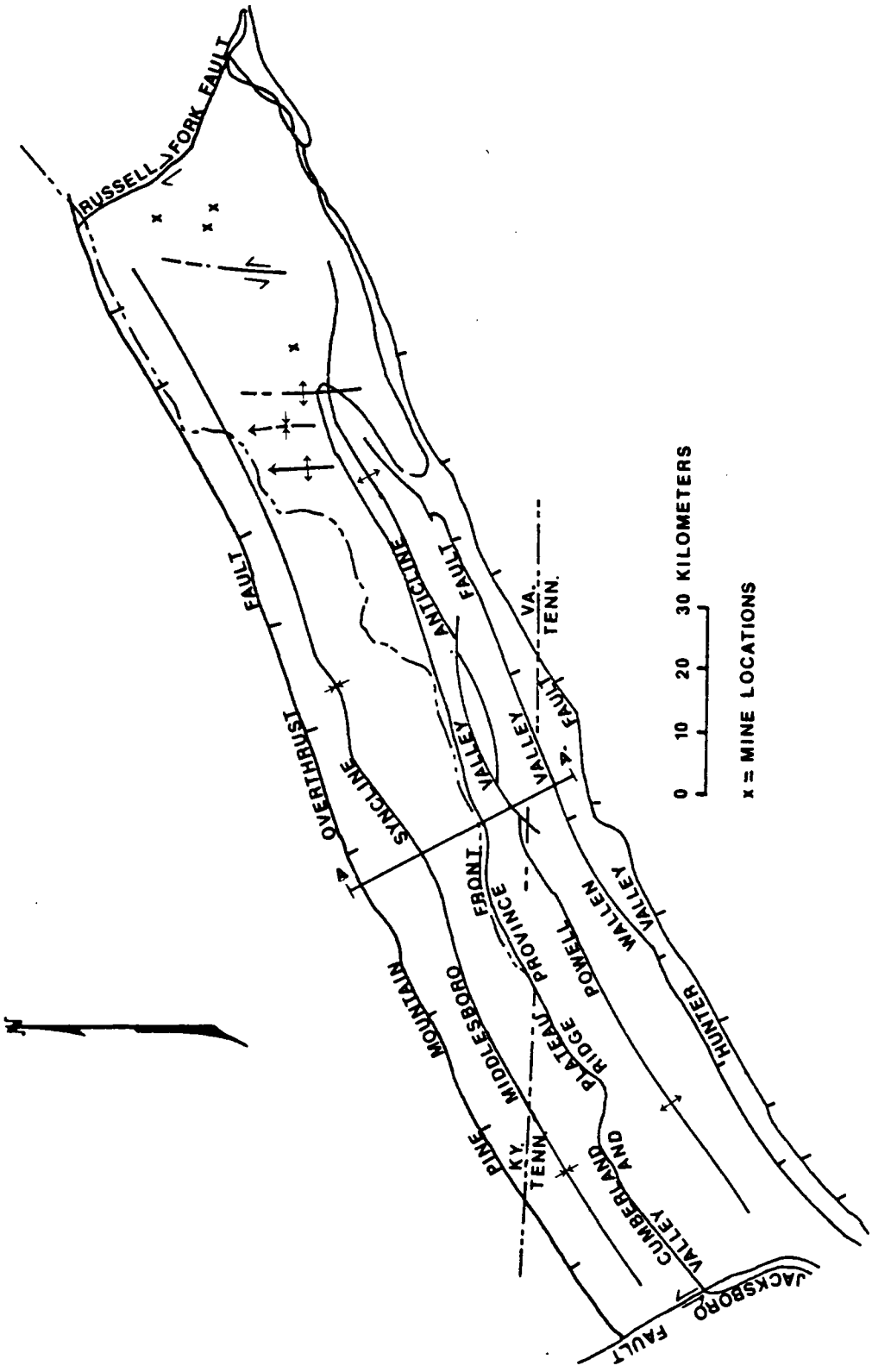

Figure 2.2: Geologic map of Pine Mountain thrust plate (after Miller, 1973).

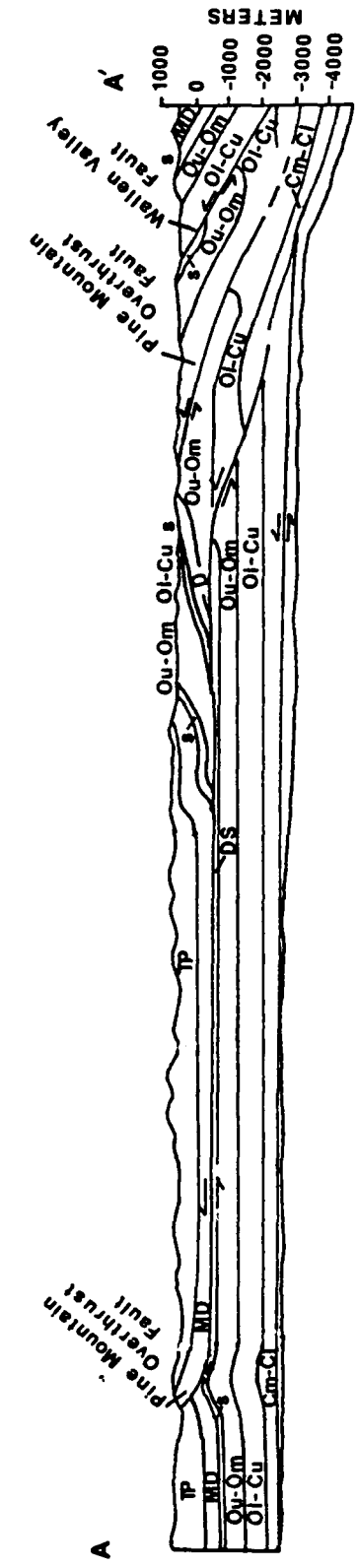

Figure 2.3: Geologic cross-section of Pine Mountain thrust plate (after Miller, 1973).

and it is here that all of the coal is found. The Middlesboro syncline also contains some cross-strike features, some of which have been named (Eby, 1923): the Gladeville anticline, Dorchester syncline, and the Buck Knob anticline. Johnston et al. (1975) located the Coeburn fault while other cross-strike structures have been described by Rich (1934). Many smaller-scale features can also be observed.

Harris and Milici (1977) used the concept of decollements, connected by structural ramps and based on the original thin-skinned version by Rich (1934), to explain the structure of the Pine Mountain block. In the basal decollement, an original master thrust fault within a zone of weak Cambrian shales, detaches the Paleozoic sedimentary rocks from the underlying Precambrian crystalline basement (Figure 2.4). As the sheet is thrust to the northwest, resistance to movement increases and the fault "ramps-up" to another, stratigraphically higher layer of weak rocks. This type of faulting may be enhanced by higher than normal fluid porepressures within the relatively impermeable shaly horizons (Hubbert and Rubey, 1959) and has been used by R. L. Miller (1973) to explain faulting in the Pine Mountain Block. This process is repeated until either the resisting forces become too great or the orogenic force is relieved. The outcome is a staircase-like effect with rootless anticlines formed over each ramp. On the Powell Valley anticline, the result is that the amplitude of the anticline decreases to the north-

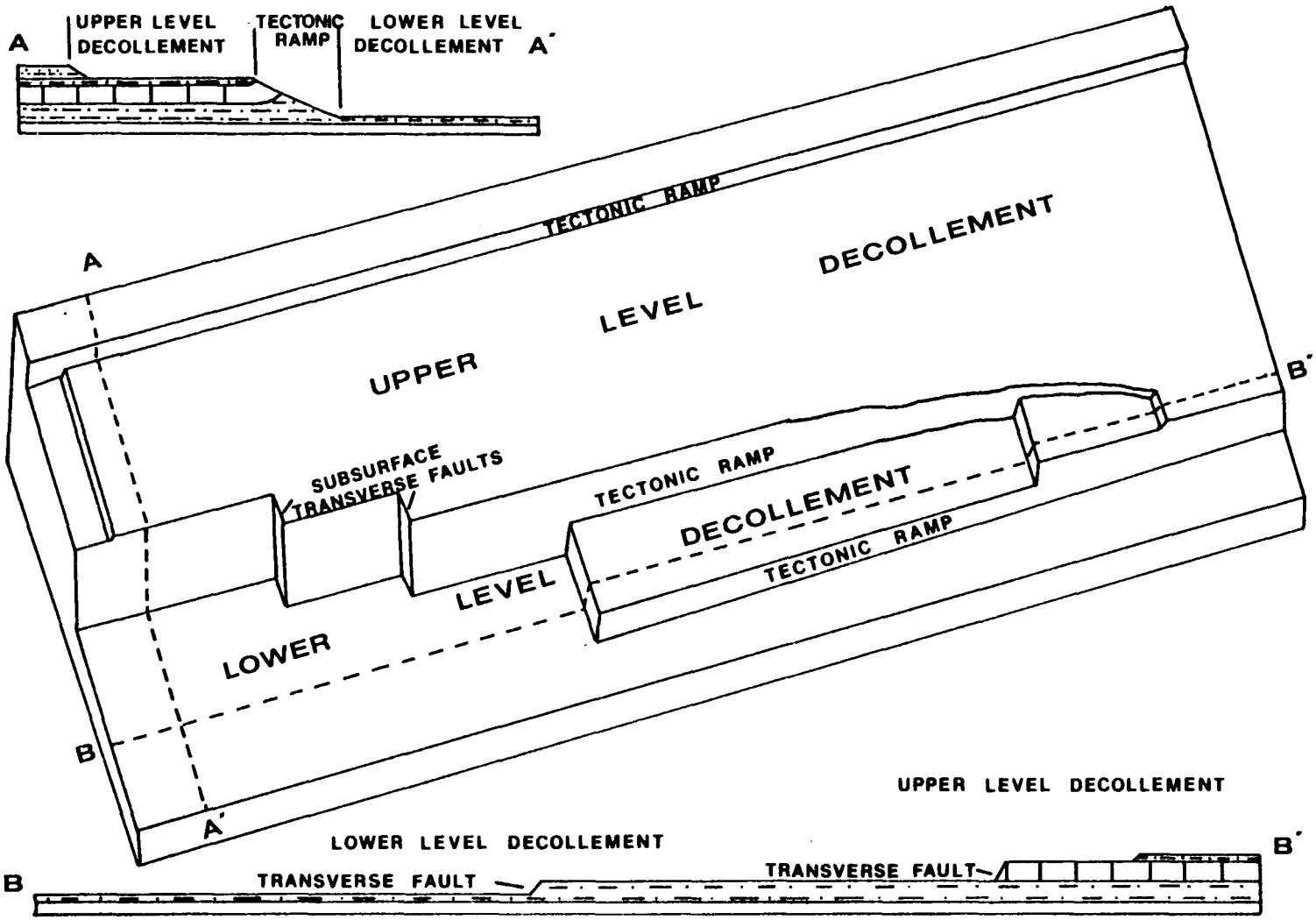

Figure 2.4: Generalized decollement (after Harris and Milici, 1977).

west as less material is duplicated above the ramp. This type of faulting has been termed shear thrust by Milici (1970) where previously unfolded strata are broken resulting in rootless, passive anticlines. Warping of the Powell Valley anticline by a later, buried thrust fault, the Bales thrust of Harris (1967), has folded the Pine Mountain thrust. Decollements on a smaller scale can be found in coal mine roof rocks within the sheet (Milici et al., 1982a, 1982b).

Unless a thrust sheet is infinitely long, it must by bounded laterally by transverse faults or by decreasing displacement. In the case of the Pine Mountain block, two tear or "wrench" faults (Moody and Hill, 1956) terminate the sheet at either end. These are the Jacksboro and Russell Fork faults. Rich (1934), utilizing the ideas of Wentworth (1921), proposed an interpretation of these faults and also explained the presence of the northerly-trending, cross-strike features. Wentworth (1921) had examined the Russell Fork fault in great detail and determined that almost all of the movement of the Pine Mountain plate was of a strike-slip nature in a north-south direction. On the other hand, the Jacksboro fault which borders the southwest end of the sheet has elements of both dip-slip and strike-slip faulting. It would appear, then, that the movement of the block on the east was hindered at some point and acted

somewhat as a hinge zone as deformation progressed. The block then pivoted northward on this northeast corner resulting in the Jacksboro fault. Because the plate was unable to move on its east end, stresses were relieved by cross-faulting rather than continued movement (Wilson and Stearns, 1958, Harris, 1970). The end result was formation of the cross-structural Buck Knob and Gladeville anticlines and Dorchester syncline. The Gladeville anticline is the sharpest of these folds and may represent an incipient failure zone or may, in fact, by underlain be a thrust fault (Rich, 1934). Rich (1934) also noted "three lines of disturbance "between Speedwell and Jellico in Tennessee, Cumberland Gap and Pineville, Kentucky, and from the eastern end of the Powell Valley anticline northward to Pine Mountain at Pound Gap.

2.2 GEOLOGIC FEATURES ASSOCIATED WITH COAL MINE ROOF FAILURES

2.2.1 General Considerations

The determination of the factors which cause roof failures has been the subject of much work in recent years. Various approaches have been utilized in this regard and range from statistical and other numeric methods, such as finite elements and beam bending theory, to empirical observations. In addition to the delineation of factors affecting mine roofs, some attempts have been made to classify various factors of the problem in order to develop certain

categories. The objective of this is to predict falls and areas of instability before they occur, or before mining has begun. In this regard, another approach is that of studying the genesis of rocks themselves. The development of such depositional models may shed some light on the relationships involved.

2.2.2 Parameters Involved in Roof Falls

Most roof falls result from geologic discontinuities in the mine roof, especially where the roof is fractured or where one type of strata is in contact with another. Moebs (1973, 1977, 1981) and Moebs and Ellenberger (1980, 1982) have investigated some of these features. They described paleochannels, scours, pinchouts, slickensides, clay veins, crevasse splays, and joints as being detrimental to roof stability.

Paleochannels are usually trough-like masses of cross-bedded sandstone often referred to by miners as "sandstone rolls" (Figures 2.5 and 2.6). These channels consist of sedimentary rocks which were deposited in ancient stream beds and tidal channels. In places, these channels cut down into the peat beds and were subsequently filled in as the channels were abandoned (Figure 2.7). The danger associated with these bodies results from the occurrence of weaker rocks, e.g. coal or shale, being poorly bonded to the adjacent sandstone channel fills. When mining occurs beneath

Figure 2.5: Paleochannel (photograph by T. M. Gathright, II).

Figure 2.6: Paleochannel seen underground (photograph by T. M. Gathright, II).

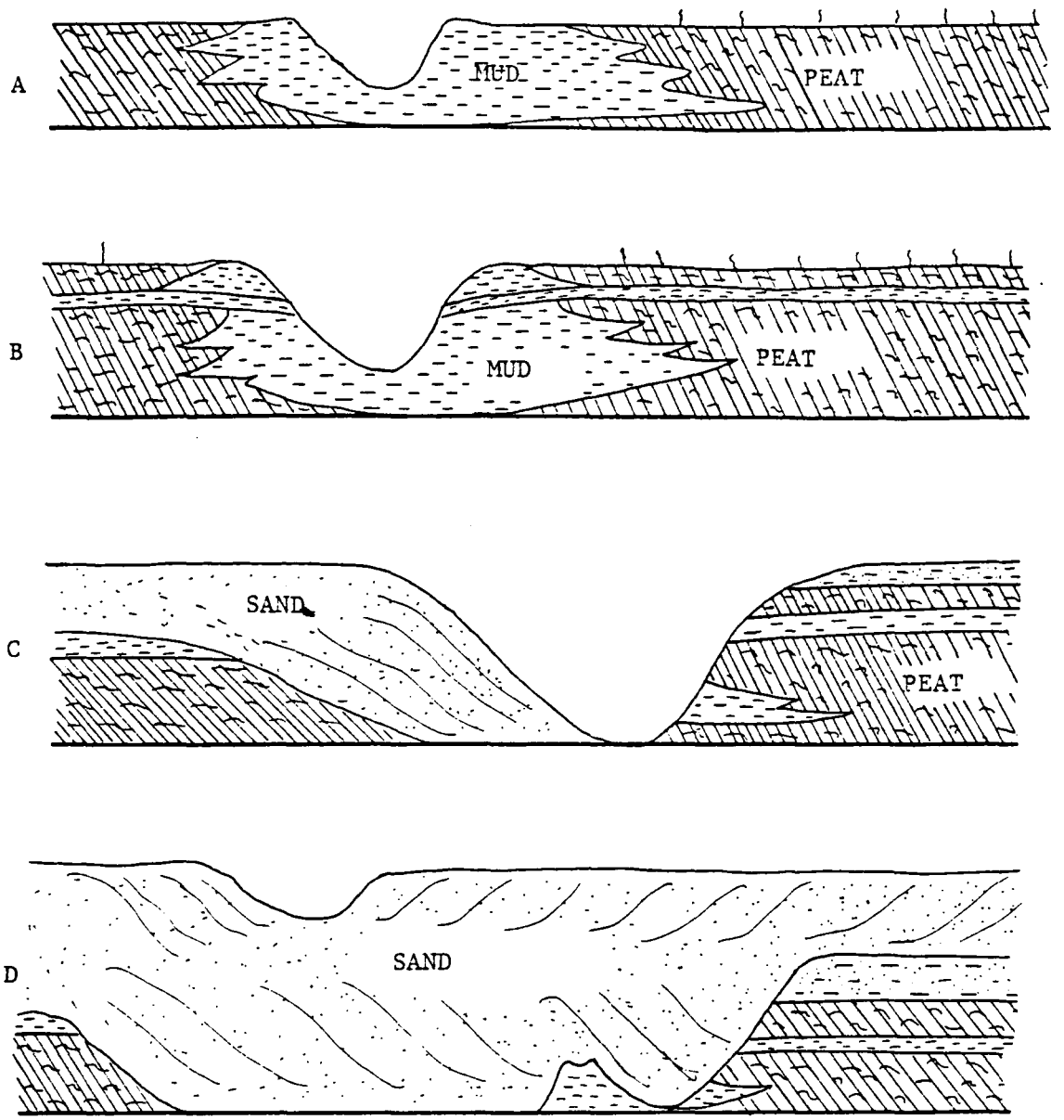

Figure 2.7: Formation of a paleochannel (after Moebs, 1981).

the channel boundary, rocks along the weak interface are likely to pull away. Moebs and Ellenberger (1980) differentiate scours from paleochannels since they have a curved or saucer shape rather than the linear shape of a channel. The origin of the two is the same, however. Two distinct types of sandstone channels have been noted by Jeran and Jansky (1983). The first is referred to as a "cut-out" in which each individual coal layer has been cut by the sandstone. This type of channel does not affect the coal thickness as it is approached by mining. The second occurs when the coal has been subjected to pressure by the overlying sandstone. This results in the coal being squeezed to either side of the channel and its thickness may even be doubled. The layers of coal, in this case, may be wrinkled as they are bent downward.

A pinch-out is defined to be "the termination or end of a stratum, vein, or other bed of rock that narrows or thins progressively in a given horizontal direction until it disappears and the rocks it once separated are in contact" (American Geological Institute, 1974). The rapid thinning of a sedimentary stratum during deposition is a possible mode of formation of these features. On the other hand Moebs and Ellenberger (1980), note that pinch-outs ore often found along the boundaries of channels and may be the result of the same cutting action that formed the channels (Figure

2.8).

Slickensides are, perhaps, the most dangerous of all coal mine roof features (Figure 2.9). They are also one of the most common. A slickensided surface is one which is polished and smoothly striated because of friction resulting from movement along a surface within the rock (American Geological Institute, 1974). Because of this sliding and resultant polishing, the slickensided region forms a surface of low shear strength in the rock along which additional movement can easily occur. Ferm et al. (1978) have suggested that slickensides are the major contributor to roof falls and that they result from a number of causes. They can be found in slump deposits, kettle bottoms, fire clays, channel bottoms, or anywhere the sediments have slid past each other due to differential compaction. Milici et al. (1982a, 1982b) determined that a large proportion of slickensides in coal mine roof strata in Virginia resulted from tectonic movements. Similar features are caused by decollements elsewhere in the Appalachian plateau (Harris and Milici, 1977).

Clay veins, or clay dikes, although not common in Virginia coal beds, often present a problem in West Virginia and Illinois (Figure 2.10) (Moebs, 1974, 1977, 1981, Moebs and Ellenberger, 1980, 1982, Peng, 1978, Krause et al., in press). These features consist of mudstone or claystone-filled tension cracks in a coal bed. In places, the clay

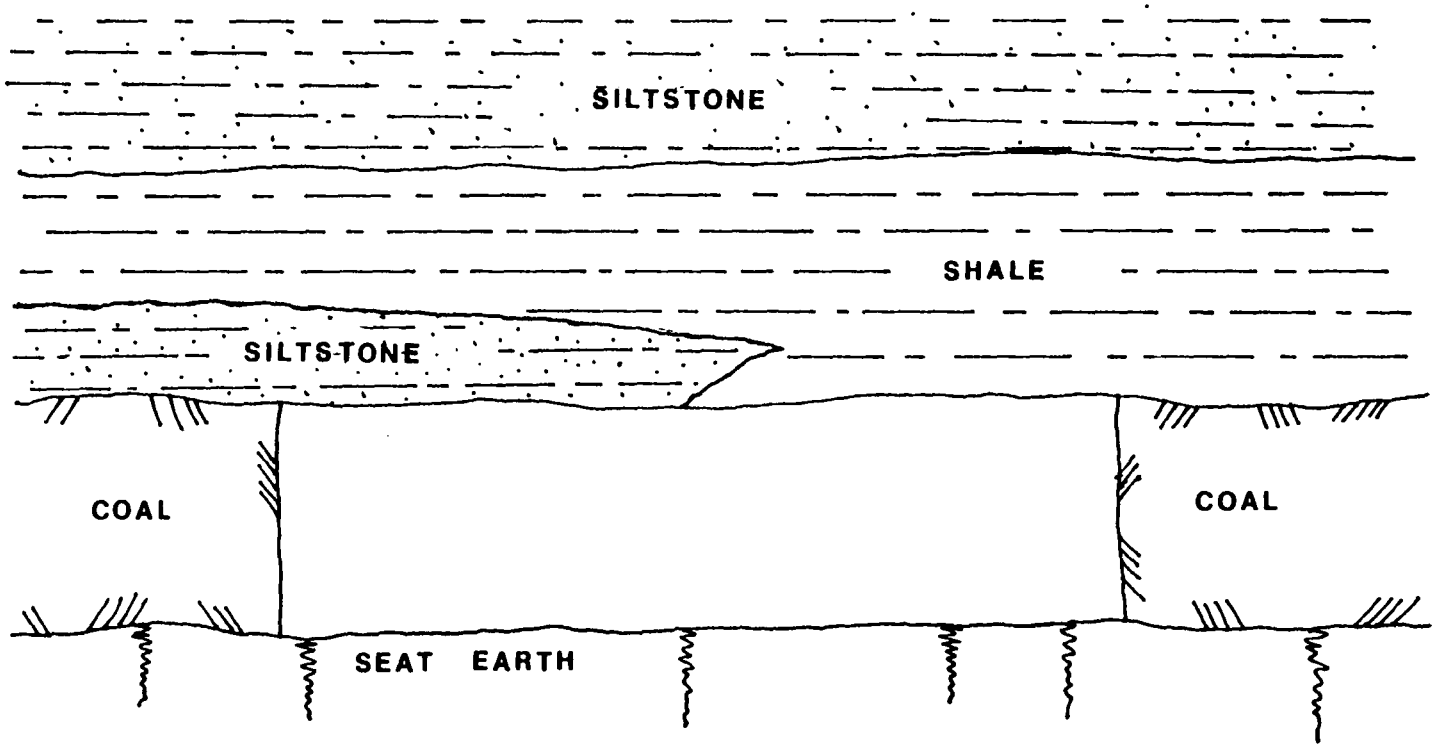

Figure 2.8: Pinch-out.

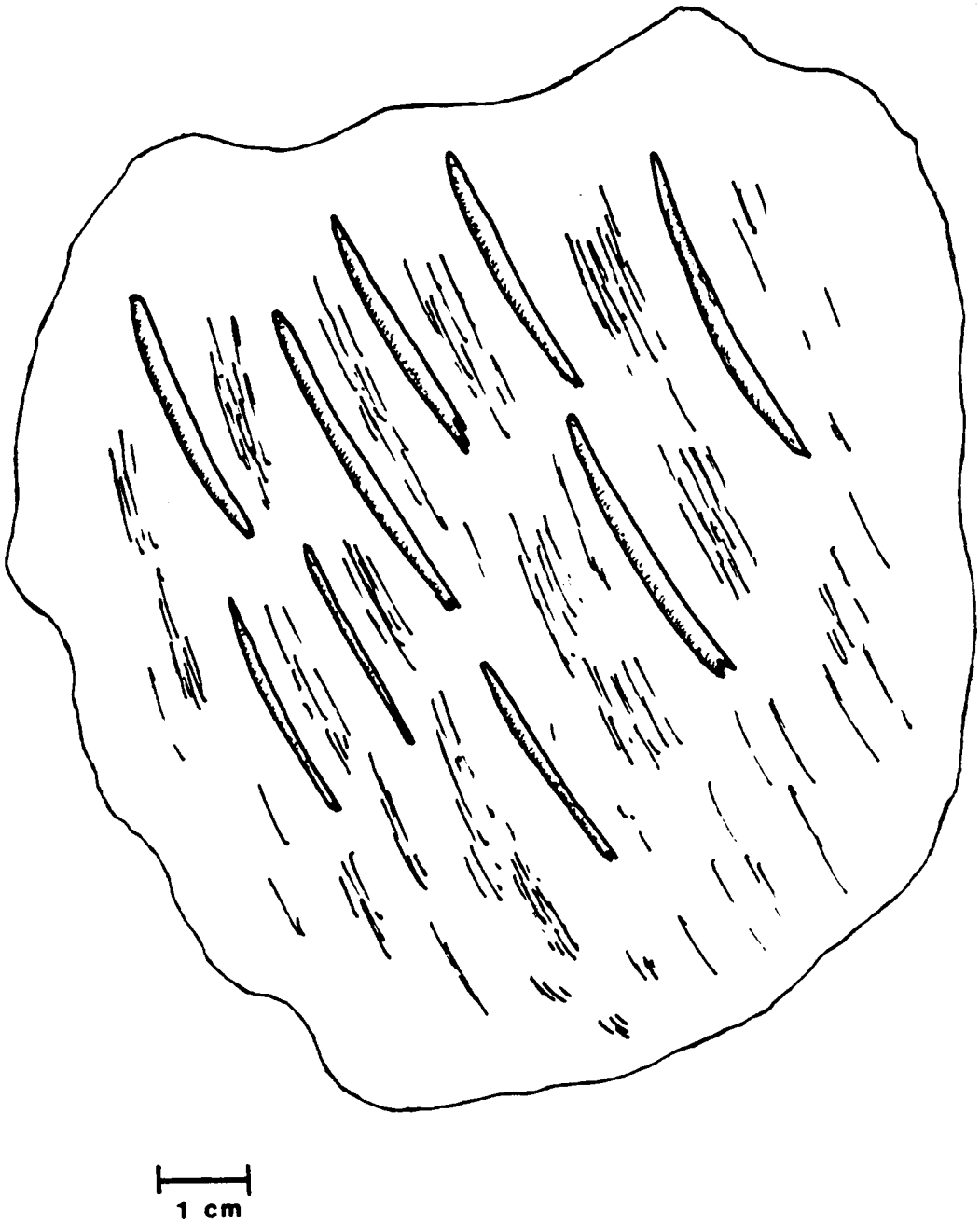

Figure 2.9: Slickensides.

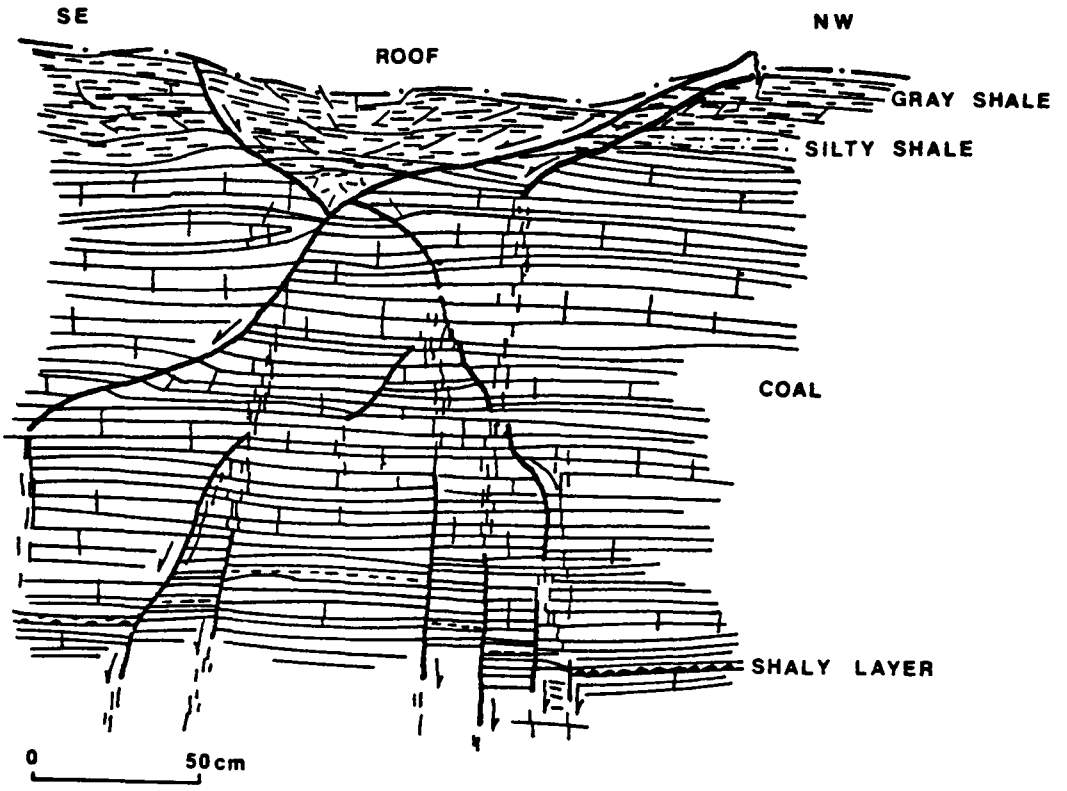

Figure 2.10: Clay vein.

filling is intruded from the roof and Krause et al. (1979) found low angle normal faults associated with veins. Slickensides often accompany clay veins further contributing to the danger.

Crevasse splays were formed when a stream breached its natural levee depositing sand on top of the mud flats bordering the channel (Figure 2.11). Repeated episodes of flooding have resulted in rock consisting of interbedded sequences of thin layers of micaceous sandstones and shales. These units can be from 2 to 9 meters thick and have a sheet-like or lenticular appearance in plan view (Moebs and Ellenberger, 1980, 1982). Their inherent weakness is attributable to the lack of cohesion between the mica and shale layers, and it is often amplified by plant remains or thin carbonaceous layers on the bedding planes.

Joints, planar fractures within the rock along which no movement has occurred, are very important as far as roof control is concerned. Joints are especially important in Virginia where folding and faulting are greater than in the central Appalachian coal fields (Moebs and Ellenberger, 1980). Situations that are particularly conducive to roof falls occur where joints are densely spaced or where joint sets parallel the mine entries (Mahtab,1973). Mahtab (1973) has explored the possibility of incorporating both geometrical properties, such as joint strike, dip, and spacing, and

Figure 2.11: Crevasse splay.

mechanical properties, such as shear strength, into a finite element analysis for coal mine design. He then distinguishes between an inhomogeneous and homogeneous model. In the inhomogeneous model, the rock mass is modeled as consisting of individual joint elements and intact rock blocks. The homogeneous model enables the assignation of directional properties to the rock mass such as orthotropic or transversely isotropic. A more thorough discussion of rock joint theory and the effects of varying conditions on joint behavior is presented by Kane (1981).

Faulting is another extremely important factor as far as roof falls are concerned. In Illinois, Nelson (1981) has written extensively on the effects of faulting in coal mines. He emphasized the consequence of faulting as primarily the weakening of the roof and ribs. In addition, it also allows the introduction of clay and other roof-derived impurities into the coal, contributing further to roof instability. He then divided faults into two groups: tectonic faults and non-tectonic faults. Tectonic faults arise from forces acting deep within the earth while non-tectonic faults are local in nature and are formed by the disturbance of only partially lithified sediments.

Tectonic faults are found to be planar or slightly curved and occur in well-defined systems. Characteristically, they are not limited to any particular rock stratum or type. Large tectonic faults are often accompanied by gouge

or breccia. Drag folding may be present, with the rock folded in the direction of net slip. Tectonic faults may be normal, reverse, strike-slip, oblique-slip, or bedding plane faults (Figure 2.12) (Nelson, 1981).

Nelson (1981) describes non-tectonic faults as being curved in strike and/or dip. This type of faulting is usually found within a single bed, such as the coal seam or shale roof. In Illinois, faulting is consistently of the normal variety with false drag, folding opposite to slip direction, often found. These faults are closely associated with the rock distribution above the seam and may include compactional faults, clay-dike faults (occurring with clay dikes or veins), and gravitational slumping and sliding that occurred prior to lithification.

The effects of both large and small scale faulting on roof conditions has been examined by Iannacchione, et al. (1981). They studied the factors affecting roof stability in the Upper Kittanning coal bed of Pennsylvania and found two well-defined trends which affect roof falls in this area. Slickensided bedding planes and thrust faulting was found to be a primary contributor to roof problems along with sandstone-shale transition zones. They found that thrust faults extended into the roof where their dip flattened and they became bedding plane faults. The authors also demonstrated how bedding orientations and coal cleat

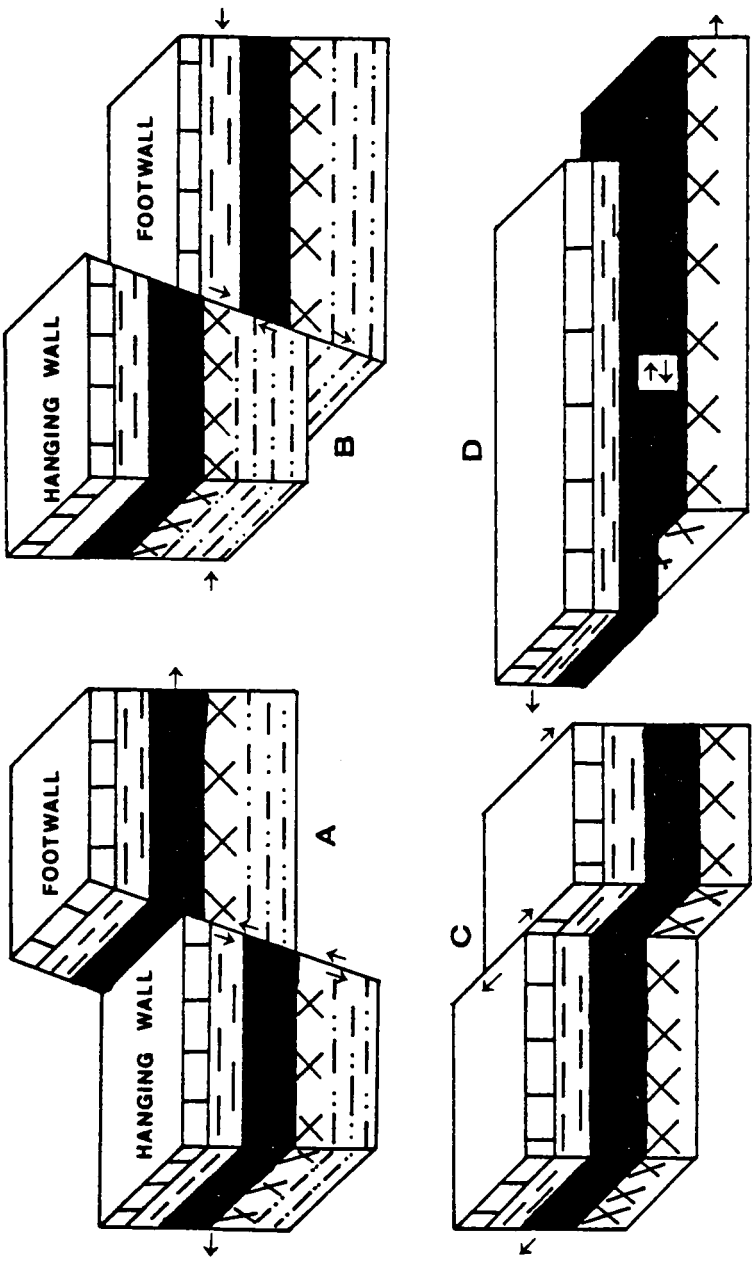

Figure 2.12: Types of faults (Nelson, 1981).

are deformed in the fault zone.

Milici et al. (1982a, 1982b), in an analysis of some southwest Virginia mines, also discovered slickensided extensional, contractional, and bedding plane faults to be a major factor in roof falls. They also noted the effects of slickensided areas due to differential compaction, sandstone channels, and the interlayering of different rock types along with jointing as being detrimental to roof quality.

The presence of an area of extensively faulted and slickensided roof rock above practically undeformed coal was discovered by Krausse and Nance (1980) in an Illinois mine. They termed this area a "shear body" and described it as being bounded on its lower surface by a series of shear faults which are sub-parallel to bedding and then curve upward into the roof along the outer margins of the shear body. This same type of faulting has been found in a number of Virginia mines by Milici et al. (1982) where the surface of decollement has been the top of an undeformed coal seam. Milici et al. (1982) have also noted much deformation in shale or siltstone partings within the coal bed before the fault ramps up through the coal and into the roof.

Shepherd and Fisher (1978) concentrated exclusively on the effects of faulting in their study of roof stability in an Australian coal mine. Statistical methods were used in examining parameters suggested by Shepherd and Burston (1977) such as fault "plane" geometry, geometry of slicken-

sides, interference of sets of slickensides, fault profile styles, fault throw, gouge, and cleat interaction. A definite correlation between the presence of faults and bad roof conditions was established in that normal dip slip faulting did not appear to influence roof failure a great deal but normal, oblique, and strike-slip faults led to severe roof problems. They hypothesized that the coal seam has a lower shear strength across oblique-slip faults than dip-slip faults due to several movements along the oblique-slip faults. Alternatively, they felt that these groups of oblique-slip faults are due to residual tectonic stresses rather than being gravity caused as in the case of dip-slip faults.

Shepherd and Fisher (1978) found that the strength of the fault-bad top association diminishes with distance from the fault. This led them to the idea of a "zone of influence" for the different types of faults. The authors also felt that the presence of certain types of faulting will affect the manner of roof failure, e.g., a dome-shaped fall will be caused by a clustering of faults.

The influence of roof lithology has been investigated by Moebs and Ferm (1982) in the Pocahontas No. 3 coal bed in southwestern Virginia. They found that many detrimental features could be seen in drill core and subsequent preparation could be made before mining. Certain rock types were

identified with poor roof. These included slump deposits, channel scours, and fire clays. Poor-to-fair roof conditions were associated with cross-bedded and pebbly sandstones, sandstone with shale streaks or interbedded shales and sandstones, and crystallized sandstone and conglomerate. Stable roof could be found in areas with massive gray sandstones or massive sandy shales.

Lithologic studies have also been carried out by Ealy, Mazurak, and Langrand (1979). By combining map overlays with statistical results, they were able to delineate key areas within a West Virginia mine where problems might ensue. They found that roof fall frequency correlated with a number of parameters. The frequency was greatest where the main roof is composed of thinly laminated shales or siltstones and was directly proportional to increases in the thickness of the shale unit. Fault and fracture zones played a large part in roof stability, especially where the roof is made up of shale or siltstone. They also noted that roof fall frequencies will increase with a corresponding increase in the extraction ratio. Finally, statistical analysis revealed that vertical load variations, that is, the effect of overlying topography, had little or no effect on either fall distribution or frequency. Most falls in this particular mine were oriented along a north-south axis, probably in response to high regional stresses.

Moebs (1974), on the other hand, has noted a definite

increase in roof fall occurrences beneath stream valleys in the Appalachian Plateau region. These falls usually develop a short time after mining, within hours or days, and he states that they may be due to a combination of topography, jointing, tectonic stress, and the geometry of the mine itself. R. A. Nelson (1979) suggests that this joint development is akin to a rock burst as the rock fractures on a plane parallel with the newly-formed free surface. These fractures follow topography and are often irregular in shape. They tend to be especially common in shales and rocks which demonstrate evidence of pressure solution.

The unloading caused by the quarrying action of a stream is responsible for increased tensile stress in the rock underlying the stream valley (Overbey et al. 1973). Falls beneath stream valleys have been found to occur in southwestern Pennsylvania by McCulloch et al. (1975). Roof falls not only occurred beneath stream valleys but also aligned themselves with the trend of the valley. This allows joints to penetrate deep within the rock and enables water to percolate down towards the coal. Ion exchange during leaching of the rocks above the coal may cause the rock to be weakened considerably, and clays may swell and increase the stress on the roof.

Stresses in the roof can be extremely important in the promotion of roof falls. High vertical stress can result in

floor heave or rib crushing. This has been documented by Morgan (1973) who suggested that floor heave and rib crushing at first resulted in lowered stress at the rib which in turn led to lowered shear stresses at the rib line. Thus, at first, the result is an improvement in roof stability. However, continued heave or pillar crushing has the net effect of rotating the maximum moment of the roof beam to the center of the span where tensile failure can take place. This phenomenon has been noted in at least one mine (Morgan et al., 1965). Parsons and Dahl (1971) have identified one of the major causes of falls at a mine in the Pittsburgh coal seam as being due to high compressive stresses in a direction perpendicular to the entries. Blevins (1982) has described problems associated with high lateral stresses in an Illinois mine. Attempts in dealing with the resulting roof conditions proved negligible. These included cutting slots in the roof to absorb rock yield and modifying mining procedure. In the end, careful determination of the orientation of the stress field allowed for reorienting entry and cross-cut directions and alleviation of the problem.

Moelle (1972) has approached the stress field problem in his concept of "directional mining." He states that an initial state of stress exists in the in situ rock. Any mining activity induces stresses which interact with the existing stress field. Roof falls will then occur along any

discontinuities if they coincide with planes of high shear stress within the stress ellipsoid.

The stress field underground has been analyzed by Aggson (1980) who used it to describe four typical failure modes depending on the state of stress. Figure 2.13 shows that where a mine with a massive roof is under the influence of high horizontal stresses in relation to the vertical stress, shear stresses will develop in the roof resulting in an arch-shaped failure. If the horizontal and vertical stresses are nearly the same, the failure surface will become somewhat more vertical and may result in "cutter roof." This type of failure, in which a vertical crack forms along the rib, is shown in Figure 2.14. The third type of stress-related failure occurs when body forces are the only ones involved. In this gravity-loaded situation, the vertical stresses are higher than the horizontal and maximum stress is of a tensile nature in the center of the roof span. Failure occurs if the tensile strength of the rock material is exceeded as shown in Figure 2.15. Finally, if a laminated roof is present, as is common in many coal mines, failure occurs progressively (Figure 2.16). First, deflection of the layer adjacent to the mined area begins to sag and delaminate from the layer immediately above it. Failure results in this first layer leaving the next layer above unconfined and free to deflect and fail in a similar

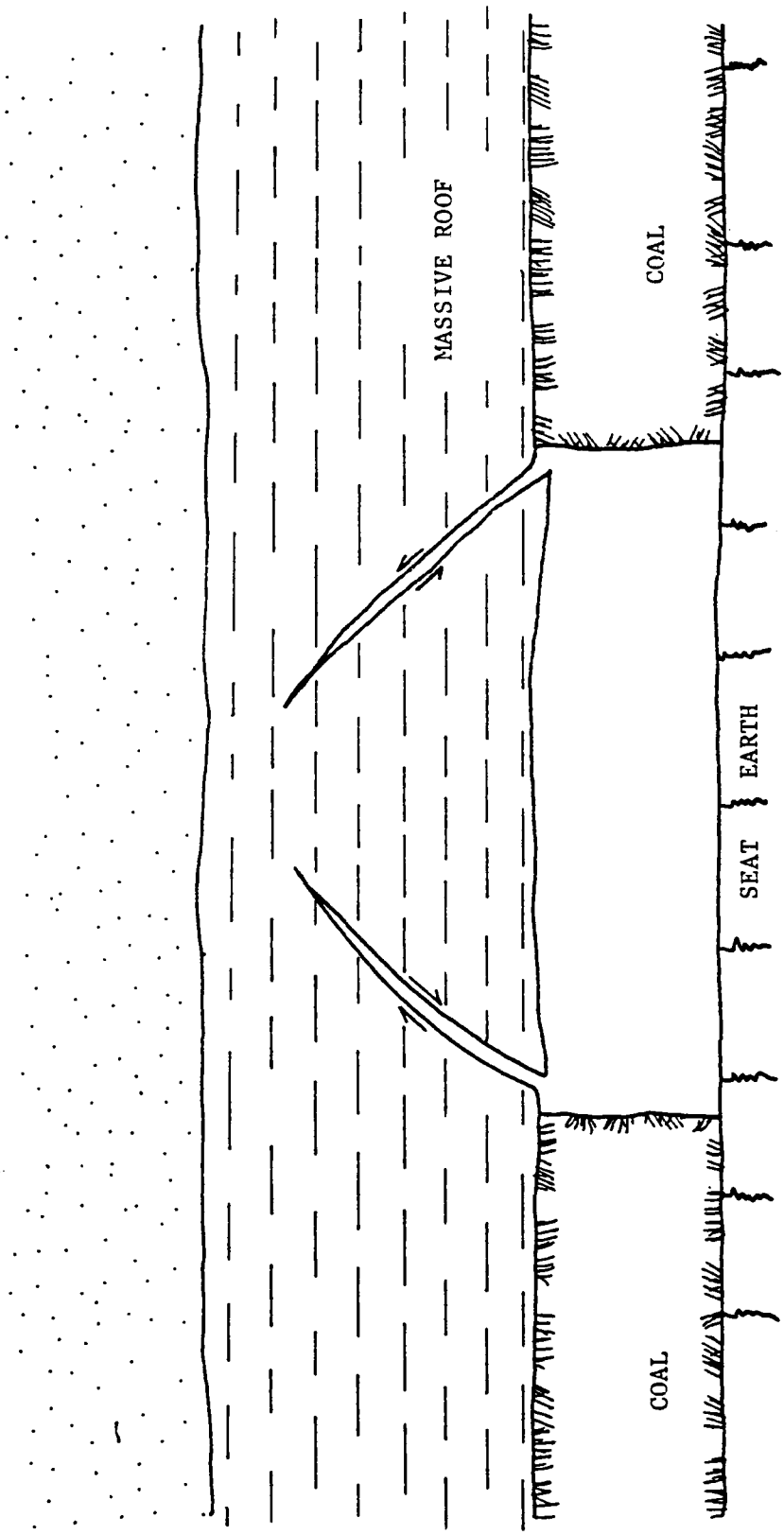

Figure 2.13: Roof failure due to high horizontal stresses (after Aggson, 1980).

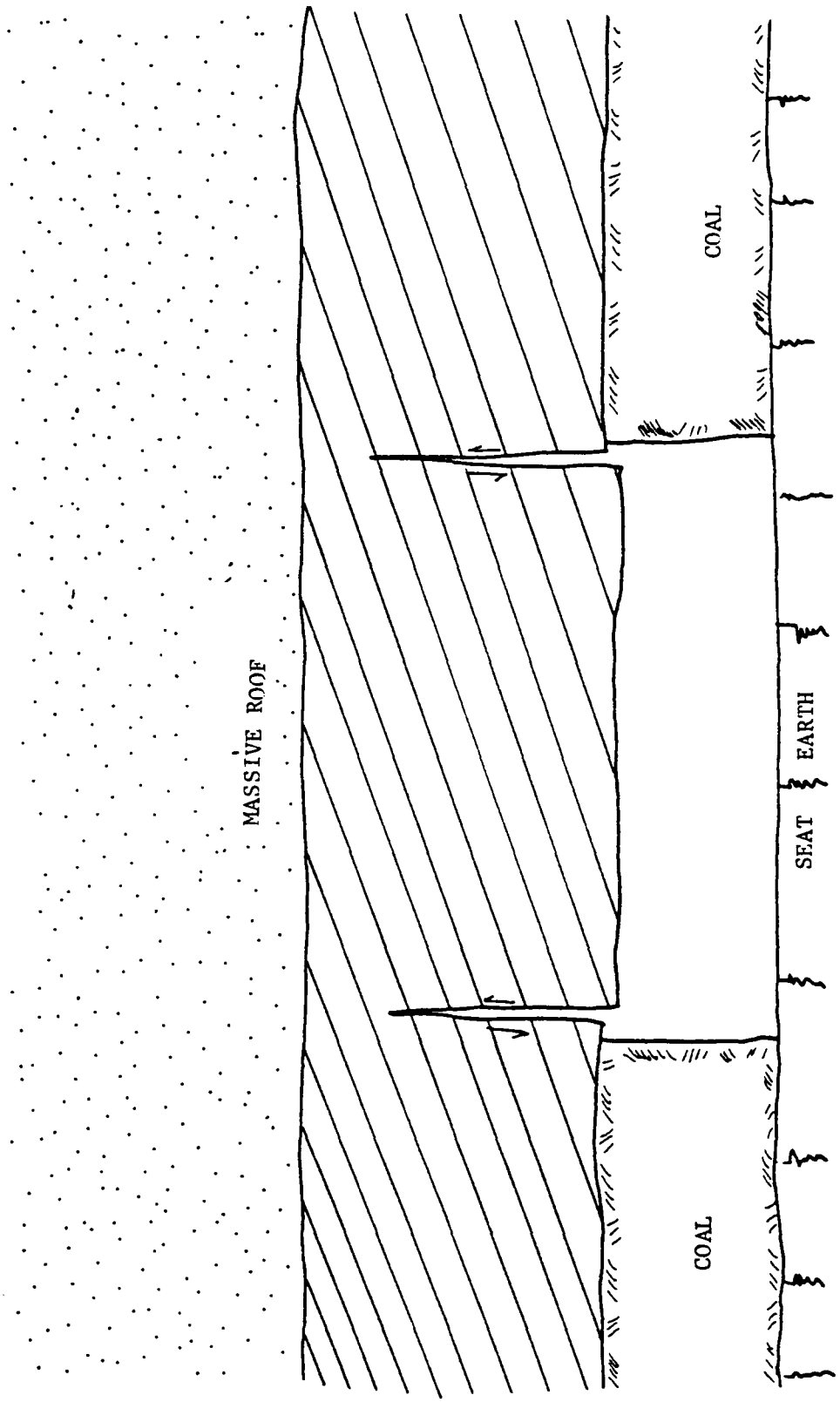

Figure 2.14: Cutter roof (after Aggson, 1980).

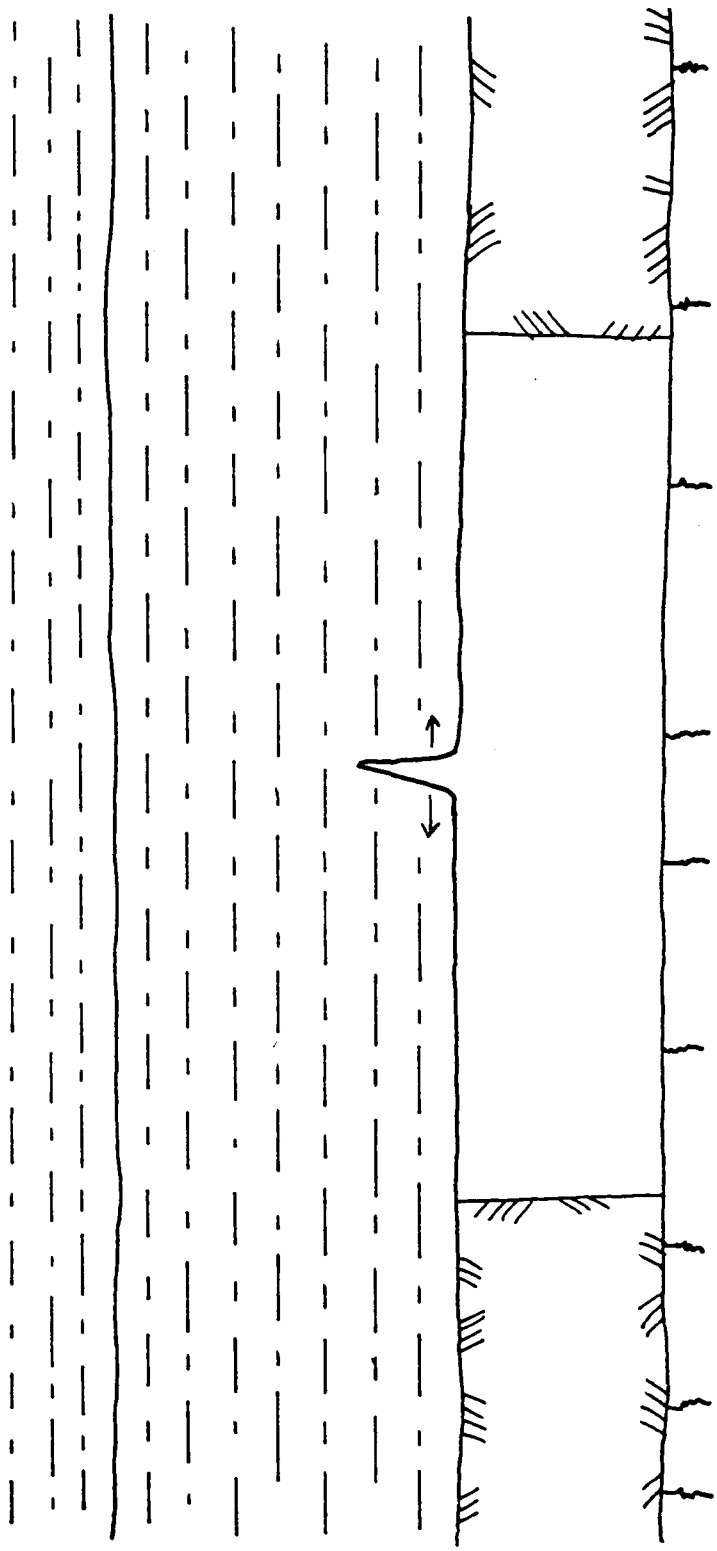

Figure 2.15: Tensile failure (after Aggson, 1980).

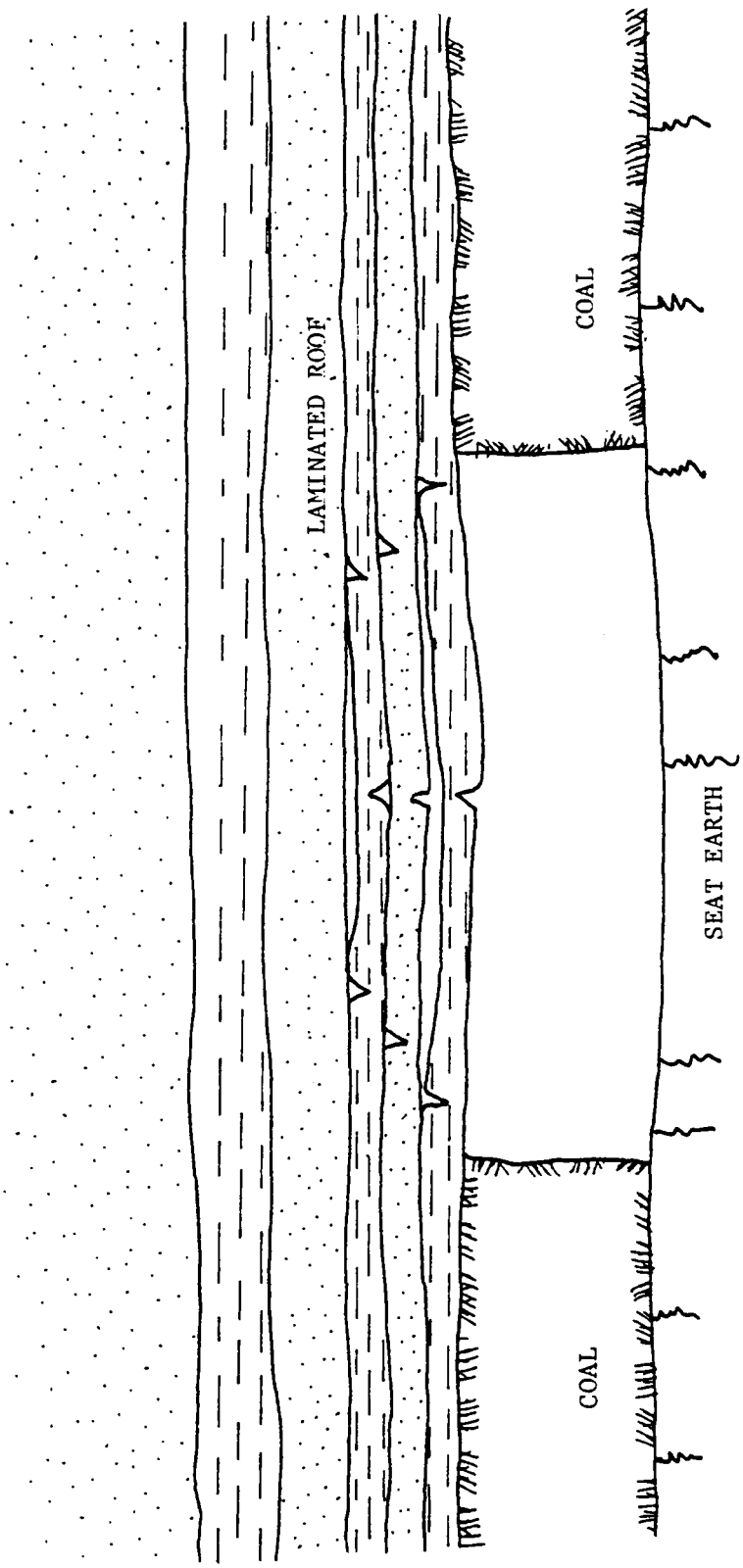

Figure 2.16: Failure in a layered roof (after Aggson, 1980).

manner. This can also be the mode of failure of a thinly-bedded floor as it heaves (Aggson, 1978). Obert et al. (1960) have addressed this subject with regards to mine design.

Stresses often originate due to folding of the rock units (Price, 1966). Beam bending considerations indicate that tensile stresses and resulting fractures will exist in the bottom of a synclinal rock layer while an anticline will undergo compression and any fractures will be closed. Roof falls, then, could be expected to be more commonplace below a syncline.

One type of roof hazard which may be erratic and unpredictable in its distribution has been described by Jeran and Jansky (1983) among others. Referred to as a "kettle-bottom", this feature is the fossil trunk or root of a fern or tree preserved as a mud cast (Figure 2.17). A kettlebottom is often surrounded by a thin layer of coalified bark and slickensides, and because it is of greater diameter on the bottom than the top, it is prone to falling suddenly when the coal is mined out from below. Kettlebottoms may vary from several inches to several meters in diameter (Peng, 1978).

Other geologic factors which may cause roof falls include gas and water pressure in the immediate roof or voids in the roof brought about by the oxidation of pyritic veins (Headlee, 1944). Wier (1969) has also identified the pre-

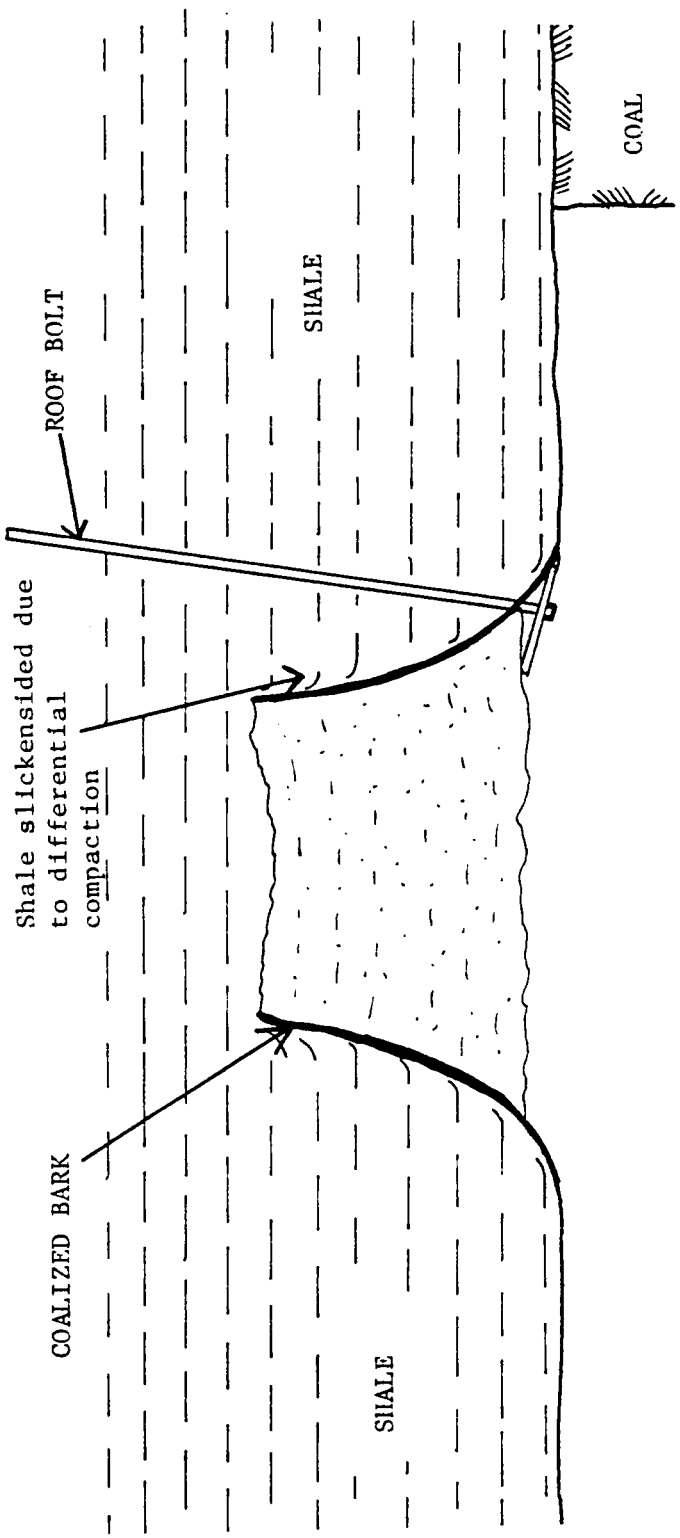

Figure 2.17: Kettlebottom.

sence of expandable clays such as illite and montmorillonite in the roof rock and the presence of fossils as being detrimental to roof stability. Burggraf (1981) suggested that the presence of, and distance to, any rider coals can be an important parameter. These seams which can vary from fractions of an centimeter to several meters thick lack any tensile strength and if located in close proximity above mine workings can cause large falls.

In areas where deposits of mineralized peat or "coal balls" are found, mining problems related to these occurrences have been noted (Demaris et al., 1983). Coal balls appear to be associated with areas of transitional roof lithology and thus may also serve as indicators of potential problems.

Coal cleat may also be associated with roof control problems as has been suggested by McCulloch et al. (1974) and (1975). This is due to the fact that local deviations in cleat orientation may be indicative of adverse geologic conditions in the immediate area. Holmes (1982) also examined the effect of cleat directions on mine operations. He devised a Roof Stability Index which reflects the effect of cleat upon roof failure (Figure 2.18). When cleat directions subtend an angle of less than 30 degrees with the face and roadway directions, instability problems within the roof are likely to develop. This is due, in part, to the inter-

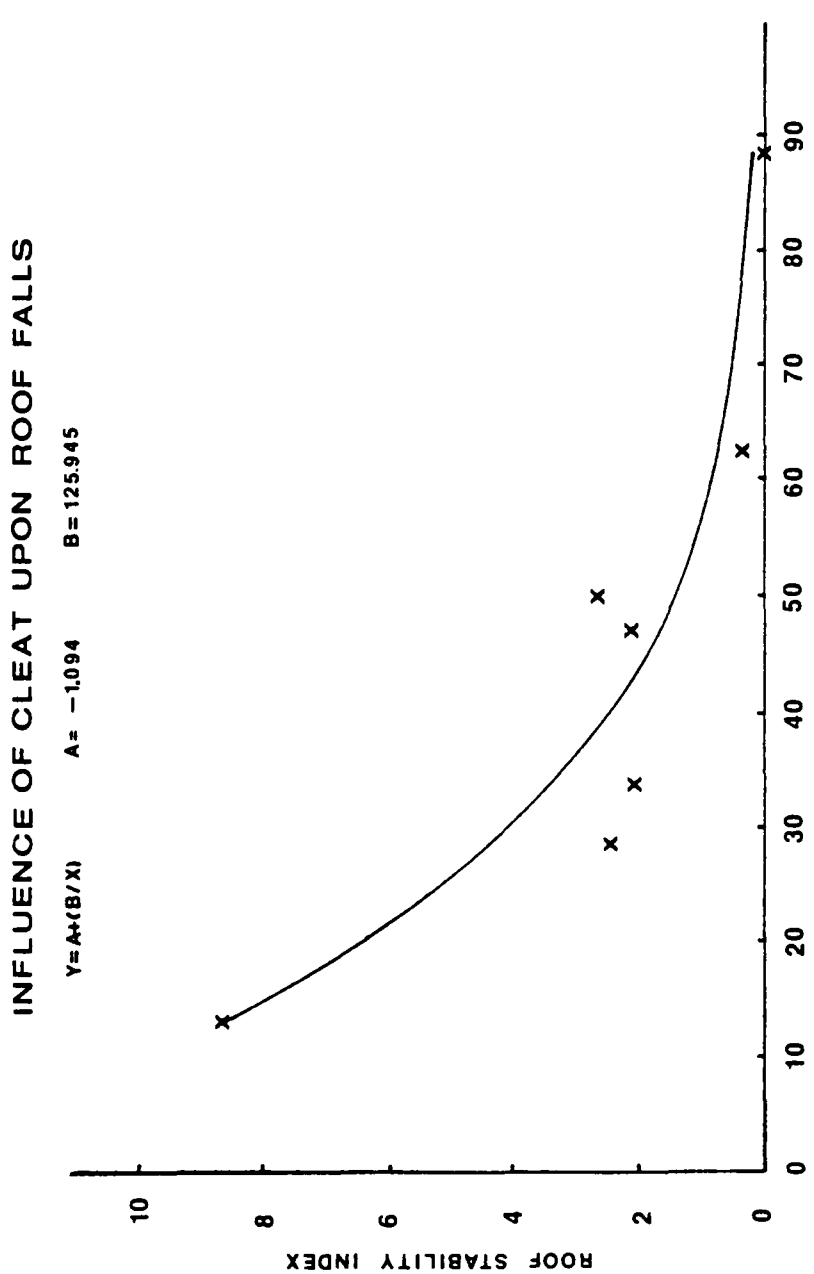

Figure 2.18: The effect of cleat on Holmes' Roof Stability Index (Holmes, 1982).

action of imposed abutment pressures ahead of the face with the cleat planes.

Peng (1980) has demonstrated that location is a major factor in roof falls. More than 71% of all fatal falls occur inby the last row of permanent supports while the majority of non-fatal falls occur at entry intersections. Because most fatal falls occur under unsupported or temporarily supported roof, the time that unsupported roof is allowed to stand may be a factor. Cox (1974) found in three Alabama mines that if poor mine roof conditions already existed, then elapsed time was of the utmost importance in roof stability. However, even under good roof, the time lapse between excavation and permanent support installation is still important. On the other hand, a Colorado mine examined by Radcliffe and Stateham (1978) revealed that the amount of elapsed time prior to the installation of support did little if anything to affect the stability of the roof once the support had been provided.

Climatic conditions have also been cited as being potentially related to roof falls (Boyer, 1964; Chenevert, 1969; Colback and Wild, 1965; Haynes, 1975; Parker, 1966; and Stateham and Radcliffe, 1978; among others). Boyer (1964) examined the relationship between barometric pressure and major disasters in coal mines while Parker (1966) and Haynes (1975) studied the effects of temperature and humidity on coal mine roof rocks. Haynes (1975) found that coal

mine roof is untowardly affected by changes in moisture. Stateham and Radcliffe (1978) were able to determine that the roof fall occurrence rate lags behind the humidity cycle by about two weeks. This is explained by the fact that a decrease in the strength of a rock depends of the amount of moisture absorbed which, in turn, is a function of clay content. Also, expansion and contraction of the clay minerals with absorption and desiccation can cause small internal cracks which reduce the strength of the rock.

Cummings et al. (1983) have also studied the effect of moisture on roof rock in West Virginia and Illinois. They suggest that the overcompacted nature of the claystone roof, as evidenced by slickensides, lends itself readily to swelling as moist air makes contact with it after mining. This swelling allows the formation of negative pore pressures within the material which, in turn, causes more water to be introduced within the claystone. The authors suggest leaving a few inches of "cap coal" to protect the roof from contact with moisture. They also recommend using portions of the mine, usually old works, as tempering or cooling entries which condition the air before it is brought into the active portion of the mine itself.

Chugh and Missavage (1981), in their review of the moisture problem, suggest that it can be approached in three ways. First, humidity changes can be controlled by using

tempering entries. They also suggest air conditioning or continuous wetting of the adversely affected sections of the mine. Neither solution has gained acceptance by the industry because of cost and time considerations. An alternate means of controlling the effects of moisture is to prevent moisture migration by leaving a layer of coal on the roof, using sealants and resin bolts, dry drilling, or controlled blasting to prevent moisture migration along bedding planes. Finally, rock reinforcement measures can be used such as wire mesh, gunite, or shotcrete.

2.3 CLASSIFICATIONS AND MAPPING

2.3.1 Objectives

Coal deposits are the result of complex geologic processes. As such, coal mine roofs and roof falls do not easily lend themselves to a broad classification scheme. However, in order to deal with roof control problems from an engineering standpoint, it is essential that some method of categorizing be used. Classifications have come from within the coal industry and there have been attempts to use rock engineering classifications derived for use in tunneling for coal mine applications. These have met with varied and limited success.

Classifications are especially valuable when used in conjunction with underground mapping programs. They enable the observer to quickly note and categorize features that

can later be analyzed with respect to the mining situation. In this regard, the subject of prediction is important. By using classification schemes for data procurement during the mapping process, the engineer may be able to make some prediction as to what roof types or problems may be encountered during the course of future mining. He, then, may be able to specify measures well in advance to be taken to alleviate any untoward effects of potential geologic hazards.

2.3.2 Roof and Roof Fall Classifications

Hylbert (1978) devised a roof classification scheme based entirely on geology, i.e., lithologic and structural features. Employing a checklist for detailed underground mapping, he was able to generate four roof categories:

1. Condition A: laminated shale containing discontinuities some of which may have slickensides.

2. Condition B: laminated shale which contains bedding plane faults with horizontal zones of crushed shale.

3. Condition C: rolling sandstone containing pockets or narrow zones of shale. This can often be an erosional contact with the sandstone. Roof control presents a problem.

4. Condition D: zone of major sandstone rolls usually due to washouts. This is a large scale example of Condition C.

Hylbert was then able to relate the roof type and thickness to the incidence of roof falls. Roof falls were found to be especially frequent at sandstone-shale boundaries, that is,

roof Condition C.

Ferm, et al. (1978) also employed geologic criteria to categorize roof rocks. Using statistical analysis to determine significant parameters, they devised the following classification:

1. Good Top: smooth, clean, crack-free roof. Minor spalling may be present.

2. Moderate Top: roof appears rough with loose pieces about a foot in length and contains some cracks and vertical separations.

3. Bad Top: rough, broken roof with many pieces greater than a foot in width. Contains a large number of vertical separations.

4. Fallen Top: self explanatory

Ferm et al. (1978) described the support measures that have been used for each roof type and then tried to relate either rock type or rock sequence to the roof quality. They found a positive association between thick sandstone and moderate, bad and fallen top while thick shale was positively associated with good top. The reasons given for this are that the sandstones often are cross-bedded or contain shale layers or coaly strips in the basal part of their units. The thick shales, on the other hand, are usually part of coarsening upward sequences. Results for other rock types such as splay deposits and orthoquartzitic sandstones were ambiguous. Ferm et al. also describe the type of support used for each kind of roof: standard bolt pattern for good top, extra bolts, half-headers, and an occasional crib for

moderate top; and extensive cribbing, extra timbers, or steel straps for bad top.

Kester and Chugh (1980) have developed a roof rating system for mines in the Illinois Basin wherein they employ both geologic and rock mechanics criteria. They evaluated a number of factors in the roof strata, coal bed, and floor strata from cores and then assigned weights to the different variables. A rating table was then devised whereby bad top had a value of 0 and excellent top a value of 4 (Table 2.2). From this, a roof control scheme can be implemented.

In a study of one coal bed in Illinois, Damberger, et al. (1980) found four major roof types.

These are:

1. Gray shale roof: gray shale, siltstone, and sandstone crevasse-splay deposits along major channels.

2. Black shale-limestone roof: black marine shales and limestone.

3. Wedge-type transitional roof: wedge-shaped deposits of gray shale overlapped by the black shale-limestone roof.

4. Pod-type transitional roof: small lenses of gray shale overlapped by the black shale-limestone roof.

Problems associated with the gray shale roof type were slaking, carbonaceous bedding planes in rare sandstones, water-saturated sandstone, slickensided shales with associated rider coals, and gravitational slides and slumps. In the black shale-limestone roof, clay dikes and accompanying

TABLE 2.2

Rating table of Kester and Chugh (1980)

Rating Table for Roof Cores - Illinois No. 6 Seam

Evaluation Factor	Bad - 0	Poor - 1	Fair - 2	Good - 3	Excellent - 4
Interval to base of limestone	>15 ft.	8-12 ft.	4-8 ft.	2-4 ft.	0-2 ft.
Number of beds in interval to limestone	numerous laminated	multiple	two	one	one
Relative strength of beds	all weak - no strong beds <3000 psi	alternating strong and weak 3000-5000 psi	moderately strong or strong lower bed with weaker intermediate beds 5000-8000 psi	moderately strong 8000-10000 psi	strong >10000 psi
Fractures or bedding in interval to limestone	highly fractured or severe bedding separation	moderate fractures or bed separation	few fractures moderately strong on bedding	occasional fractures difficult to separate on bedding	no fractures no bedding separation
Roof shale sensitivity to water (percent swell strain perpendicular to bedding)	highly sensitive >4.0	sensitive 1.5-4.0	moderately sensitive 0.5-1.5	slightly sensitive 0.2-0.5	insensitive
Unbroken limestone anchor thickness	no lime within boltable height	0-18"	18-24"	24-36"	>36"
Limestone character	none within boltable height	numerous fractures or weak shale lamination	occasional fractures or shale laminations	no fractures, occasional small shale laminae	no fractures or laminations
Projected bolt length	no anchor	10-14 ft.	6-10 ft.	4-6 ft.	3-4 ft. min.

TABLE 2.2 (continued)

Rating Table for Floor Cores - Illinois No. 6 Seam

Evaluation Factor	Bad - 0	Poor - 1	Fair - 2	Good - 3	Excellent - 4
Floor clay thickness	>5 ft.	3-5 ft.	2-3 ft.	1-2 ft.	0-1 ft.
Floor clay sensitivity to water	highly sensitive	sensitive	moderately sensitive	slightly sensitive	insensitive
Floor clay hardness or strength	very soft >100 psi	soft 100-300 psi	firm 300-700 psi	medium hard 700-1500 psi	hard >1500 psi
Interval base coal to first competent strata	>10 ft.	>6 ft.	4-6 ft.	2-4 ft.	>2 ft.
Composition of first competent strata	none, reworked clays, slickensided, few lime nodules	thin interbedded strata, fractured, >25% lime nodules in claystone or mudstone matrix, slickensided	limestone nodules 25-50% by volume at least 5' thick in claystone matrix, moderate fracturing and matrix, slickensides	shales and limestone, nodules 50-75% by volume, at least 3' thick in claystone matrix, few fractures slickensides	shales, limestone, nodular lime 75% by volume in claystone matrix
Substrata below first competent bed	all weak members	strong beds with weak beds below	beds increase in strength with depth	moderately strong beds below nodular lime for at least 5 feet	strong beds immediately below nodular lime
Moisture content substrata below first competent member	>10%	8-10%	6-8%	5-6%	<5%
Clay mineralogy of weaker strata within 5 ft. below first competent bed	>70% montmorillonite	0-25% montmorillonite 75-100% mixed layer	no montmorillonite <75% mixed layer	no montmorillonite <50% mixed layer	no montmorillonite <40% mixed layer

clay-dike faults present a major problem. Wedge-type transitional roof suffers mostly from rolls of gray shale while the gray shale of the pod-type transition has the highest incidence of failure.

Milici et al. (1982) have developed a geological roof classification. After extensive mapping in the coal fields of southwestern Virginia, they proposed a classification and derived a roof instability index (RII). The RII is the ratio of favorable roof types to unfavorable types depending on their category. Briefly, relatively stable roofs are classified as such, whether sandstone or shale, while relatively poorer ones are classified into categories depending on those characteristics which cause instability (Table 2.3). For example, a Type A roof is a shale or siltstone roof which is characterized by small-to-moderate scale bedding faults whose surfaces are polished and slickensided. This would be considered an undesirable roof. Stable roofs such as SH are also included. This type of roof would likely be a coarsening upward particle size sequence containing few, if any, discontinuities. Of course, gradations between roof types exist. In this example, a relatively stable, slickensided shale roof would be classified as A-SH. Transitional zones are also accounted for. The shale-sandstone interface at a channel boundary would be categorized as CB roof (Figure 2.19).

In Australia, Shepherd and Burston (1977) have proposed

TABLE 2.3

Roof Rating Classification of Milici et al. (1982a)

Roof Type	Description
A	Roof surface uneven, slickensided and polished by faulting. Failure occurs along slickensided and polished surfaces.
B	Roof is composed of rock which tends to break along subhorizontal bedding planes, cross beds, rider seams, shale and clay partings and other stratigraphic zones of weakness, excluding those related to channel sandstones. Includes soft sediment slump features.
C	Roof consists of channel sandstone with irregular base. Channel bottoms, load casts and other protuberances extend downward into shale above coal. Differential compaction may result in numerous slickensided and polished fractures in shales and siltstones between tops of coal beds and channel bottoms.
Cb	Channel boundary condition in immediate roof occurs where sandstone cuts down sharply through shale and siltstone to or near the top of a coal bed.
SS	Stable sandstone roof occurs where undeformed planar bedded sandstone with few zones of stratigraphic weakness lies directly on coal.
Sh	Stable shale roof occurs where undeformed planar bedded shale or siltstone constitutes immediate roof. These may be bases of coarsening upward sequences or relatively homogeneous strata which contain few zones of internal weakness.
Ash	Roof is intermediate between major roof types; it contains some polished and slickensided beds, but not to a large degree.
AB	Slickensided surfaces related to faulting in shale intersect zones of stratigraphic weakness.
AC	Slickensided surfaces related to faulting in shale intersect channel bottoms or sides.

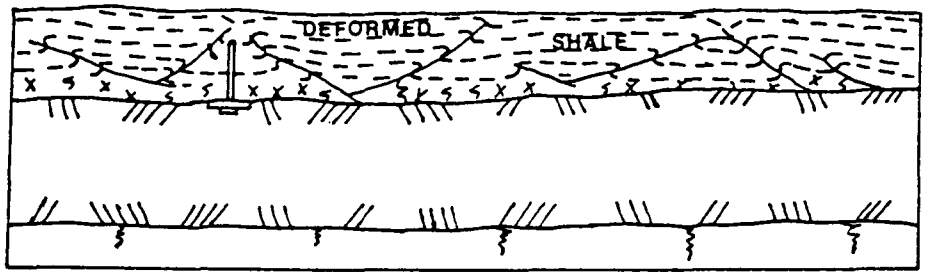

TYPE A ROOF

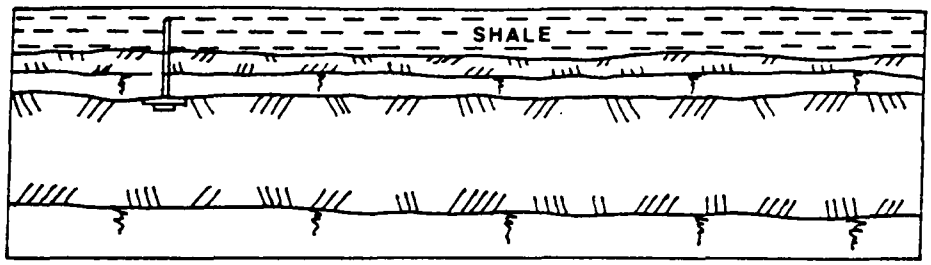

TYPE B ROOF

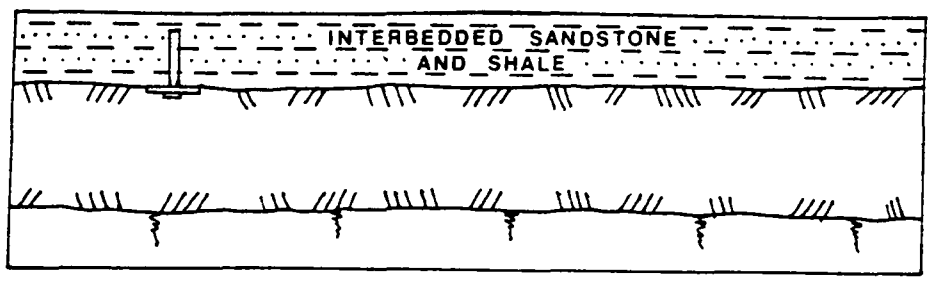

TYPE B ROOF

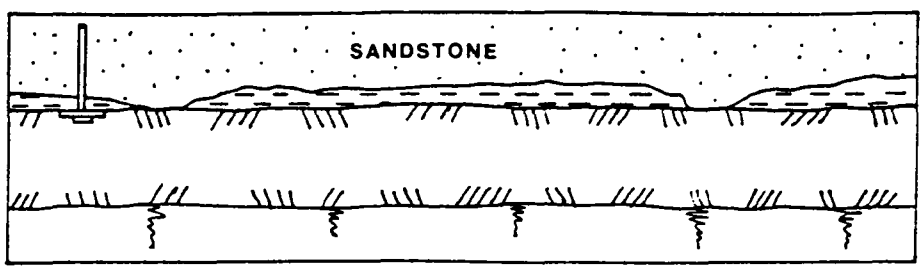

TYPE C ROOF

Figure 2.19: Geological roof classification of Milici et al. (1982).

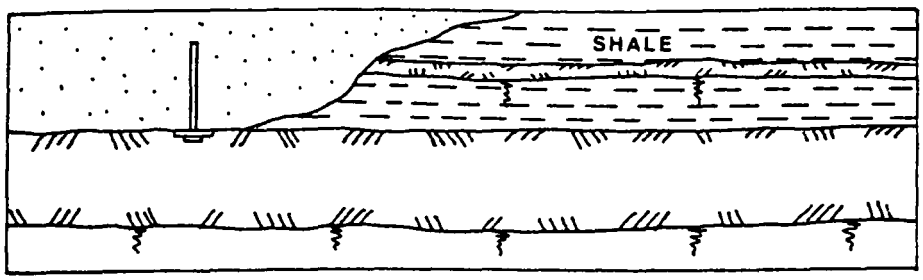

TYPE Cb ROOF

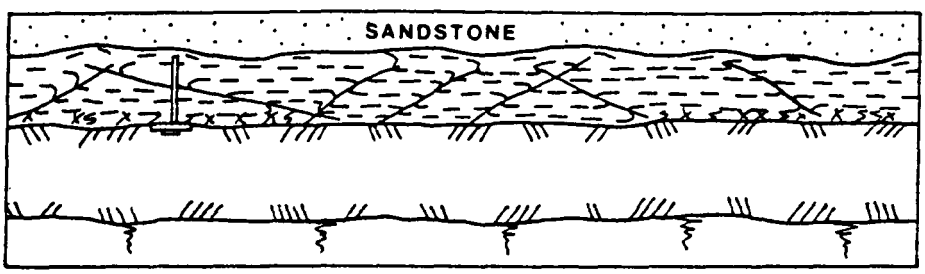

TYPE AC ROOF

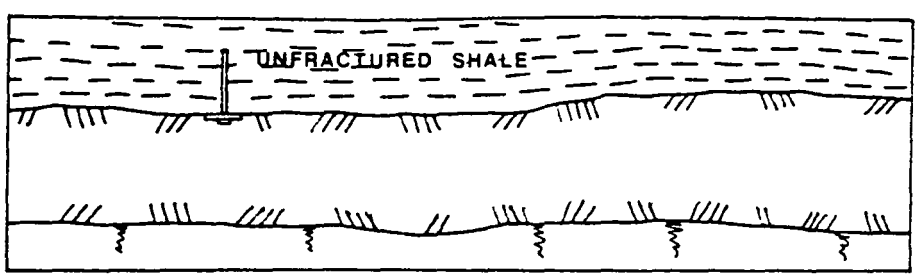

TYPE Sh ROOF

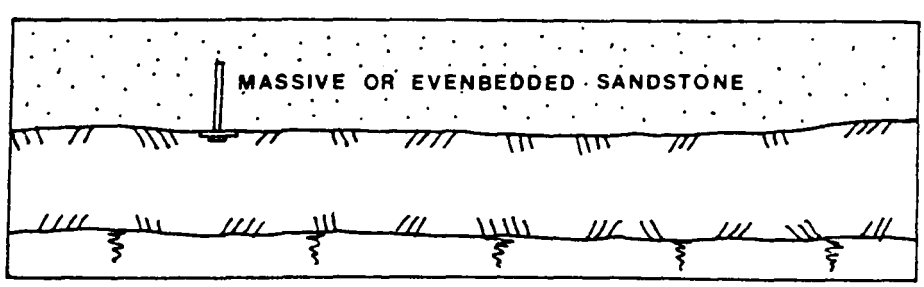

TYPE SS ROOF

Figure 2.19: (continued)

a roof classification based on the shape and height of falls. The classification is as follows:

1. Good (competent) Roof: a roof which shows no signs of deterioration and for which support is minimal.

2. Scaly Roof: slabbing of the roof but condition is still relatively good.

3. Heavy Roof: deterioration is present and timbers are taking weight.

4. Very Heavy Roof: roof is highly fractured and timbers show a great deal of deformation. Failure would occur if timbers were removed.

5. Gutter Falls: falls occurring which are much longer than wide where the width is less than half that of the entry.

6. Falls: blocks greater than six inches in height have fallen from the roof.

Roof falls themselves have also been classified (Milici et al., 1982a; Patrick and Aughenbaugh, 1979; Aggson, 1980; and Caudle, 1973). Milici et al. (1982a) proposed a roof fall classification based on their roof classification. In other words, a Type A roof would experience a Type A fall. Alternatively, a classification has been proposed by Patrick and Augenbaugh (1979) in which only the geometry of the fall is used without any attempt to include geology or any other parameters (Table 2.4). This allows subclassification according to other variables such as location, geology, stress field, etc. Falls are classified as follows:

1. Dome Type: a fall which is approximately circular or oval in plan view and having either a curved contour and/or a flat upper surface.

TABLE 2.4

Roof fall classification of Patrick and Aughenbaugh (1979)

GENERAL DESCRIPTION OF FALL		GEOMETRY OF FALL					
		NO DISCONTINUITY PRESENT AT UPPER BOUNDARY OF FALL			DISCONTINUITY PRESENT AT UPPER BOUNDARY OF FALL		
I. REGULAR GEOMETRY	A. 0.9m (3') < h < w	CURVED CONTOUR CIRCULAR DOME 1		CURVED CONTOUR OVAL DOME 2	FLAT-TOPPED CIRCULAR DOME 3		FLAT-TOPPED OVAL DOME 4
	B. h > w	CURVED CONTOUR OVAL ARCH 5	CURVED CONTOUR LINEAR ARCH 6	CURVED CONTOUR SERPENTINE ARCH 7	FLAT-TOPPED OVAL ARCH 8	FLAT-TOPPED LINEAR ARCH 9	FLAT-TOPPED SERPENTINE ARCH 10
II. IRREGULAR GEOMETRY	A. 0.46m (1.5') < h < 1.2m(4')	MINOR AREAL 11		MINOR LINEAR 12		MINOR SERPENTINE 13	
	B. h < 0.46m (1.5')	AREAL SLOUGHING 14		LINEAR SLOUGHING 15		SERPENTINE SLOUGHING 16	

2. Arch Type: a fall which is basically linear or serpentine in plan view.

3. Minor Type: any fall which is areal, linear, or serpentine which is smaller in extent than the above and has an irregular cross-section.

4. Sloughing or Rashing: smaller than a minor type fall.

The type of fall has been correlated with location, e.g., at intersections, stress conditions, and the presence of rib rashing. The rationale for this system is that it is a quick and efficient means by which the engineer can easily describe and record roof falls. It also allows him to make decisions regarding the best means of support for a given situation.

Finally, another means of describing roof falls has been advanced by Caudle (1973) and Aggson (1980) as mentioned previously. In this approach, the mechanism of roof failure is classified and from this design recommendations can be made. Failure in massive rocks can be by shear or by tensile failure. In shear failure, large horizontal stresses cause cracks to begin at entry corners and propagate upwards into the roof producing an arch fall. The steepness of the failure surface is a function of the relationship of the horizontal and vertical stresses. A lower angle will result if the horizontal stress is much higher than the vertical stress. For high vertical and horizontal stresses of nearly equal magnitudes, a vertical failure

surface will result. This is known as a "cutter roof". Tensile failure occurs when the vertical stress is greater than the horizontal such as in gravity loading. Then, the rock acts as a beam and tensile stresses are concentrated on the lower side. If stress exceeds the tensile strength of the rock, failure occurs. In a layered roof, the mode of failure will be quite different as each member delaminates and loads the bottom-most layer eventually leading to failure. This mechanism also causes floor heave in thinly bedded floor (Aggson, 1979). Other roof failures may be due to much more complex roof, pillar, and floor interactions such as floor heave itself (Caudle, 1973). It should be noted that the type of failure influences the failure geometry as described in Patrick and Aughenbaugh's (1978) classification. For example, shear failure will produce an arch or dome-shaped fall while tensile failure may produce only a minor-type fall.

2.3.3 Engineering Classifications

Rock engineering classifications have been used in tunneling for some years with considerable success (Barton, 1976). One of the most widely used classification systems is the one developed by Barton (1974), the Q-System, which incorporates a number of geotechnical variables into a single rating parameter, Q, from which a particular means of support can be recommended. The parameters it utilizes are

RQD, the number of joint sets (J_n), the roughness of the weakest joints (J_r), the degree of alteration or filling along the weakest joints (J_a), and two parameters which account for rock load and water inflow (SRF and J_w). The rock mass quality, Q, is found by the following formula:

$$Q = (RQD/J_n) + (J_r/J_a) + (J_w/SRF) \qquad \text{Eqn. 2.1}$$

It has not been used in the coal mine applications as it requires a great deal of information not readily available in most premining investigations. In addition it ignores geotechnical factors of great importance to coal mining tunnels.

The Geomechanics Classification of Bieniawski (1980) is one engineering classification which has been applied and modified for use in coal mines. This approach assigns weighted values for six geomechanics parameters (Table 2.5). These are:

- uniaxial compressive strength of the rock material,
- rock quality designation (RQD),
- spacing of discontinuities,
- condition of discontinuities,
- orientation of discontinuities,
- groundwater conditions.

The weighted values for each parameter are summed in order to obtain a rock mass rating (RMR). This rating, in turn,

TABLE 2.5

Geomechanics Classification of Bieniawski (1980)

A. CLASSIFICATION PARAMETERS AND THEIR RATINGS

PARAMETER			RANGES OF VALUES				
1	Strength of intact rock material	Point-load strength index	> 10 MPa	4 - 10 MPa	2 - 4 MPa	1 - 2 MPa	For this low range - uniaxial compressive test is preferred
		Uniaxial compressive strength	> 250 MPa	100 - 250 MPa	50 - 100 MPa	25 - 50 MPa	5-25 MPa | 1-5 MPa | < 1 MPa
	Rating		15	12	7	4	2 | 1 | 0
2	Drill core quality RQD		90% - 100%	75% - 90%	50% - 75%	25% - 50%	< 25%
	Rating		20	17	13	8	3
3	Spacing of discontinuities		> 2 m	0.6 - 2 m	200 - 600 mm	60 - 200 mm	< 60 mm
	Rating		20	15	10	8	5
4	Condition of discontinuities		Very rough surfaces Not continuous No separation Unweathered wall rock	Slightly rough surfaces Separation < 1 mm Slightly weathered walls	Slightly rough surfaces Separation < 1 mm Highly weathered walls	Slickensided surfaces OR Gouge < 5 mm thick OR Separation 1-5 mm Continuous	Soft gouge > 5 mm thick OR Separation > 5 mm Continuous
	Rating		30	25	20	10	0
5	Ground water	Inflow per 10 m tunnel length	None	< 10 litres/min	10-25 litres/min	25 - 125 litres/min	> 125
		Ratio $\frac{\text{joint water pressure}}{\text{major principal stress}}$	OR 0	OR 0.0-0.1	OR 0.1-0.2	OR 0.2-0.5	OR > 0.5
		General conditions	OR Completely dry	OR Damp	OR Wet	OR Dripping	OR Flowing
	Rating		15	10	7	4	0

B. RATING ADJUSTMENT FOR JOINT ORIENTATIONS

Strike and dip orientations of joints		Very favourable	Favourable	Fair	Unfavourable	Very unfavourable
Ratings	Tunnels	0	-2	-5	-10	-12
	Foundations	0	-2	-7	-15	-25
	Slopes	0	-5	-25	-50	-60

C. ROCK MASS CLASSES DETERMINED FROM TOTAL RATINGS

Rating	100 ← 81	80 ← 61	60 ← 41	40 ← 21	< 20
Class No	I	II	III	IV	V
Description	Very good rock	Good rock	Fair rock	Poor rock	Very poor rock

D. MEANING OF ROCK MASS CLASSES

Class No	I	II	III	IV	V
Average stand-up time	10 years for 15 m span	6 months for 8 m span	1 week for 5 m span	10 hours for 2.5 m span	30 minutes for 1 m span
Cohesion of the rock mass	> 400 kPa	300 - 400 kPa	200 - 300 kPa	100 - 200 kPa	< 100 kPa
Friction angle of the rock mass	< 45°	35° - 45°	25° - 35°	15° - 25°	< 15°

Strike perpendicular to tunnel axis				Strike parallel to tunnel axis		Dip $0^{\circ}-20^{\circ}$ irrespective of strike
Drive with dip		Drive against dip				
Dip $45^{\circ}-90^{\circ}$	Dip $20^{\circ}-45^{\circ}$	Dip $45^{\circ}-90^{\circ}$	Dip $20^{\circ}-45^{\circ}$	Dip $45^{\circ}-90^{\circ}$	Dip $20^{\circ}-45^{\circ}$	
Very favourable	Favourable	Fair	Unfavourable	Very unfavourable	Fair	Unfavourable

provides a measure of the roof rock quality and also its stand-up time for a given span. The author found that, for a number of coal mines in Pennsylvania and West Virginia, top coal and claystone had a poor rock mass rating, shale had a fair rating, while limestone was of very good quality.

2.3.4 Mapping and Prediction

The ultimate goal of any roof stability investigation is not necessarily to determine how an event took place but, rather, prevent a similar occurrence in the future. A careful underground mapping program coupled with surface and subsurface exploration can be very useful. In this regard, Hopkins (1980) has stated,

> Regional changes have to some extent been mapped; local variations normally cannot be mapped from subsurface data but their presence can usually be recognized by careful observations of cores and logs. . . . Careful evaluation of these factors during mine planning can often minimize future problems.

Mapping programs can be very successful. Stritzel (1980) has used underground mapping for dealing with a series of ground control problems. He compiled a checklist of needed information to aid in roof fall analysis and which is shown in Table 2.6. Geologic mapping enabled Nelson and Nance (1980) to make predictions as to faults, fracture zones, and channels ahead of the face which, they felt, would have been impossible if only exploratory drilling was utilized.

Mapping and map overlays were used by Ealy, Mazurak,

TABLE 2.6

Checklist for underground mapping (Stritzel, 1980)

1. The shape of the fall, such as low angle or high angle arch, etc.

2. Location of fall (at an intersection, crosscut, face, etc.).

3. The dimensions of the fall, entries, crosscuts, and intersections.

4. Location of roof failure (e.g. above anchorage zone, below anchorage zone, etc.).

5. Type of roof support used (resin bolts, conventional bolts, trusses, etc.).

6. Type of supplementary roof support used and effectiveness (e.g. timbers, crossbars, rails, cribs, etc.).

7. Evaluation for defective material (e.g. bolt, expansion shell, bolt head, etc.).

8. Determination of mining practices and whether approved roof control plan was followed.

9. Length of time roof was standing before failure was first evidenced.

10. Types of warning observed prior to failure (e.g. sounds of fracturing in the roof, dribbling or flaking of the roof in the center of the entry, along the rib, etc.), and length of time the warning lasted.

11. Unusual geologic features such as slips, rolls, joints, faults, soft material in roof, thin-bedded strata, etc.

12. Was fall localized or was it a part of a series of falls consisting of a certain pattern within a particular area of the mine.

13. Evidence of any high stresses in the area and their location.

14. Evidence of localized heaving of bottoms in the area.

15. Load distribution across the entire area including excessive pressures and their location.

and Langrand (1979) and Ealy and Mazurak (1980) to successfully forecast potentially hazardous areas. These areas were rated according to instability based on actual experience. The result was an 80% decrease in roof fall frequencies over two years as mine plans were modified to accommodate the hazardous zones.

One of the most effective means of roof prediction is a combination of geologic mapping and hazard maps using an overlay technique as shown in Table 2.7 (Ellenberger, 1981). In this process, geologic, and geomechanical factors, are plotted on acetate sheets and overlain on the base mine map. Areas where problems may occur can be seen where a number of undesirable characteristics coincide. Overbey et al. (1973) had earlier used this technique and found that a very high degree of potential risk occurred where several combinations of undesirable geologic factors overlapped. For their mapping program, the authors made maps of structure and lithofacies, drainage, overburden thickness, and fracture traces. A method similar to the multiple overlay technique is known as hazard analysis. In this method, overlays are made but a numerical rating system is employed, sometimes with a cost multiplier, to evaluate a site (Seegmiller, 1982). This approach is amenable to computer applications. McDonough (1976) has used geologic mapping in the metal mining industry with notable results.

In the field of tunneling a somewhat different approach

TABLE 2.7

Overlay hazard mapping considerations (Ellenberger, 1981)

Class I: Geographic, Pre-exploration
- A. Valley configuration
  - 1. shape
  - 2. size
- B. Topographic gradients
- C. Regional location
- D. Surrounding mine properties
- E. Photolinears

Class IIa: Geologic; Exploration Related
- A. Overburden
  - 1. amount
  - 2. variations
  - 3. composition (general)
  - 4. roof stratigraphy
- B. Rock properties from core
  - 1. strength
  - 2. RQD
  - 3. weatherability
- C. Hydrology
  - 1. groundwater
  - 2. surface ponds or lakes
  - 3. permeability
- D. Major structures (deformational)
  - 1. faults
  - 2. folds
- E. Major structures (sedimentary)
  - 1. washouts
  - 2. want
- F. Coal quality

Class IIb: Geologic: Underground Mine Data
- A. Minor structures
  - 1. joints
  - 2. faults
  - 3. slumps
  - 4. clay veins
  - 5. roof rolls
  - 6. concretions
  - 7. kettlebottoms
  - 8. slips or slickensides
- B. Stratigraphy
  - 1. roof
  - 2. coal
  - 3. floor
  - 4. lenticular units
  - 5. critical thickness units

TABLE 2.7 (continued)

- C. Rock properties
  - 1. weatherability
  - 2. strength
  - 3. lateral changes
- D. Evidence of paleostresses
  - 1. oriented falls
  - 2. oriented general ground control problems

Class III: Mining Related Considerations

- A. Pillar configuration
- B. Entry configuration
  - 1. entry width and height
  - 2. number of entries per set (total width)
  - 3. overburden
- C. Mining systems
  - 1. continuous
  - 2. conventional
  - 3. panel
- D. Roof support
- E. Experience of personnel
  - 1. in entire basin under consideration
  - 2. in seam under consideration
  - 3. in mine under consideration
- F. Over/Under/Adjacent Mining

has been taken. Probabilistic methods are now being applied to geologic hazards (Ashley et al., 1981). This type of analysis uses decision theory to design support methods given a probability of a particular geologic condition being encountered. Uncertainty is reduced since the geologic information is continually updated as tunneling progresses. Although used in some tunneling projects, this probabilistic approach has not been used in coal mine design to date.

Besides the standard Brunton compass used in geologic mapping, there are several other devices which warrant mention. For examining the condition of intact roof strata, the borescope (Tennant, 1982) and the TV borehole camera have been used to gather data on roof fractures that would otherwise have been impossible to obtain. The vacuum tester developed by V. deKorompay (1980) can also be used to detect fractures in the intact roof and to determine their continuity as well.

2.4 Depositional Models

Though not often mentioned as a means of predicting potential roof problems, depositional models can be of significant interest. By studying the depositional environment of coal beds, geologists and engineers can gain the knowledge necessary, not only to estimate reserves but, also, to predict such potential trouble spots as channel

boundaries and crevasse splay deposits as well as good sandstone or shale top. Paleoenvironmental modeling can be accomplished on a regional as well as local scale (Mullenex and Miller, 1981). Underground mapping techniques can often be combined with such preliminary models in order to achieve fairly accurate prediction on a local scale.

Ferm (1974) and Horne et al. (1978) have reported a detailed work in the use of depositional models. Ferm (1974) applied depositional modeling to accurately predict lateral facies changes in different lithologic units. Horne et al. (1978) examined the depositional environments of Appalachian coal seams and found that, not only was the sulfur content of the coal predictable, but, also, the type of roof problems that might occur. They attempted to relate specific roof problems to particular paleoenvironments (Figure 2.20). For example, graywacke sandstone roof is common where migrating channels have existed. This is usually in an upper delta plain-fluvial and transitional lower delta-plain environment. Lag deposits of shale and coal pebbles, however, can present a problem as they usually formed near the bottom of the channel and can weaken the roof. Beach barrier deposits frequently contain clear, well-cemented orthoquartzic sandstones which provide excellent top but, due to their brittle nature, are often jointed and can result in large falls. Where sandstones are flat-bedded or interbedded with shales, roof traits depend on bed thickness. Thin beds, as

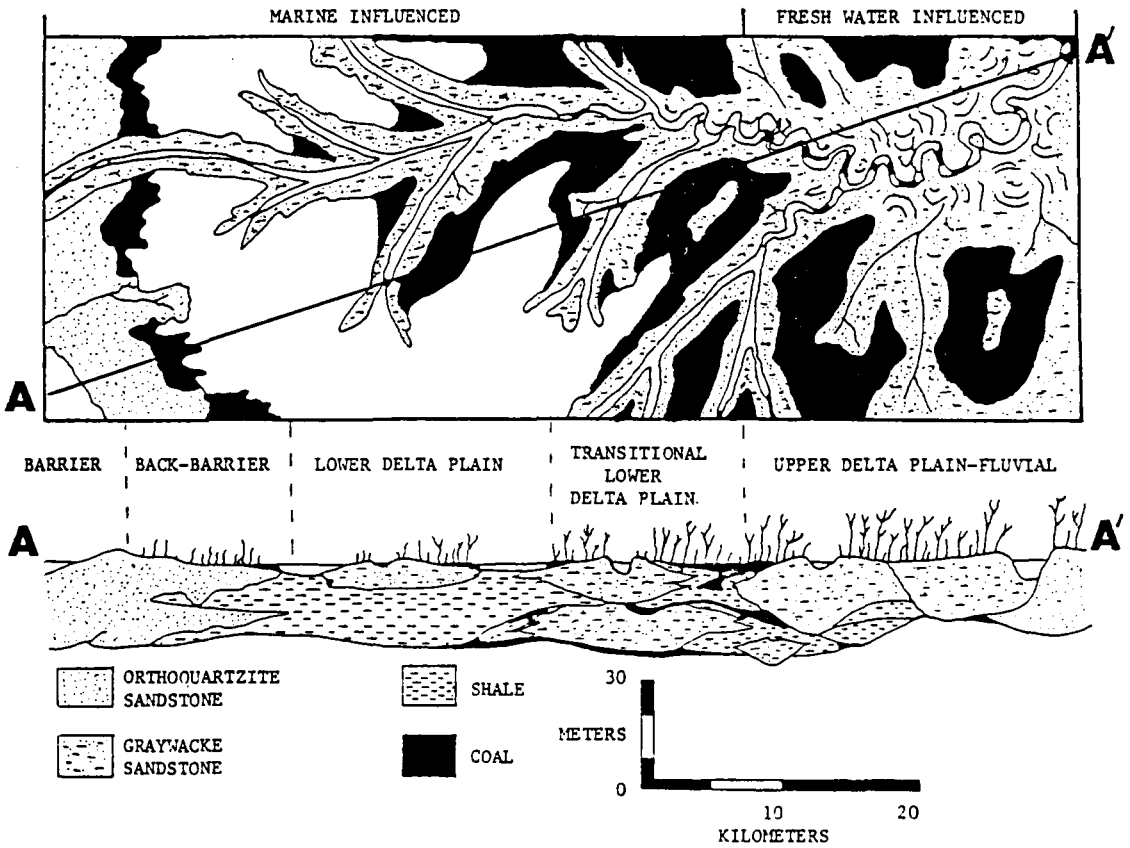

Figure 2.20: Depositional environments of coal (Horne et al., 1978).

well as thick beds accompanied by slickensided fractures are hazardous. Beds 0.6 to 3.0 meters thick are considered best by the authors for the bridging effect the thick rock beam provides. These beds are characteristic of the flanks of any areas prone to periodic flooding such as the sides of distributary mouth bars and splay deposits and, thus, are found in either lower delta-plain or transitional lower delta-plain areas. Slickensided slump deposits can also be found in these locales.

Coarsening upward sequences, that is, lithologies grading from shale upwards through sandstones, provide excellent support when bolted. These deposits are characteristic of bay fills and are found in the transitional lower delta-plain.

Carbonaceous black shales are also typical of the transitional lower delta-plain or the lower delta-plain. They can be bay fill or lagoonal deposits which are indicative of low-energy reworking of the surface of the coal swamps as water begins to cover them. Roof problems are possible as the rock tends to be brittle and jointed.

The burrowing of shales, siltstones, and sandy shales can appreciably lower the strength of the rock. Depositional environments where a large degree of animal activity could occur are those open to influxes of marine or brackish water. These would be back-barrier, lower delta-plain, and

transitional lower delta plain.

Seat earths are silty clays which served as the soil for growing plants. As such, they were subject to a great deal of disturbance by root activity. Slickensided surfaces are very common in these rocks and the combination of root penetrations, fine grain sizes, and slickensides make for extremely hazardous roof conditions. The areas most likely to contain seat earth are the upper delta plain-fluvial and the transitional lower delta-plain.

Kettlebottoms, as mentioned previously, are the fossilized, upright stumps of trees. These can be dangerous and are found in most coal-forming environments. However, because rapid sedimentation during flooding and the large areas available for plant growth, some upper delta plain-fluvial and transitional lower delta plain environments contain a great deal of kettlebottoms, usually in interdistributary regions.

Differential compaction with consequent slickensides at the sandstone-shale interface can easily lead to a roof failure. Channel boundaries in the lower delta plain or the back barrier tidal channels can be conducive to this type of problem.

Slumps occur on the cutbank sides of meandering stream channels. The resulting blocks are often large and heavily slickensided, presenting roof control problems. Tidal channels in the back barrier environment or channels of the

upper delta plain-fluvial and the transitional lower delta plain areas are the most likely to contain such structures.

Finally, rider seams are a major source of large-scale roof problems. Rider coals developed when natural stream levees were breached and sediment covered sections of the adjoining swamps. When the flood waters abated, swamps re-expanded and supplied the material for more peat. Rider seams can be found in any of the delta settings.

2.5 Lineaments

The use of remote sensing, that is, the depiction of linear features observed from high altitude and satellite imagery onto mine maps, has become a controversial topic in hazard prediction. It has been suggested (Overlick, 1978; Rinkenberger, 1978; Dimick and Barnum, 1978; and Jansky and McCabe, 1979) that poor roof conditions correlate with the density of linears. Other writers (Gregory, 1981 and Milici et al., 1982) have found such a relationship to be not quite as simple as proponents would suggest.

McCabe (1981) states that "linears are real and show a high potential to disrupt mine workings" and notes that of 300 mines analyzed by the Roof Control Branch of the Mine Safety and Health Administration (MSHA), over 95 percent were detrimentally affected by linears. McCabe also feels that not only are syn- and post-Appalachian orogeny linears

important in roof control, but that ancient linears, i.e., discontinuities, controlled drainage patterns during the time of coal deposition. This discontinuities have since propagated up to the surface and are now visible from Landsat. Thus, these linears can be used to predict sandstone channels formed by the rivers that followed these ancient fractures. It should be noted that one of the many assumptions McCabe makes is that most linears are vertical features.

By using lineations in a Utah coal mine, Dimick and Barnum (1978) state that they have a "relatively high degree of confidence that lineations do indicate the presence of some type of fracturing." They further suggest that the number of lineation intersections which occur determines, to a large degree, the severity of a problem. For example, one linear indicates a fault or fracture which may only cause a minimal amount of trouble. The intersection of two linear features usually resulted in fractures oriented in the same direction with minor problems in about half the cases. A three linear intersection indicates a widespread problem and the need for additional roof support. The authors note that problem areas may not occur directly under the linears but can vary as much as 37 meters away. They feel, however, that a determination of the fracture dip would enable the fault to be placed more precisely.

In the eastern United States, Rinkenberger (1978) has

described a correlation of mine problems with linears in eastern Kentucky. Oberlick (1978) has used remote sensing in mine development in southwestern West Virginia. Although many linears could be found on the surface, no underground work had yet been carried out to verify their existence at depth. Other work in West Virginia (Hock and Pascoe, 1982) has shown that linear zones contain closer joint spacing in the roof rock and coal which cannot withstand high stresses. On the other hand, the authors state that the severity and extent of poor conditions related to lineaments still cannot be predicted without further research.

Studies have been conducted in southwestern Virginia regarding linear analysis. Gathright (1981) studied the use of lineaments and fracture patterns on LANDSAT imagery as a means of predicting oil production in Lee County. He concluded that the fracture patterns observed correlate well with those that would be expected from known stress-strain history of the region and that oil production is greater from wells within 30 meters of lineaments. This work, then, suggests that linears are representations of existing geologic fractures.

In Buchanan County, Virginia, Elder et al. (1974) used Side Looking Airborne Radar (SLAR) lineaments to find a number of previously undiscovered geologic features. They also found that poor roof conditions in mines in the Poca-

hontas No. 3 coal bed correlated with SLAR lineaments which they interpreted as faults and fracture zones. The worst roof conditions coincided with the strongest lineaments or where lineaments intersected.

Other studies have not been so positive about the value of lineament analysis. Gregory (1981) attempted to statistically relate lineaments as well as joints and roof fractures to the roof quality of mines in East Gulf, West Virginia. The author was unable to correlate any of the variables, especially lineaments, with roof quality. An analysis of lineament trends in eastern Kentucky and the Dunkard Basin (Hylbert, 1980) revealed that lineaments correlated with roof falls only 50-65 percent of the time. The author did find a close correlation of "snap-top" zones in West Virginia with lineament directions. Finally, in the southwestern Virginia coal fields, Milici et al. (1982) attempted to correlate LANDSAT imagery with roof falls. Although there did appear to be a general relationship with their Types A and AC Roof, they stated (p. 55):

> It can be concluded from this study that LANDSAT and air-photo lineaments cannot be used to predict specific occurrences of roof falls. High concentrations of lineaments, however, appear to be related to general areas of roof instability.

2.6 THEORETICAL ASPECTS

2.6.1 General Considerations

Although this research is primarily concerned with the

geomechanical aspects of coal mine roof failures, a section on the theoretical aspects of roof behavior is also included in the interest of completeness. Most mine layout and support systems today are designed using these theories of strata movement.

A brief discussion of roof bolting and support has also been written in order to place the topic of roof failures in the proper perspective, that is, roof failures and support techniques are intimately related and cannot be separated in any literature review.

2.6.2 Ground Control Theories

There are several theories regarding the stress distribution and the corresponding behavior of the roof rock above an excavated opening. Some of these theories also account for surface subsidence which will not be included in this discussion. The theories themselves are: pressure arch, dome, beam, and voussoir arch theory.

According to Hackell (1962), the first qualitative pressure arch theory was advanced in 1911. This was the result of thinking in the latter part of the 19th century based on the observation that unsupported underground excavations in soil or rock would often remain stable if the roofs had a vaulted or peaked shape. It is interesting to note that many coal mine roof falls also have this shape once they have reached equilibrium.

The mechanism of the pressure arch is as follows (Karabin, Cybulski, and Kramer, 1982). As mining beneath the coal proceeds, the overlying strata above the tunnel sag and delaminate from the layers above. This leads to a distressed area from which the stress is placed on the ribs to either side. A "primary" arch is thus developed as is shown in Figure 2.21. If three entries are developed, as shown in Figure 2.22, then primary arches form around each entry. With the passage of time, the stress levels between the pillars will cause deformation and the stress will move outside to form concentrated stress abutments (Figure 2.23).

Karabin et al. (1982) have introduced the term "transient mining-induced abutment stresses" to describe high-stress zones that occur as a result of the mining sequence. These pressure arches will shift as mining progresses. They have used this concept to account for roof instability as shown in Figure 2.24. Entries which are turned off mains can penetrate the abutment zone of the pressure arch and experience roof control problems.

Pothini et al. (1976) have used the concept of the pressure arch to increase extraction ratio by using small, "soft" pillars in the panel and large stiff abutments on the edges for carrying most of the load (Figure 2.25).

Adler and Sun (1976) state that the width of the arch can be determined from the empirical formula:

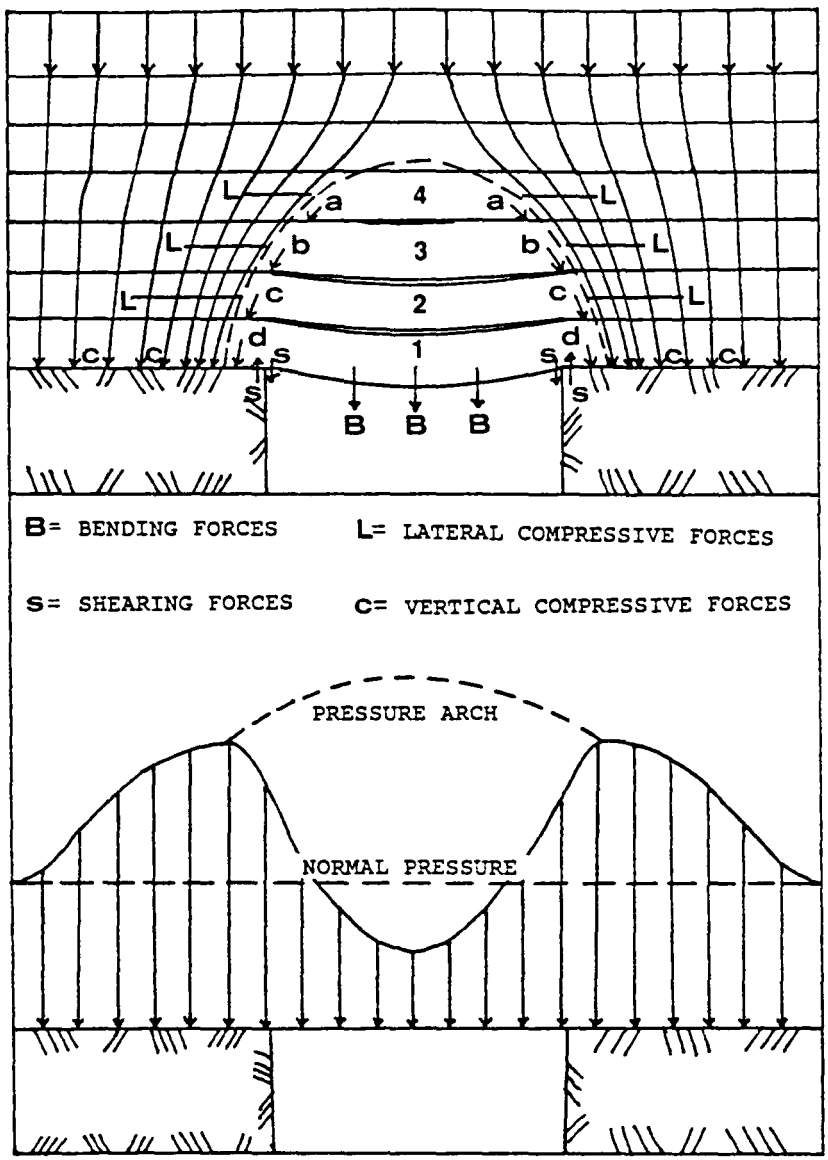

Figure 2.21: Pressure arch above an entry (Adler and Sun, 1976).

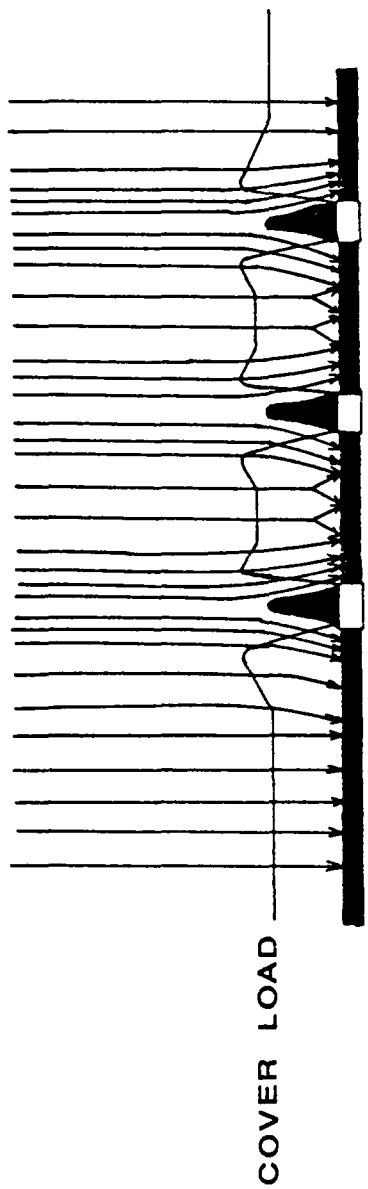

Figure 2.22: Pressure arches above several entries.

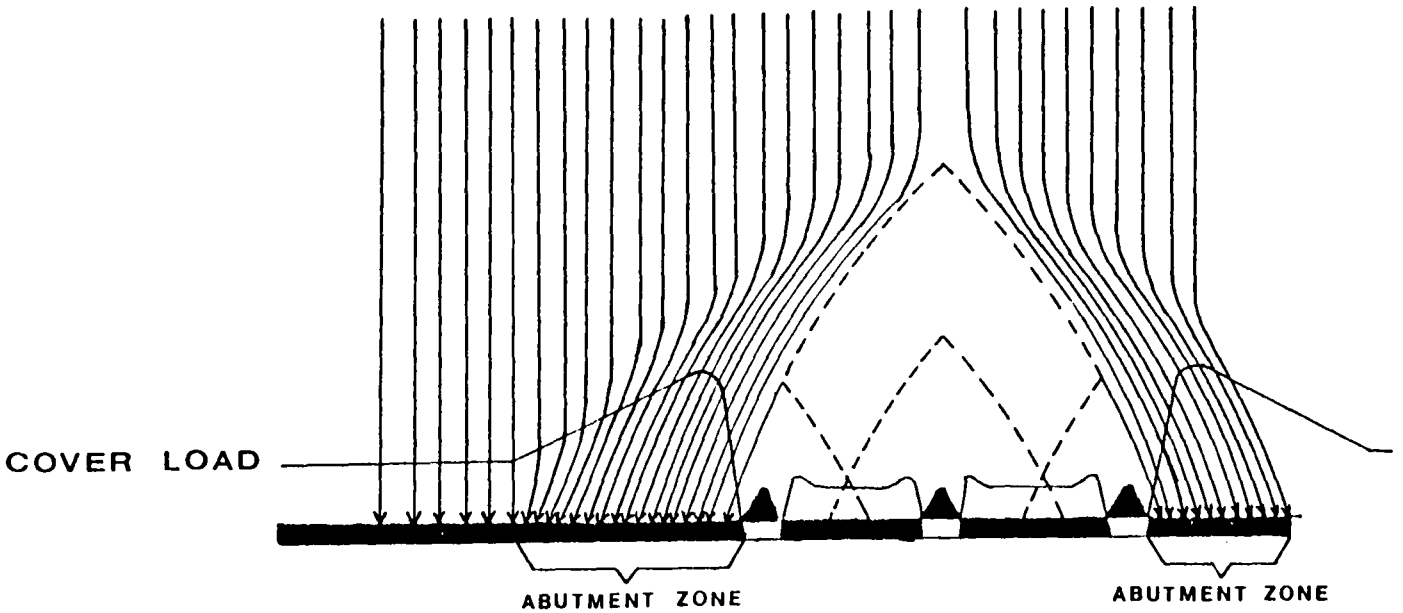

Figure 2.23: Secondary pressure arch above three entries (after Karabin et al., 1982).

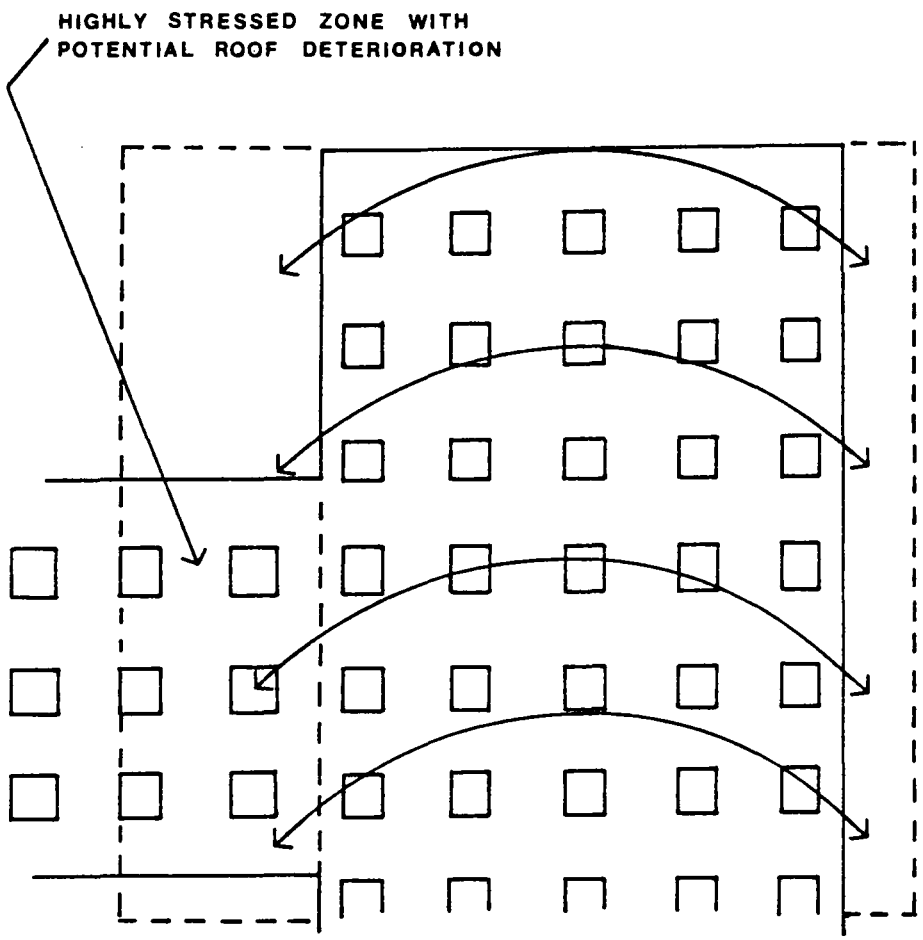

Figure 2.24: Transient pressure arch (after Karabin et al., 1982).

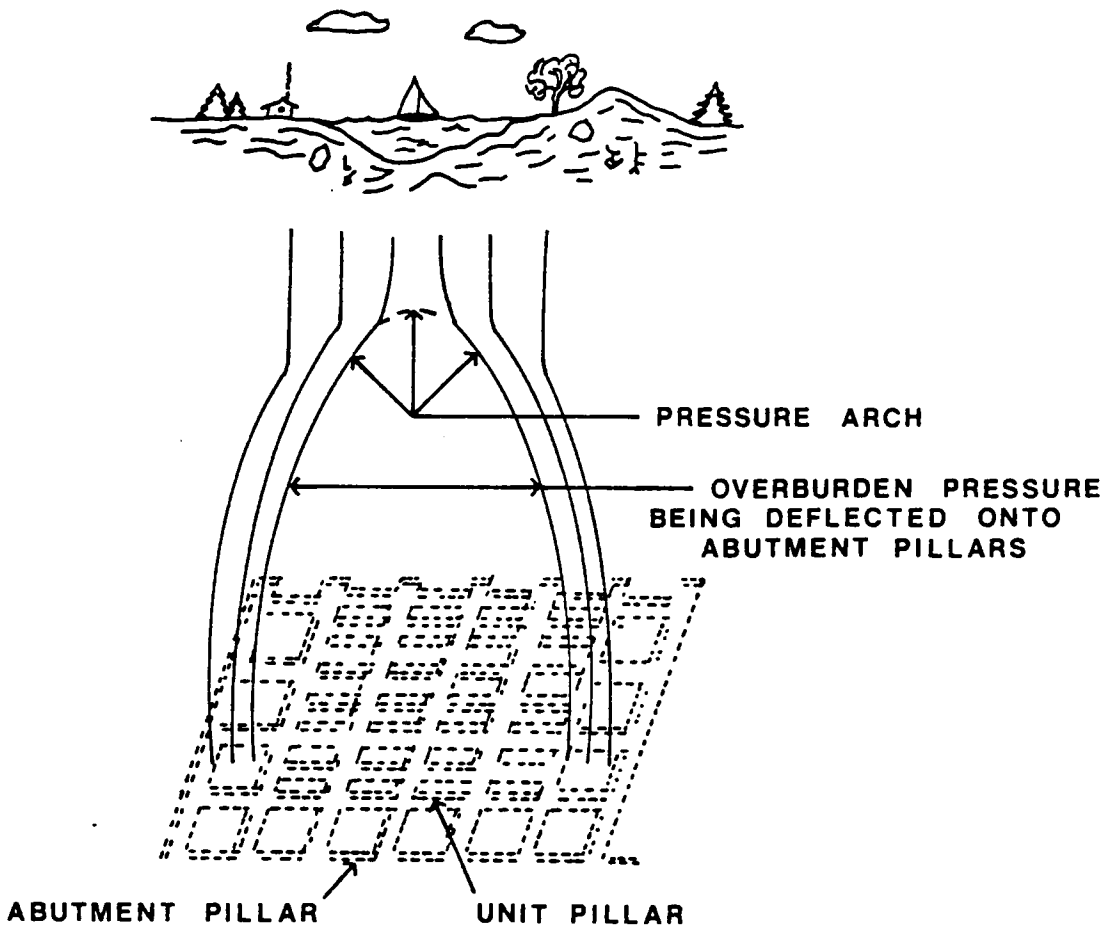

Figure 2.25: "Soft" pillars and stiff abutments (Pothini et al., 1976).

$$W = 0.15 \times D + 60 \qquad \text{Eqn. 2.2}$$

Where: W = width of maximum pressure arch in feet

D = depth of arch below surface surface in feet

The authors further state that if the width of the excavation exceeds the width of the pressure arch, intense roof fracturing will occur.

Dome theory can be viewed as a three-dimensional extension of arch theory. Dinsdale (1935) describes the problem as one of a pressure ring around the mine opening (Figure 2.26). The rock within the ring is separated from that without due to horizontal shearing and vertical tension, and thus rests entirely on the roof supports. Pressures on the immediate ribs and the supports are small when compared with those within the pillar, and the increase in pressure on the supports is proportion to the increase in depth. From Figure 2.27, assuming that the value of L is known, the location of R and H is at the center of the abutment, and the values of P and H are known, the height of the dome can be calculated as follows:

$$\sum_{Y} F = 0: \quad R = P(2L + b)/2$$

$$\sum_{B} M = 0: \quad \text{(of only 1/2 diagram)}$$

$$M_B = P[(2L + b)/2] \times [(2L + b)/4] + H \times h - R[(L + b)/2]$$

Therefore, $$h = (P/8H) \times (2Lb + b^2) \qquad \text{Eqn. 2.3}$$

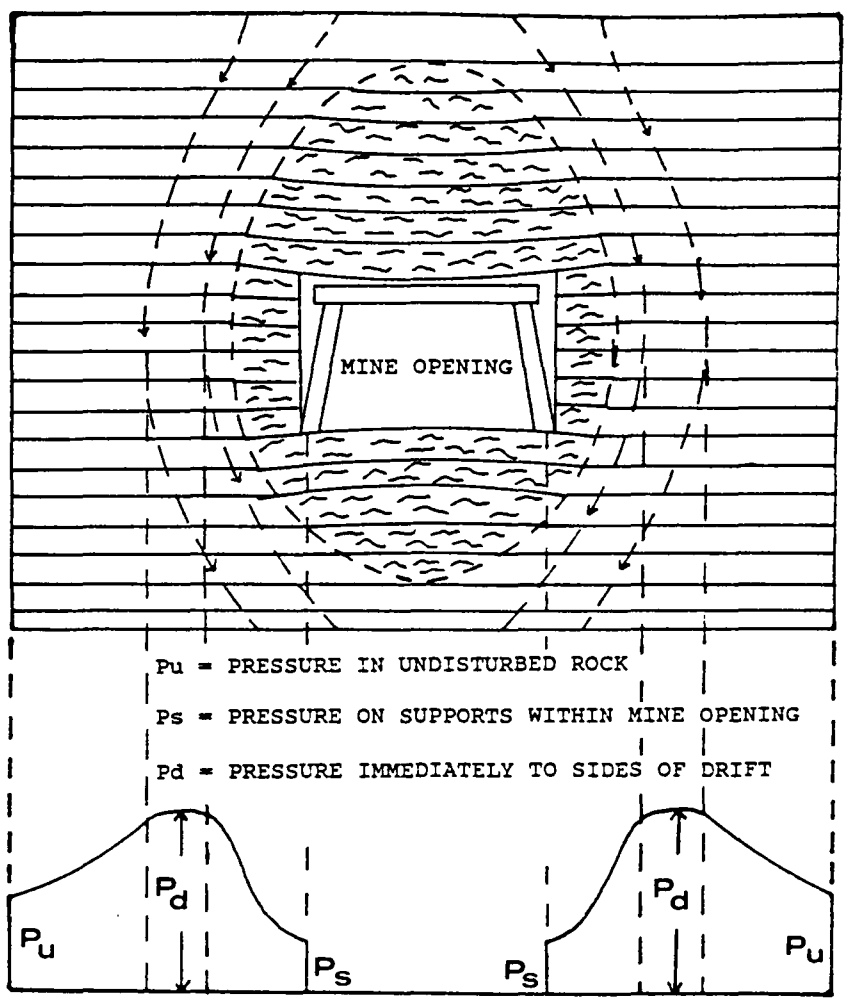

Figure 2.26: Pressure dome (Dinsdale, 1935).

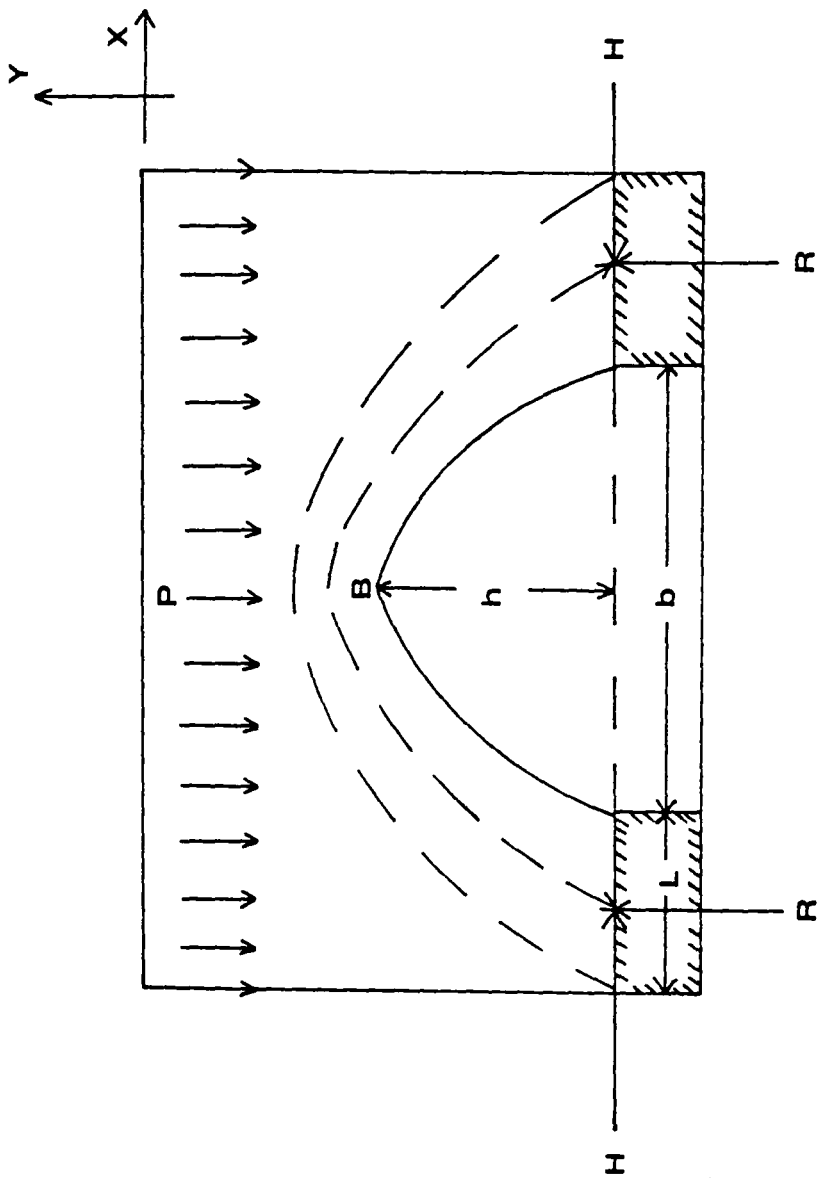

Figure 2.27: Forces acting on a pressure dome (Dinsdale, 1935).

Where: P = pressure on dome exerted by the overlying rock (lbs/ft)

R = vertical force. (lbs)

H = horizontal force. (lbs)

h = height of dome. (ft)

b = span of opening. (ft)

L = width of abutments. (ft)

From this analysis, it is clear that the height, h, of the dome is directly proportional to the vertical pressure. Schoemaker (1949) believes that the relationship between P and H is to difficult to estimate and that the above analysis is probably too simplistic.

Denkhaus (1964) has suggested that the stress distribution for an elastic dome be calculated based on the equilibrium of forces at the dome boundary. Deformations are not accounted for but only the failure load which occurs when loads reach a critical value (Figure 2.28).

The author makes the distinction between sufficiently cohesive and insufficently cohesive strata. Sufficiently cohesive rock will not separate from the dome boundary and, as a result, carries the weight of the core. Failure, if it occurs, is sudden and catastrophic. If portions of the core separate from the dome boundary as the span increases and the face is advanced, the rock is said to be insufficiently cohesive. The core thus rests gradually on the supports and is the more desirable condition. Denkhaus has arrived at the

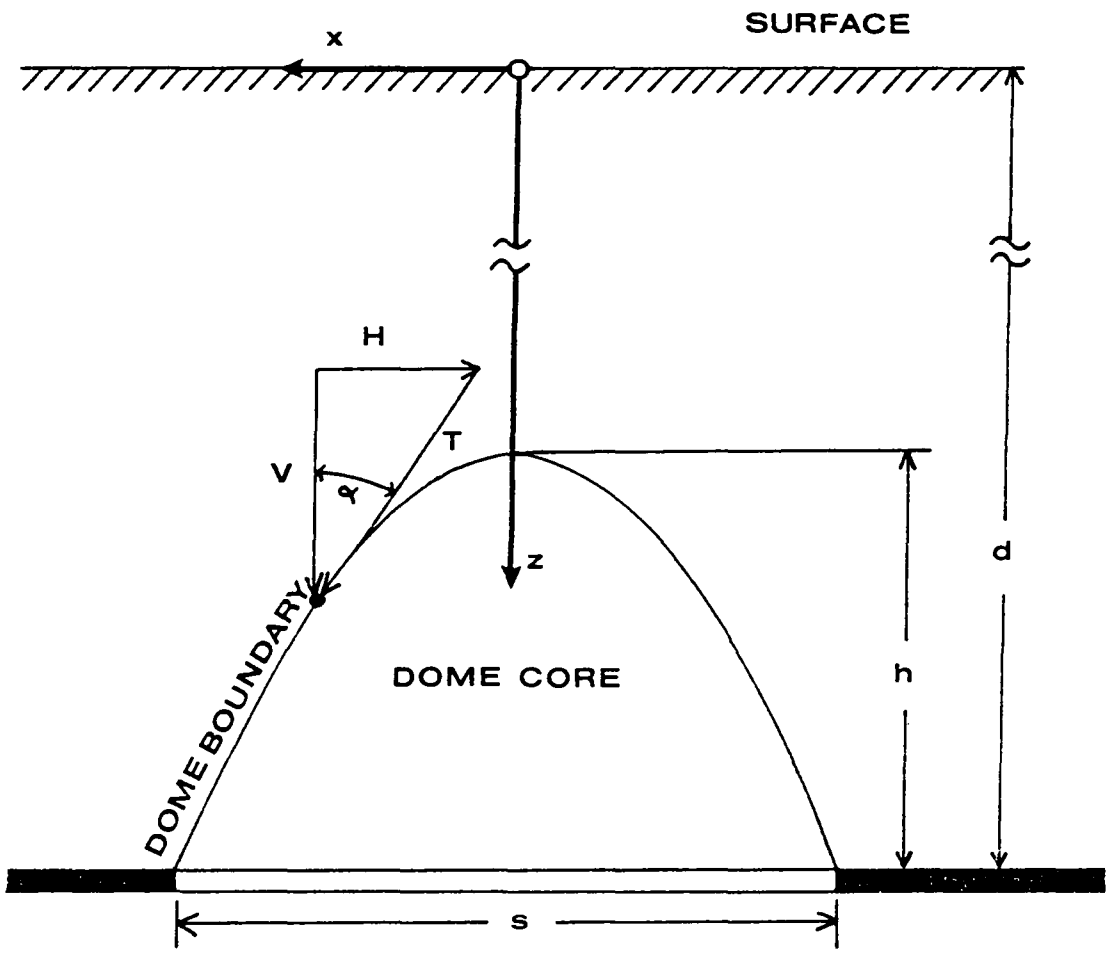

Figure 2.28: Forces at a dome boundary (Denkhaus, 1964).

shape of these domes, shown in Figure 2.29, mathematically.

Because coal mine roofs are composed of bedded rock and not the homogeneous and isotropic materials assumed in arch and dome theory, the application of the theory of beams to roof rock behavior is not inappropriate. Beam theory is well-known and contained in any engineering handbook, and, therefore, will not be included here. One problem with using elementary beam theory is that the abutments are assumed to be rigid. It has been found by Lehr (1935) that if the abutments are elastic, the point of maximum stress and, consequently, potential failure shifts inward towards the midspan. As a result, the point of inflection of the sagging beam also shifts toward the midspan. Plate theory can also be used in this approach but becomes cumbersome when applied to mine roofs.

Failure, according to the application of beam theory, is in the following manner. The lowermost layer of the immediate roof begins to sag almost immediately after mining thereby breaking the weak bond with the layer above. Because rock is weaker in tension then compression, failure will occur in midspan as a tensile failure. Shear failure is also a possibility as shown in Figure 2.30. The second beam, i. e. the beam above the initial one will then deflect and fail. Due to bending of the beam below, the second beam will be smaller and the process will continue until the thickness

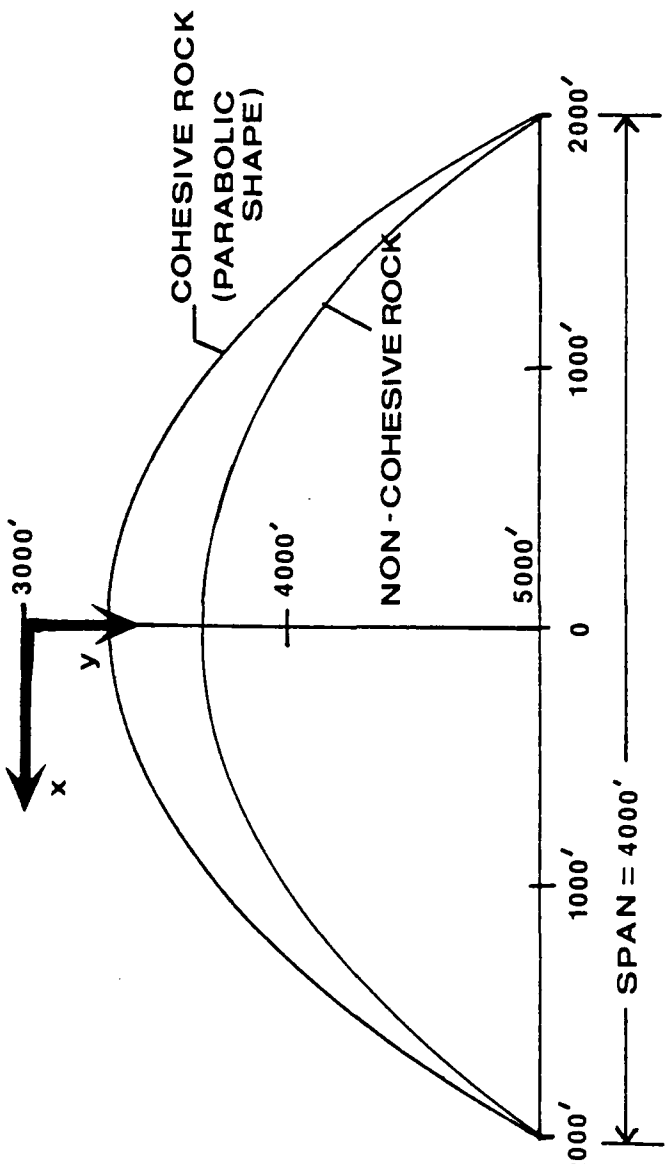

Figure 2.29: Pressure dome shapes (Denkhaus, 1964).

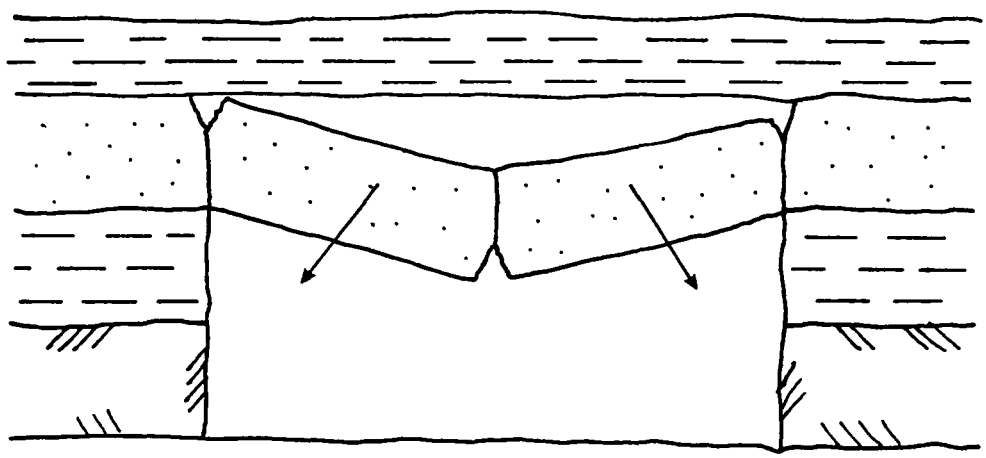

a

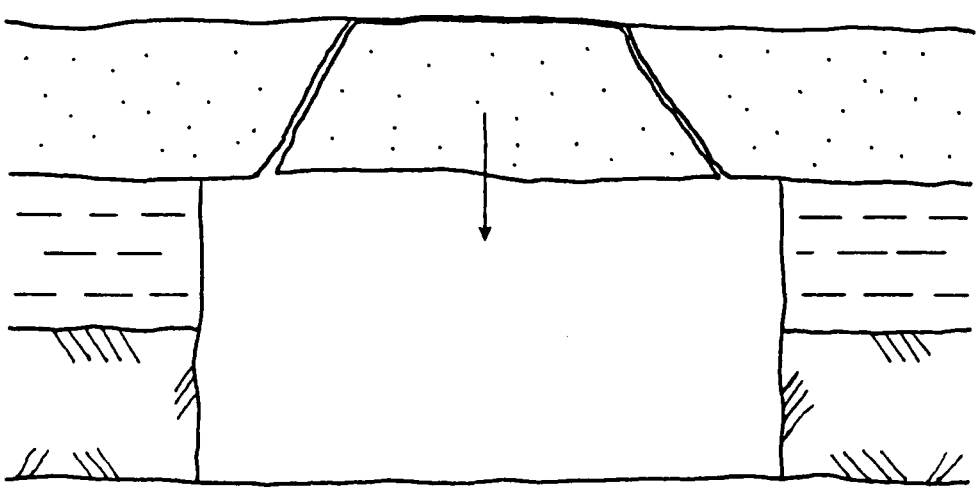

b

Figure 2.30: Types of beam failure: (a) snap through (tensile) (b) shear (after Beer and Meek, 1982).

and elastic modulus of the beams becomes too great for failure to occur. The failure surface will take the form shown in Figure 2.31. It is possible that the beams will deflect rather than fail. This results in a gap between the rock beams known as the Weber cavity (Denkhaus, 1964). Besides taking into account the effect of overlying beds any inclination in the immediate roof strata must be included (Adler and Sun, 1976).

From beam theory, the calculation of mine roof span can be made. Kidybinski (1982) has used this approach and calculated the critical span for different mining systems and roof support types.

The voussoir arch is that used by ancient builders to construct arches of wedge-shaped blocks with or without mortared joints (Figure 2.32). Because highly fractured roof rock often remained stable, yet unsupported, for long periods of time, the concept of the voussoir arch was employed to account for such behavior. Three conditions must be fulfilled for a voussoir arch to remain stable (Morley, 1948):

1. Rotation or tension must not occur. Therefore the eccentricity of thrust must fall with the middle third of the joint--the "middle third rule."

2. The stability of the arch is dependent on the angle that the resultant of the normal and transverse forces at any joint make with the normal to that joint. For stability, this angle must be less than the angle of friction for the material.

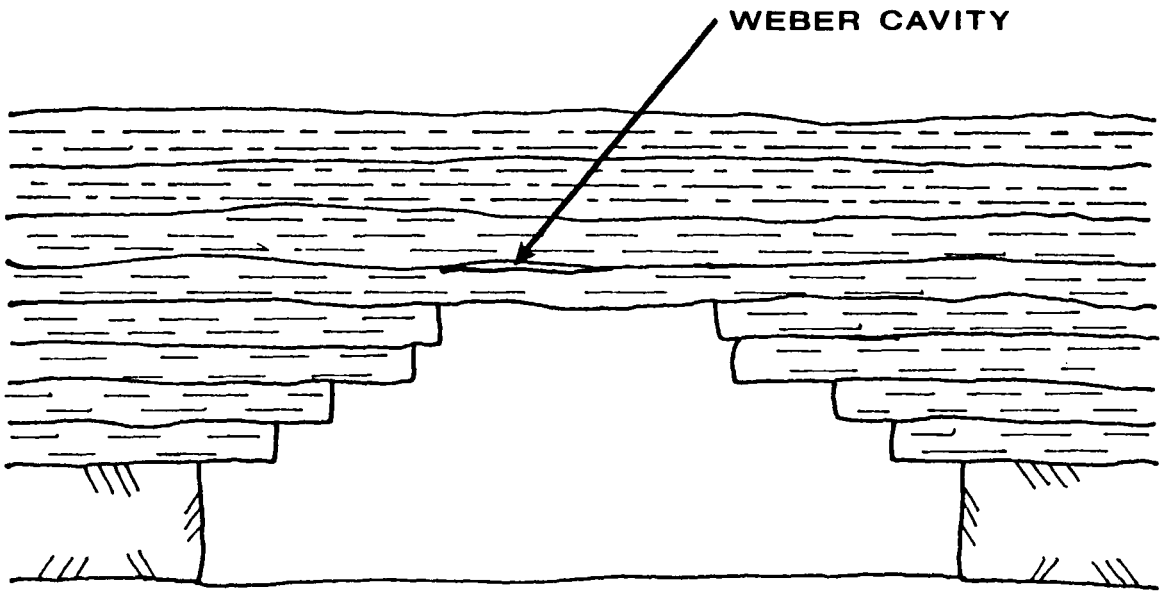

Figure 2.31: Beam fracture arch with Weber cavity (after Denkhaus, 1964).

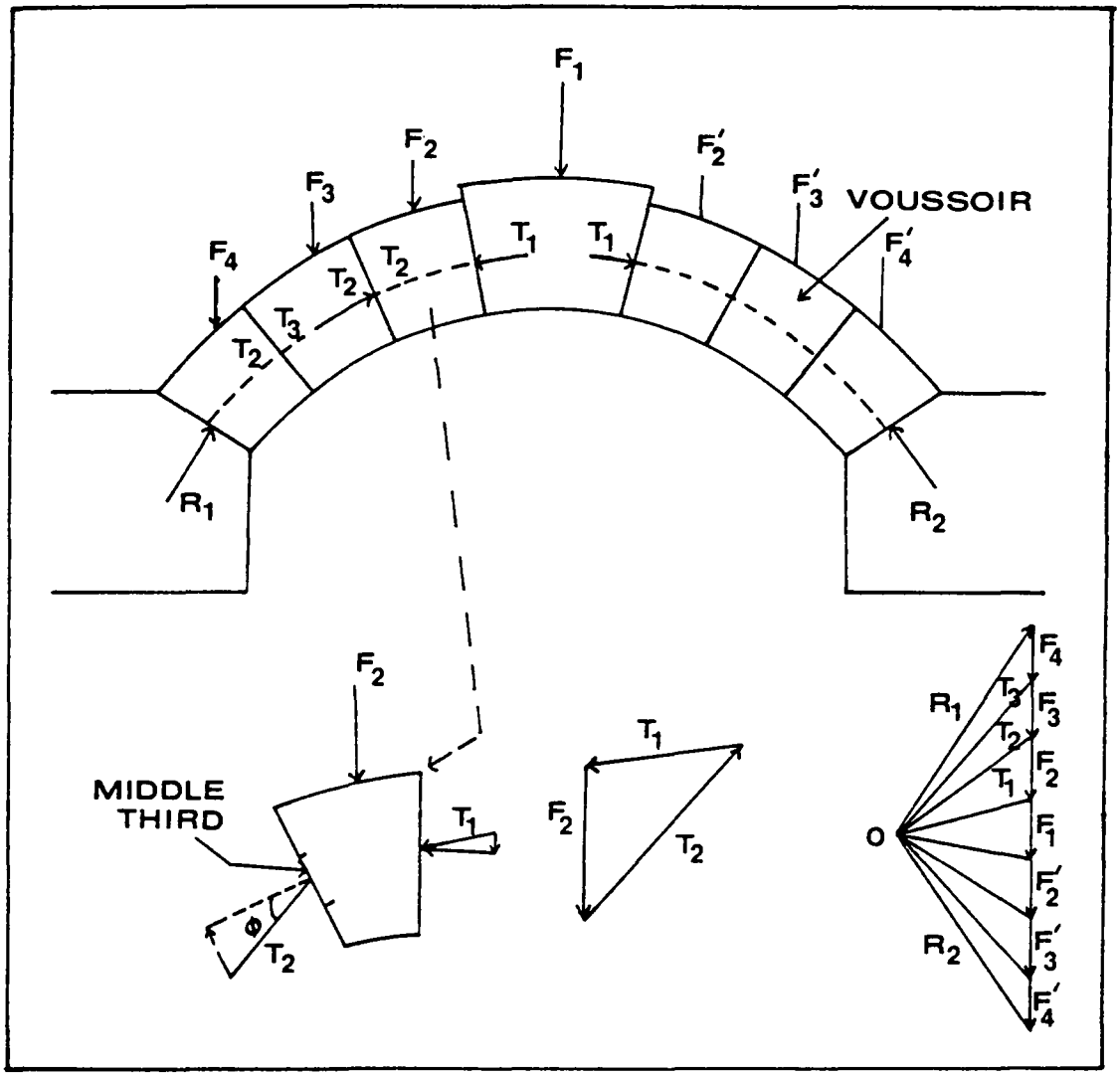

Figure 2.32: Forces acting on a voussoir arch (Adler and Sun, 1976).

3. The crushing resistance of the material must not be exceeded.

Because the voussoir arch is an arch of forces rather than a material arch, it can be straight or convex depending on the force regime in effect.

Beer and Meek (1982) have developed a series of design curves for safe roof span based on voussoir beam theory.

2.6.3 Roof Supports

The most widely used type of roof support in underground coal mining in the United States is the roof bolt. Bolts provide excellent support in day-to-day mining situations, require less storage space than other means of support, and make for a relatively unobstructed mine opening. Although there are many other support types in use, the thrust of this research is in the area of roof bolt supported top and a brief review of the types of bolts encountered in the study is included.

Three basic theories have been advanced to describe the mechanism of roof bolt-roof rock interaction. The first has been described by Panek (1962) and is shown in Figure 2.33. This is known as suspension. When the immediate roof sags after mining, the layers delaminate. Roof bolts then anchor the roof beam into a stronger layer above the immediate roof. The effect, then, is one of suspending the weaker, sagging layers from a more rigid layer above.

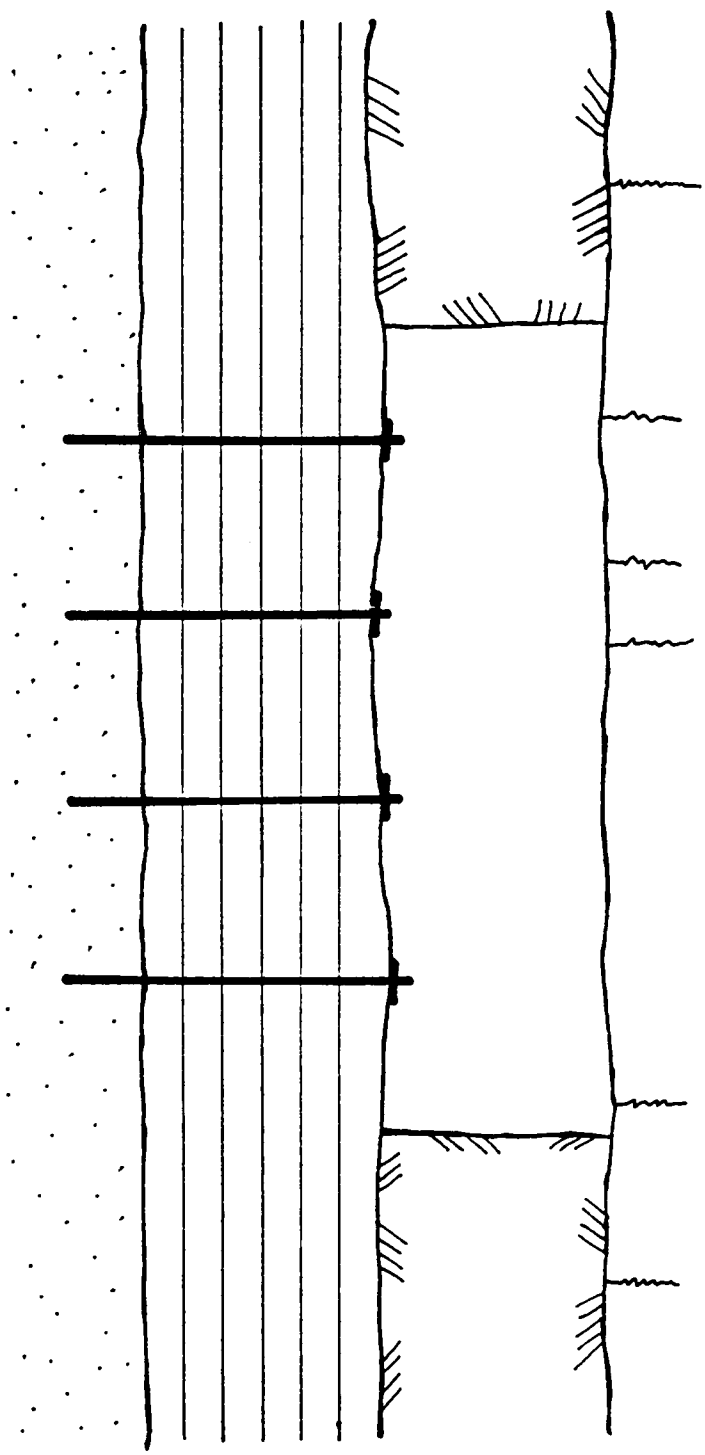

Figure 2.33: Suspension of immediate roof by roof bolts.

The second theory deals with friction (Panek, 1956) and is depicted in Figure 2.34. Often, in underground coal mines, there is no strong layer in close proximity to the immediate roof to suspend the weaker strata. In this case the frictional effects of rock bolts are important. The bolts, in effect, clamp the roof layers together and thus form a thicker, more rigid beam. This results in decreased strain at the beam ends and a safer roof. The roof layers are held together by the frictional forces induced along the bedding planes by the bolts. The magnitude of this force is dependent on bolt tension.

Obert and Duvall (1967) have described the keying effect of rock bolts. In many instances, the roof of a coal mine is dissected with fractures which can lead to roof failure. Bolts can be used to bolt through these planes of weakness and thus reduce movement as shown in Figure 2.35.

There are two types of bolts commonly used: the point-anchored bolt and the full-length anchored bolt or fully-grouted bolt. The point-anchored bolt is anchored at the tip and then tensioned. The fully-grouted bolt is un-tensioned and resin grouted along its entire length.

Point-anchored bolts can be of the slot-and-wedge, expansion shell, or resin anchor variety. The slot-and-wedge has a center slot with a wedge on it. It achieves anchorage by being pushed against the bottom of the hole and forcing

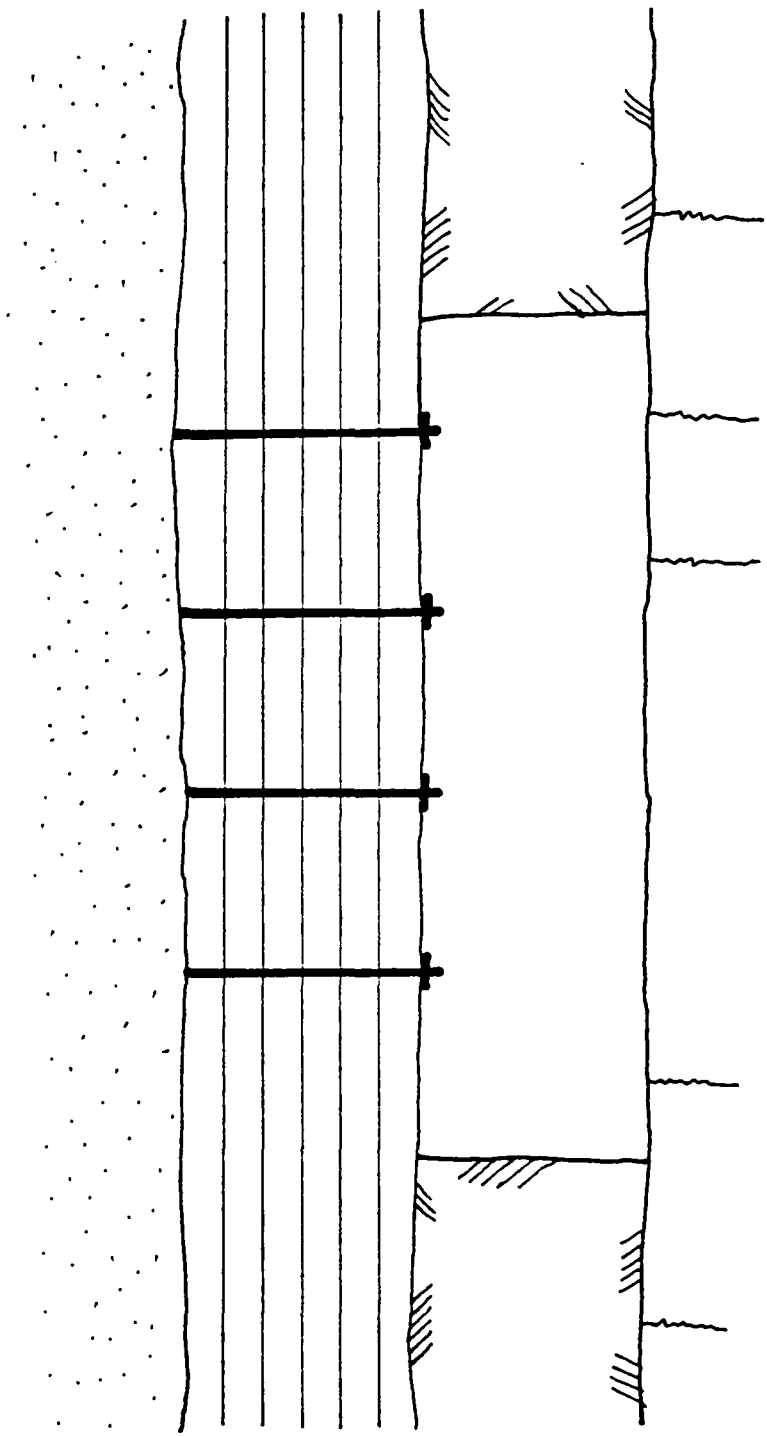

Figure 2.34: Support of immediate roof by friction of roof bolts.

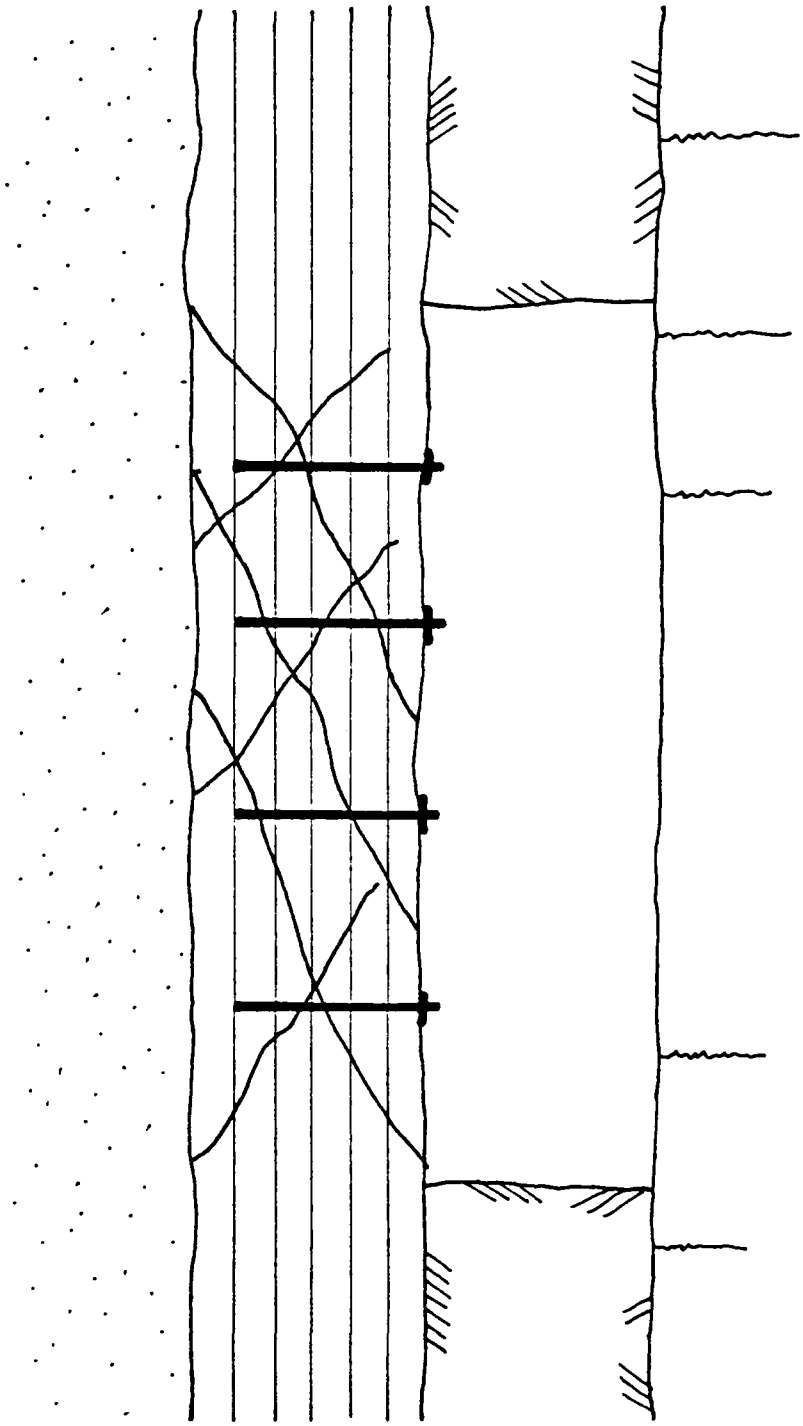

Figure 2.35: Keying of immediate roof by roof bolts.

the wedge into the slot thus enlarging the end against the hole sides. Hole length must be closely controlled and, as a result, these types of bolts are obsolete. Expansion shell bolts have a threaded, serrated end piece. When the bolt is threaded into the end, it forces the serrations against the rock. A problem results in that extremely high stress concentrations form at the tips of the serrations and crush the wall rock, thus inducing slippage (Stefanko and Dela Cruz, 1964). Finally, the resin point anchor bolt is the type most widely used in Virginia. The end last one-third meter of the bolt is grouted in the hole and tension is applied.

Resin bolting utilizes fast setting polyester resins to achieve a bond with the wall rock. Resin bolts work in two manners. The resin bolt maintains complete contact with the wall rock along its entire length. In doing so, it can prevent roof separation by the frictional shear resistance of the resin (Karabin and Debevec, 1976). Fairhurst and Singh (1974) suggested that resin bolts also work because of their rigidity. This rigidity is similar to those of the sedimentary rocks in which they are placed. Because the resin completely fills the hole, horizontal displacement between the strata is eliminated and so is any consequent sagging or delamination.

CHAPTER 3

RESEARCH PROGRAM

3.1 INTRODUCTION

In order to carry out this research, it was necessary to design a program which could collect a large amount of data, which could be analyzed using the most up-to-date methods. In order to accomplish this, a number of variables were mapped extensively in underground coal mines and the results were processed by statistical means. Finite element modeling using a nonlinear elastic-plastic model was also conducted to complement the previous analysis.

3.2 FIELD MAPPING

After reviewing the literature and discussing the situation with mine personnel, a list of potentially hazardous geologic and mining variables was compiled (Table 3.1). An attempt was made to limit the variables to those which could be easily determined and whose measurement was not time-consuming. This was done for two reasons:

(i) It was felt that mapping should be conducted in a manner which could easily be done by coal operators. Thus, any results could be duplicated or enhanced by each operator without a great deal of expense or expertise.

(ii) Emphasis was placed on establishing a data base as large and as quickly as possible. The prevailing philosophy was that the more roof

TABLE 3.1

Geologic and Mining Variables Mapped in Study

GEOMECHANICAL VARIABLES	MINING VARIABLES
ROOF	BOLT (SUPPORT TYPE)
1. Type	
2. Presence of Slickensides	ENTRY TREND AND WIDTH
3. Presence of Fossils	
4. Strike and Dip of Bedding	CROSSCUT TREND AND WIDTH
FALL	
1. Dimensions	
2. Type	
3. Location	
4. Time (Before or After Bolting)	
5. Trend	
FRACTURES	
1. Type	
2. Strike and Dip	
3. Density	
COAL	
1. Height	
2. Presence of Faults	
a. strike and dip	
b. type	
3. Cleat Strike and Dip	
PRESENCE OF WATER	

> falls that could be mapped, the greater the possibility for establishing an idea of the controlling mechanisms of roof failures in Virginia.

For this reason, several variables were eliminated from the list. Probably the most important was the influence of overburden, or the lithostatic stress, at a given location. The difficulty here was in the time-consuming task of pinpointing each station on the mine map on the larger scale topographic maps with any accuracy. The effect of tectonic, or residual, stresses was neglected due to the extremely expensive equipment involved and the inconsistent results which are often obtained when making these measurements. The thickness of the rock layers in the immediate roof was not used since the only data available consisted of drill logs taken on nearly one kilometer centers. It was felt that interpolation of rock types and thicknesses between these points would be much too vague for detailed mapping of the type conducted in this study. Finally, the distance that the fall occurred from the face was not measured due to the time-of-fall problem described below.

Two coal seams, the Jawbone and the Upper Banner of the Norton Formation, were selected for study in order to reduce the problem of differing tectonic regimes and minimize the influence of stratigraphic variation. Four mines were chosen within the thrust plate.

Mapping was conducted in a systematic manner at specif-

ic intersections in each mine. Measurements between intersections were not taken unless a fall had occurred or something unusual, such as a fault in the coal or a channel boundary, was observed. Data collection was performed in this manner to allow a systematic procedure and to ensure that a large variety of both stable and unstable roof conditions were sampled. A typical data record sheet is shown in Figure 3.1.

At each station, the roof lithology was recorded as well as the presence of individual geologic features, both in the roof and in the coal. Examination of the roof provided data on the presence or absence of slickensides and fossils, and descriptions of any roof fractures. The strike and dip of roof-rock bedding and fractures was recorded with a Brunton compass. Fractures were described as being joints if no slickensides were found on their surfaces, tear faults if slickensides indicated the last direction of movement to be horizontal, or dip-slip faults if slickensides indicated the last direction of movement to be along the dip of the fault. The fracture density was determined as the number of fractures of a given joint set in a linear distance of 3 meters along the roof. The fracture density for each joint set was then summed to yield a total fracture density.

If a roof fall had occurred at a station, its location was plotted on the mine map and its dimensions recorded. The fall was classified according to a modified version of the

ROOF FALL DATA SHEET

MINE: SEAM: Upper Banner

STATION: FALL LOCATION (Spad):

ROOF TYPE:

SUPPORT TYPE: ___Resin Bolt ___ Mech. Bolt ___Pt. Anchor Cribs
Posts Headers Other:

FALL: BEFORE AFTER BOLTING UNKNOWN NA

FALL Length (ft.) Width: Height:

FALL TYPE:

TREND OF FALL:

FRACTURES PRESENT:

strike/dip	strike of intersect.	Density(per 10 feet)
A		A
B		B
C		C
D		D
E		E
		Total

If bedding is involved in fall: (strike/dip)

SLICKENSIDES: Yes No Orientation:

INTERSECTION? 3-way 4-way No

TREND OF ENTRY: CROSSCUT:

WIDTH OF ENTRY: ft. CROSSCUT: ft.

COAL HEIGHT (ft.):

FAULT IN COAL: Yes No Contractional Extensional Strike-slip

strike/dip

COAL CLEAT (strike/dip): Face: Butt:

WATER PRESENT? Yes No

COMMENTS:

Figure 3.1: Sample roof data sheet.

scheme proposed by Patrick and Aughenbaugh (1979) as shown in Table 3.2. Any compass trend of the fall was noted as well as the time the fall occurred. There is a great deal of difficulty involved in determining the time of a roof failure. Unless the mine has been continuously monitored over a period of years, only large falls are recorded as to time and date on the mine foreman's map. For this reason the time of fall was divided into two categories--either the fall occurred before supports were in place or it occurred after. This was only done for falls in which the time of the event was obvious and, for the majority of falls, the time of failure was listed as unknown. If water was associated with the fall, its presence was noted also.

The condition of the coal was examined. The height of the coal was measured as was the strike and dip of both the face and butt cleats. Faults within the coal were characterized, as described above, for roof fractures as to type and their orientations noted.

Several mining variables were also used in this study. The bolt and/or support type was observed and the entry trend and width as well as the cross-cut trend and width was measured. Obviously, some stations were located at points where only a cross-cut or entry existed.

TABLE 3.2

Modified version of roof fall classification (after Patrick and Aughenbaugh, 1979)

GENERAL DESCRIPTION OF FALL	GEOMETRY OF FALL					
	NO DISCONTINUITY AT UPPER BOUNDARY			DISCONTINUITY AT UPPER BOUNDARY		
REGULAR GEOMETRY	Curved Contour Circular Dome circular $l \approx w > 1M$ $1M < h < w$	Curved Contour Oval Dome $w < l < 2w$ $1M < h < w$		Flat-topped Circular Dome circular $l \approx w > 1M$ $1M < h < w$	Flat-topped Oval Dome $w < l < 2w$ $1M < h < w$	
	Curved Contour Oval Arch	Curved Contour Linear Arch	Curved Contour Serpentine Arch	Flat-topped Oval Arch	Flat-topped Linear Arch	Flat-topped Serpentine Arch
	$w < l < 2w$ $h > w$	$l > 2w$ $h > 1M$	$l > 2w$ $h > 1M$	$w < l < 2w$ $h > w$	$l > 2w$ $h > 1M$	$l > 2w$ $h > 1M$
IRREGULAR GEOMETRY (Plan and/or Cross-section)	Minor Areal $l \leq 2w$ $0.5M \leq h < 1.3M$		Minor Linear $l > 2w$ $0.5M \leq h < 1.3M$		Minor Serpentine $l > 2w$ $0.5M \leq h < 1.3M$	
	Areal Sloughing $l > 2w$ $h < 0.5M$		Linear Sloughing $l > 2w$ $h < 0.5M$		Serpentine Sloughing $l > 2w$ $h < 0.5M$	

3.3 STATISTICAL ANALYSIS

3.3.1 Introduction

Data analysis was carried out by means of the Statistical Analysis System, or SAS, package (Statistical Analysis System, 1982a). Statistical tests were run in order to determine the controlling factors for particular roof and fall types as well as the most successful means of support. This was accomplished by means of frequency analysis, chi-square analysis, and regression analysis.

3.3.2 Frequency Analysis

For frequency analysis, i.e. bar charts, frequency counts of data, percentages, and averages, the CHART procedure of SAS was utilized. This procedure allows for the production of both two and three dimensional bar charts. It also provides for the determination of means for all variables as well as midpoints for continuous variables such as strike and dip.

3.3.3 Chi-square Analysis

As mentioned previously, chi-square analysis was performed on the majority of the data. This took the form of bivariate contingency tables. Data was summarized into a table by the SAS FREQ command and tested for independence. Ott (1977) discusses independence of variables as follows:

> Two variables that have been categorized in a two-way table are independent if the probability that a measurement is classified into a given cell of

> the table is equal to the probability of being classified into that row times the probability of being classified into that column. This must be true for all cells of the table.

This results in the following test statistic for two variables arranged into a two-way table:

$$X^2 = \sum_i \sum_j (n_{ij} - E_{ij})^2 / E_{ij} \qquad \text{Eqn. 3.1}$$

where n_{ij} and E_{ij} are the observed and expected number of measurements falling in the cell for th i row and the j th column. When the two variables are independent, the expected number of measurements E_{ij} falling in the i,j cell is taken to be:

$$E_{ij} = (\text{row i total})(\text{column j total})/n.$$

For a chi-square test the null hypothesis (H_0) assumes that the variables are independent while the alternative hypothesis is that the two variables are dependent. The rejection criteria for H_0 in this analysis was taken to be a = 0.05 and the degrees of freedom = (r-1)(c-1). In this case, "a" is the probability that the null hypothesis, i.e., the variables are independent, will be rejected when it is, indeed, true, r = the number of rows in the table, and c = the number of columns. The degrees of freedom is a measure which allows the specification of one of the many chi-square distributions (Ott, 1977).

As mentioned previously, SAS allows the compilation of two-way tables, and also computes the chi-square as well as

the probability of the null hypothesis being rejected accidentally. This is done by means of the FREQ procedure with appropriate options specified.

One problem with the two-way chi-square analysis performed on the type of variables in this study is that the interactions of the different variables are not accounted for. Preliminary model building in which three- and four-way tables were formed showed little distinction from the two-way tables as far as chi-square effects went. Another approach is to model functions of categorical responses. This is known as the GSK method after its proposal by Grizzle, Starmer, and Koch (1969). However, according to SAS (1982b), both the GSK and contingency table methods yield similar results. The contingency table method of chi-square testing is much better for testing for independence and was chosen for this reason.

3.3.4 Regression Analysis

Regression analysis was performed in two ways, i.e, using the REG and RSQUARE procedures. In the first the correlation coefficient between fall size and each of the several numerical variables was calculated. The REG procedure of SAS was used to fit least squares estimates to linear models. The value of the correlation coefficient lies between -1 and 1 and gives a measure of how well data fit a

line of the form (SAS, 1982b):

$$Y_i = B_0 + B_1 X1_i + B_2 X2_i + e_i \qquad \text{Eqn. 3.2}$$

where Y is the dependent variable and X1 and X2 are the independent variables, B_1 and B_2 are coefficients of the regression line, and e is the error involved. If the correlation coefficient is greater than zero than a positive linear relationship exists between the data points and the regression line. If the correlation coefficient is less than zero a negative linear relationship exists. A value of r equal to zero indicates that no linear relationship whatsoever exists between the data points and a least squares derived line. The square of the correlation coefficient provides for the proportion of variability in Y that can be accounted for by the independent variable X. In other words, the closer the value of R^2 to unity, the stronger the relationship between X and Y, and the more linear the data will be.

In the REG procedure, the models must be expressed within the computer program. Sometimes this is inconvenient if many independent variables are being used. For this reason, SAS has provided the RSQUARE procedure. This is useful if many regression models are being investigated in conjunction with a dependent variable. RSQUARE evaluates each possible combination of independent variable with the dependent variable and provides the R^2 value for each

combination. This enables the quick determination of the most important variables for further testing such as in the REG procedure.

As will be mentioned in the results section of this thesis, the analysis conducted on the linear regression models yielded far-from-significant results. For this reason, a full and further investigation of the numerical variables was not deemed necessary.

3.3.5 Summary

In summary, the CHART, FREQ, REG, and RSQUARE procedures of SAS were chosen to evaluate the data. CHART was used to provide bar charts and graphs of the different numeric variables. FREQ was used to perform chi-square tests for independence of the categorical variables as well as tabulate the different parameters and responses. REG and RSQUARE were used for testing the numerical data as it related to fall size.

3.4 FINITE ELEMENT ANALYSIS

3.4.1 Introduction

Finite element analysis was chosen to further investigate the behavior of certain roof types. This was decided because, as will be discussed in the next chapter, the mapped parameters failed to yield any insight into the failure behavior of these roof types. The finite element approach seemed to be the logical choice since different

situations could be modeled on the computer quickly and easily.

The advantages of the finite element method have been summarized by Wilson (1965) and include the following:

(i) With respect to material properties and problem geometry, the method is completely general.

(ii) Complex bodies composed of diverse materials are easily represented.

(iii) Displacement or stress boundary conditions may be specified at any nodal point.

(iv) In formulation, a symmetric, positive-definite matrix in a banded form usually occurs. This results in a solution which utilizes a minimum of computer storage and time.

A complete description of the method would be complex and well beyond the scope of this research. Thorough texts such as Desai and Abel (1972), Zienkiewicz (1977), or Reddy (1984) are recommended.

3.4.2 Formulation

Because a two-dimensional code with eight node quadrilateral elements was utilized in this analysis, only its formulation will be discussed. It should be noted that triangular and four node quadrilateral elements have also been used.

An eight node element is shown in Figure 3.2. The displacements, u and v, of any nodal point in the x and y

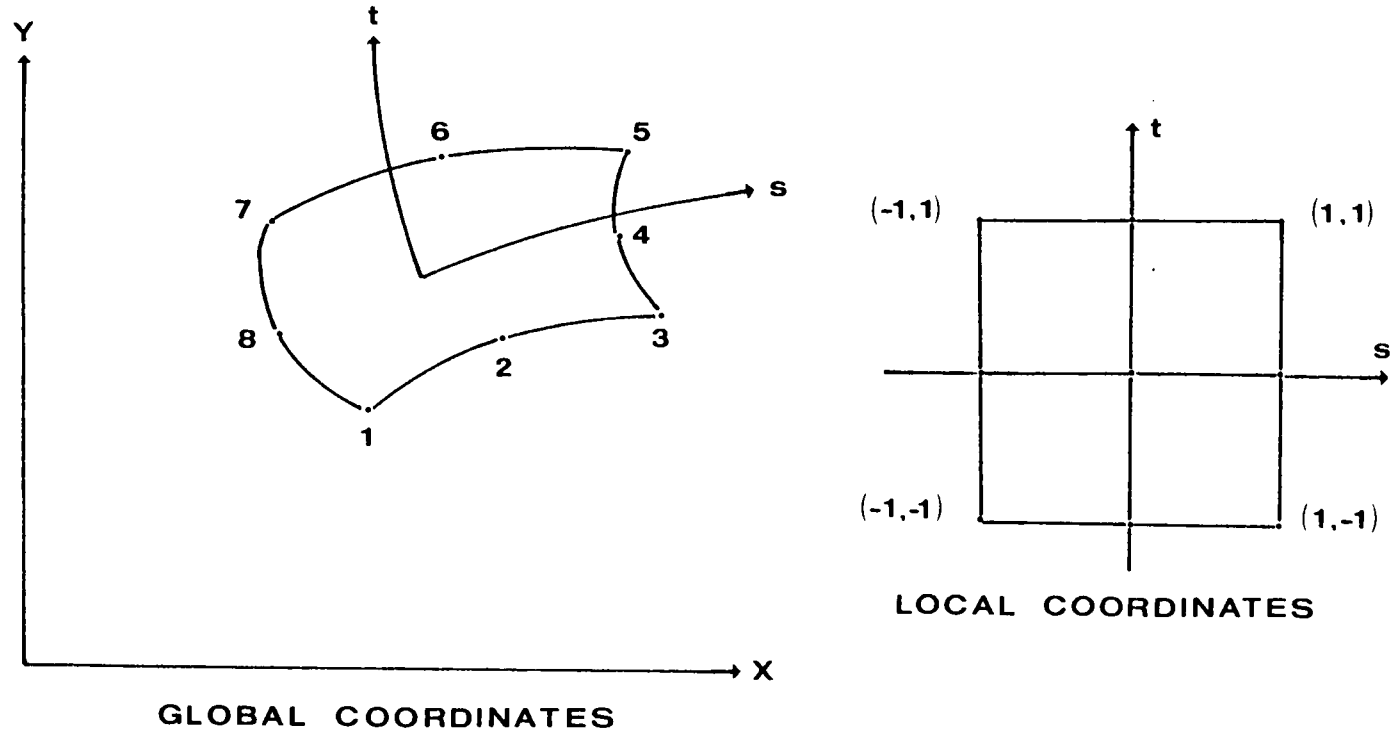

Figure 3.2: Eight node quadrilateral element.

directions, respectively, can be expressed as:

$$U = N_1 u_1 + N_2 u_2 + \ldots + N_8 u_8 \qquad \text{Eqn. 3.3}$$

$$V = N_1 v_1 + N_2 v_2 + \ldots + N_8 v_8 \qquad \text{Eqn. 3.4}$$

where $N_1 \ldots N_8$ are interpolation functions which provide interelement compatibility. Equations 3.3 and 3.4 can be expressed in vecor form as:

$$\begin{Bmatrix} U \\ V \end{Bmatrix} = [N] \{q\} \qquad \text{Eqn. 3.5}$$

where

$$[N] = \begin{bmatrix} N_1 & 0 & N_2 & 0 & \ldots\ldots & N_8 & 0 \\ 0 & N_1 & 0 & N_2 & \ldots\ldots & 0 & N_8 \end{bmatrix}$$

and

$$\{q\}^T = [u_1 \; v_1 \; u_2 \; v_2 \; \ldots\ldots \; u_8 \; v_8]$$

The interpolation functions can be expressed in terms of local coordinates s and t which vary from -1 to +1 (Reddy, 1984):

$$N_1 = (1/4)(1 - s)(1 - t)(-1 - s - t)$$

$$N_2 = (1/2)(1 - s^2)(1 - t)$$

$$N_3 = (1/4)(1 + s)(1 - t)(s - t - 1)$$

$$N_4 = (1/2)(1 - s)(1 - t^2)$$

$$N_5 = (1/2)\ (1 + s)\ (1 - t^2)$$

$$N_6 = (1/4)\ (1 - s)\ (1 + t)\ (-1 - s + t)$$

$$N_7 = (1/2)\ (1 - s^2)\ (1 + t)$$

$$N_8 = (1/4)\ (1 + s)\ (1 + t)\ (-1 + s + t)$$

Assuming small strains, the strain-displacement relation can be expressed as (Reddy, 1984):

$$\varepsilon_x = \frac{\partial u}{\partial x} \qquad \varepsilon_y = \frac{\partial v}{\partial y} \qquad \gamma_{xy} = \frac{\partial u}{\partial y} + \frac{\partial u}{\partial x} \qquad \text{Eqn. 3.6}$$

By, substitution of Equation 3.5 into Equation 3.6, the strain vector $\{ \varepsilon \}$ can be obtained:

$$\{ \varepsilon \} = \begin{Bmatrix} \frac{\partial u}{\partial x} \\ \frac{\partial v}{\partial y} \\ \frac{\partial u}{\partial y} + \frac{\partial v}{\partial x} \end{Bmatrix} \qquad \text{Eqn. 3.7}$$

or

$$\{ \varepsilon \} = [B]\ \{q\} \qquad \text{Eqn. 3.8}$$

where the matrix [B] is called the strain-displacement transformation matrix. By chain-rule differentiation, the transformation from local to global coordinates can be made:

$$\frac{\partial}{\partial s} = \frac{\partial}{\partial x}\frac{\partial x}{\partial s} + \frac{\partial}{\partial y}\frac{\partial y}{\partial s}$$

$$\frac{\partial}{\partial t} = \frac{\partial}{\partial x}\frac{\partial x}{\partial t} + \frac{\partial}{\partial y}\frac{\partial y}{\partial t}$$

In terms of the Jacobian matrix this becomes:

$$\begin{Bmatrix} \frac{\partial}{\partial s} \\ \frac{\partial}{\partial t} \end{Bmatrix} = [J] \begin{Bmatrix} \frac{\partial}{\partial x} \\ \frac{\partial}{\partial y} \end{Bmatrix}$$

where

$$[J] = \begin{bmatrix} \frac{\partial}{\partial s} \sum N_i X_i & \frac{\partial}{\partial s} \sum N_i Y_i \\ \frac{\partial}{\partial t} \sum N_i X_i & \frac{\partial}{\partial t} \sum N_i Y_i \end{bmatrix}$$

Thus, the global derivatives of the interpolation functions can be derived

$$\begin{Bmatrix} \frac{\partial N_1}{\partial x} \\ \frac{\partial N_1}{\partial y} \end{Bmatrix} = [J]^{-1} \begin{Bmatrix} \frac{\partial N_1}{\partial s} \\ \frac{\partial N_1}{\partial t} \end{Bmatrix}$$

where $[J^{-1}]$ is the inverse of the Jacobian matrix.

The next step in the formulation requires the constitutive, or stress-strain, relation:

$$\begin{Bmatrix} \sigma_x \\ \sigma_y \\ \sigma_{xy} \end{Bmatrix} = \begin{bmatrix} C_{11} & C_{12} & C_{13} \\ C_{21} & C_{22} & C_{23} \\ C_{31} & C_{32} & C_{33} \end{bmatrix} \begin{Bmatrix} \varepsilon_x \\ \varepsilon_y \\ \varepsilon_{xy} \end{Bmatrix}$$

It can also be expressed in vector form:

$$\{ \sigma \} = [C] \{ \varepsilon \} \qquad \text{Eqn. 3.9}$$

where $\{ \sigma \}$ is the stress vector and [C] is the constitutive matrix.

The element stiffness equations can now be derived by using the principle of minimum potential energy. In essence,

this principle states that under given geometric constraints or boundary condtions, the potential energy of the deformed body will be a stationary value (Desai, 1979). For stable equilibrium to be maintained, the potential energy must be some minimum value. The potential energy of any body can be expressed as the sum of the internal strain energy, and the potential energy of the body forces and surface tractions:

$$\pi_p = \iiint_V U(u,v,w)\, dv - \iiint_V (\bar{X}u + \bar{Y}v + \bar{Z}w)\, dv - \iint_{S_1} (\bar{T}_x u + \bar{T}_y v + \bar{T}_z w)\, ds \qquad \text{Eqn. 3.10}$$

where V is the volume of the body, U(u,v,w,) is the strain energy per unit volume, $\bar{X}$, $\bar{Y}$, and $\bar{Z}$ are the body forces per unit volume, and $\bar{T}_x$, $\bar{T}_y$, $\bar{T}_z$ are the surface loading or traction per unit surface, and S_1 is that part of the body surface over which the surface loading acts. By substituting [B], [C], [N] and {q}, and inserting the vector of initial stresses { σ_o } the integrals can be expressed in terms of the nodal displacements.

Minimizing the potential energy yields:

$$[k]\ \{q\} = \{Q\} \qquad \text{Eqn. 3.11}$$

where [k] is the first term of Equation 3.10 and {Q} is the sum of terms on the right hand side of the equal sign. Numerical integration is used to evaluate the interal in the following form:

$$\iiint_V [B]^T\ [C]\ [B]\ dv = \int_{-1}^{+1}\int_{-1}^{+1}\int_{-1}^{+1} [B]^T\ [C]\ [B]\ \det[J]\ dr\,ds\,dt$$

where r, s, and t, are the local coordinate system.

The element equations are assembled from the from the element property matrix and take the form:

$$[K]\{r\} = \{R\} \qquad \text{Eqn. 3.12}$$

where [K] is the assemblage property matrix,

{r} is the assemblage vector of nodal displacements

{R} is the assemblage vector of nodal forces.

Boundary conditions are then input and the system can then be solved for the displacements as the primary unknowns. This is done because a displacement formulation based on potential energy has been used. Secondary unknowns, i.e., strains and stresses, can then be calculated.

3.4.3 Drucker-Prager Yield Criterion

The Drucker-Prager model (Drucker and Prager, 1952) is one of the simplest plasticity models. It has also been referred to as the extended von Mises yield criterion because it not only incoporates the effects of the intermediate principal stress, but accounts for frictional effects as well (Desai and Christian, 1977). It is widely used, primarily, due to its mathematical convenience.

In this yield criterion, the idea of incremental relations between stress and strain is utilized. The Mohr-Coulomb law is generalized so that it incorporates all the principal stresses and is given by Desai and Christian

(1977) as:

$$J_2^{1/2} = k - \alpha I_1$$

where

$$J_2 = \frac{(\sigma_{xx}-\sigma_{yy})^2 + (\sigma_{yy}-\sigma_{zz})^2 + (\sigma_{xx}-\sigma_{zz})^2}{6} + \sigma_{xy}^2 + \sigma_{yz}^2 + \sigma_{xz}^2$$

$$I_1 = \sigma_{xx} + \sigma_{yy} + \sigma_{zz}$$

α, k = material constants

The yield surface is depicted in Figure 3.3. Below the yield surface, the stress-strain behavior is assumed to be linear elastic.

A major obstacle in employing this criterion is that the Drucker-Prager model predicts large volumetric plastic strains which have not been observed in laboratory tests (Lightner, 1979).

3.4.4 Program Description

As will be described in Chapter 4, Interface Roof did not show signicant results from the statistical analysis. Therefore, further modelling of this roof type by finite element methods was attempted. Two Interface Roof situations were modeled. The first varied the height of the rider seam from 0.25 to 2.0 meters above the coal bed in an effort to determine critical stress distributions with regard to rider distance above the seam. The second model utilized sandstone and shale units of thicknesses varying between 0.25 an 1.0

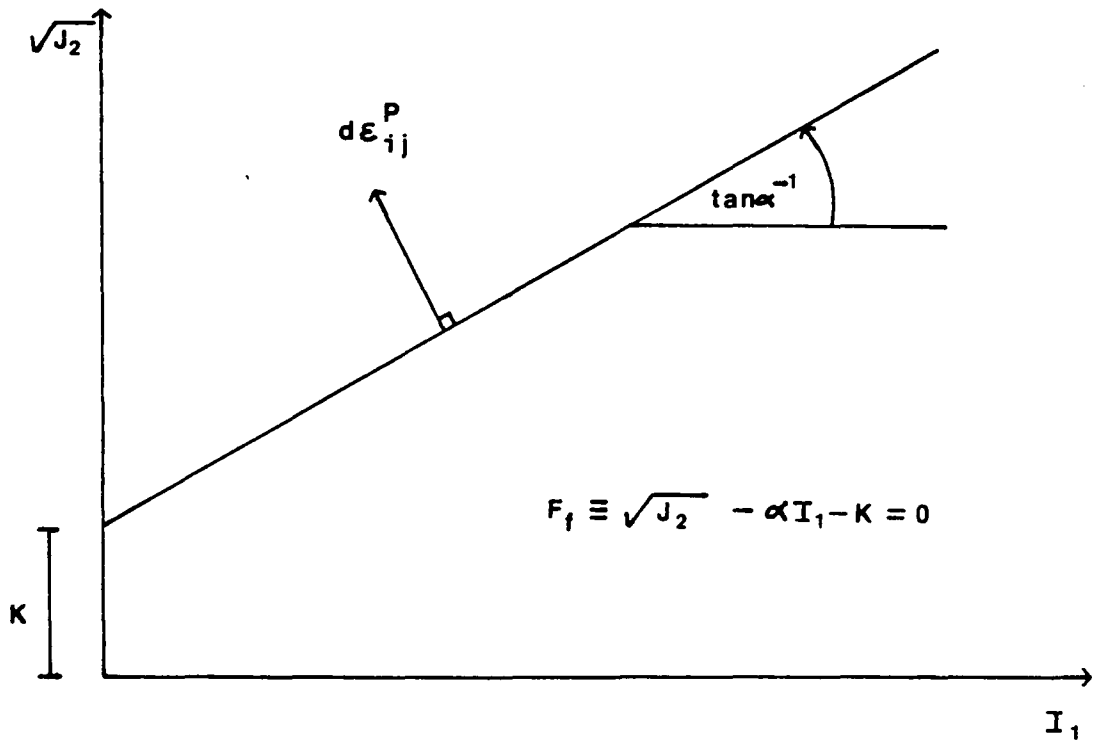

Figure 3.3: Drucker-Prager yield surface.

meters in an effort to simulate a crevasse splay roof deposit. This was done in hopes of determining what thicknesses of rock layers in the roof were responsible for unstable roof.

The finite element code used in this research was developed at Virginia Polytechnic Institute and State University by T. Kuppusamy (1984). It utilizes the Drucker-Prager yield criterion and allows for the sequential removal of elements so as to simulate mining excavation. Excavation was simulated by removing first six, and then five elements, from the virgin coal conditions.

Rock properties input to the program were derived from the literature and are shown in Table 3.3. They were modified somewhat to more realistically reflect joint and in situ properties (Protod'iakonov, 1964). Properties for the excavted elements were taken to be extremely small in order to avoid renumbering the mesh. A finite element mesh with 528 nodes and 483 elements was used (Figure 3.4). Two-dimensional plane strain analysis was conducted in all cases.

Output from the program consists of displacements and stresses. Stresses are given at the four Gaussian quadrature points and displacements are given for the nodes in the x- and y-coordinate directions. A feature of this code is that the elemental state is also output. That is, the program reports whether a given element is in the elastic region or

TABLE 3.3

Rock properties used in finite element analysis (Modified from Hustrulid, 1976; Jaeger and Cook, 1979; and Jumikis, 1979)

Material	Young's Modulus (kPa)	Poisson's Ratio	Density kN/m3
Shale	67.57×10^6	0.23	24.9
Coal	4.46×10^6	0.23	20.1
Sandstone	88.43×10^6	0.23	22.7

Material	Angle of Internal Friction (degrees)	Cohesion (kPa)	Tensile Strength (kPa)
Shale	55	1.15×10^6	5.32×10^3
Coal	15	0.42×10^6	0.20×10^3
Sandstone	43	2.5×10^6	8.40×10^3

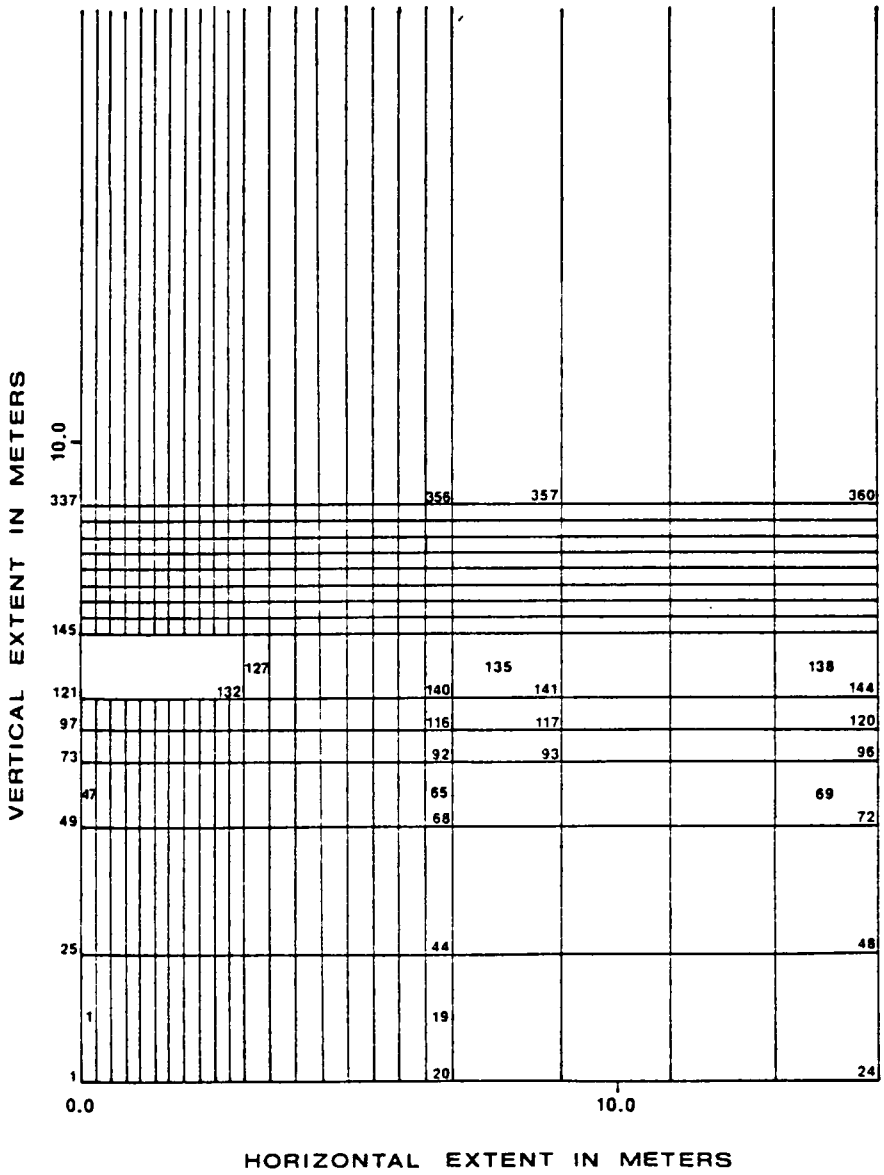

Figure 3.4: Finite element mesh used in analysis.

if it has failed in tension or yielded plastically according to the Drucker-Prager criterion.

CHAPTER 4

STATISTICAL ANALYSIS

4.1 Introduction

Very early in this study, it was discovered that certain relationships existed between stratigraphic and structural features within the immediate roof of both the Upper Banner and Jawbone seams. Some roof conditions appeared to be dependent on the stratigraphic relationships between different materials while others, usually more homogeneous lithologically, seemed dependent on structural characteristics. This led to the formulation of a relatively simple roof classification for which the different survey parameters could by recorded. The classification is as follows:

Interface Roof: Characterized by heterogenous strata in immediate and main roof and dependent on these differences in lithology for its degree of stability. Examples include channel boundaries where sandstone cuts down into the immediate roof or where slickensided fractures in shale intersect a channel bottom or sides. Interbedded sandstones, siltstones and shales such as splay deposits. Rider coals are also included but not smaller features such as carbonaceous bedding planes (Figure 4.1).

Sandstone Roof: Evenly bedded, smooth sandstone or a sandstone with an irregular base due to channel bottoms, load casts, and other features extending downward. No shale or siltstone beds are present, or else the top would

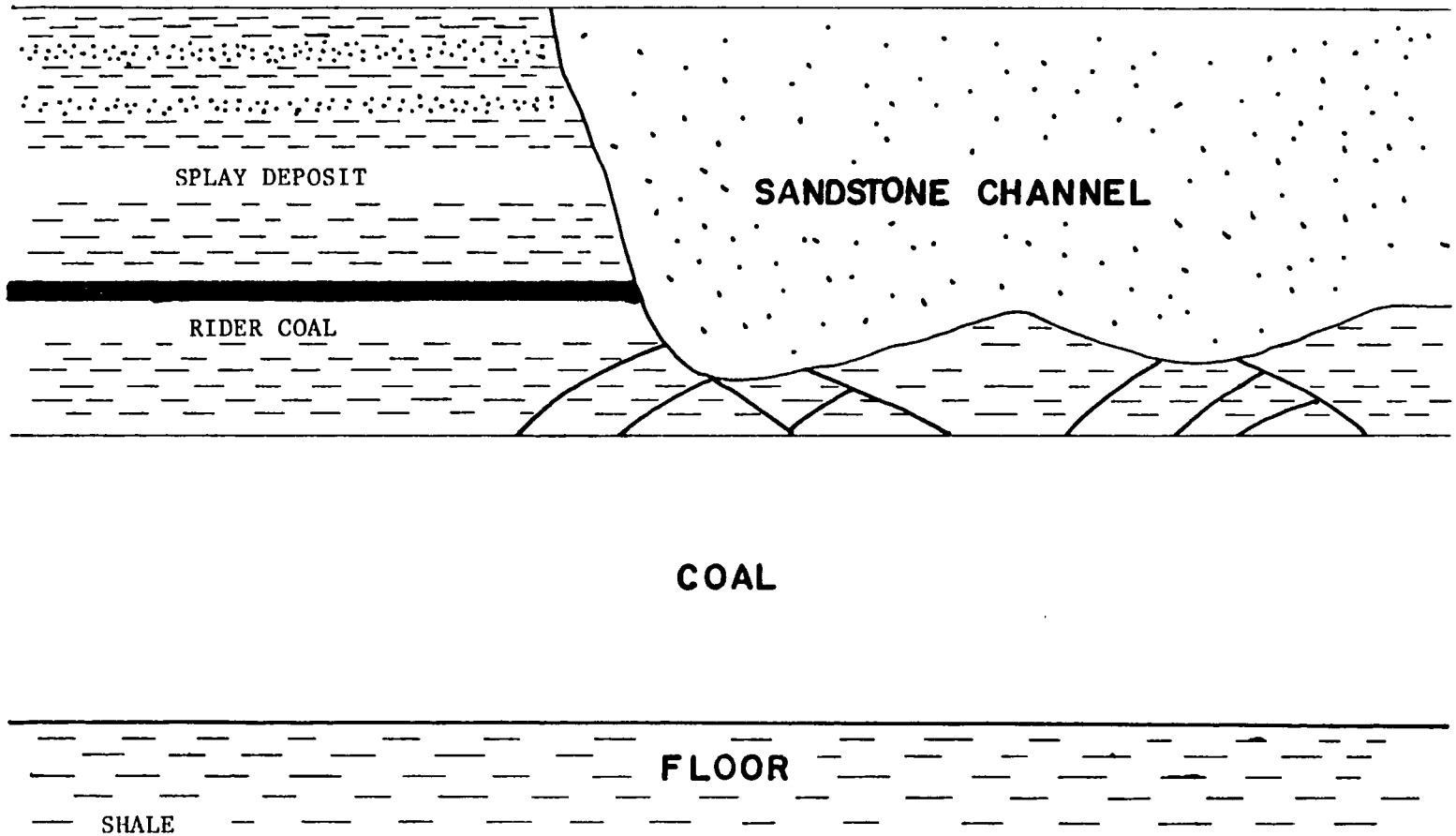

Figure 4.1: Interface roof.

be classified as Interface Roof (Figure 4.2).

Shale Roof: Shales or siltstones which may be planar-bedded, faulted, slickensided, or deformed. Can also include coarsening upward sequences (Figure 4.3).

The data base employed in the statistical analysis consisted of 260 actual roof falls and 286 instances of stable roof conditions. Ninety-eight examples of Interface Roof, 144 cases of Sandstone Roof, and 304 samples of Shale Roof were examined. Figure 4.4 shows a breakdown in the percentage of observations made for each roof type at different locations.

For statistical analysis, the parameters were divided into two groups; classification variables and numerical variables. Tests of independence were carried out by means of the chi-square test for the classification variables while regression analysis was performed on the numerical variables.

Correlations were tested for each roof type between the occurrence of a fall and (1) fall location, (2) faulting and deformation within the coal itself, (3) the presence of fossils, (4) the presence of slickensides, (5) the presence of water, and (6) support type. Fall type and roof type were investigated in an effort to determine possible relationships. Average, approximate fall sizes were also analyzed with respect to time as well as the previously mentioned variables. Finally, the influence of both fracture

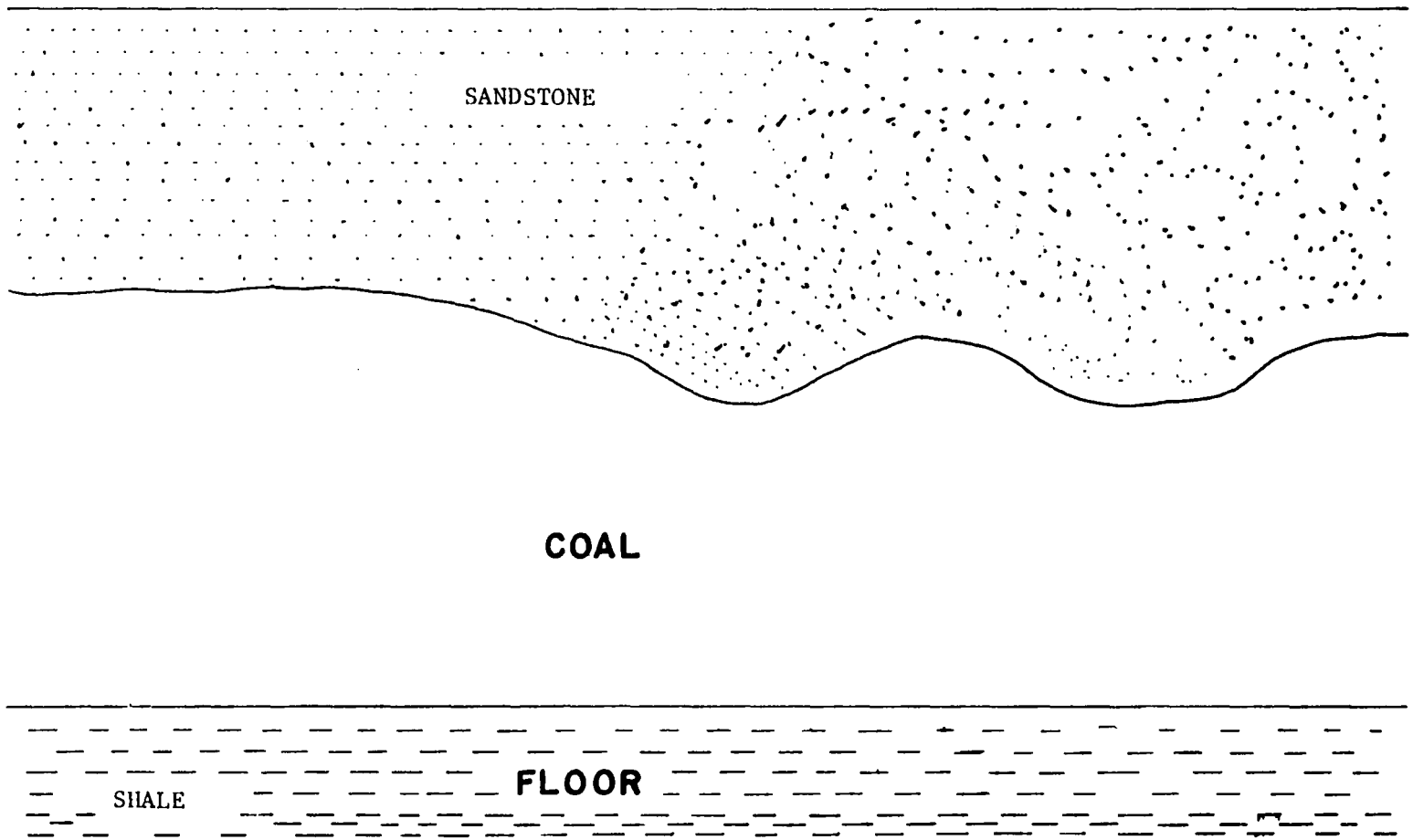

Figure 4.2: Sandstone Roof.

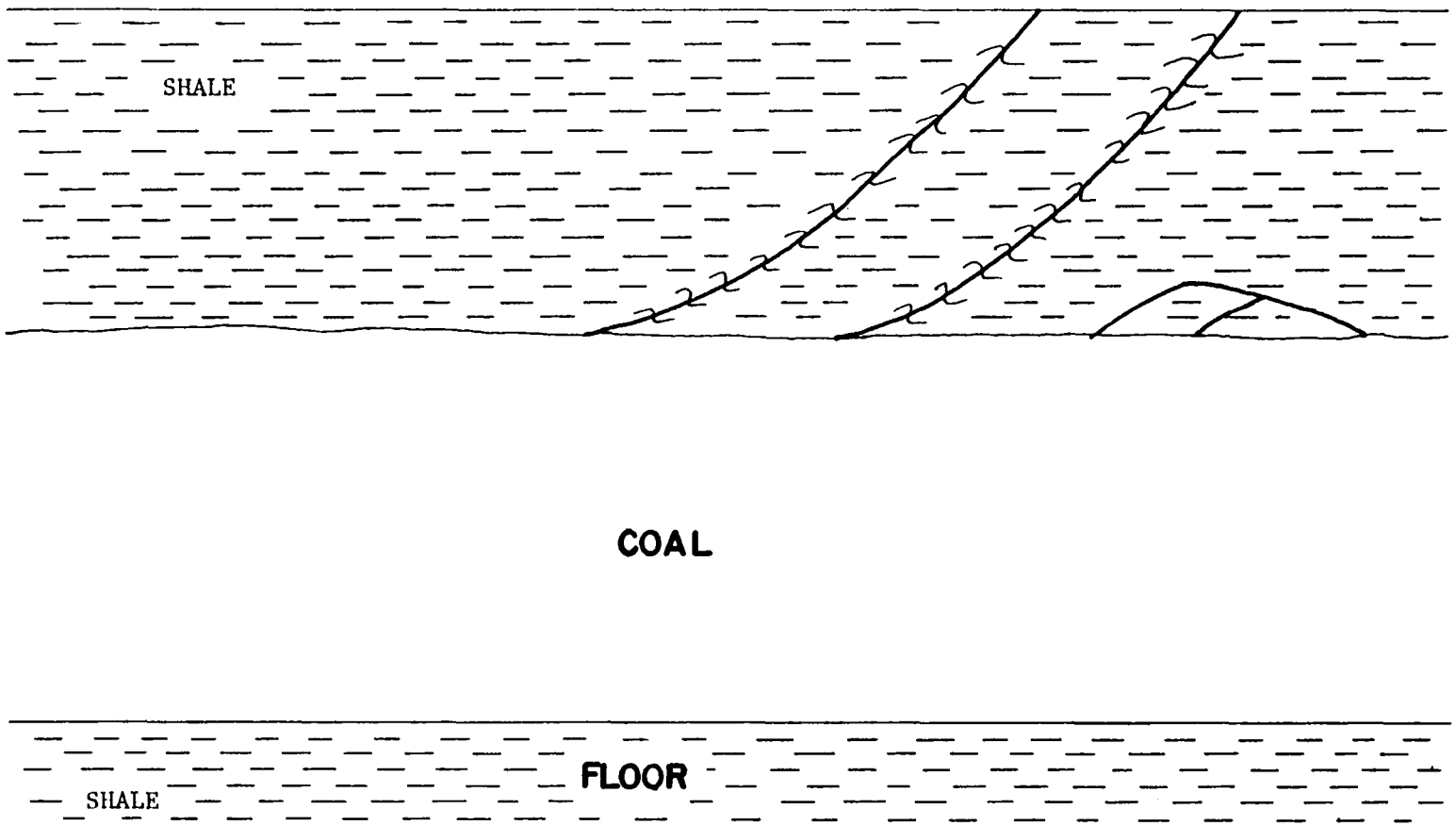

Figure 4.3: Shale Roof.

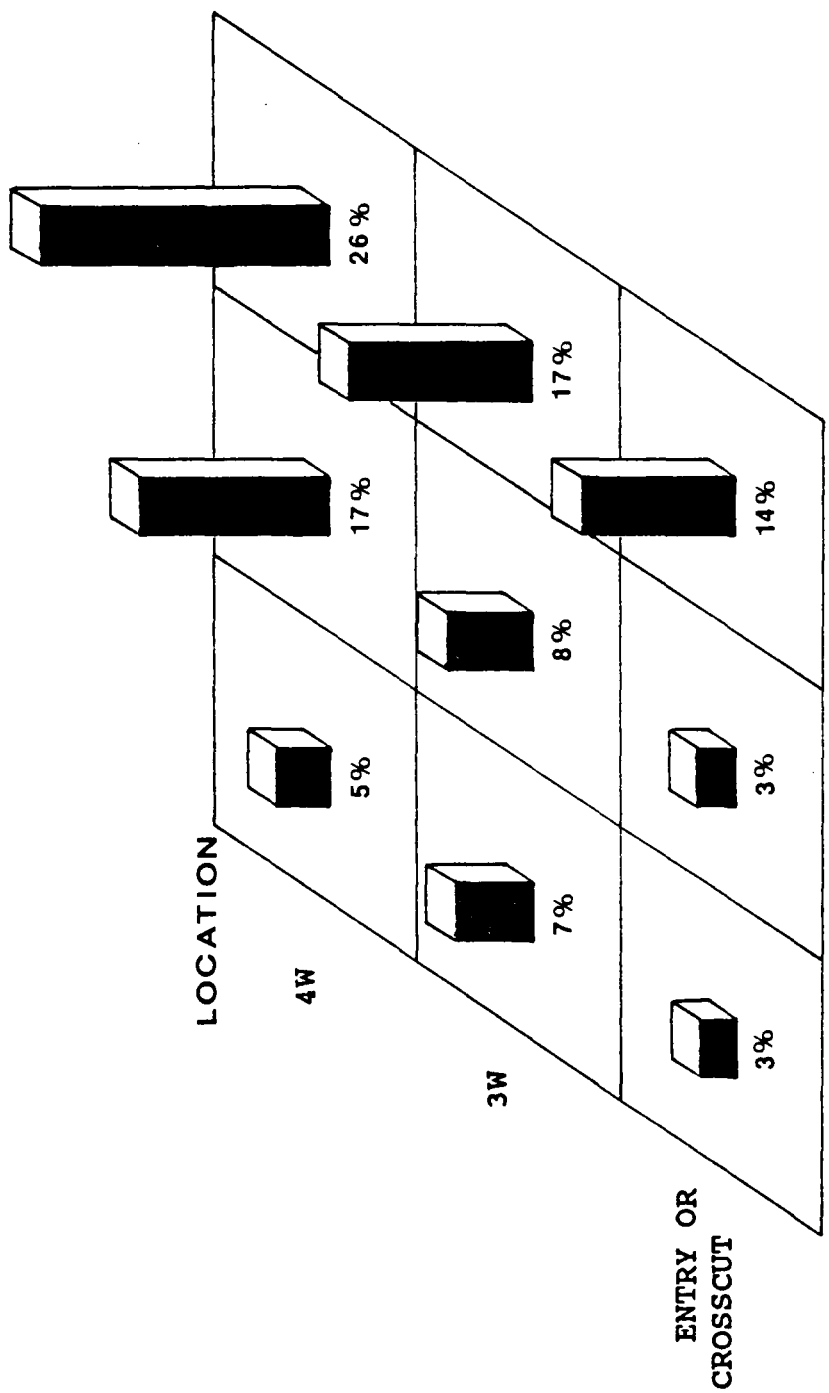

Figure 4.4: Percentage of observations for each roof type at different locations.

orientation and dip angle were analyzed for their effect on roof stability.

Regression analysis was performed to determine the strength of any relationships between fall size and such numeric variables as coal height, roof fracture density, entry width, cross-cut width, deviation of roof fracture trend from entry and cross-cut trends, and the dip angle of roof fractures.

4.2 RESULTS OF THE STATISTICAL ANALYSIS

4.2.1 Location

Location within the mine plays a significant role in roof stability. Chi-square analysis for the three roof types shows that for Interface Roof, position is not a factor (Table 4.1). However, for Sandstone and Shale Roof, strong correlations between location and roof failure are found (Tables 4.2 and 4.3). Sandstone Roof has a chi-square probability of 0.0017 and Shale Roof one of 0.0001, both of which are well below the 0.05 significance level recommended for chi-square analysis.

Location has been shown to be a factor in the occurrence of a fall for shale and sandstone roofs. Entries or cross-cuts had a greater chance of failure. The mean approximate fall size for each roof type at a particular location shows the opposite trend (Figure 4.5). The smallest falls occur in entries in cross-cuts and the largest in

TABLE 4.1

Chi-square analysis of location versus roof failure for Interface Roof

Frequency
Percent
Row Percent
Column Percent

LOCATION	FALL: NO	YES	TOTAL
Entry or Cross-cut	5	11	16
	7.04	15.49	22.54
	31.25	68.75	
	15.63	28.21	
3-Way Intersection	17	16	33
	23.94	22.54	46.48
	51.52	48.48	
	53.13	41.03	
4-Way Intersection	10	12	22
	14.08	16.90	30.99
	45.45	54.55	
	31.25	30.77	
TOTAL	32	39	71
	45.07	54.93	100.00

CHI-SQUARE 1.789 DEGREES OF FREEDOM = 2

PROBABILITY = 0.4087

TABLE 4.2

Chi-square analysis of location versus roof failure for Sandstone Roof

Frequency
Percent
Row Percent
Column Percent

LOCATION	FALL: NO	YES	TOTAL
Entry or Cross-cut	5	12	17
	3.68	8.82	12.50
	29.41	70.59	
	5.56	26.09	
3-Way Intersection	24	13	37
	17.65	9.56	27.21
	64.86	35.14	
	26.67	28.26	
4-Way Intersection	61	21	82
	44.85	15.44	60.29
	74.39	25.61	
	67.78	45.65	
TOTAL	90	46	136
	66.18	33.82	100.00

CHI-SQUARE 12.766 DEGREES OF FREEDOM = 2

PROBABILITY = 0.0017

TABLE 4.3

Chi-square analysis of location versus roof failure for Shale Roof

Frequency
Percent
Row Percent
Column Percent

LOCATION	FALL: YES	NO	TOTAL
Entry or Cross-cut	6	62	68
	2.26	23.31	25.56
	8.82	91.18	
	5.26	40.79	
3-Way Intersection	42	37	79
	15.79	13.91	29.70
	53.16	46.84	
	36.84	24.34	
4-Way Intersection	66	53	119
	24.81	19.92	44.74
	55.46	44.54	
	57.89	34.87	
TOTAL	114	152	266
	42.86	57.14	100.00

CHI-SQUARE 43.310 DEGREES OF FREEDOM = 2

PROBABILITY = 0.0001

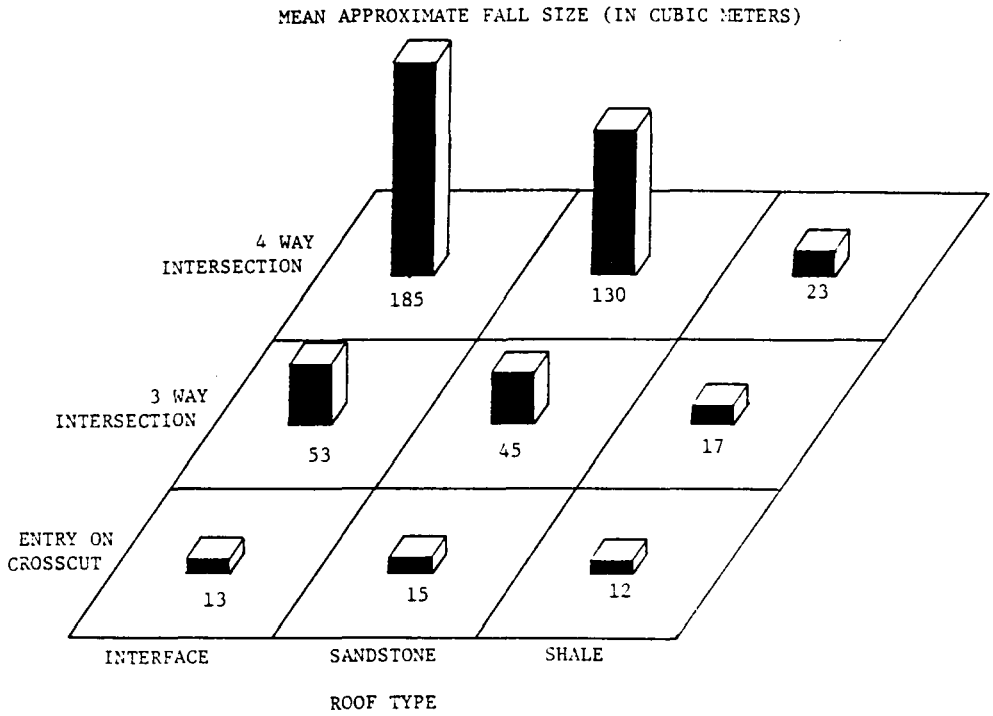

Figure 4.5: Mean approximate fall sizes for each roof type and location.

4-way intersections. This indicates that the unsupported span is probably the most important factor in controlling fall size. The effect is most noticeable in Interface Roof where the average fall size, in a 4-way intersection, is three times that of an entry fall. Shale roof, on the other hand, shows the smallest average approximate fall size and also the smallest relative increase. The overriding influence of other factors,therefore, has to be considered whose importance is by far more significant in stability than the geometry of the opening as expressed by its span.

4.2.2 Faulting within the Coal

Since intense faulting within the coal might imply a highly fractured roof, it was felt that faulting and deformation within the coal seam itself would be an indicator of roof stability. Interface roof (Table 4.4), and Sandstone Roof (Table 4.5), do not demonstrate any correlation between roof fall occurrence and the presence of fault within the coal. This is believed to be due to the somewhat rigid nature of these roof types. Sandstone Roof, when stressed by tectonic forces, is more likely to crush the coal beneath it before actually fracturing itself. Figure 4.6 shows a highly faulted coal beneath a massive sandstone top. Interface roof, which has interbedded sandstone, can also act as a stiff composite material through which stress is trans-

TABLE 4.4

Chi-square analysis of faulting in coal versus roof failure for Interface Roof

Frequency
Percent
Row Percent
Column Percent

COAL	FALL : NO	YES	TOTAL
Fault Not Present	10	12	22
	24.39	29.27	53.66
	45.45	54.55	
	52.63	54.55	
Fault Present	9	10	19
	21.95	24.39	46.34
	47.37	52.63	
	47.37	45.45	
TOTAL	19	22	41
	46.34	53.66	100.00

CHI-SQUARE 0.015 DEGREES OF FREEDOM = 1

PROBABILITY = 0.9025

TABLE 4.5

Chi-square analysis of faulting in coal versus roof failure for Sandstone Roof

Frequency
Percent
Row Percent
Column Percent

COAL	FALL : NO	YES	TOTAL
Fault Not Present	46	14	60
	46.00	14.00	60.00
	76.67	23.33	
	62.16	53.85	
Fault Present	28	12	40
	28.00	12.00	40.00
	70.00	30.00	
	37.84	46.15	
TOTAL	74	26	100
	74.00	26.00	100.00

CHI-SQUARE 0.554 DEGREES OF FREEDOM = 1

PROBABILITY = 0.4565

Figure 4.6: Faulted coal beneath massive Sandstone Roof.

mitted to the coal beneath it.

Shale roof shows a remarkable degree of correlation between the presence of faulting in the coal and roof failure (Table 4.6). The chi-square probability of 0.0165 establishes a high degree of dependence between the two variables. This can be explained by the presence of bedding parallel thrust faults, or decollements, which are relatively common in this area of Virginia. These decollements ramp up through the coal and flatten in shales along the top of the coal bed (Figures 4.7 and 4.8). These zones (1.0 - 5.0 centimeters thick) of polished and slickensided shales are commonly seen on the tops of the coal beds in these areas. This is the result of the entire roof having slid, unfractured, a short distance along the top of the coal during the late Paleozoic (Appalachian) orogeny (Milici et al., 1982). Due to changing stress conditions in some places, the faults ramp up again this time into the roof, and problems may result. This phenomenon is found almost exclusively in Shale Roof. As mentioned previously, massive sandstones, and rigid Interface Roof, probably act to confine faulting and movement to the coal itself. Thus, faulted coal may be viewed as a strong indicator of roof instability for Shale Roof.

An attempt to determine if faulting within the coal might serve as an indicator of fall type and, hence, approximate size and shape, yielded no positive results (Tables

TABLE 4.6

Chi-square analysis of faulting in coal versus roof failure for Shale Roof

Frequency
Percent
Row Percent
Column Percent

COAL	FALL : NO	YES	TOTAL
Fault Not Present	51	35	86
	30.54	20.96	51.50
	59.30	40.70	
	60.71	42.17	
Fault Present	33	48	81
	19.76	28.74	48.50
	40.74	59.26	
	39.29	57.83	
TOTAL	84	83	167
	50.30	49.70	100.00

CHI-SQUARE 5.749 DEGREES OF FREEDOM = 1

PROBABILITY = 0.0165

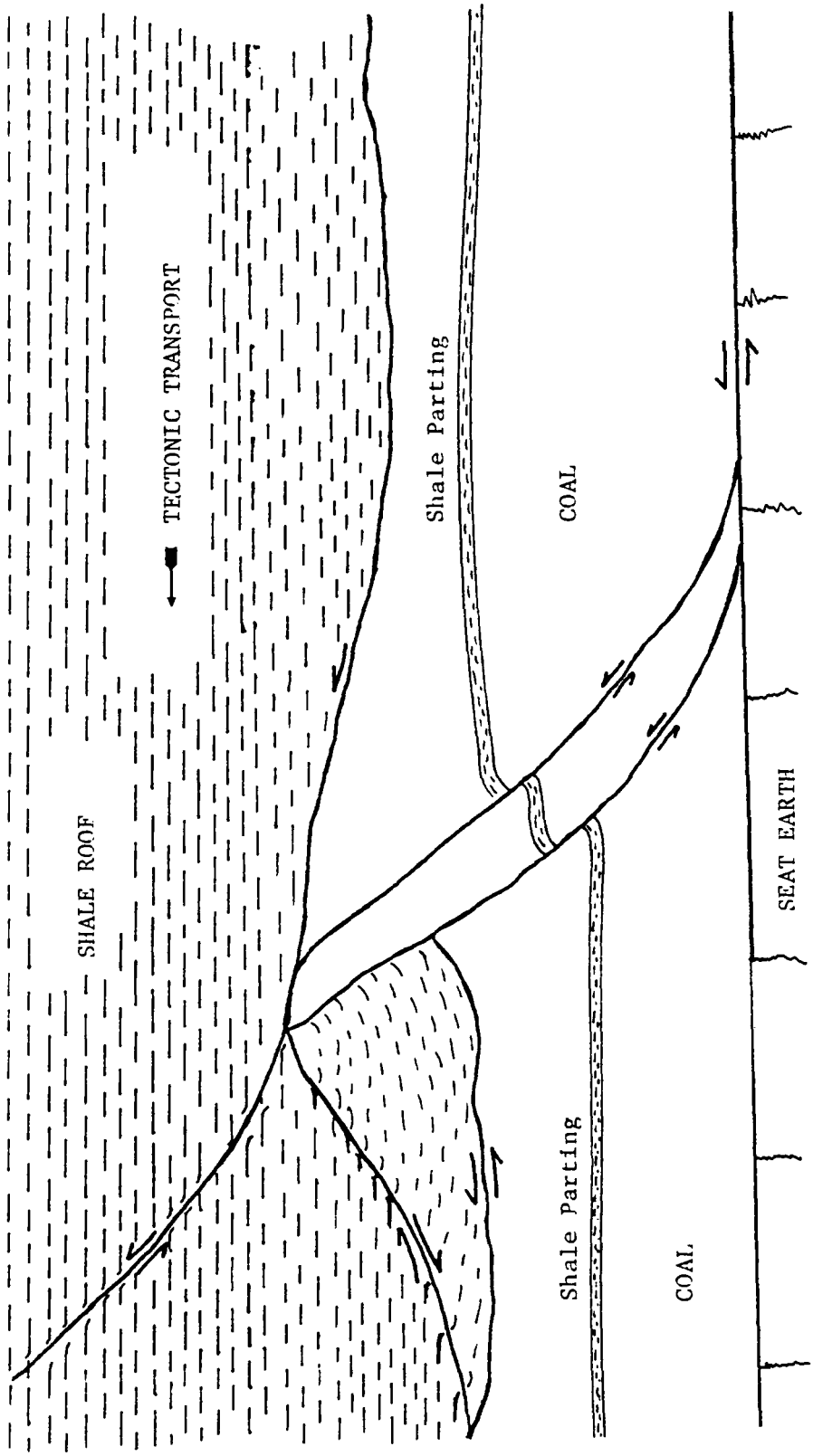

Figure 4.7: Generalized diagram of a decollement within a coal seam.

Figure 4.8: Decollement seen in mine roof (photograph by T. M. Gathright, II).

4.7, 4.8, and 4.9). No chi-square probabilities were low enough to suggest a correlation. Not enough data was available for falls occurring after the roof was bolted, but the limited data available also indicate that fall type and fracturing of the coal is independent (Tables 4.10, 4.11, and 4.12).

4.2.3 Fossils

Figure 4.9 shows the relative percentage of stations containing fossils for the different roof types. The presence of fossils may be an indicator of potential roof failure. When examinining Interface Roof, fossils do not appear to be an important factor in roof stability (Table 4.13). The same is true for Shale Roof (Table 4.14), although the chi-square probability is lower, 0.4347 as opposed to 1.000 for Interface Roof. Sandstone Roof is the only roof type demonstrating a strong correlation, chi-square probability of 0.0251 (Table 4.15). The risk of a fall increases by a factor of about 2.5 when fossils are found within the sandstone. This can be attributed to the fact that carbonaceous bedding planes and beds with large concentrations of fossils can be common in sandstone channels. These bedding planes can constitute a major plane of weakness as they possess little or no tensile strength, and can cause a roof fall if they occur within close proximity above the coal seam.

TABLE 4.7

Chi-square analysis of faulting in coal versus fall type for Interface Roof

Frequency
Percent
Row Percent
Column Percent

FAILURE TYPE	FAULTED COAL : NO	YES	TOTAL
Domal	3	0	3
	13.64	0.00	13.64
	100.00	0.00	
	25.00	0.00	
Minor	2	1	3
	9.09	4.55	13.64
	66.67	33.33	
	16.67	10.00	
Sloughing	7	9	16
	31.82	40.91	72.73
	43.75	56.25	
	58.33	90.00	
TOTAL	12	10	22
	54.55	45.45	100.00

CHI-SQUARE 3.430 DEGREES OF FREEDOM = 2

PROBABILITY = 0.1800

TABLE 4.8

Chi-square analysis of faulting in coal versus fall type for Sandstone Roof

Frequency
Percent
Row Percent
Column Percent

FAILURE TYPE	FAULTED COAL : NO	YES	TOTAL
Arch	1	1	2
	3.85	3.85	7.69
	50.00	50.00	
	7.14	8.33	
Domal	0	1	1
	0.00	3.85	3.85
	0.00	100.00	
	0.00	8.33	
Minor	4	4	8
	15.38	15.38	30.77
	50.00	50.00	
	28.57	33.33	
Sloughing	9	6	15
	34.62	23.08	57.69
	60.00	40.00	
	64.29	50.00	
TOTAL	14	12	26
	53.85	46.15	100.00

CHI-SQUARE 1.455 DEGREES OF FREEDOM = 3

PROBABILITY = 0.6927

TABLE 4.9

Chi-square analysis of faulting in coal versus fall type for Shale Roof

Frequency
Percent
Row Percent
Column Percent

FAILURE TYPE	FAULTED COAL : NO	YES	TOTAL
Arch	4	5	9
	4.82	6.02	10.84
	44.44	55.56	
	11.43	10.42	
Domal	2	4	6
	2.41	4.82	7.23
	33.33	66.67	
	5.71	8.33	
Minor	14	18	32
	16.87	21.69	38.55
	43.75	56.25	
	40.00	37.50	
Sloughing	15	21	36
	18.07	25.30	43.37
	41.67	58.33	
	42.86	43.75	
TOTAL	35	48	83
	42.17	57.83	100.00

CHI-SQUARE 0.248 DEGREES OF FREEDOM = 3

PROBABILITY = 0.9695

TABLE 4.10

Chi-square analysis of faulting in coal versus fall type for Interface Roof after bolting

Frequency
Percent
Row Percent
Column Percent

FAILURE TYPE	FAULTED COAL : NO	YES	TOTAL
Domal	1	0	1
	50.00	0.00	50.00
	100.00	0.00	
	50.00	0.00	
Sloughing	1	0	1
	50.00	0.00	50.00
	100.00	0.00	
	50.00	0.00	
TOTAL	2	0	2
	100.00	0.00	100.00

TABLE 4.11

Chi-square analysis of faulting in coal versus fall type for Sandstone Roof after bolting

Frequency
Percent
Row Percent
Column Percent

FAILURE TYPE	FAULTED COAL : NO	YES	TOTAL
Arch	1	1	2
	11.11	11.11	22.22
	50.00	50.00	
	20.00	25.00	
Minor	0	1	1
	0.00	11.11	11.11
	0.00	100.00	
	0.00	25.00	
Sloughing	4	2	6
	44.44	22.22	66.67
	66.67	33.33	
	80.00	50.00	
TOTAL	5	4	9
	55.56	44.44	100.00

CHI-SQUARE 1.575 DEGREES OF FREEDOM = 2

PROBABILITY = 0.4550

TABLE 4.12

Chi-square analysis of faulting in coal versus fall type for Shale Roof after bolting

Frequency
Percent
Row Percent
Column Percent

FAILURE TYPE	FAULTED COAL : NO	YES	TOTAL
Arch	1	0	1
	10.00	0.00	10.00
	100.00	0.00	
	33.33	0.00	
Domal	1	2	3
	10.00	20.00	30.00
	33.33	66.67	
	33.33	28.57	
Minor	1	4	5
	10.00	40.00	50.00
	20.00	80.00	
	33.33	57.14	
Sloughing	0	1	1
	0.00	10.00	10.00
	0.00	100.00	
	0.00	14.29	
TOTAL	3	7	10
	30.00	70.00	100.00

CHI-SQUARE 3.016 DEGREES OF FREEDOM = 3

PROBABILITY = 0.3892

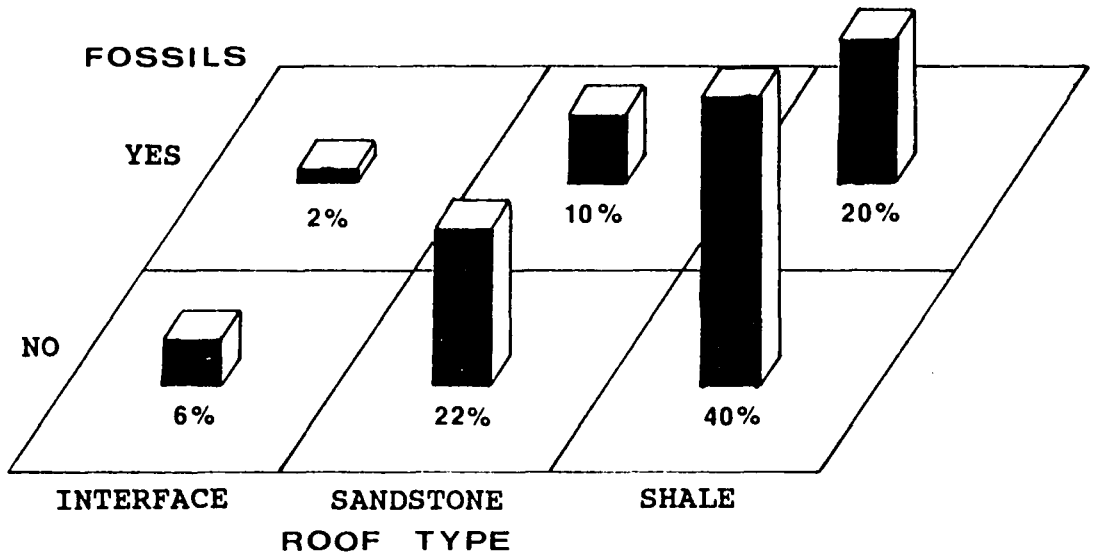

Figure 4.9: Percentage of observations where fossils were present.

TABLE 4.13

Chi-square analysis of the presence of fossils versus roof failure for Interface Roof

Frequency
Percent
Row Percent
Column Percent

FOSSILS	FALL : NO	YES	TOTAL
Absent	3	12	15
	15.00	60.00	75.00
	20.00	80.00	
	75.00	75.00	
Present	1	4	5
	5.00	20.00	25.00
	20.00	80.00	
	25.00	25.00	
TOTAL	4	16	20
	20.00	80.00	100.00

CHI-SQUARE 0.000 DEGREES OF FREEDOM = 1

PROBABILITY = 1.0000

TABLE 4.14

Chi-square analysis of the presence of fossils versus roof failure for Shale Roof

Frequency
Percent
Row Percent
Column Percent

FOSSILS	FALL : NO	YES	TOTAL
Absent	39	57	96
	26.71	39.04	65.75
	40.63	59.38	
	69.64	63.33	
Present	17	33	50
	11.64	22.60	34.25
	34.00	66.00	
	30.36	36.67	
TOTAL	56	90	146
	38.36	61.64	100.00

CHI-SQUARE 0.610 DEGREES OF FREEDOM = 1

PROBABILITY = 0.4347

TABLE 4.15

Chi-square analysis of the presence of fossils versus roof failure for Sandstone Roof

Frequency
Percent
Row Percent
Column Percent

FOSSILS	FALL : NO	YES	TOTAL
Absent	46	8	54
	58.97	10.26	69.23
	85.19	14.81	
	75.41	47.06	
Present	15	9	24
	19.23	11.54	30.77
	62.50	37.50	
	24.59	52.94	
TOTAL	61	17	78
	78.21	21.79	100.00

CHI-SQUARE 5.017 DEGREES OF FREEDOM = 1

PROBABILITY = 0.0251

The results of a comparison of fall type versus the presence of fossils is shown in Tables 4.16, 4.17, and 4.18. Interface Roof fails to show any correlation (Table 4.16). Surprisingly, Sandstone Roof has a high chi-square probability, 0.4501, also (Table 4.17). Chi-square analysis for Shale Roof, on the other hand, indicates somewhat of a relationship. Fossils seem to be most important in sloughing where 50% of falls had fossils present. Larger falls tended to be correlated with the absence of fossils.

4.2.4 Slickensides

Slickensides are another deleterious feature found within coal mine roof. As Figure 4.10 shows, most occurrences of Shale Roof were found to have slickensides present while the opposite was true for Sandstone Roof. Roughly half the examples of Interface Roof were found to have slickensides.

The presence of slickensides in Interface Roof does not seem to indicate a potential problem as seen in Table 4.19. It should be noted however, that slickensides are not common in this roof type. The occurrence of slickensides in Sandstone Roof demonstrates a stronger correlation with roof falls (Table 4.20). The value of 0.1430 for the chi-square probability is still not great enough to use these features as an indicators. Shale Roof, on the other hand, is greatly affected by slickensides (Table 4.21). In fact, the possi-

TABLE 4.16

Chi-square analysis of the presence of fossils versus roof fall type for Interface Roof

Frequency
Percent
Row Percent
Column Percent

FAILURE TYPE	FOSSILS : NO	YES	TOTAL
Arch	1	0	1
	6.25	0.00	6.25
	100.00	0.00	
	8.33	0.00	
Domal	2	1	3
	12.50	6.25	18.75
	66.67	33.33	
	16.67	25.00	
Minor	2	0	2
	12.50	0.00	12.50
	100.00	0.00	
	16.67	0.00	
Sloughing	7	3	10
	43.75	18.75	62.50
	70.00	30.00	
	58.33	75.00	
TOTAL	12	4	16
	75.00	25.00	100.00

CHI-SQUARE 1.244 DEGREES OF FREEDOM = 3

PROBABILITY = 0.7424

TABLE 4.17

Chi-square analysis of the presence of fossils versus roof failure for Sandstone Roof

Frequency
Percent
Row Percent
Column Percent

FAILURE TYPE	FOSSILS : NO	YES	TOTAL
Arch	1	0	1
	5.88	0.00	5.88
	100.00	0.00	
	12.50	0.00	
Domal	1	0	1
	5.88	0.00	5.88
	100.00	0.00	
	12.50	0.00	
Minor	1	1	2
	5.88	5.88	11.76
	50.00	50.00	
	12.50	11.11	
Sloughing	5	8	13
	29.41	47.06	76.47
	38.46	61.54	
	62.50	88.89	
TOTAL	8	9	17
	47.06	52.94	100.00

CHI-SQUARE 2.643 DEGREES OF FREEDOM = 3

PROBABILITY = 0.4501

TABLE 4.18

Chi-square analysis of the presence of fossils versus roof fall type for Shale Roof

Frequency
Percent
Row Percent
Column Percent

FAILURE TYPE	FOSSILS : NO	YES	TOTAL
Arch	3	2	5
	3.33	2.22	5.56
	60.00	40.00	
	5.26	6.06	
Domal	6	2	8
	6.67	2.22	8.89
	75.00	25.00	
	10.53	6.06	
Minor	24	6	30
	26.67	6.67	33.33
	80.00	20.00	
	42.11	18.18	
Sloughing	24	23	47
	26.67	25.56	52.22
	51.06	48.94	
	42.11	69.70	
TOTAL	57	33	90
	63.33	36.67	100.00

CHI-SQUARE 7.128 DEGREES OF FREEDOM = 3

PROBABILITY = 0.0679

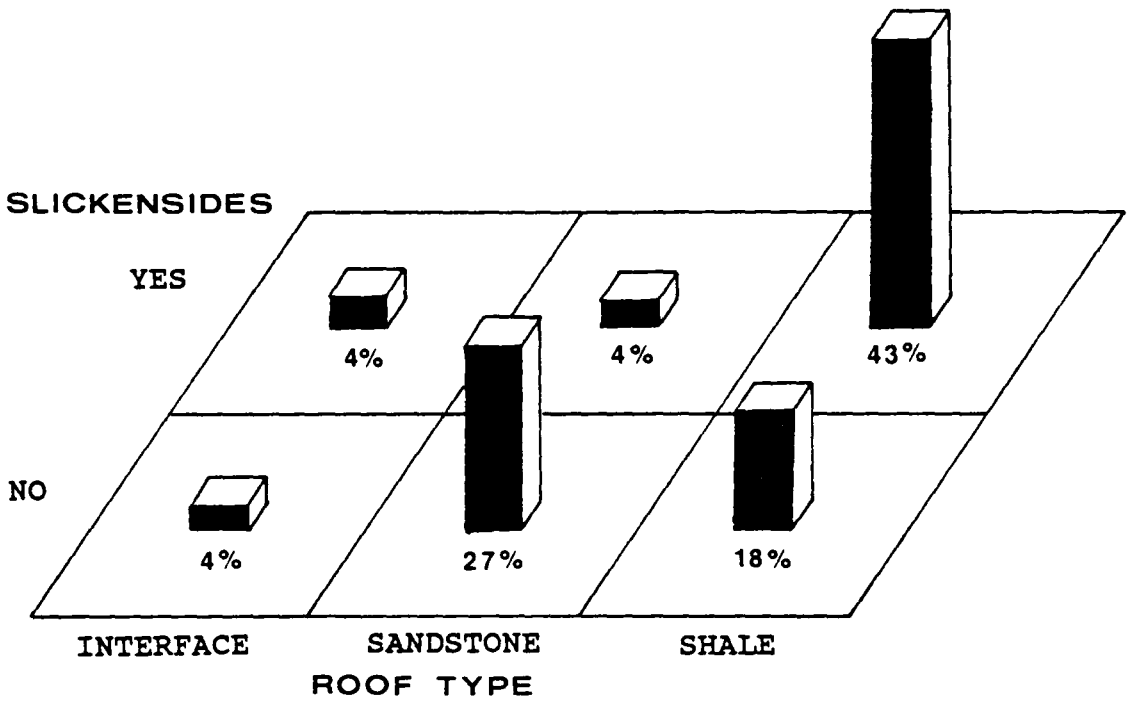

Figure 4.10: Percentage of observations where slickensides were found.

TABLE 4.19

Chi-square analysis of the presence of slickensides versus roof failure for Interface Roof

Frequency
Percent
Row Percent
Column Percent

SLICKENSIDES	FALL : NO	YES	TOTAL
Absent	2	6	8
	10.53	31.58	42.11
	25.00	75.00	
	50.00	40.00	
Present	2	9	11
	10.53	47.37	57.89
	18.18	81.82	
	50.00	60.00	
TOTAL	4	15	19
	21.05	78.95	100.00

CHI-SQUARE 0.130 DEGREES OF FREEDOM = 1

PROBABILITY = 0.7189

TABLE 4.20

Chi-square analysis of the presence of slickensides versus roof failure for Sandstone Roof

Frequency
Percent
Row Percent
Column Percent

SLICKENSIDES	FALL : NO	YES	TOTAL
Absent	54	13	67
	70.13	16.88	87.01
	80.60	19.40	
	90.00	76.47	
Present	6	4	10
	7.79	5.19	12.99
	60.00	40.00	
	10.00	23.53	
TOTAL	60	17	77
	77.92	22.08	100.00

CHI-SQUARE 2.146 DEGREES OF FREEDOM = 1

PROBABILITY = 0.1430

TABLE 4.21

Chi-square analysis of the presence of slickensides versus roof failure for Shale Roof

Frequency
Percent
Row Percent
Column Percent

SLICKENSIDES	FALL : NO	YES	TOTAL
Absent	35	9	44
	23.97	6.16	30.14
	79.55	20.45	
	62.50	10.00	
Present	21	81	102
	14.38	55.48	69.86
	20.59	79.41	
	37.50	90.00	
TOTAL	56	90	146
	38.36	61.64	100.00

CHI-SQUARE 45.191 DEGREES OF FREEDOM = 1

PROBABILITY = 0.0001

bility of a fall almost triples when slickensides are present in this roof type. The chi-square probability in this case is 0.0001 which shows an extremely high degree of dependence between roof falls and the presence of slickensides. Not only are falls more common in Shale Roof where slickensides occur, but they also tend to be much larger. Mean approximate fall sizes are almost three times larger for areas with slickensided zones in Shale Roof (Figure 4.11). This relationship does not hold true for Interface or Sandstone Roof (Figures 4.12 and 4.13).

An analysis was made of the relationship of roof failure type to the presence of slickensides in the different roof types. In no case was it possible to establish a correlation between these variables. This is evidenced in Tables 4.22, 4.23, and 4.24.

4.2.5 Water

As noted previously, records were made concerning the effect of water in roof stability. It has been noted in the literature (Headlee, 1944 and others) that water and water pressure can have a detrimental effect on coal mine roof stability. During the course of this study, it was found that water was not present in most roof falls. In fact, it can be stated that for the mines surveyed in southwestern Virginia, the role of water in the roof failure process is negligible. This is borne out by an examination of Figure

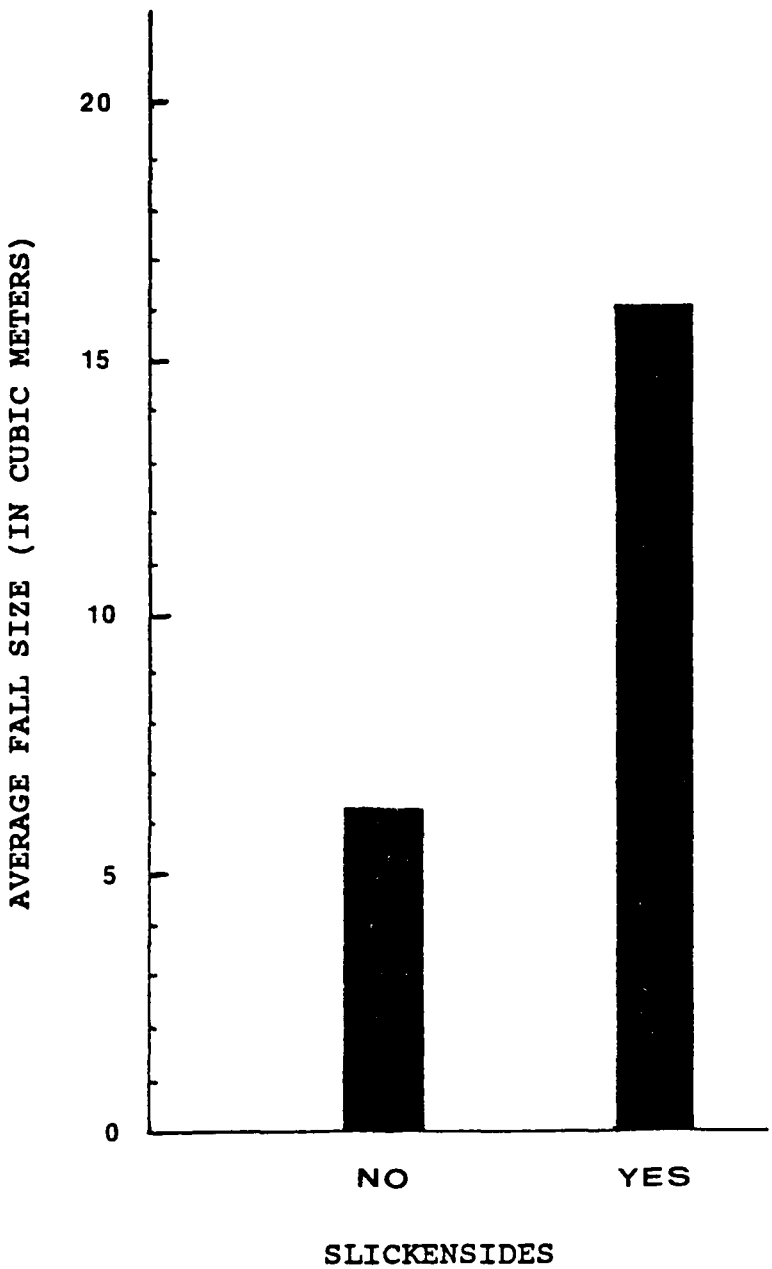

Figure 4.11: Mean approximate fall sizes for Shale Roof with and without slickensides.

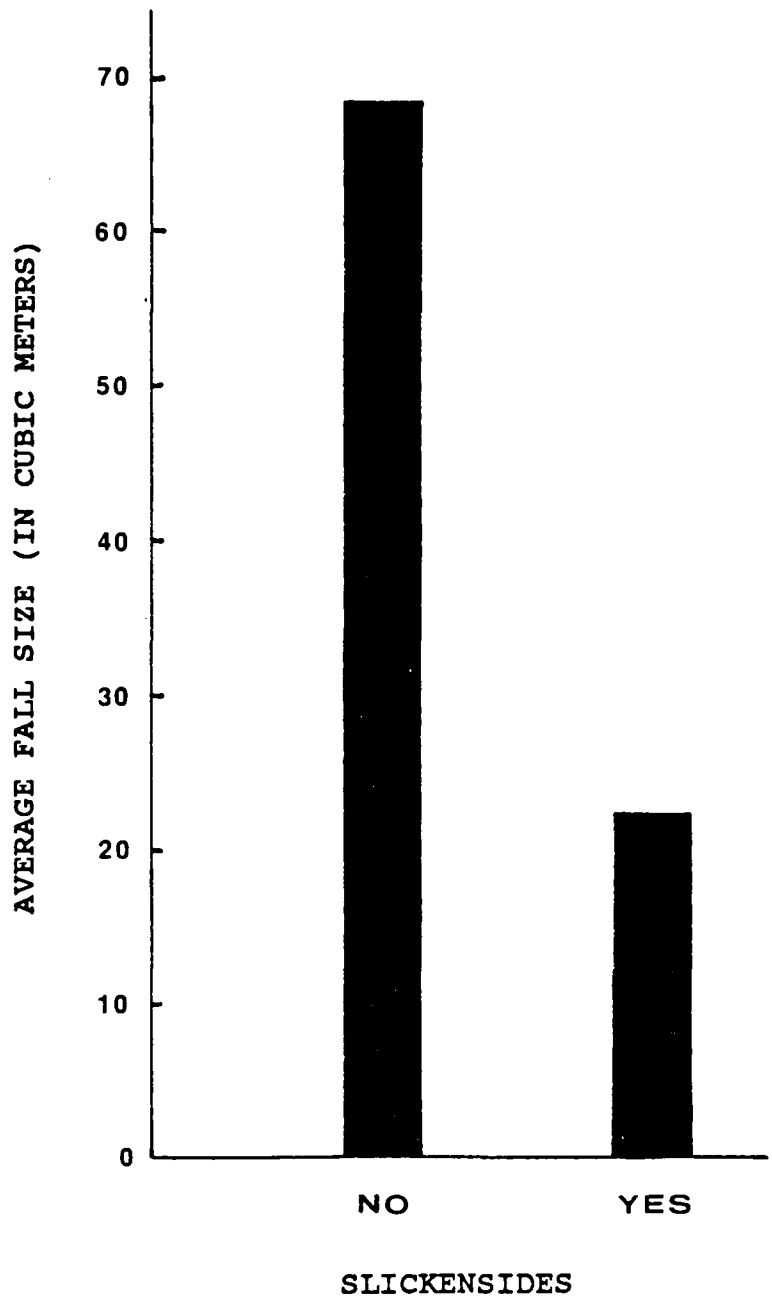

Figure 4.12: Mean approximate fall sizes for Interface Roof with and without slickensides.

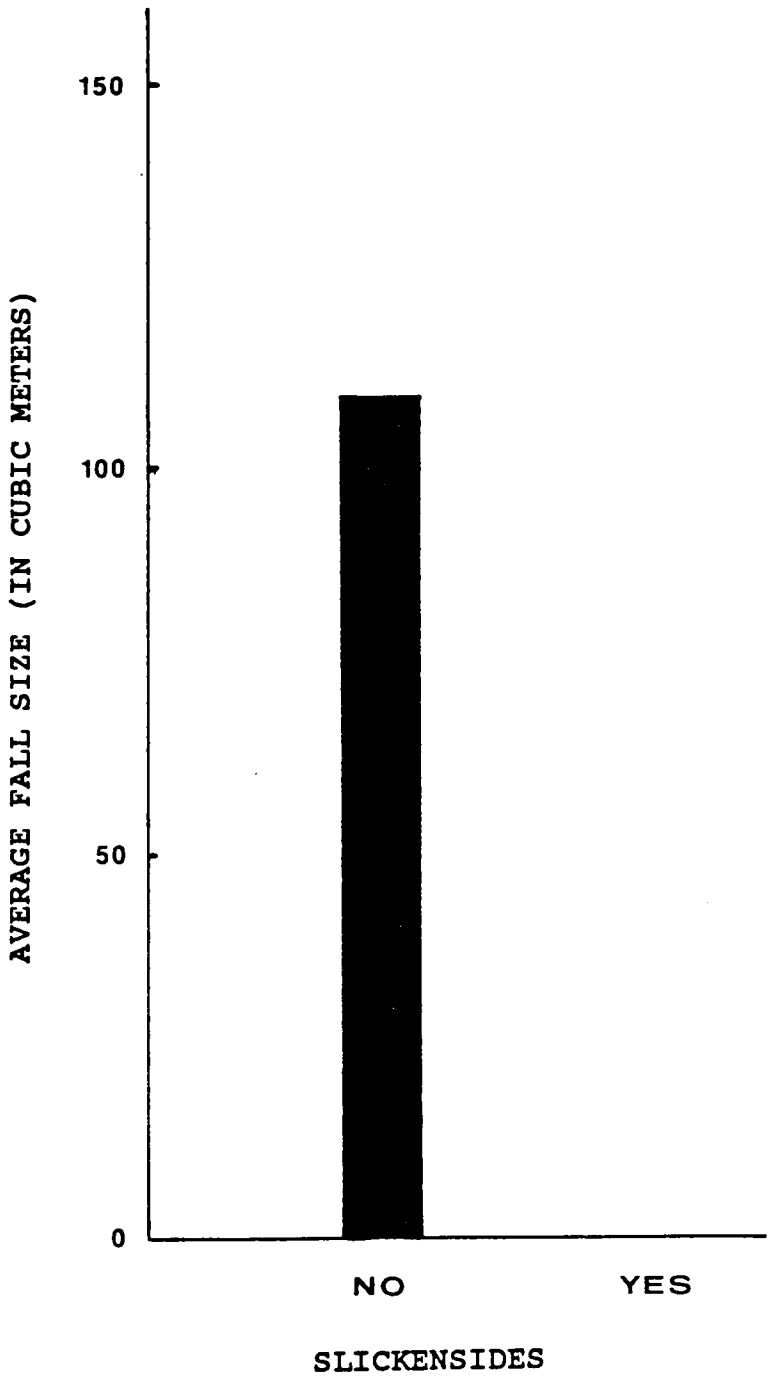

Figure 4.13: Mean approximate fall sizes for Sandstone Roof with and without slickensides.

TABLE 4.22

Chi-square analysis of the presence of slickensides versus roof fall type for Interface Roof

Frequency
Percent
Row Percent
Column Percent

FAILURE TYPE	SLICKEN-SIDES : NO	YES	TOTAL
Arch	0	1	1
	0.00	6.67	6.67
	0.00	100.00	
	0.00	11.11	
Domal	1	2	3
	6.67	13.33	20.00
	33.33	66.67	
	16.67	22.22	
Minor	1	1	2
	6.67	6.67	13.33
	50.00	50.00	
	16.67	11.11	
Sloughing	4	5	9
	26.67	33.33	60.00
	44.44	55.56	
	66.67	55.56	
TOTAL	6	9	15
	40.00	60.00	100.00

CHI-SQUARE 0.880 DEGREES OF FREEDOM = 3

PROBABILITY = 0.8303

TABLE 4.23

Chi-square analysis of the presence of slickensides versus roof fall type for Sandstone Roof

Frequency
Percent
Row Percent
Column Percent

FAILURE TYPE	SLICKEN-SIDES : NO	YES	TOTAL
Arch	1	0	1
	5.88	0.00	5.88
	100.00	0.00	
	7.69	0.00	
Domal	1	0	1
	5.88	0.00	5.88
	100.00	0.00	
	7.69	0.00	
Minor	2	0	2
	11.76	0.00	11.76
	100.00	0.00	
	15.38	0.00	
Sloughing	9	4	13
	52.94	23.53	76.47
	69.23	30.77	
	69.23	100.00	
TOTAL	13	4	17
	76.47	23.53	100.00

CHI-SQUARE 1.609 DEGREES OF FREEDOM = 3

PROBABILITY = 0.6572

TABLE 4.24

Chi-square analysis of the presence of slickensides versus roof fall type for Shale Roof

Frequency
Percent
Row Percent
Column Percent

FAILURE TYPE	SLICKEN-SIDES : NO	YES	TOTAL
Arch	0	5	5
	0.00	5.56	5.56
	0.00	100.00	
	0.00	6.17	
Domal	0	8	8
	0.00	8.89	8.89
	0.00	100.00	
	0.00	9.88	
Minor	3	27	30
	3.33	30.00	33.33
	10.00	90.00	
	33.33	33.33	
Sloughing	6	41	47
	6.67	45.56	52.22
	12.77	87.23	
	66.67	50.62	
TOTAL	9	81	90
	10.00	90.00	100.00

CHI-SQUARE 1.844 DEGREES OF FREEDOM = 3

PROBABILITY = 0.6054

4.14 and Tables 4.25, 4.26, and 4.27. In only three cases of Shale Roof water was found to be present in a large enough volume to be noticeable; and in two cases, failure did occur. Water was not found in any measurable amount in any cases of Interface or Sandstone Roof. Thus, it was concluded that water, most notably water pressure was not a significant factor in this analysis.

4.2.6 Time

Time plays an important part in the stability of coal mine roofs. Table 4.28 demonstrates just how important this role is.

By grouping all roof types together, it can be seen that a very strong chi-square relationship exists for roof falls and time. Arch and domal falls which, by definition, are large falls usually occur after bolting. Minor falls and sloughing failures, on the other hand, take place almost immediately after the coal is mined. This dependence is true for all three roof types: Interface (Table 4.29), Sandstone (Table 4.30), and Shale (Table 4.31).

The influence of time on roof failures is further evidenced by Figure 4.15. In this figure, it can be seen that roof falls which occur after bolting are much larger than those which happen before bolting. This is most noticeable in Interface Roof where falls are almost nine times larger after the roof has been bolted. The volume of rock

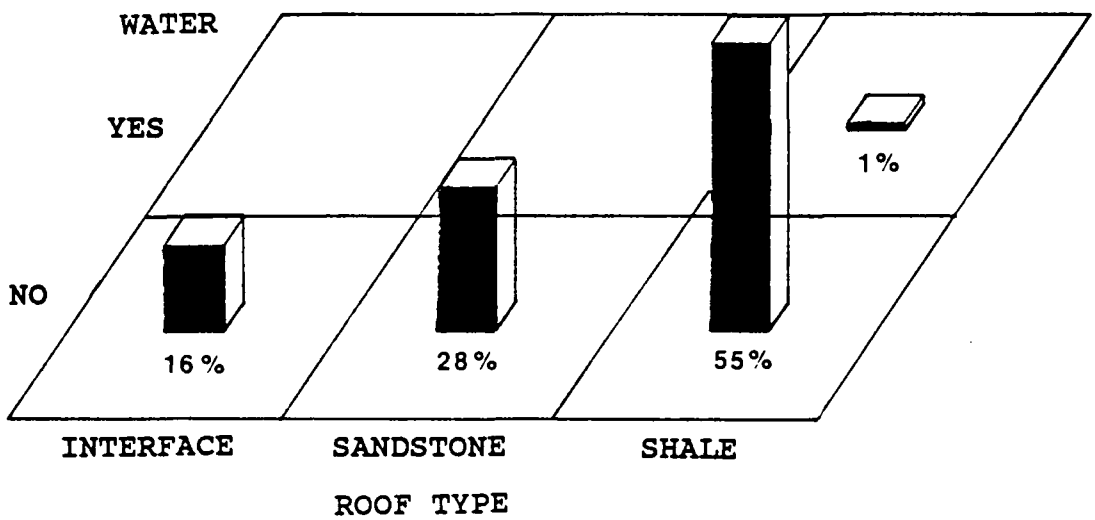

Figure 4.14: Percentage of observations with and without water with regard to roof stability.

TABLE 4.25

Chi-square analysis of the presence of water versus roof fall type for Interface Roof

Frequency
Percent
Row Percent
Column Percent

WATER	FALL : NO	YES	TOTAL
Absent	31	39	70
	44.29	55.71	100.00
	44.29	55.71	
	100.00	100.00	
Present	0	0	0
	0.00	0.00	0.00
	0.00	0.00	
	0.00	0.00	
TOTAL	31	39	70
	44.29	55.71	100.00

TABLE 4.26

Chi-square analysis of the presence of water versus roof fall type for Sandstone Roof

Frequency
Percent
Row Percent
Column Percent

WATER	FALL : NO	YES	TOTAL
Absent	84	34	118
	71.19	28.81	100.00
	71.19	28.81	
	100.00	100.00	
Present	0	0	0
	0.00	0.00	0.00
	0.00	0.00	
	0.00	0.00	
TOTAL	84	34	118
	71.19	28.81	100.00

TABLE 4.27

Chi-square analysis of the presence of water versus roof fall type for Shale Roof

Frequency
Percent
Row Percent
Column Percent

WATER	FALL : NO	YES	TOTAL
Absent	108	126	234
	45.57	53.16	98.73
	46.15	53.85	
	99.08	98.44	
Present	1	2	3
	0.42	0.84	1.27
	33.33	66.67	
	0.92	1.56	
TOTAL	109	128	237
	45.99	54.01	100.00

CHI-SQUARE 0.196 DEGREES OF FREEDOM = 1

PROBABILITY = 0.6580

TABLE 4.28

Chi-square analysis of the role time plays in the occurrence of roof falls

Frequency
Percent
Row Percent
Column Percent

FAILURE TYPE	TIME : POST BOLT	PRE-BOLT	TOTAL
Arch	9	5	14
	8.74	4.85	13.59
	64.29	35.71	
	20.93	8.33	
Domal	10	3	13
	9.71	2.91	12.62
	76.92	23.08	
	23.26	5.00	
Minor	10	23	33
	9.71	22.33	32.04
	30.30	69.70	
	23.26	38.33	
Sloughing	14	29	43
	13.59	28.16	41.75
	32.56	67.44	
	32.56	48.33	
TOTAL	43	60	103
	41.75	58.25	100.00

CHI-SQUARE 12.809 DEGREES OF FREEDOM = 3

PROBABILITY = 0.0051

TABLE 4.29

Chi-square analysis of the effect of time on Interface Roof Stability

Frequency
Percent
Row Percent
Column Percent

FAILURE TYPE	TIME : POST BOLT	PRE-BOLT	TOTAL
Domal	4	0	4
	28.57	0.00	28.57
	100.00	0.00	
	50.00	0.00	
Minor	0	2	2
	0.00	14.29	14.29
	0.00	100.00	
	0.00	33.33	
Sloughing	4	4	8
	28.57	28.57	57.14
	50.00	50.00	
	50.00	66.67	
TOTAL	8	6	14
	57.14	42.86	100.00

CHI-SQUARE 5.833 DEGREES OF FREEDOM = 2

PROBABILITY = 0.0541

TABLE 4.30

Chi-square analysis of the effect of time on Sandstone Roof stability

Frequency
Percent
Row Percent
Column Percent

FAILURE TYPE	TIME : POST BOLT	PRE-BOLT	TOTAL
Arch	5	0	5
	16.13	0.00	16.13
	100.00	0.00	
	31.25	0.00	
Domal	2	0	2
	6.45	0.00	6.45
	100.00	0.00	
	12.50	0.00	
Minor	2	8	10
	6.45	25.81	32.26
	20.00	80.00	
	12.50	53.33	
Sloughing	7	7	14
	22.58	22.58	45.16
	50.00	50.00	
	43.75	46.46	
TOTAL	16	15	31
	51.61	48.39	100.00

CHI-SQUARE 10.579 DEGREES OF FREEDOM = 3

PROBABILITY = 0.0142

TABLE 4.31

Chi-square analysis of the effect of time on Shale Roof Stability

Frequency
Percent
Row Percent
Column Percent

FAILURE TYPE	TIME : POST BOLT	PRE-BOLT	TOTAL
Arch	3	5	8
	5.88	9.80	15.69
	37.50	62.50	
	18.75	14.29	
Domal	3	2	5
	5.88	3.92	9.80
	60.00	40.00	
	18.75	5.71	
Minor	8	10	18
	15.69	19.61	35.29
	44.44	55.56	
	50.00	28.57	
Sloughing	2	18	20
	3.92	35.29	39.22
	10.00	90.00	
	12.50	51.43	
TOTAL	16	35	51
	31.37	68.63	100.00

CHI-SQUARE 7.715 DEGREES OF FREEDOM = 3

PROBABILITY = 0.0523

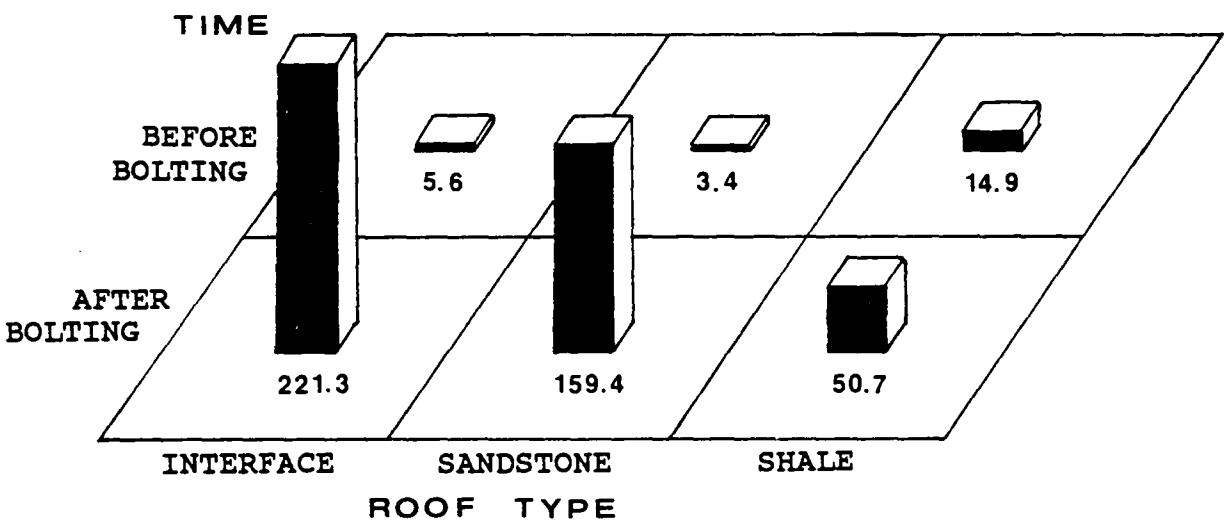

Figure 4.15: Influence of time on fall size (m^3).

involved in Sandstone roof failures is five times larger after bolting and three times larger for Shale Roof.

The best explanation for this strong dependence of both fall type and fall size with time lies in the fact that roof bolts by their nature, bind the rock into massive beams which serve to maintain the roof above the mine. When failure does occur, the amount of material which is held together is much larger than had it been unbolted. Layered Interface Roof is a good example. If left to delaminate without bolting, failure would only be limited to a few layers. However, bolts hold more strata together which, when a failure occurs, provide a much larger mass of material. On the other hand, unstable Shale Roof is often cut through with slickensided fracture planes which serve to break the roof into smaller pieces. Nevertheless, the disparity between roof fall sizes before and after bolting in Shale Roof is still large.

4.2.7 Relation of Fall Type to Roof Type

An attempt was made to determine if a relationship existed between fall types and roof types. When fall types were grouped into four broad categories and chi-square analysis carried out, no clear relationship was found (Table 4.32). Some trends were observed; the most striking being that when Interface and Sandstone Roofs were compared, domal

TABLE 4.32

Chi-square analysis of the effect of roof type on fall type

Frequency
Percent
Row Percent
Column Percent

	ROOF TYPE			
FAILURE TYPE	INTERFACE	SANDSTONE	SHALE	TOTAL
Arch	1	5	13	19
	0.41	2.05	5.33	7.79
	5.26	26.32	68.42	
	2.56	10.64	8.23	
Domal	7	3	10	20
	2.87	1.23	4.10	8.20
	35.00	15.00	50.00	
	17.95	6.38	6.33	
Minor	10	12	57	79
	4.10	4.92	23.36	32.38
	12.66	15.19	72.15	
	25.64	25.53	36.08	
Sloughing	21	27	78	126
	8.61	11.07	31.97	51.64
	16.67	21.43	61.90	
	53.85	57.45	49.37	
TOTAL	39	47	158	244
	15.98	19.26	64.75	100.00

CHI-SQUARE 9.678 DEGREES OF FREEDOM = 6

PROBABILITY = 0.1389

falls favored Interface Roof while arch falls demonstrated a stronger dependence for Sandstone Roof. Once more, it was found that the smaller minor and sloughing failures were the predominant form of roof fall for Shale Roof.

An analysis of falls occurring after bolting was hampered by a lack of data as shown in Table 4.33. However, the trend mentioned above can be seen. Domal falls are predominant in Interface Roof and arch falls more frequent in Sandstone Roof. This is true even in comparison with Shale Roof. An interesting feature is that, although minor falls still occur most readily in Shale Roof, sloughing failures are most frequent in Sandstone Roof.

4.2.8 Roof Failure and Support Type

Tables 4.34, 4.35, and 4.36 present the results of chi-square testing for roof falls and the different roof bolts utilized in the mines studied. This study,however, was hampered by a paucity of data. Determining the time of a fall was often difficult and by dividing these observations between the different bolt types and roof types the data became too sparse to allow any valid conclusions. It was decided to condense the bolt types into two categories irrespective of length: point anchor bolts and fully-grouted resin bolts. When this was achieved, Interface and Sandstone Roof, once more, failed to produce any relationships (Tables 4.37 and 4.38). Table 4.39 shows that bolt

TABLE 4.33

Chi-square analysis of the effect of roof type on fall type for falls after bolting

Frequency
Percent
Row Percent
Column Percent

	ROOF TYPE			
FAILURE TYPE	INTERFACE	SANDSTONE	SHALE	TOTAL
Arch	0	5	3	8
	0.00	12.50	7.50	20.00
	0.00	62.50	37.50	
	0.00	31.25	18.75	
Domal	4	2	3	9
	10.00	5.00	7.50	22.50
	44.44	22.22	33.33	
	50.00	12.50	18.75	
Minor	0	2	8	10
	0.00	5.00	20.00	25.00
	0.00	20.00	80.00	
	0.00	12.50	50.00	
Sloughing	4	7	2	13
	10.00	17.50	5.00	32.50
	30.77	53.85	15.38	
	50.00	43.75	12.50	
TOTAL	8	16	16	40
	20.00	40.00	40.00	100.00

CHI-SQUARE 16.471 DEGREES OF FREEDOM = 6

PROBABILITY = 0.0114

TABLE 4.34

Chi-square analysis of the effect of bolt type on roof stability for Interface Roof

Frequency
Percent
Row Percent
Column Percent

BOLT TYPE	FALL : NO	YES	TOTAL
Point Anchor 60"	1	0	1
	2.44	0.00	2.44
	100.00	0.00	
	3.13	0.00	
Point Anchor 72"	1	0	1
	2.44	0.00	2.44
	100.00	0.00	
	3.13	0.00	
Resin 48"	6	4	10
	14.63	9.76	24.39
	60.00	40.00	
	18.75	44.44	
Resin 60"	24	4	28
	58.54	9.76	68.29
	85.71	14.29	
	75.00	44.44	
Resin 72"	0	1	1
	0.00	2.44	2.44
	0.00	100.00	
	0.00	11.11	
TOTAL	32	9	41
	78.05	21.95	100.00

CHI-SQUARE 6.980 DEGREES OF FREEDOM = 4

PROBABILITY = 0.1370

TABLE 4.35

Chi-square analysis of the effect of bolt type on roof stability for Sandstone Roof

Frequency
Percent
Row Percent
Column Percent

BOLT TYPE	FALL : NO	YES	TOTAL
Point Anchor 60"	3	1	4
	2.78	0.93	3.70
	75.00	25.00	
	3.30	5.88	
Point Anchor 72"	9	2	11
	8.33	1.85	10.19
	81.82	18.18	
	9.89	11.76	
Resin 48"	53	6	59
	49.07	5.56	54.63
	89.83	10.17	
	58.24	35.29	
Resin 60"	25	7	32
	23.15	6.48	29.63
	78.13	21.88	
	27.47	41.18	
Resin 72"	1	1	2
	0.93	0.93	1.85
	50.00	50.00	
	1.10	5.88	
TOTAL	91	17	108
	84.26	15.74	100.00

CHI-SQUARE 4.366 DEGREES OF FREEDOM = 4

PROBABILITY = 0.3587

TABLE 4.36

Chi-square analysis of the effect of bolt type on roof stability for Shale Roof

Frequency
Percent
Row Percent
Column Percent

BOLT TYPE	FALL : NO	YES	TOTAL
Point Anchor 60"	5	2	7
	4.06	1.63	5.69
	71.43	28.57	
	4.80	10.53	
Point Anchor 72"	5	3	8
	4.07	2.44	6.50
	62.50	37.50	
	4.81	15.79	
Resin 48"	33	2	35
	26.83	1.63	28.46
	94.29	5.71	
	31.73	10.53	
Resin 60"	60	12	72
	48.78	9.76	58.54
	83.33	16.67	
	57.69	63.16	
Resin 72"	1	0	1
	0.81	0.00	0.81
	100.00	0.00	
	0.96	0.00	
TOTAL	104	19	123
	84.55	15.45	100.00

CHI-SQUARE 8.455 DEGREES OF FREEDOM = 4

PROBABILITY = 0.1329

TABLE 4.37

Chi-square analysis of the effect of bolt type on roof stability for Interface Roof (condensed)

Frequency
Percent
Row Percent
Column Percent

BOLT TYPE	FALL : NO	YES	TOTAL
Point Anchor	2	0	2
	4.88	0.00	4.88
	100.00	0.00	
	6.25	0.00	
Resin	30	9	39
	73.17	21.95	95.12
	76.92	23.08	
	93.75	100.00	
TOTAL	32	9	41
	78.05	21.95	100.00

CHI-SQUARE 0.591 DEGREES OF FREEDOM = 1

PROBABILITY = 0.4419

TABLE 4.38

Chi-square analysis of the effect of bolt type on roof stability for Sandstone Roof (condensed)

Frequency
Percent
Row Percent
Column Percent

BOLT TYPE	FALL : NO	YES	TOTAL
Point Anchor	12	3	15
	11.11	2.78	13.89
	80.00	20.00	
	13.19	17.65	
Resin	79	14	93
	73.15	12.96	86.11
	84.95	15.05	
	86.81	82.35	
TOTAL	91	17	108
	84.26	15.74	100.00

CHI-SQUARE 0.238 DEGREES OF FREEDOM = 1

PROBABILITY = 0.6255

TABLE 4.39

Chi-square analysis of the effect of bolt type on roof stability for Shale Roof (condensed)

Frequency
Percent
Row Percent
Column Percent

BOLT TYPE	FALL : NO	YES	TOTAL
Point Anchor	10	5	15
	8.13	4.07	12.20
	66.67	33.33	
	9.62	26.32	
Resin	94	14	108
	76.42	11.38	87.80
	87.04	12.96	
	90.38	73.68	
TOTAL	104	19	123
	84.55	15.45	100.00

CHI-SQUARE 4.184 DEGREES OF FREEDOM = 1

PROBABILITY = 0.0408

types are, indeed, important in Shale Roof stability. Nearly 13% of Shale Roofs bolted with resin bolts experienced a failure while one-third of those roofs bolted with point anchor bolts had a fall. It would appear, then, that Shale Roof is most sensitive to the type of bolt used.

An examination of the influence of bolt type on the mode of failure was carried out and the results are shown in Tables 4.40, 4.41, and 4.42. The lack of data proved to be a problem and no conclusions could be drawn.

Finally, the influence of bolt type on fall size can be seen in Figure 4.16. Point anchor bolts appear to be associated with larger falls in Sandstone Roof. Shale Roof demonstrates a remarkable turn-around from the results mentioned above. Even though fully-grouted resin bolts were shown to be less frequently involved in roof falls, Figure 4.16 indicates that they are involved in the largest falls in a Shale Roof. This may somehow be related to the layer-binding effect of the fully grouted bolts. Pieces of material could much more easily fall out between point anchor bolts since the glue is only at the anchoring end.

4.2.9 Fractures in the Roof

Fractures, that is, faults and joints, can be detrimental to mine roof stability. Roof fractures were analyzed with regard to type and orientation. Figure 4.17 shows the

TABLE 4.40

Chi-square analysis of the effect of bolt type on roof fall type for Interface Roof (condensed)

Frequency
Percent
Row Percent
Column Percent

FAILURE TYPE	BOLT : POINT ANCHOR	RESIN	TOTAL
Domal	0	4	4
	0.00	57.14	57.14
	0.00	100.00	
	0.00	57.14	
Sloughing	0	3	3
	0.00	42.86	42.86
	0.00	100.00	
	0.00	42.86	
TOTAL	0	7	7
	0.00	100.00	100.00

TABLE 4.41

Chi-square analysis of the effect of bolt type on roof fall type for Sandstone Roof

Frequency
Percent
Row Percent
Column Percent

FAILURE TYPE	BOLT : POINT ANCHOR	RESIN	TOTAL
Arch	1	4	5
	6.25	25.00	31.25
	20.00	80.00	
	50.00	28.57	
Domal	1	1	2
	6.25	6.25	12.50
	50.00	50.00	
	50.00	7.14	
Minor	0	2	2
	0.00	12.50	12.50
	0.00	100.00	
	0.00	14.29	
Sloughing	0	7	7
	0.00	43.75	43.75
	0.00	100.00	
	0.00	50.00	
TOTAL	2	14	16
	12.50	87.50	100.00

CHI-SQUARE 4.114 DEGREES OF FREEDOM = 3

PROBABILITY = 0.2494

TABLE 4.42

Chi-square analysis of the effect of bolt type on roof fall type for Shale Roof

Frequency
Percent
Row Percent
Column Percent

FAILURE TYPE	BOLT : POINT ANCHOR	RESIN	TOTAL
Arch	0	3	3
	0.00	18.75	18.75
	0.00	100.00	
	0.00	27.27	
Domal	2	1	3
	12.50	6.25	18.75
	66.67	33.33	
	40.00	9.09	
Minor	2	6	8
	12.50	37.50	50.00
	25.00	75.00	
	40.00	54.55	
Sloughing	1	1	2
	6.25	6.25	12.50
	50.00	50.00	
	20.00	9.09	
TOTAL	5	11	16
	31.25	68.75	100.00

CHI-SQUARE 3.588 DEGREES OF FREEDOM = 3

PROBABILITY = 0.3095

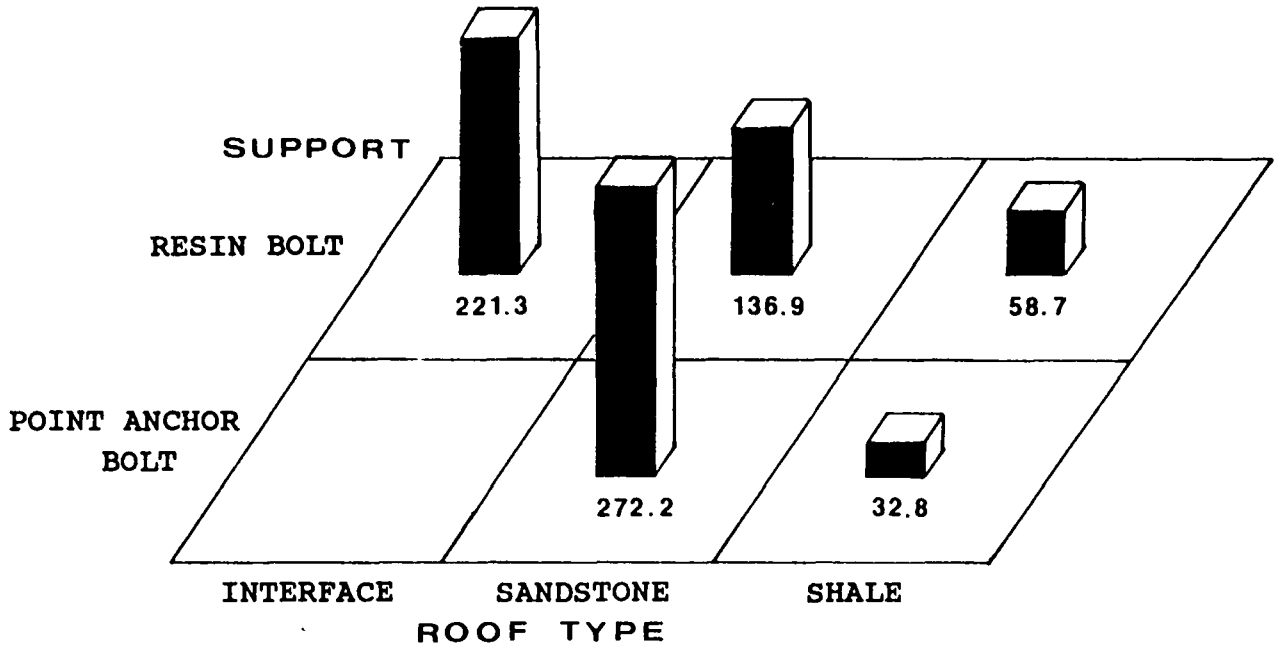

Figure 4.16: Influence of roof bolt type on fall size (m^3).

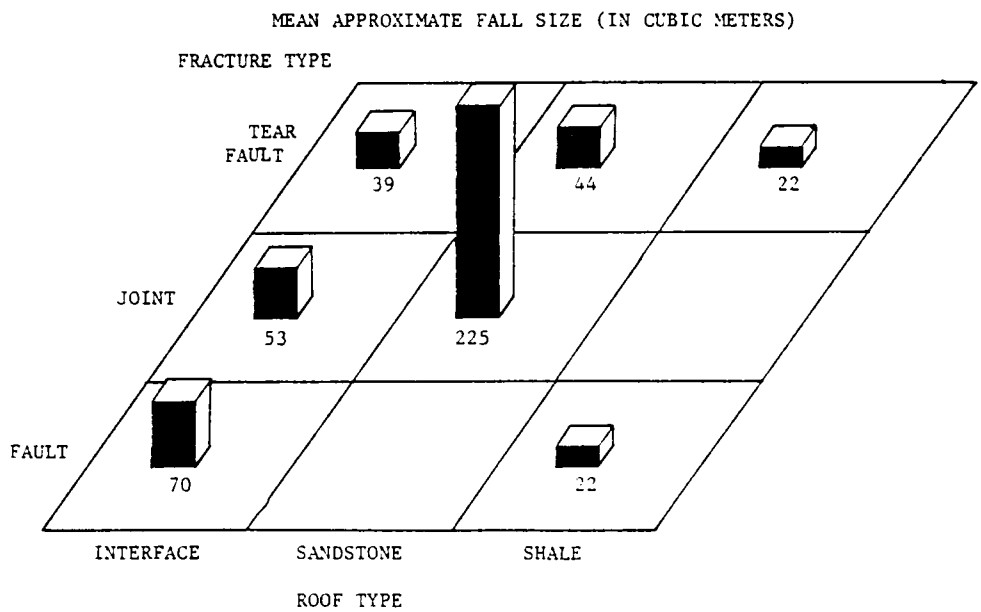

Figure 4.17: Mean approximate fall size for different roof types containing faults or joints.

mean approximate fall size for the different roof types with faults or joints present. As can be seen, joints cause the largest falls in Sandstone Roof while Interface Roof is most affected by dip- or oblique-slip faults and least affected by tear faults. Joints are not common in Shale Roof and fall size, in general, does not seem to be influenced by differences in fracture type.

A study was made of the influence of roof fracture type and orientation on roof stability. Chi-square analysis was performed for the three main fracture types: faults (contractional and extensional), tear faults, and joints. The results are shown in Tables 4.43 through 4.45.

Table 4.43 demonstrates that Interface Roof is most affected by joints and contractional and extensional faults. The chi-square probability of 0.0688 shows that there is a definite trend toward dependence of roof stability and fracture type. A more rigorous correlation could not be established since the data is somewhat sparse. The importance of jointing can be attributed to the sandstone component in this roof type. Tear faults do not have much affect on Interface Roof stability.

A scarcity of data is also a problem with Sandstone Roof (Table 4.44). The data available suggests that roof falls in this type roof are probably not related very strongly to roof fracture type as evidenced by the chi-square probability of 0.2077.

TABLE 4.43

Chi-square analysis of the effect of roof fracture type on roof stability for Interface Roof

Frequency
Percent
Row Percent
Column Percent

ROOF FRACTURE TYPE	FALL : NO	YES	TOTAL
Dip-slip Fault	5	24	29
	9.62	46.15	55.77
	17.24	82.76	
	38.46	61.54	
Joint	1	7	8
	1.92	13.46	15.38
	12.50	87.50	
	7.69	17.95	
Tear Joint	7	8	15
	13.46	15.38	28.85
	46.67	53.33	
	53.85	20.51	
TOTAL	13	39	52
	25.00	75.00	100.00

CHI-SQUARE 5.353 DEGREES OF FREEDOM = 2

PROBABILITY = 0.0688

TABLE 4.44

Chi-square analysis of the effect of roof fracture type on roof stability for Sandstone Roof

Frequency
Percent
Row Percent
Column Percent

ROOF FRACTURE TYPE	FALL : NO	YES	TOTAL
Dip-slip Fault	7	4	11
	21.21	12.12	33.33
	63.64	36.36	
	46.67	22.22	
Joint	4	10	14
	12.12	30.30	42.42
	28.57	71.43	
	26.67	55.56	
Tear Fault	4	4	8
	12.12	12.12	24.24
	50.00	50.00	
	26.67	22.22	
TOTAL	15	18	33
	45.45	54.55	100.00

CHI-SQUARE 3.143 DEGREES OF FREEDOM = 2

PROBABILITY = 0.2077

Once again, Shale Roof is strongly affected by a variable. Table 4.45 shows that almost 92% of all falls in this roof type have some kind of dip-slip faulting present in the roof rock. The probability of 0.0096 shows that this is a very strong indicator of stability. There is a possibility that, since faults are indicated by slickensides, there may be a combined effect between these two variables. This is not the case, however, Table 4.45 also shows that tear faults do not lend themselves as indicators of roof instability although they, too, have the characteristic slickensides. Joints appear to be very uncommon in Shale Roof and, therefore, should not be used in roof stability analysis.

A comparison of fall types and fracture types was also made (Tables 4.46 through 4.48). Interface Roof was found to have a strong probability of dependence, 0.0017, especially where sloughing-type failures were associated with contractional and extensional faulting. Since enough data was not available for Sandstone Roof conclusions were not possible. (Table 4.47). Finally, for Shale Roof no preference was shown for fall type and fracture type (Table 4.48) as all falls were associated with contractional and extensional dip-slip faulting.

Fracture orientation with regard to entry and cross-cut direction can be very important for some roof types. Table 4.49 demonstrates the results of chi-square testing of the

TABLE 4.45

Chi-square analysis of the effect of roof fracture type on roof stability for Shale Roof

Frequency
Percent
Row Percent
Column Percent

ROOF FRACTURE TYPE	FALL : NO	YES	TOTAL
Dip-slip Fault	32	101	133
	20.92	66.01	86.93
	24.06	75.94	
	74.42	91.82	
Joint	1	0	1
	0.65	0.00	0.65
	100.00	0.00	
	2.33	0.00	
Tear Fault	10	9	19
	6.54	5.88	12.42
	52.63	47.37	
	23.26	8.18	
TOTAL	43	110	153
	28.10	71.90	100.00

CHI-SQUARE 9.292 DEGREES OF FREEDOM = 2

PROBABILITY = 0.0096

TABLE 4.46

Chi-square analysis of the effect of roof fracture type on fall type for Interface Roof

Frequency
Percent
Row Percent
Column Percent

	ROOF FRACTURE TYPE			
FAILURE TYPE	DIP-SLIP	JOINT	TEAR	TOTAL
Domal	3	3	2	8
	7.69	7.69	5.13	20.51
	37.50	37.50	25.00	
	12.50	42.86	25.00	
Minor	4	3	6	13
	10.26	7.69	15.38	33.33
	30.77	23.08	46.15	
	16.67	42.86	75.00	
Sloughing	17	1	0	18
	43.59	2.56	0.00	46.15
	94.44	5.56	0.00	
	70.83	14.29	0.00	
TOTAL	24	7	8	39
	61.54	17.95	20.51	100.00

CHI-SQUARE 17.290 DEGREES OF FREEDOM = 4

PROBABILITY = 0.0017

TABLE 4.47

Chi-square analysis of the effect of roof fracture type on fall type for Sandstone Roof

Frequency
Percent
Row Percent
Column Percent

	ROOF FRACTURE TYPE			
FAILURE TYPE	DIP-SLIP	JOINT	TEAR	TOTAL
Arch	0	3	0	3
	0.00	16.67	0.00	16.67
	0.00	100.00	0.00	
	0.00	30.00	0.00	
Domal	0	1	0	1
	0.00	5.56	0.00	5.56
	0.00	100.00	0.00	
	0.00	10.00	0.00	
Minor	0	3	2	5
	0.00	16.67	11.11	27.78
	0.00	60.00	40.00	
	0.00	30.00	50.00	
Sloughing	4	3	2	9
	22.22	16.67	11.11	50.00
	44.44	33.33	22.22	
	100.00	30.00	50.00	
TOTAL	4	10	4	18
	22.22	55.56	22.22	100.00

CHI-SQUARE 7.840 DEGREES OF FREEDOM = 6

PROBABILITY = 0.2501

TABLE 4.48

Chi-square analysis of the effect of roof fracture type on fall type for Shale Roof

Frequency
Percent
Row Percent
Column Percent

	ROOF FRACTURE TYPE		
FAILURE TYPE	DIP-SLIP	TEAR	TOTAL
Arch	8	1	9
	7.27	0.91	8.18
	88.89	11.11	
	7.92	11.11	
Domal	8	2	10
	7.27	1.82	9.09
	80.00	20.00	
	7.92	22.22	
Minor	41	2	43
	37.27	1.82	39.09
	95.35	4.65	
	40.59	22.22	
Sloughing	44	4	48
	40.00	3.64	43.64
	91.67	8.33	
	43.56	44.44	
TOTAL	101	9	110
	91.82	8.18	100.00

CHI-SQUARE 2.677 DEGREES OF FREEDOM = 3

PROBABILITY = 0.4442

TABLE 4.49

Chi-square analysis of the effect of roof fracture strike on the stability of Interface Roof

Frequency
Percent
Row Percent
Column Percent

FALL	FRACTURE DEVIATION IN DEGREES:	0-10	11-20	21-30	31-40	41-50	51-60	61-70	71-80	81-90	TOTAL
NO		10	4	6	3	2	2	5	5	8	45
		6.58	2.63	3.95	1.97	1.32	1.32	3.29	3.29	5.26	29.61
		22.22	8.89	13.33	6.67	4.44	11.11	11.11	17.78		
		43.48	26.67	35.29	23.08	10.00	18.18	27.78	29.41	44.44	
YES		13	11	11	10	18	9	13	12	10	107
		8.55	7.24	7.24	6.58	11.84	5.92	8.55	7.89	6.58	70.39
		12.15	10.28	10.28	9.35	16.82	8.41	12.15	11.21	9.35	
		56.52	73.33	64.71	76.92	90.00	81.82	72.22	70.59	55.56	
TOTAL		23	15	17	13	20	11	18	17	18	152
		15.13	9.87	11.18	8.55	13.16	7.24	11.84	11.18	11.84	100.00

CHI-SQUARE 9.024 DEGREES OF FREEDOM = 8

PROBABILITY = 0.3402

influence of fault-plane strike on the stability of Interface Roof. The high probability suggests that fracture strike is not an important factor in roof falls for this roof type. The same holds true for Sandstone Roof as reflected in Table 4.50. In this case, the probability is 0.9556 which is much too high to even suggest a nuance of a relationship. However, Table 4.51 for Shale Roof reveals a strong chi-square probability of 0.0050. Fractures whose strike differs from that of the entry or cross-cut trend by a difference of approximately 20 degrees to either side are more likely to be involved in a fall. Of all roof falls, 52% occurred where fracture trends varied between 0 to 20 degrees and 71 to 90 degrees entry and cross-cut trends.

The dip of a fracture, that is, its vertical angle from a horizontal plane is important for two roof types. Interface Roof (Table 4.52) does not show any dependence on fracture dip. Sandstone Roof, on the other hand, seems to be affected. Its chi-square probability of 0.0847 is only slightly above the 0.05 cut-off level. Fractures with relatively steep dips, 70 to 80 degrees from the horizontal, are the most dangerous, while those with flatter dips, 20 to 50 degrees, experience fewer falls. This is probably due to the fact that the shallower dipping fractures can be bolted through. Those with steeper dips, on the other hand, would require much longer bolts to anchor them in sound strata. Noteworthy, is the fact that Sandstone Roof (Table 4.53)

TABLE 4.50

Chi-square analysis of the effect of roof fracture strike on the stability of Sandstone Roof

Frequency
Percent
Row Percent
Column Percent

FALL	FRACTURE DEVIATION IN DEGREES:	0-10	11-20	21-30	31-40	41-50	51-60	61-70	71-80	81-90	TOTAL
NO		12	10	4	9	16	9	6	9	12	87
		5.66	4.72	1.89	4.25	7.55	4.25	2.83	4.25	5.66	41.04
		13.79	11.49	4.60	10.34	18.39	10.34	6.90	10.34	13.79	
		38.71	52.63	33.33	39.13	37.21	36.00	42.86	45.00	48.00	
YES		19	9	8	14	27	16	8	11	13	125
		8.96	4.25	3.77	6.60	12.74	7.55	3.77	5.19	6.13	58.96
		15.20	7.20	6.40	11.20	21.60	12.80	6.40	8.80	10.40	
		61.29	47.37	66.67	60.87	62.79	64.00	57.14	55.00	52.00	
TOTAL		31	19	12	23	43	25	14	20	25	212

CHI-SQUARE 2.626 DEGREES OF FREEDOM = 8

PROBABILITY = 0.9556

TABLE 4.51

Chi-square analysis of the effect of roof fracture strike on the stability of Shale Roof

Frequency
Percent
Row Percent
Column Percent

FALL	FRACTURE DEVIATION IN DEGREES:	0-10	11-20	21-30	31-40	41-50	51-60	61-70	71-80	81-90	TOTAL
NO		27	22	13	1	14	8	12	17	28	142
		3.92	3.19	1.89	0.15	2.03	1.16	1.74	2.47	4.06	20.61
		19.01	15.49	9.15	0.70	9.86	5.63	8.45	11.97	19.72	
		25.47	29.73	24.07	2.00	18.42	11.27	19.35	19.77	25.45	
YES		79	52	41	49	62	63	50	69	82	547
		11.47	7.55	5.95	7.11	9.00	9.14	7.26	10.01	11.90	79.39
		14.44	9.51	7.50	8.96	11.33	11.52	9.14	12.61	14.99	
		74.53	70.27	75.93	98.00	81.58	88.73	80.65	80.23	74.55	
TOTAL		106	74	54	50	76	71	62	86	110	689

CHI-SQUARE 21.957 DEGREES OF FREEDOM = 8

PROBABILITY = 0.0050

TABLE 4.52

Chi-square analysis of the effect of roof fracture dip on the stability of Interface Roof

Frequency
Percent
Row Percent
Column Percent

FALL	FRACTURE DEVIATION IN DEGREES:	0-10	11-20	21-30	31-40	41-50	51-60	61-70	71-80	81-90	TOTAL
NO		0	2	8	4	4	4	13	4	2	41
		0.00	1.37	5.48	2.74	2.74	2.74	8.90	2.74	1.37	28.08
		0.00	4.88	19.51	9.76	9.76	9.76	31.71	9.76	4.88	
		0.00	28.57	22.22	25.00	20.00	23.53	46.43	33.33	20.00	
YES		0	5	28	12	16	13	15	8	8	105
		0.00	3.42	19.18	8.22	10.96	8.90	10.27	5.48	5.48	71.92
		0.00	4.76	26.67	11.43	15.24	12.38	14.29	7.62	7.62	
		0.00	71.43	77.78	75.00	80.00	76.47	53.57	66.67	80.00	
TOTAL		0	7	36	16	20	17	28	12	10	146
		0.00	4.79	24.66	10.96	13.70	11.64	19.18	8.22	6.85	100.00

CHI-SQUARE 6.663 DEGREES OF FREEDOM = 7

PROBABILITY = 0.4648

TABLE 4.53

Chi-square analysis of the effect of roof fracture dip on the stability of Sandstone Roof

Frequency
Percent
Row Percent
Column Percent

FALL	FRACTURE DEVIATION IN DEGREES:	0-10	11-20	21-30	31-40	41-50	51-60	61-70	71-80	81-90	TOTAL
NO		0	1	16	13	10	16	19	4	6	85
		0.00	0.47	7.58	6.16	4.74	7.58	9.00	1.90	2.84	40.28
		0.00	1.18	18.82	15.29	11.76	18.82	22.35	4.71	7.06	
		0.00	33.33	59.26	52.00	43.48	32.00	35.85	20.00	60.00	
YES		0.00	2	11	12	13	34	34	16	4	126
		0.00	0.95	5.21	5.69	6.16	16.11	16.11	7.58	1.90	59.72
		0.00	1.59	8.73	9.52	10.32	26.98	26.98	12.70	3.17	
		0.00	66.67	40.74	48.00	56.52	68.00	64.15	80.00	40.00	
TOTAL		0	3	27	25	23	50	53	20	10	211
		0.00	1.42	12.80	11.85	10.90	23.70	25.12	9.48	4.74	100.00

CHI-SQUARE 12.522 DEGREES OF FREEDOM = 7

PROBABILITY = 0.0847

with dips approaching 90 degrees are not associated with many falls. This can be attributed to a " Poisson effect" which transfers stress across the joint in order to mobilize shear strength along it. Finally, Shale Roof shows an excellent correlation between fracture dip and the occurrence of roof falls (Table 4.54). Although the chi-square probability is very low 0.0003, no real pattern emerges. Shallow dipping fractures have a high degree of fall incidence as do those which dip from 30-40 degrees and 80 to 90 degrees. The best explanation for this is that other factors, most notably fracture density, play a role. A high fracture density, especially in a shale can lead to falls in which the material falls out between bolts and this may favor certain fracture dips (Figure 4.18).

Regression analysis was performed on the numeric data in order determine if a linear relationship exists between selected numeric variables. Table 4.55 displays the correlation coefficients for the variables of dip angle and fracture deviation from entry trend for roof falls. For Interface Roof the correlation coefficient is -0.01121, for Sandstone Roof, it is -.01110, and for Shale Roof the coefficient is 0.03827. All these values are so close to zero that it can be stated that no linear relationship exists between fracture dip angles and deviations. The data is too scattered to provide any preferential combination of the two

TABLE 4.54

Chi-square analysis of the effect of roof fracture dip on the stability of Shale Roof

Frequency
Percent
Row Percent
Column Percent

FALL	FRACTURE DEVIATION IN DEGREES:	0-10	11-20	21-30	31-40	41-50	51-60	61-70	71-80	81-90	TOTAL
NO		0	9	27	21	40	18	12	9	3	139
		0.00	1.31	3.92	3.05	5.81	2.62	1.74	1.31	0.44	20.20
		0.00	6.47	19.42	15.11	28.78	12.95	8.63	6.47	2.16	
		0.00	13.43	22.31	12.65	32.26	15.79	30.00	34.62	16.67	
YES		12	58	94	145	84	96	28	17	15	549
		1.74	8.43	13.66	21.08	12.21	13.95	4.07	2.47	2.18	79.80
		2.19	10.56	17.12	26.41	15.30	17.49	5.10	3.10	2.73	
		100.00	86.57	77.69	87.35	67.74	84.21	70.00	65.38	83.33	
TOTAL		12	67	121	166	124	114	40	26	18	688
		1.74	9.74	17.59	24.13	18.02	16.57	5.81	3.78	2.62	100.00

CHI-SQUARE 29.577 DEGREES OF FREEDOM = 8

PROBABILITY = 0.0003

Figure 4.18: Highly fractured mine roof falling out between roof bolts (photograph by T. M. Gathright, II).

TABLE 4.55

Correlation coefficients for falls: fracture deviation and dip angle

Key:
Correlation Coefficients
Probability > R Under Ho: Rho = 0
Number of Observations

INTERFACE ROOF

	FRACTURE DEVIATION	DIP ANGLE
FRACTURE DEVIATION	1.00000 0.0000 117	-0.01121 0.9097 105
DIP ANGLE	-0.01121 0.9097 105	1.00000 0.0000 105

SANDSTONE ROOF

	FRACTURE DEVIATION	DIP ANGLE
FRACTURE DEVIATION	1.00000 0.0000 136	-0.01110 0.9019 126
DIP ANGLE	-0.01110 0.9019 126	1.00000 0.0000 126

SHALE ROOF

	FRACTURE DEVIATION	DIP ANGLE
FRACTURE DEVIATION	1.00000 0.0000 614	0.03827 0.3708 549
DIP ANGLE	0.03827 0.3708 549	1.00000 0.0000 549

variables that would combine to increase the chance of a fall. It was then decided to confine the data into two groups in order to eliminate any outliers which might influence the regression analysis. Separate tests were run for falls which were larger than 280 cubic meters and for falls which had a volume of less than 280 cubic meters. The results were similar to those above. Correlation coefficients were either zero or so close to zero for the greater-than-280-cubic-meter group as to eliminate any possible suggestion of a relationship (Table 4.56). The same holds true for the smaller fall group as can be seen in Table 4.57.

An attempt was then made to study the effect of fracture deviation as well as fracture dip on fall size. In Table 4.58, it can be seen that the deviation of a fracture from the entry or cross-cut trend has virtually no effect on fall size as correlation coefficients are once again close to zero. Falls were once again grouped according to size with the larger ones, those greater than 280 cubic meters, treated separately. The results were inconclusive as shown in Table 4.59 and Table 4.60 although the relationship for Sandstone Roof did show a little strength with a correlation coefficient of -0.28457.

Next, a similar series of tests were run in order to determine if a linear relationship existed between fall size and fracture dip angle. Table 4.61 shows the results of

TABLE 4.56

Correlation coefficients for falls larger than 280 cubic meters: fracture deviation and dip angle

Key:
Correlation Coefficients
Probability > R Under Ho: Rho = 0
Number of Observations

INTERFACE ROOF

	FRACTURE DEVIATION	DIP ANGLE
FRACTURE DEVIATION	1.00000 0.0000 5	0.00000 1.0000 4
DIP ANGLE	0.00000 1.0000 4	1.00000 0.0000 4

SANDSTONE ROOF

	FRACTURE DEVIATION	DIP ANGLE
FRACTURE DEVIATION	1.00000 0.0000 15	0.05800 0.8439 14
DIP ANGLE	0.05800 0.8439 14	1.00000 0.0000 14

SHALE ROOF

	FRACTURE DEVIATION	DIP ANGLE
FRACTURE DEVIATION	1.00000 0.0000 9	0.01920 0.9609 9
DIP ANGLE	0.01920 0.9609 9	1.00000 0.0000 9

TABLE 4.57

Correlation coefficients for falls smaller than 280 cubic meters: fracture deviation and dip angle

Key:
Correlation Coefficients
Probability > R Under Ho: Rho = 0
Number of Observations

INTERFACE ROOF

	FRACTURE DEVIATION	DIP ANGLE
FRACTURE DEVIATION	1.00000 0.0000 112	0.01352 0.8933 101
DIP ANGLE	0.01352 0.8933 101	1.00000 0.0000 101

SANDSTONE ROOF

	FRACTURE DEVIATION	DIP ANGLE
FRACTURE DEVIATION	1.00000 0.0000 121	-0.02189 0.8188 112
DIP ANGLE	-0.02189 0.8188 112	1.00000 0.0000 112

SHALE ROOF

	FRACTURE DEVIATION	DIP ANGLE
FRACTURE DEVIATION	1.00000 0.0000 605	0.03850 0.3719 540
DIP ANGLE	0.03850 0.3719 540	1.00000 0.0000 540

TABLE 4.58

Correlation coefficients for falls: fall size and fracture deviation

Key:
Correlation Coefficients
Probability > R Under Ho: Rho = 0
Number of Observations

INTERFACE ROOF

	FALL SIZE	FRACTURE DEVIATION
FALL SIZE	1.00000 0.0000 205	-0.03020 0.7850 84
FRACTURE DEVIATION	-0.03020 0.7850 84	1.00000 0.0000 117

SANDSTONE ROOF

	FALL SIZE	FRACTURE DEVIATION
FALL SIZE	1.00000 0.0000 245	0.02971 0.7558 112
FRACTURE DEVIATION	0.02971 0.7558 112	1.00000 0.0000 136

SHALE ROOF

	FALL SIZE	FRACTURE DEVIATION
FALL SIZE	1.00000 0.0000 995	-0.02264 0.6121 504
FRACTURE DEVIATION	-0.02264 0.6121 504	1.00000 0.0000 614

TABLE 4.59

Correlation coefficients for falls larger than 280 cubic meters: fall size and fracture deviation

Key:
Correlation Coefficients
Probability > R Under Ho: Rho = 0
Number of Observations

INTERFACE ROOF

	FALL SIZE	FRACTURE DEVIATION
FALL SIZE	0.00000 1.0000 10	0.00000 1.0000 5
FRACTURE DEVIATION	0.00000 1.0000 5	1.00000 0.0000 5

SANDSTONE ROOF

	FALL SIZE	FRACTURE DEVIATION
FALL SIZE	1.00000 0.0000 20	0.10036 0.7219 15
FRACTURE DEVIATION	0.10036 0.7219 15	1.00000 0.0000 15

SHALE ROOF

	FALL SIZE	FRACTURE DEVIATION
FALL SIZE	1.00000 0.0000 15	-0.05573 0.8868 9
FRACTURE DEVIATION	-0.05573 0.8868 9	1.00000 0.0000 9

TABLE 4.60

Correlation coefficients for falls smaller than 280 cubic meters: fall size and fracture deviation

Key:
Correlation Coefficients
Probability > R Under Ho: Rho = 0
Number of Observations

INTERFACE ROOF

	FALL SIZE	FRACTURE DEVIATION
FALL SIZE	1.00000 0.0000 195	0.01661 0.8845 79
FRACTURE DEVIATION	0.01661 0.8845 79	1.00000 0.0000 112

SANDSTONE ROOF

	FALL SIZE	FRACTURE DEVIATION
FALL SIZE	1.00000 0.0000 225	-0.28457 0.0047 97
FRACTURE DEVIATION	-0.28457 0.0047 97	1.00000 0.0000 121

SHALE ROOF

	FALL SIZE	FRACTURE DEVIATION
FALL SIZE	1.00000 0.0000 980	-0.05495 0.2223 495
FRACTURE DEVIATION	-0.05495 0.2223 495	1.00000 0.0000 605

TABLE 4.61

Correlation coefficients for falls: fall size and dip angle

Key:
Correlation Coefficients
Probability > R Under Ho: Rho = 0
Number of Observations

INTERFACE ROOF

	FALL SIZE	DIP ANGLE
FALL SIZE	1.00000 0.0000 205	0.33409 0.0030 77
DIP ANGLE	0.33409 0.0030 77	1.00000 0.0000 105

SANDSTONE ROOF

	FALL SIZE	DIP ANGLE
FALL SIZE	1.00000 0.0000 245	0.33214 0.0006 104
DIP ANGLE	0.33214 0.0006 104	1.00000 0.0000 126

SHALE ROOF

	FALL SIZE	DIP ANGLE
FALL SIZE	1.00000 0.0000 995	-0.09076 0.0536 453
DIP ANGLE	-0.09076 0.0536 453	1.00000 0.0000 549

tests for all fall sizes. The results are slightly more encouraging as the correlation coefficient for Interface Roof is 0.33409 and that for Sandstone Roof is 0.33214. Shale Roof, however, demonstrated no trend towards linearity with a coefficient of -0.09076. Results for falls divided on the basis of size were also encouraging. For large falls, the correlation coefficient jumped to 0.64528 for Sandstone Roof (Table 4.62). The other two roof types little if any improvement. Interface fell to zero while Shale Roof did improve to -.28911. Smaller falls, Table 4.63, did not show any significant results.

In order to further investigate the role of fractures in coal mine roof stability, charts were made of mean fall sizes and fracture deviations and angles. Figure 4.19 shows that for Interface Roof average fall sizes were larger for fracture deviations less than 10 degrees and also for between 60 and 70 degrees. The first phenomenon is understandable since the unsupported beam delineated by the fractures is longer and thus will be inherently less stable as well as supplying a larger volume of rock to the fall. The second peak, however, remains rather mysterious as to its genesis. Sandstone Roof (Figure 4.20) demonstrates no trends at all with regards to increased fall size with different fracture trends. Finally, Shale Roof has a very large mean fall size for deviations between 30 and 40 de-

TABLE 4.62

Correlation coefficients for falls larger than 280 cubic meters fall size and dip angle

Key:
Correlation Coefficients
Probability > R Under Ho: Rho = 0
Number of Observations

INTERFACE ROOF

	FALL SIZE	DIP ANGLE
FALL SIZE	0.00000 1.0000 10	0.00000 1.0000 4
DIP ANGLE	0.00000 1.0000 4	1.00000 0.0000 4

SANDSTONE ROOF

	FALL SIZE	DIP ANGLE
FALL SIZE	1.00000 0.0000 20	0.64528 0.0127 14
DIP ANGLE	0.64528 0.0127 14	1.00000 0.0000 14

SHALE ROOF

	FALL SIZE	DIP ANGLE
FALL SIZE	1.00000 0.0000 15	-0.28911 0.4505 9
DIP ANGLE	-0.28911 0.4505 9	1.00000 0.0000 9

TABLE 4.63

Correlation coefficients for falls smaller than 280 cubic meters: fall size and dip angle

Key:
Correlation Coefficients
Probability > R Under Ho: Rho = 0
Number of Observations

INTERFACE ROOF

	FALL SIZE	DIP ANGLE
FALL SIZE	1.00000 0.0000 195	0.07415 0.5330 73
DIP ANGLE	0.07415 0.5330 73	1.00000 0.0000 101

SANDSTONE ROOF

	FALL SIZE	DIP ANGLE
FALL SIZE	1.00000 0.0000 225	0.07002 0.5120 90
DIP ANGLE	0.07002 0.5120 90	1.00000 0.0000 112

SHALE ROOF

	FALL SIZE	DIP ANGLE
FALL SIZE	1.00000 0.0000 980	0.00898 0.8504 444
DIP ANGLE	0.00898 0.8504 444	1.00000 0.0000 540

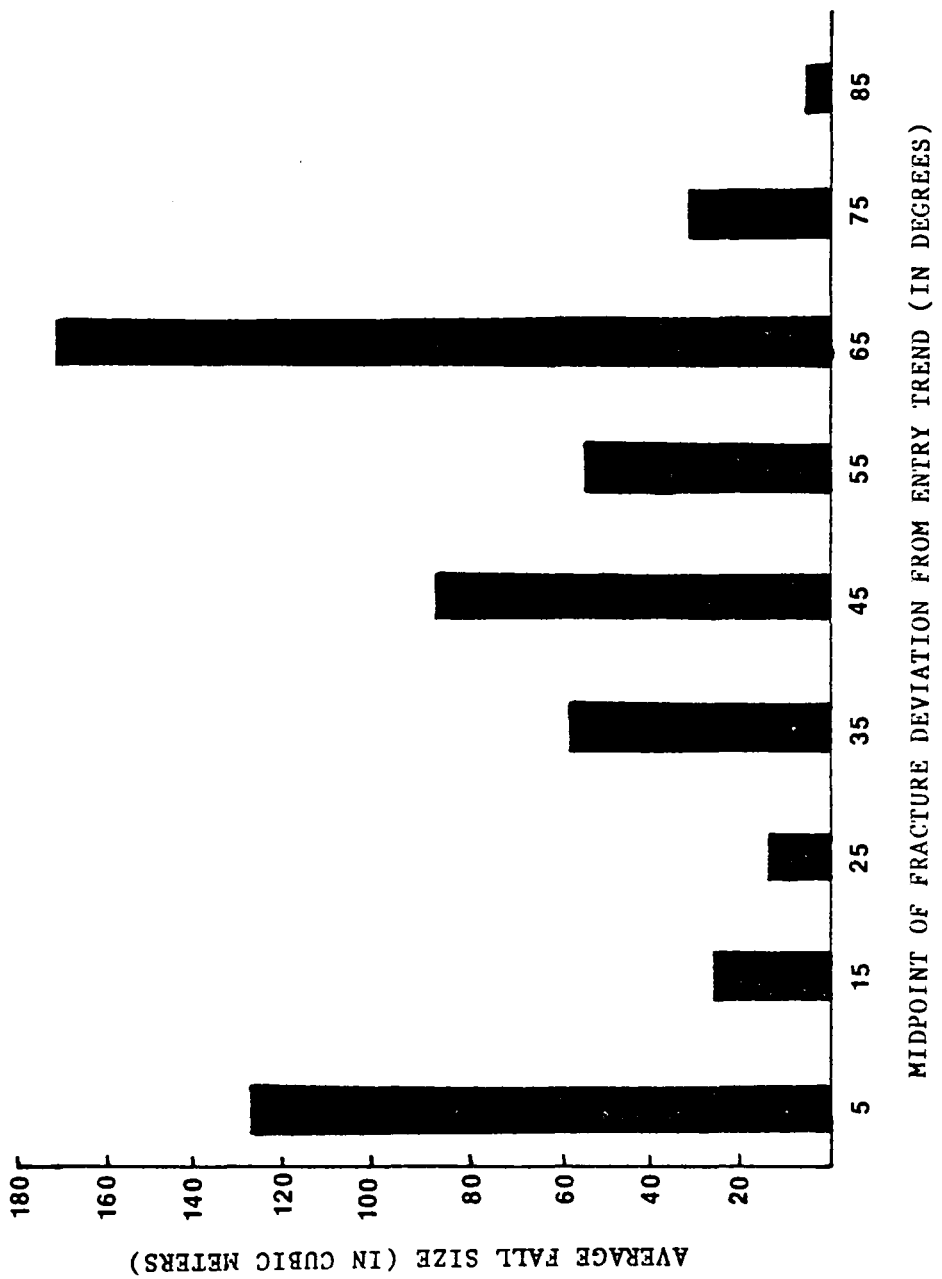

Figure 4.19: Bar chart of roof fall sizes and fracture deviations for Interface Roof.

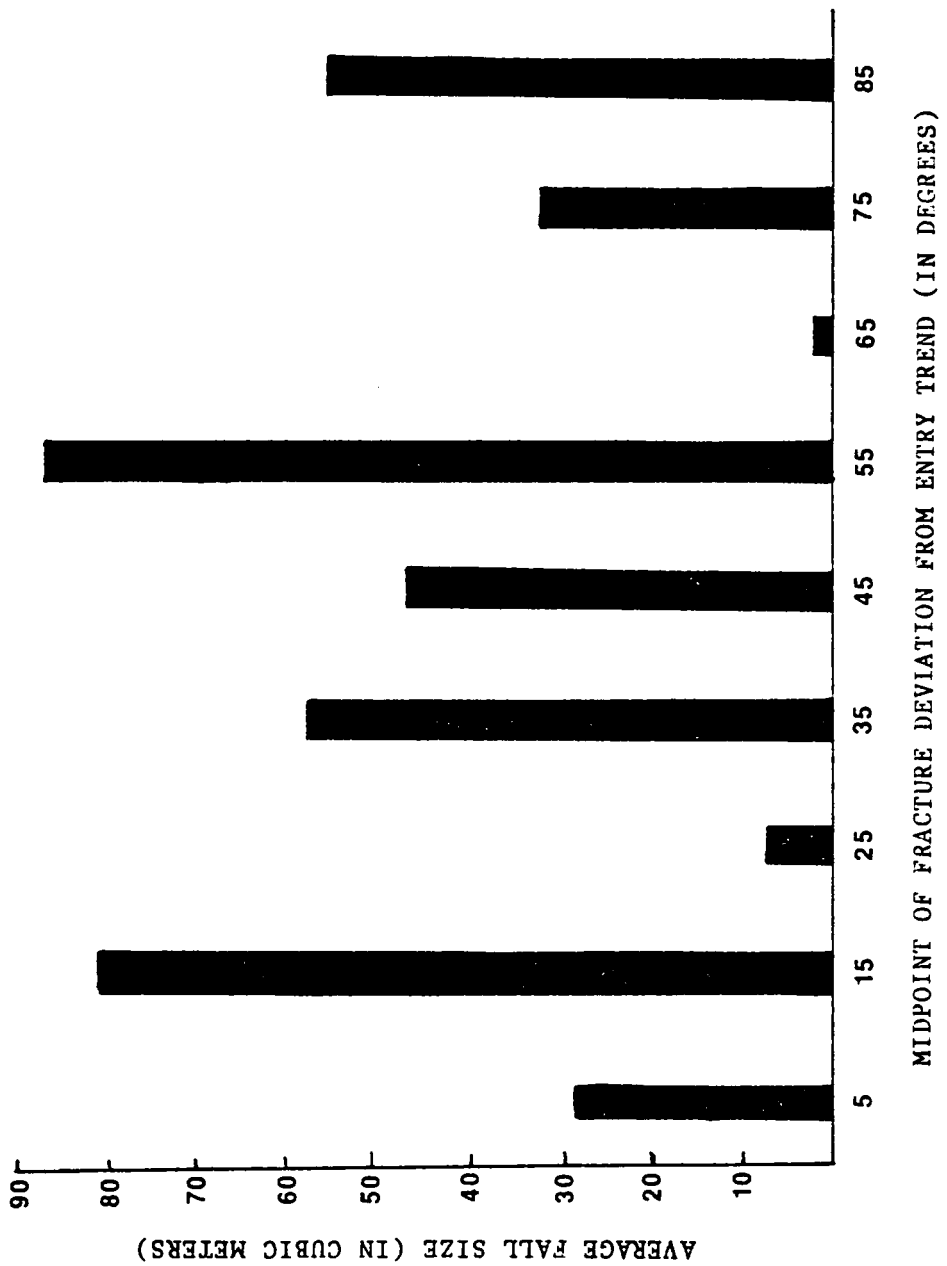

Figure 4.20: Bar chart of roof fall sizes and fracture deviations for Sandstone Roof.

grees and two smaller peaks at either end of the fracture deviation spectrum as shown in Figure 4.21.

Diagrams for fracture angles show some very encouraging results. Fall sizes for Interface Roof are largest between 70 and 90 degrees (Figure 4.22). This can be explained by the fact that higher angle fractures will delineate larger blocks resulting in greater fall sizes. Note that fall sizes for this roof type are very small for the shallower dipping fractures. This same relationship is even more pronounced for Sandstone Roof as seen in Figure 4.23. Very high angles, that is, greater than 80 degrees have small falls. One possible explanation for this is that the Poisson's effect coupled with the high cohesion due to joint friction of sandstone prevents any large blocks from falling. That this is not always true, however, can be seen in Figures 4.24 and 4.25 where vertical jointing is responsible for a massive failure in a Sandstone Roof. It should be noted that the carbonaceous bedding planes along which the sandstone delaminated are also responsible in a large part for this fall and that it is possible that failure may not have taken place if only the vertical jointing was present. Although large falls occurred in Shale Roof for high fracture angles (Figure 4.26) the largest falls occurred where dips were shallow. It would appear, in this case, that some other variable might contribute to the fall size. Fracture density is a possibility in that a roof with shallow frac-

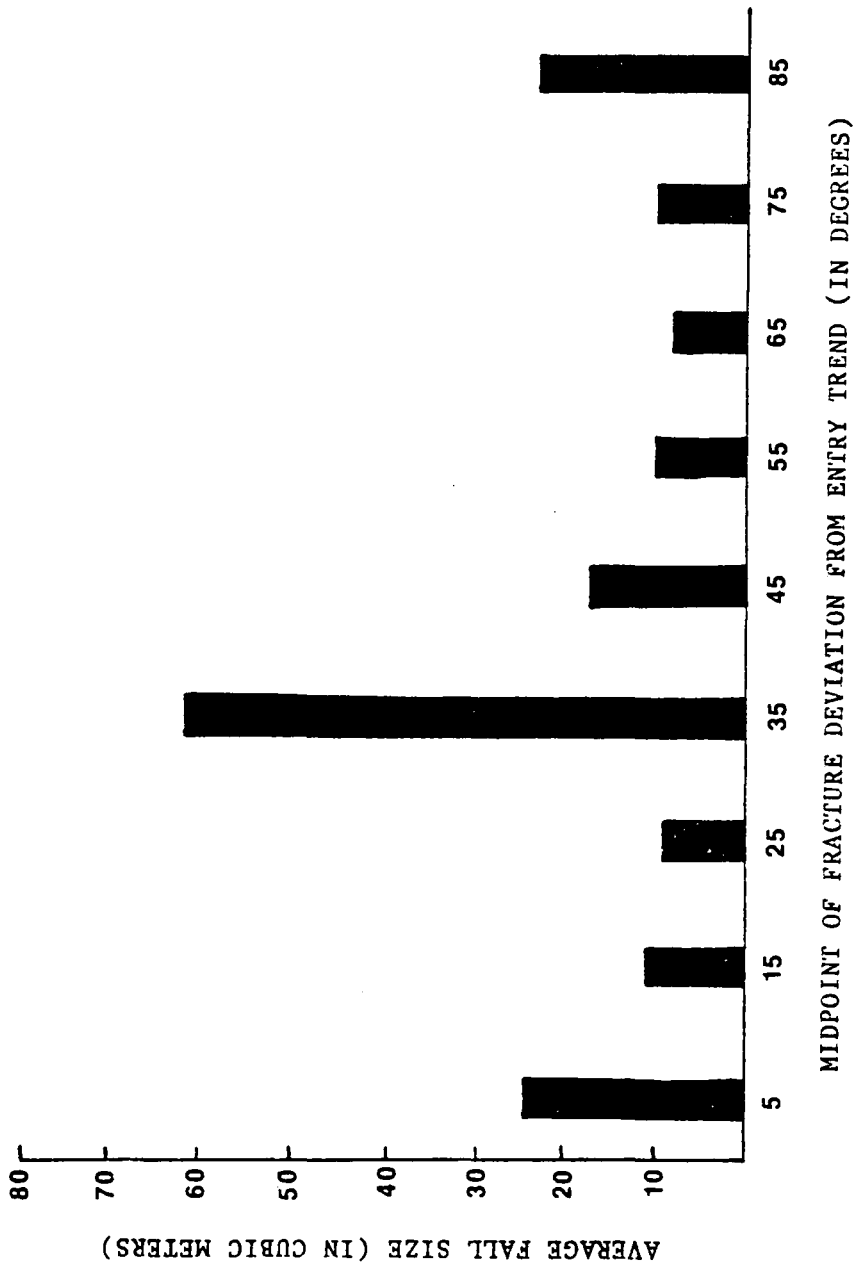

Figure 4.21: Bar chart of roof fall sizes and fracture deviations for Shale Roof.

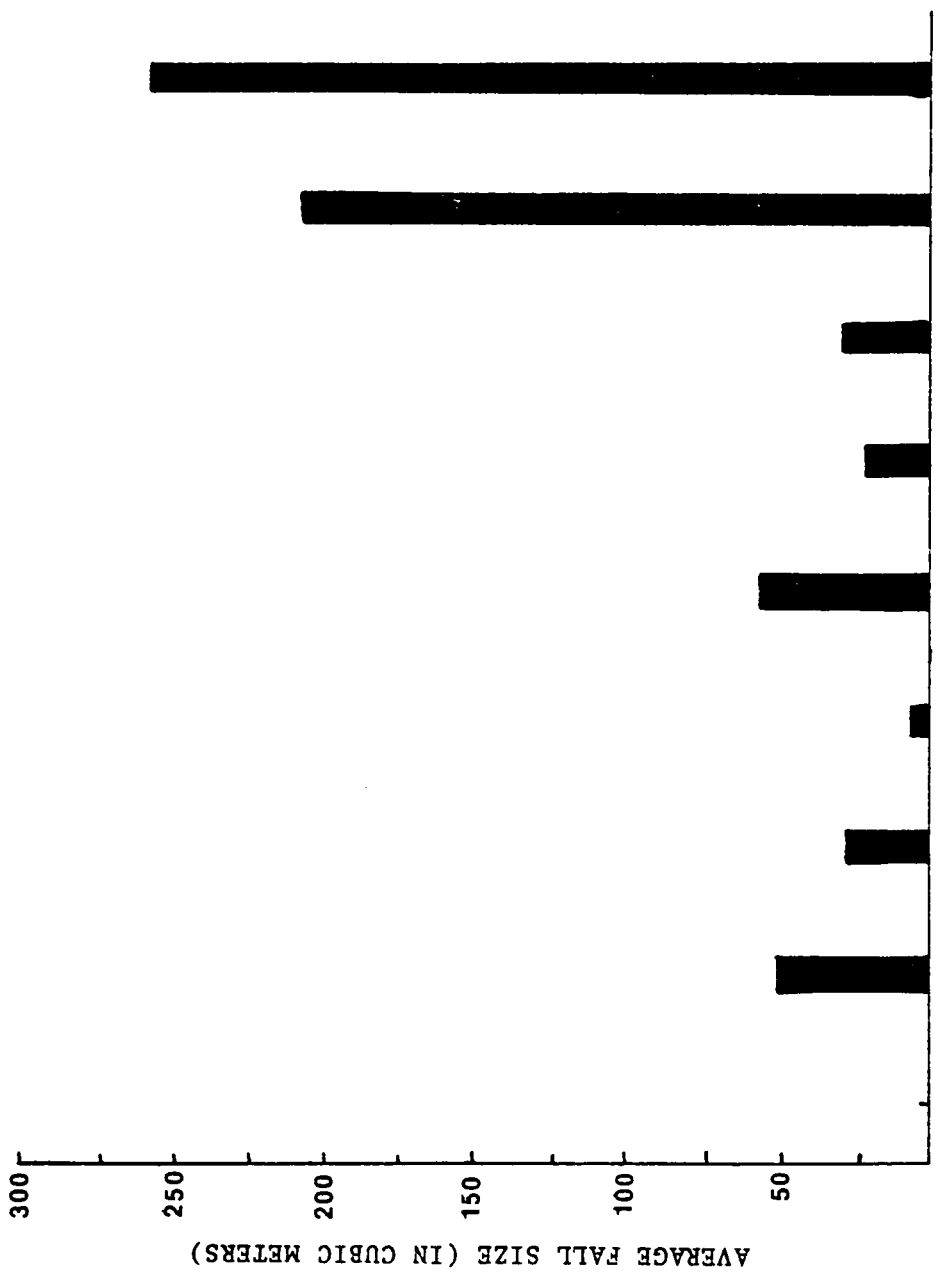

Figure 4.22: Bar chart of roof fall sizes and fracture angles for Interface Roof.

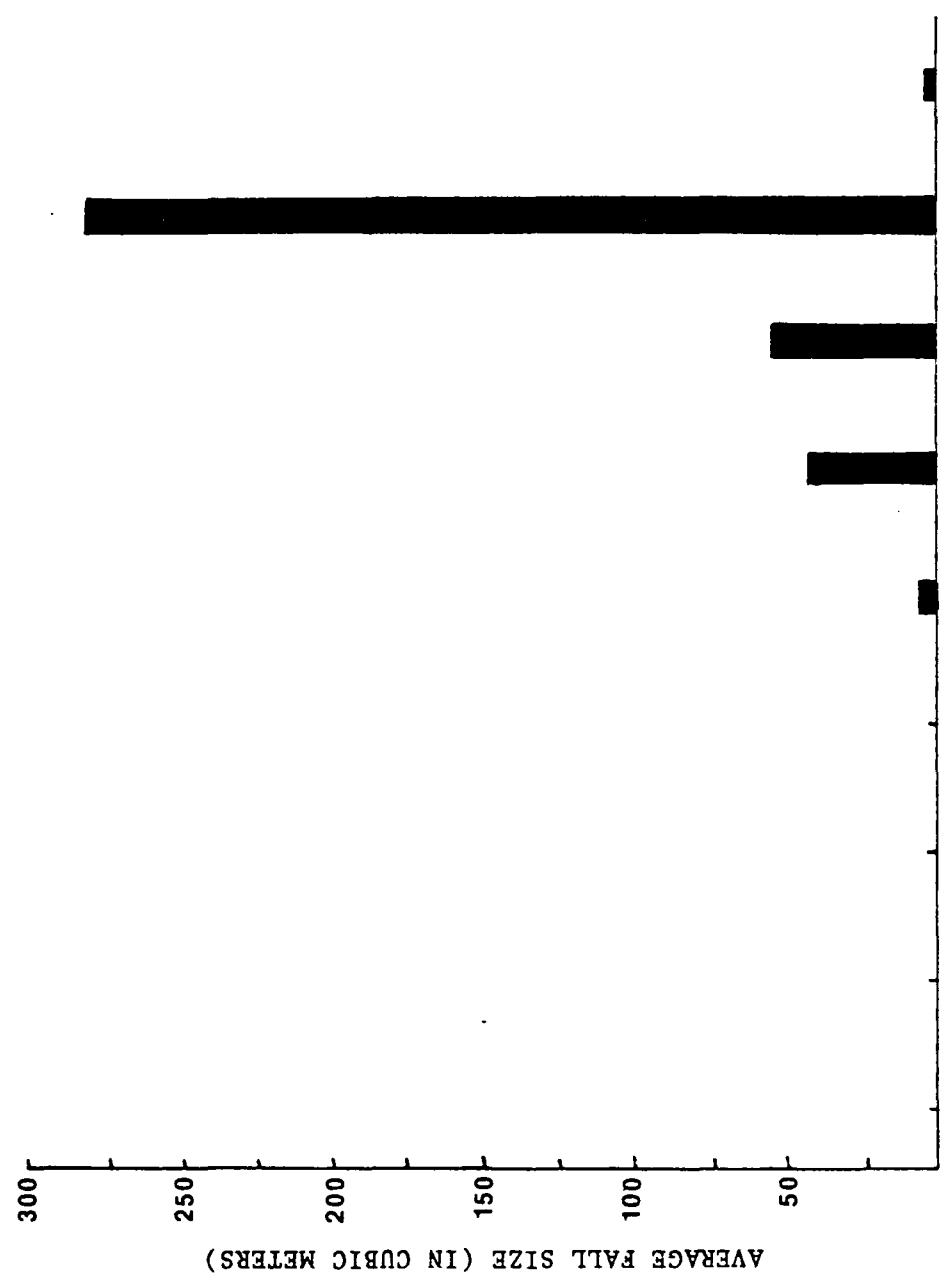

Figure 4.23: Bar chart of roof fall sizes and fracture angles for Sandstone Roof.

Figure 4.24: Roof fall due to vertical jointing of Sandstone Roof (photograph by T. M. Gathright, II).

Figure 4.25: Another view of roof fall in Figure 4.24 (photograph by T. M. Gathright, II).

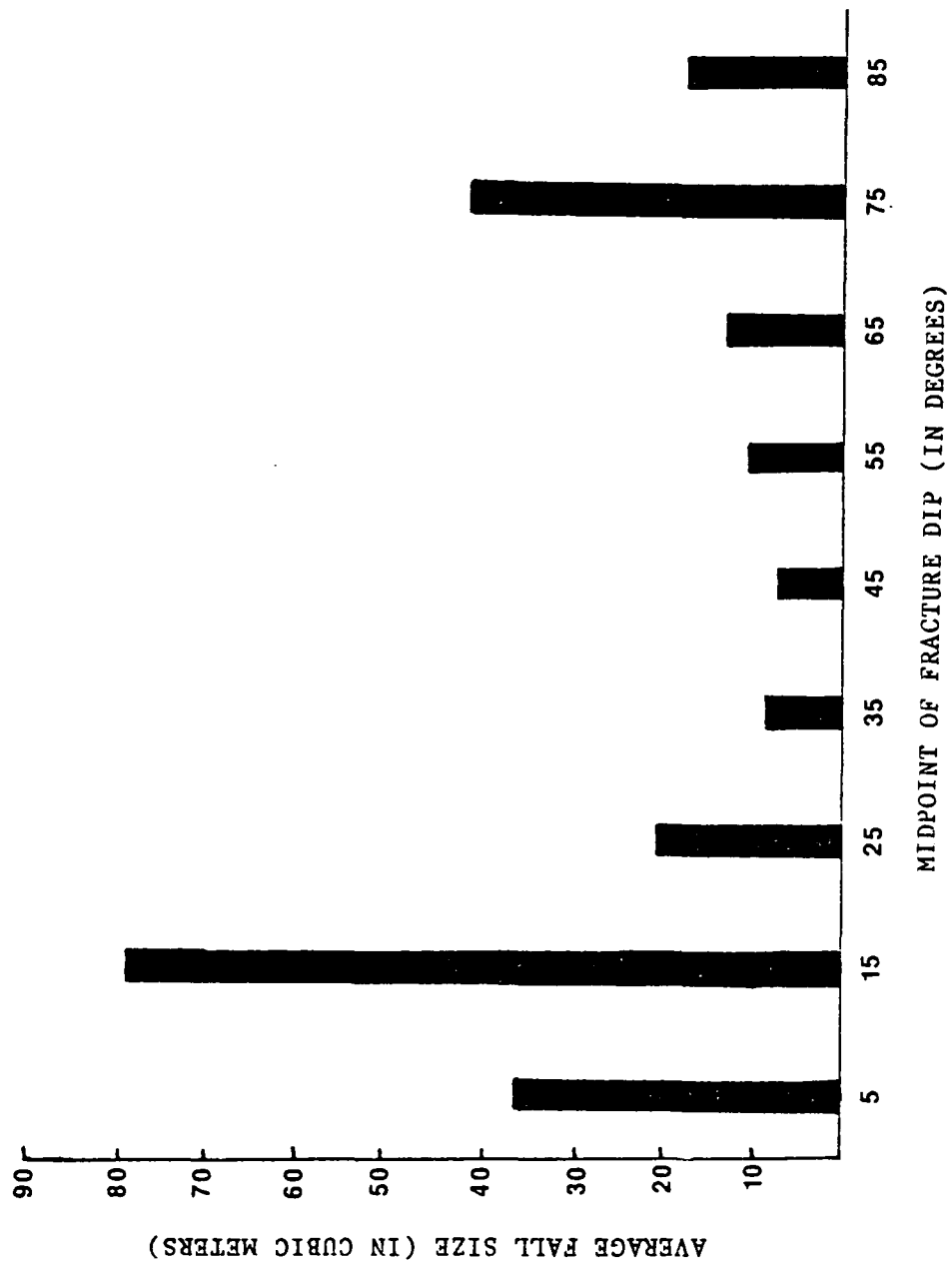

Figure 4.26: Bar chart of roof fall sizes and fracture angles for Shale Roof.

ture dips could lose a large amount of rock if that material was broken-up enough. For example, see Figure 4.18 for a Shale Roof where the fracture density was so great that the roof rock fell out between the bolts.

Frequency charts were also prepared for the respective roof types and fracture deviations. Figure 4.27 for Interface Roof reveals a high number of falls in the 40 to 50 degree category smaller peaks at either end. The same holds true for Sandstone Roof (Figure 4.28). Shale Roof, on the other hand, shows peaks on either end as seen in Figure 4.29.

There is a great deal of variability for the frequency charts for fracture angles and roof falls. Interface Roof (Figure 4.30) has the greatest number of falls in the 20 to 30 degree fracture angle range. Figure 4.31 shows that the greatest number of falls in Sandstone Roof occur when the fracture dip is between 50 and 70 degrees. Finally, the highest frequency of roof falls for Shale Roof was recorded between 30 and 40 degrees (Figure 4.32).

4.2.10 Regression Analysis

The last statistical processing attempted on the data was a linear regression analysis in which fall size was established as the dependent variable. Regression models were then fitted using fracture density, coal height, deviation of fracture direction from entry or cross-cut direc-

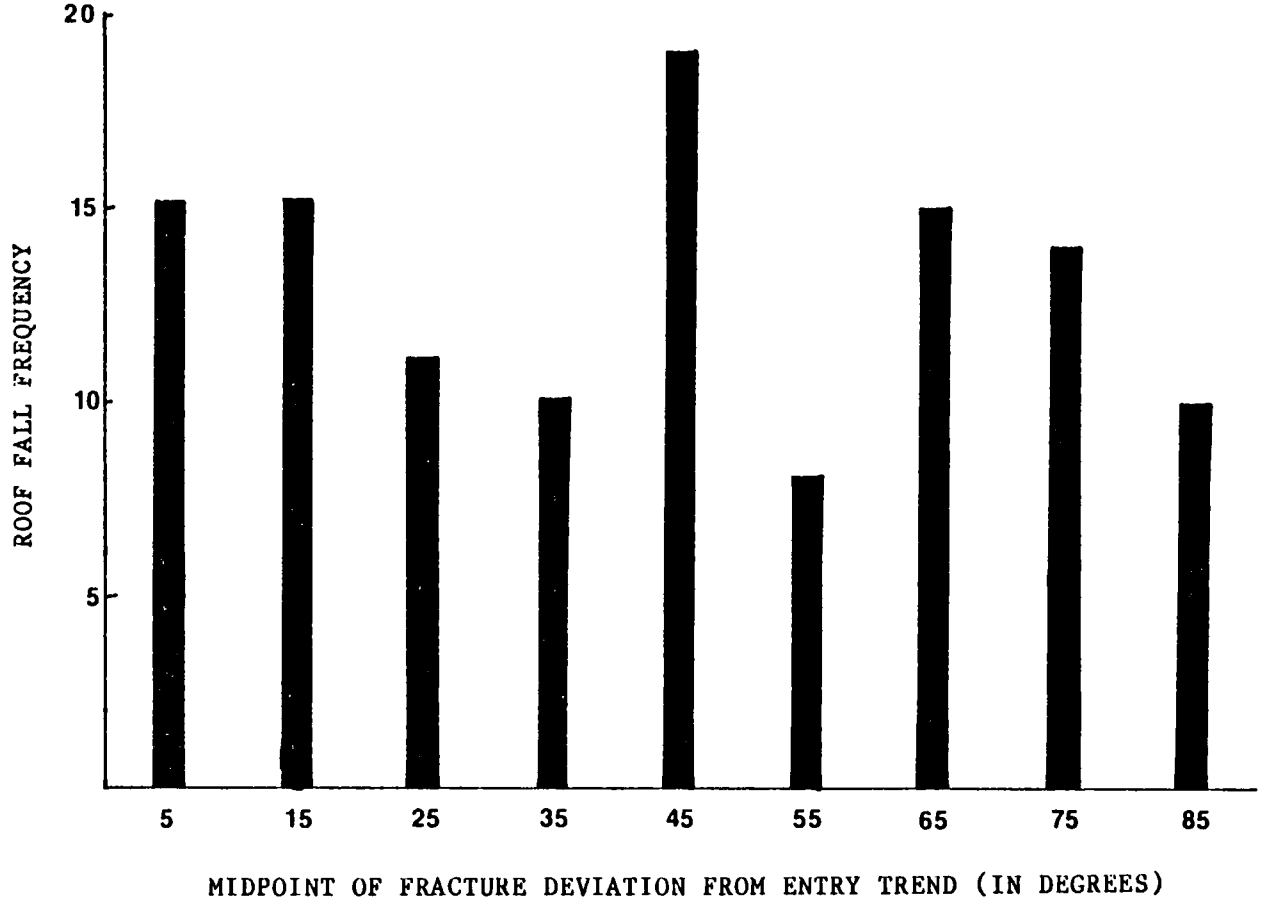

Figure 4.27: Frequency of roof falls for Interface Roof and different fracture deviations.

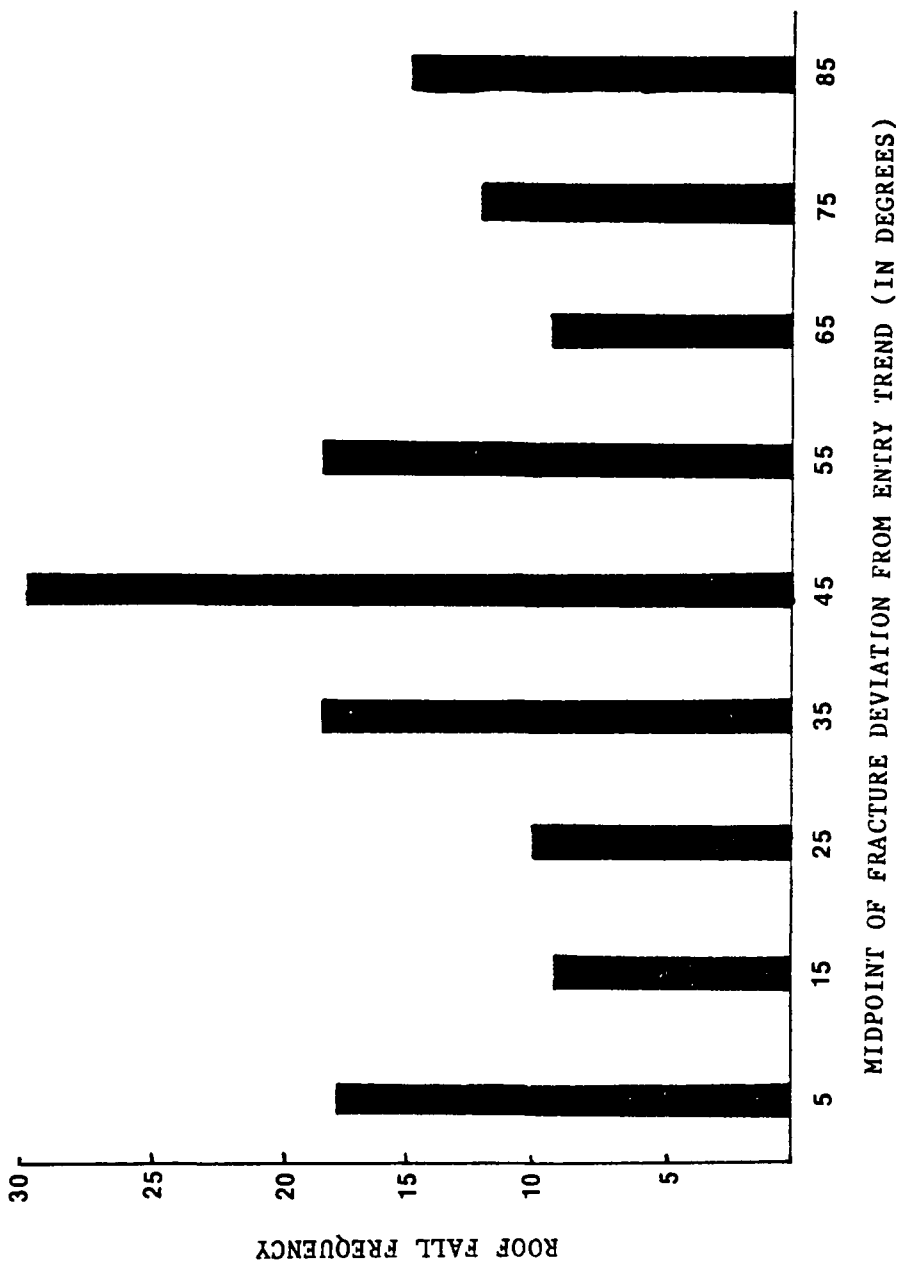

Figure 4.28: Frequency of roof falls for Sandstone Roof and different fracture deviations.

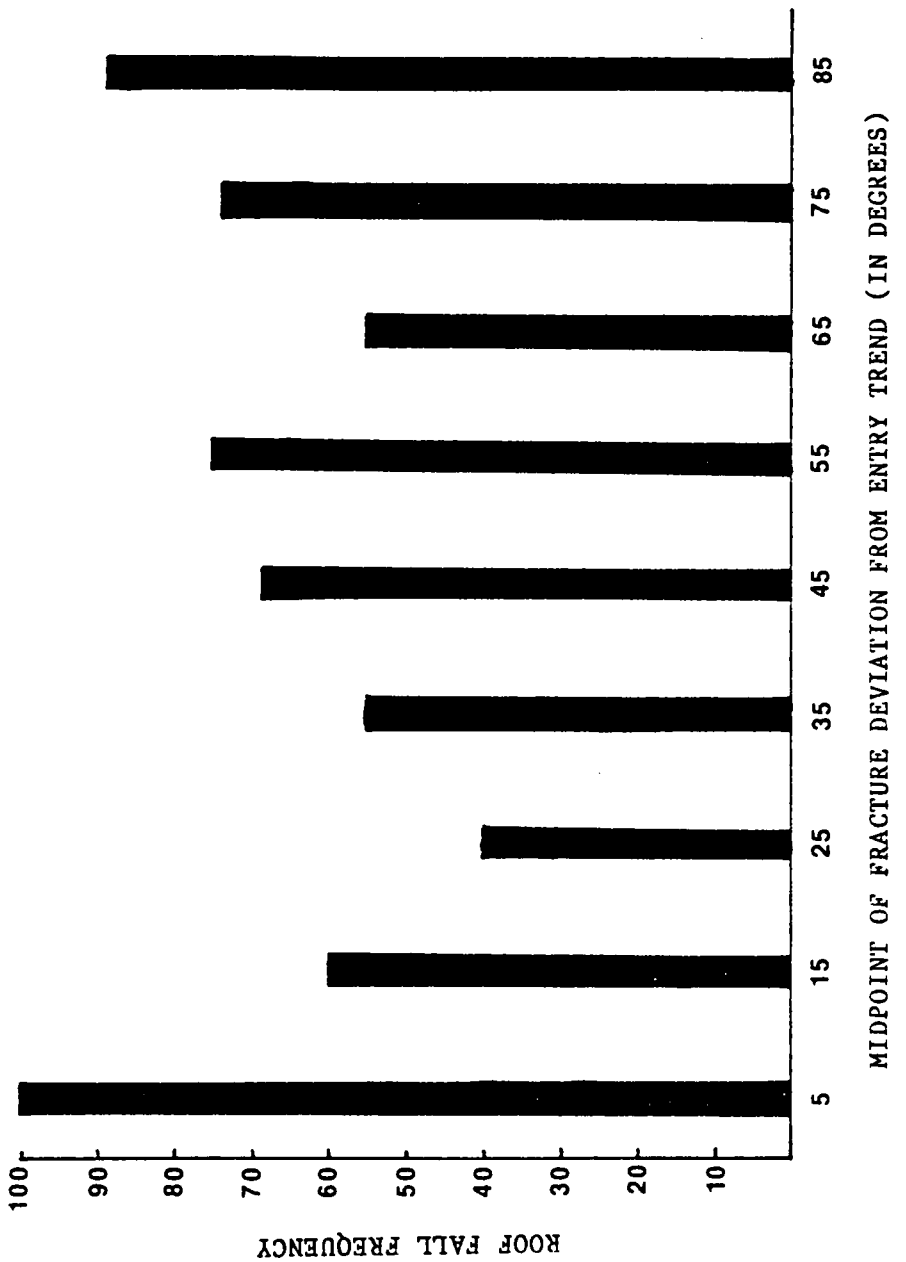

Figure 4.29: Frequency of roof falls for Shale Roof and different fracture deviations.

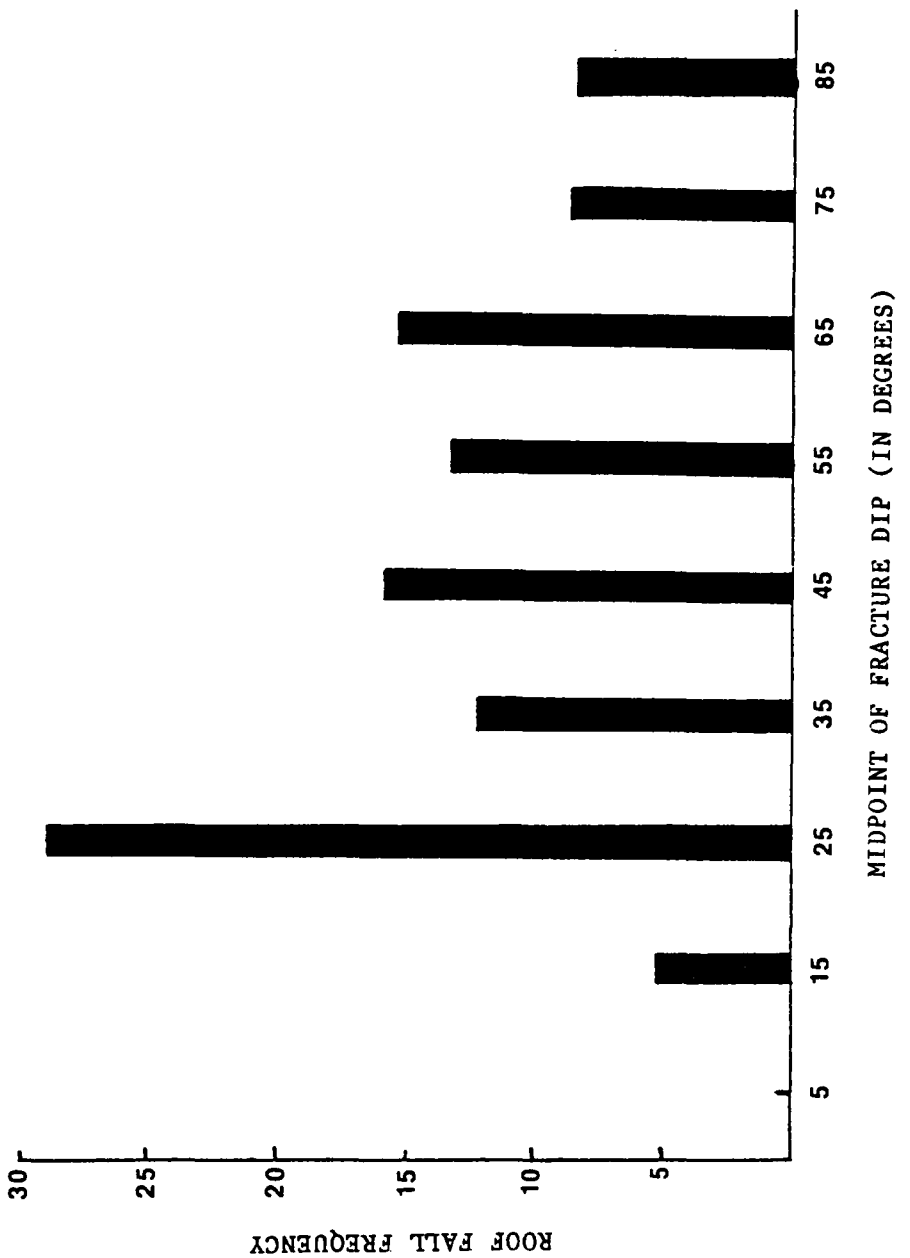

Figure 4.30: Frequency of roof falls for Interface Roof and different fracture angles.

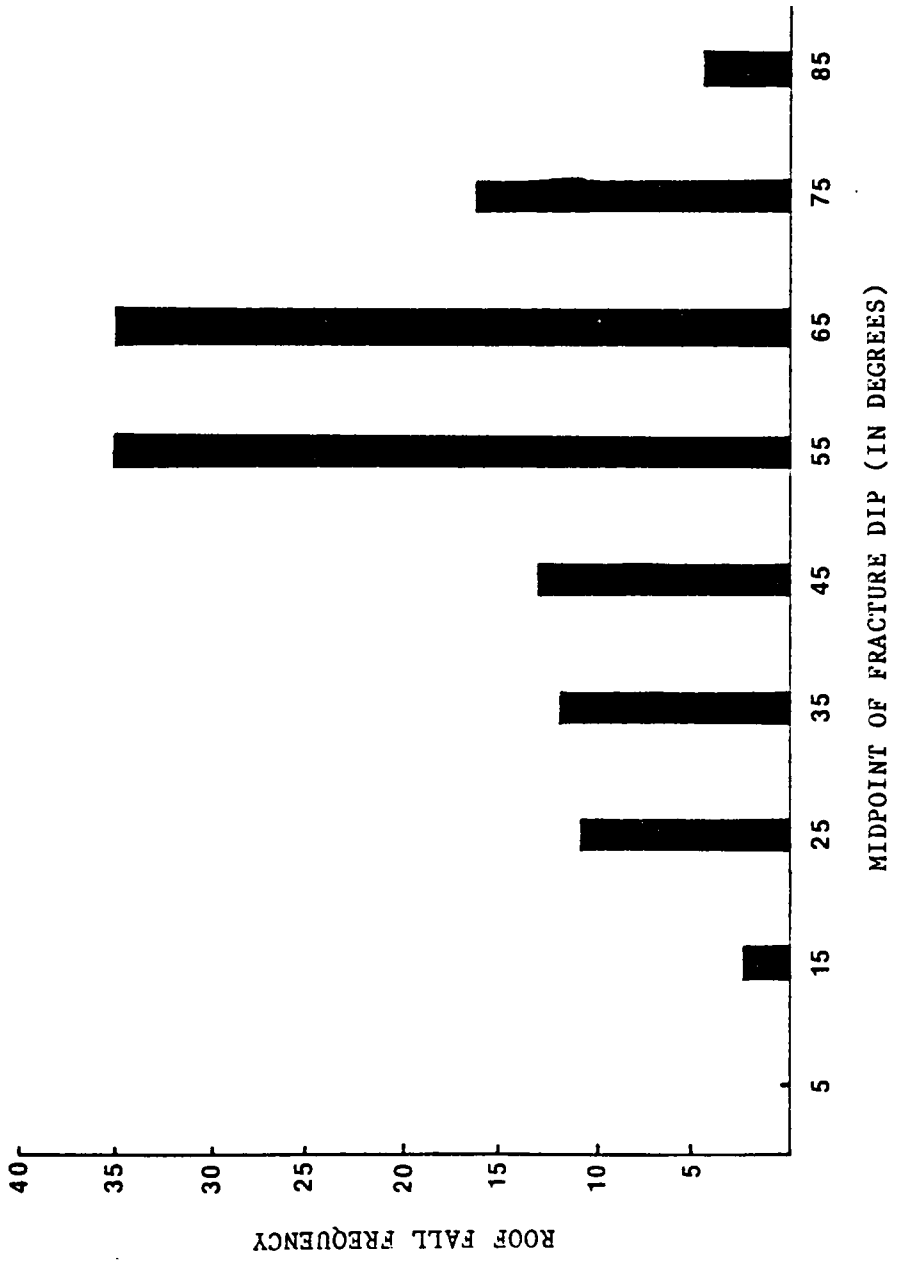

Figure 4.31: Frequency of roof falls for Sandstone Roof and different fracture angles.

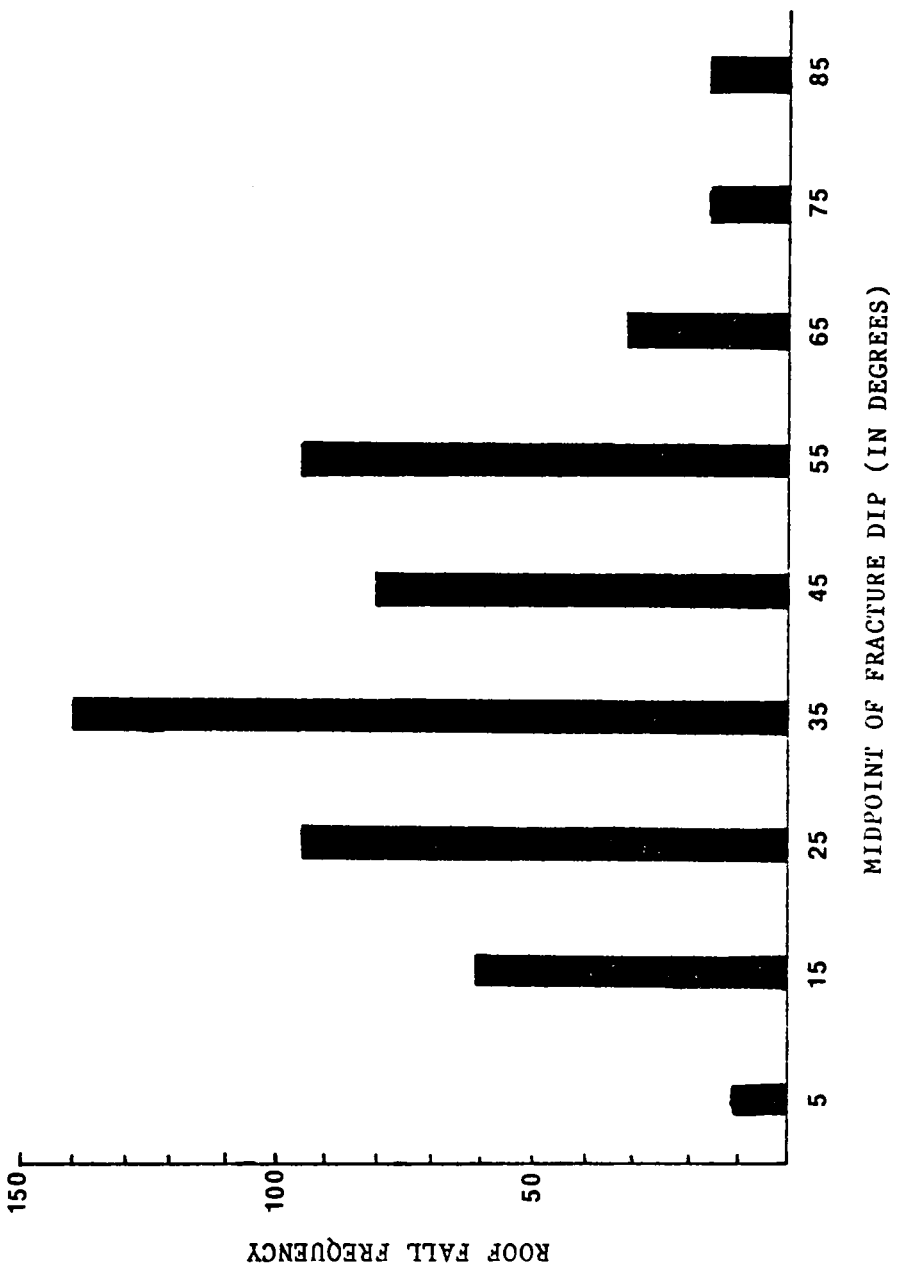

Figure 4.32: Frequency of roof falls for Shale Roof and different fracture angles.

tion, and dip of fracture angle as independent variables.

Table 4.64 shows the results for Interface Roof. The original one variable models yielded R-square values ranging from 0.2344 for fracture density to 0.3308 for coal height. Two variable models showed little improvement as was true with the three variable models also. Combining all four independent variables together resulted in an R-square of 0.3609, not as strong as one would hope for this type of analysis.

Sandstone Roof (Table 4.65) had a better R-square overall. The one variable models had values ranging from 0.0526 for fracture deviation to 0.4010 for fracture density. This R-square was improved to 0.4552 for the four variable model. However, the strength of the correlation was derived mostly from the effect of fracture density and the other variables contributed but a small amount to the final R-square.

Fracture density is extremely important in fall size determination for Shale Roof, as seen in Table 4.66. The one variable models show an R-square of only 0.0034 for fracture deviation, 0.0814 for coal height, and 0.1296 for fracture angle. The R-square for fracture density is 0.7424 which, for variables of this nature is fairly good. Improvement of the R-square by adding variables to the model resulted in a final R-square value of 0.7714 for the four variable model.

TABLE 4.64

Stepwise regression model for Interface Roof

NUMBER IN MODEL	R-SQUARE	VARIABLES IN MODEL
1	0.23441762	FRACDENS
1	0.29064297	DEVIATE
1	0.32318540	ANGLE
1	0.33085298	COALHT
2	0.32544520	DEVIATE ANGLE
2	0.32840403	FRACDENS ANGLE
2	0.33130317	FRACDENS COALHT
2	0.33640272	FRACDENS DEVIATE
2	0.35477719	COALHT DEVIATE
2	0.35955703	COALHT ANGLE
3	0.33807901	FRACDENS DEVIATE ANGLE
3	0.35673707	FRACDENS COALHT DEVIATE
3	0.36051607	FRACDENS COALHT ANGLE
3	0.36084991	COALHT DEVIATE ANGLE
4	0.36095987	FRACDENS COALHT DEVIATE ANGLE

NUMBER OF OBSERVATIONS = 12

ANGLE = Fracture Dip
COALHT = Coal Thickness
DEVIATE = Fracture Deviation From Entry Trend
FRACDENS = Fracture Density

TABLE 4.65

Stepwise regression model for Sandstone Roof

NUMBER IN MODEL	R-SQUARE	VARIABLES IN MODEL
1	0.05262285	DEVIATE
1	0.15213809	COALHT
1	0.26037015	ANGLE
1	0.40096106	FRACDENS
2	0.15247066	COALHT DEVIATE
2	0.28156089	DEVIATE ANGLE
2	0.39171048	COALHT ANGLE
2	0.40100395	FRACDENS COALHT
2	0.40437115	FRACDENS ANGLE
2	0.40587023	FRACDENS DEVIATE
3	0.40806012	FRACDENS COALHT DEVIATE
3	0.41895789	FRACDENS DEVIATE ANGLE
3	0.41989535	COALHT DEVIATE ANGLE
3	0.43477256	FRACDENS COALHT ANGLE
4	0.45525587	FRACDENS COALHT DEVIATE ANGLE

NUMBER OF OBSERVATIONS = 10

ANGLE = Fracture Dip
COALHT = Coal Thickness
DEVIATE = Fracture Deviation From Entry Trend
FRACDENS = Fracture Density

TABLE 4.66

Stepwise regression model for Shale Roof

NUMBER IN MODEL	R-SQUARE	VARIABLES IN MODEL
1	0.00339805	DEVIATE
1	0.08143211	COALHT
1	0.12962373	ANGLE
1	0.74240115	FRACDENS
2	0.08303684	COALHT DEVIATE
2	0.13261842	DEVIATE ANGLE
2	0.15817274	COALHT ANGLE
2	0.74274933	FRACDENS DEVIATE
2	0.76806741	FRACDENS COALHT
2	0.77016011	FRACDENS ANGLE
3	0.15905262	COALHT DEVIATE ANGLE
3	0.76943005	FRACDENS COALHT DEVIATE
3	0.77021717	FRACDENS COALHT ANGLE
3	0.77129353	FRACDENS DEVIATE ANGLE
4	0.77145440	FRACDENS COALHT DEVIATE ANGLE

NUMBER OF OBSERVATIONS = 64

ANGLE = Fracture Dip
COALHT = Coal Thickness
DEVIATE = Fracture Deviation From Entry Trend
FRACDENS = Fracture Density

4.3 DEVELOPMENT OF A ROOF RATING INDEX (RRI)

By utilizing the results of the statistical analysis (Table 4.67), a Roof Rating Index (RRI) was devised (Table 4.68). An effort was made to assign weighted values to each variable for a particular roof type. These weights reflect the strength of the chi-square as well as the regression analysis relationships. Values of from 0 to 10 were given to each variable depending on its influence in roof stability. The lower the value, the more unstable the condition. Thus, a value of 1 would reflect a very hazardous condition while that of 10 would indicate very stable roof. For example, since slickensides increase the possibility of a roof fall in shale by three times, the value for slickensided Shale Roof is one-third that of unslickensided roof. This weighting was carried out for all variables and was modified in some instances if observation warranted another value. Once the assigning of weighted values for an observation was completed, the Roof Rating Index (RRI) was obtained by finding the sum of all the categories. From this, it is possible to make some determination of the relative stability of a particular roof type with regards to the probability of a rock fall. It should be noted that observations in which more than six of the categories were missing were not included in the Index.

Table 4.69 shows the results of a chi-square test in

TABLE 4.67

Chi-square measures of independence for coal mine variables and roof failure (summary)

ROOF TYPE	LOCATION	FAULTED COAL	FOSSILS	SLICKENSIDES	ROOF FRACTURE TYPE	FRACTURE DEVIATION FROM ENTRY TREND	FRACTURE DIP	FRACTURE DENSITY
INTERFACE	0.4087	0.9025	1.0000	0.7189	0.0688	0.3402	0.4648	0.4396
SANDSTONE	0.0017	0.4565	0.0251	0.1430	0.2077	0.9556	0.0847	0.0001
SHALE	0.0001	0.0165	0.4347	0.0001	0.0096	0.0050	0.0003	0.0001

TABLE 4.68

Roof Rating Index

ROOF TYPE	A LOCATION			B FOSSILS		C SLICKENSIDES		D FAULTED COAL	
	4-Way Intersection	3-Way Intersection	Entry or Crosscut	Present	Absent	Present	Absent	Yes	No
INTERFACE	2	6	8	1	6	5	8	3	10
SANDSTONE	4	6	10	3	8	7	9	7	9
SHALE	3	4	8	6	10	3	10	2	10

ROOF TYPE	E FIRST FRACTURE TYPE				F SECOND FRACTURE TYPE				G THIRD FRACTURE TYPE			
	Joint	Tear	Fault	Dip-or Oblique-Slip Fault	Joint	Tear	Fault	Dip- or Oblique-Slip Fault	Joint	Tear	Fault	Dip- or Oblique Slip Fault
INTERFACE	2		8	8	2		8	8	2		8	8
SANDSTONE	1		8	8	1		8	8	1		8	8
SHALE	8		7	4	8		7	4	8		7	4

ROOF TYPE	H MINIMUM DEVIATION OF ROOF FRACTURES FROM ENTRY TREND									I MAXIMUM DIP ANGLE OF ROOF FRACTURES								
	0-9	10-19	20-29	30-39	40-49	50-59	60-69	70-79	80-90	0-9	10-19	20-29	30-39	40-49	50-59	60-69	70-79	80-90
INTERFACE	8	6	8	6	1	3	6	6	8	8	8	8	8	8	8	9	9	8
SANDSTONE	6	8	6	6	6	6	8	8	8	3	8	8	6	6	3	3	2	9
SHALE	6	6	6	3	4	4	4	4	6	4	4	6	3	6	4	4	3	4

ROOF TYPE	J FRACTURE DENSITY (Number of Fractures/3 Meters)					
	0-2	3-4	5-6	7-8	9-10	10
INTERFACE	7	5	6	5	5	4
SANDSTONE	10	8	3	7	6	1
SHALE	10	7	6	5	2	0

ROOF RATING INDEX (RRI) = A + B + C + D + E + F + G + H + I + J

TABLE 4.69

Chi-square analysis of Roof Rating Index for Interface Roof

Frequency
Percent
Row Percent
Column Percent

ROOF RATING INDEX	FALL : NO	YES	TOTAL
Index = 0 - 19	0	0	0
	0.00	0.00	0.00
	0.00	0.00	0.00
	0.00	0.00	0.00
Index = 20 - 29	5	7	12
	7.04	9.86	16.90
	41.67	58.33	
	15.63	17.95	
Index = 30 - 39	10	8	18
	14.08	11.27	25.35
	55.56	44.44	
	31.25	20.51	
Index = 40 - 49	2	10	12
	2.82	14.08	16.90
	16.67	83.33	
	6.25	25.64	
Index = 50 - 59	0	2	2
	0.00	2.82	2.82
	0.00	100.00	
	0.00	5.13	
Index = 60 - 100	15	12	27
	21.13	16.90	38.03
	55.56	44.44	
	46.88	30.77	
TOTAL	32	39	71
	45.07	54.93	100.00

CHI-SQUARE 7.606 DEGREES OF FREEDOM = 4

PROBABILITY = 0.1071

which the Roof Rating Index was compared to roof stability for Interface Roof. No data was available for an RRI of less than 20, however, the probabilities of roof falls were 58% for an RRI of 20-29, 44% for an RRI of 30-39, 83% for an RRI of 40-49, and 48% for an RRI greater than 50. The chi-square measure of independence for this test is 0.1071 which indicates that the test does not show a strong dependence for this roof type. The best explanation for this lack of dependence lies in the fact that Interface Roof did not show many strong correlations between the variables tested and roof failure. This is reflected in the poor performance of the RRI as a predictor for this roof type. Interface Roof, as determined from the field study portion of this research, is much more dependent stability-wise on the localized lithologic differences present between rock types. For example, channel boundaries are dependent on the differing properties of the material on either side of the interface rather than on, say, fossils. Rider coals depend on the tensile strength of the coal in the rider seam as well as its distance above the main seam. By design, these variables were not part of the survey as they are not universal and apply only to the particular type of Interface Roof in question. Another problem inherent in dealing with Interface Roof is that it is relatively rare and by creating subsets within the classification, field data would become too sparse to

make any conclusions.

The results for Sandstone Roof are quite encouraging (Table 4.70). The chi-square probability for the analysis is 0.0001 which demonstrates a very strong dependence between stability and RRI. The probability of a failure for a roof with an RRI of 0-19 is 71%; this decreases to 69% for an RRI of 20-29. An RRI of 30-39 yields a fall probability of 44%, and that of 40-49, only 33%. Finally, observations with an RRI of greater than 50 experienced a percentage of failure of only 15%.

Shale Roof also had a strong chi-square probability of 0.0001. This is shown in Table 4.71. However, results for Shale Roof did not show quite as good a trend as those for Sandstone Roof. A Roof Rating Index of 0-19 had probability of failure of 77%, but a roof with an RRI of 20-29 had the probability jump slightly to 79%. An RRI of 30-39 had a 77% chance of a fall and RRI from 40-49 also fell a small amount to 72%. When the RRI was greater than 50, the probability of failure dropped tremendously to only 28%. Although, the figures for Shale Roof are not as good as those for Sandstone Roof, the fact remains that increasing RRI is indicative of better and more stable roof rock in Shale Roof.

This information is summarized in Table 4.72.

A computer code in BASIC was written to compute the Roof Rating Index given the variables used in this research. A simplified flowchart is shown in Figure 4.33. Data is read

TABLE 4.70

Chi-square analysis of Roof Rating Index for Sandstone Roof

Frequency
Percent
Row Percent
Column Percent

ROOF RATING INDEX	FALL : NO	YES	TOTAL
Index = 0 - 19	2	5	7
	1.72	4.31	6.03
	28.57	71.43	
	2.67	12.20	
Index = 20 - 29	8	18	26
	6.90	15.52	22.41
	30.77	69.23	
	10.67	43.90	
Index = 30 - 39	5	4	9
	4.31	3.45	7.76
	55.56	44.44	
	6.67	9.76	
Index = 40 - 49	10	5	15
	8.62	4.31	12.93
	66.67	33.33	
	13.33	12.20	
Index = 50 - 59	1	0	1
	0.86	0.00	0.86
	100.00	0.00	
	1.33	0.00	
Index = 60 - 100	49	9	58
	42.24	7.76	50.00
	84.48	15.52	
	65.33	21.95	
TOTAL	75	41	116
	64.66	35.34	100.00

CHI-SQUARE 27.930 DEGREES OF FREEDOM = 5

PROBABILITY = 0.0001

TABLE 4.71

Chi-square analysis of Roof Rating Index for Shale Roof

Frequency
Percent
Row Percent
Column Percent

ROOF RATING INDEX	FALL : NO	YES	TOTAL
Index = 0 - 19	5	17	22
	2.37	8.06	10.43
	22.73	77.27	
	7.04	12.14	
Index = 20 - 29	10	39	49
	4.74	18.48	23.22
	20.41	79.59	
	14.08	27.86	
Index = 30 - 39	14	47	61
	6.64	22.27	28.91
	22.95	77.05	
	19.72	33.57	
Index = 40 - 49	9	24	33
	4.27	11.37	15.64
	27.27	72.73	
	12.68	17.14	
Index = 50 - 59	2	9	11
	0.95	4.27	5.21
	18.18	81.82	
	2.82	6.43	
Index = 60 - 100	31	4	35
	14.69	1.90	16.59
	88.57	11.43	
	43.66	2.86	
TOTAL	71	140	211
	33.65	66.35	100.00

CHI-SQUARE 57.217 DEGREES OF FREEDOM = 5

PROBABILITY = 0.0001

TABLE 4.72

Chi-square analysis of Roof Rating Index for the different roof types

INTERFACE ROOF
(Chi-square Probability = 0.1071)

ROOF INDEX	PROBABILITY OF FAILURE
0 - 19	(No Data Available)
20 - 29	58%
30 - 39	44%
40 - 49	83%
> 50	48%

SANDSTONE ROOF
(Chi-square Probability = 0.0001)

ROOF INDEX	PROBABILITY OF FAILURE
0 - 19	71%
20 - 29	69%
30 - 39	44%
40 - 49	33%
> 50	15%

SHALE ROOF
(Chi-square Probability = 0.0001)

ROOF INDEX	PROBABILITY OF FAILURE
0 - 19	77%
20 - 29	79%
30 - 39	77%
40 - 49	72%
> 50	28%

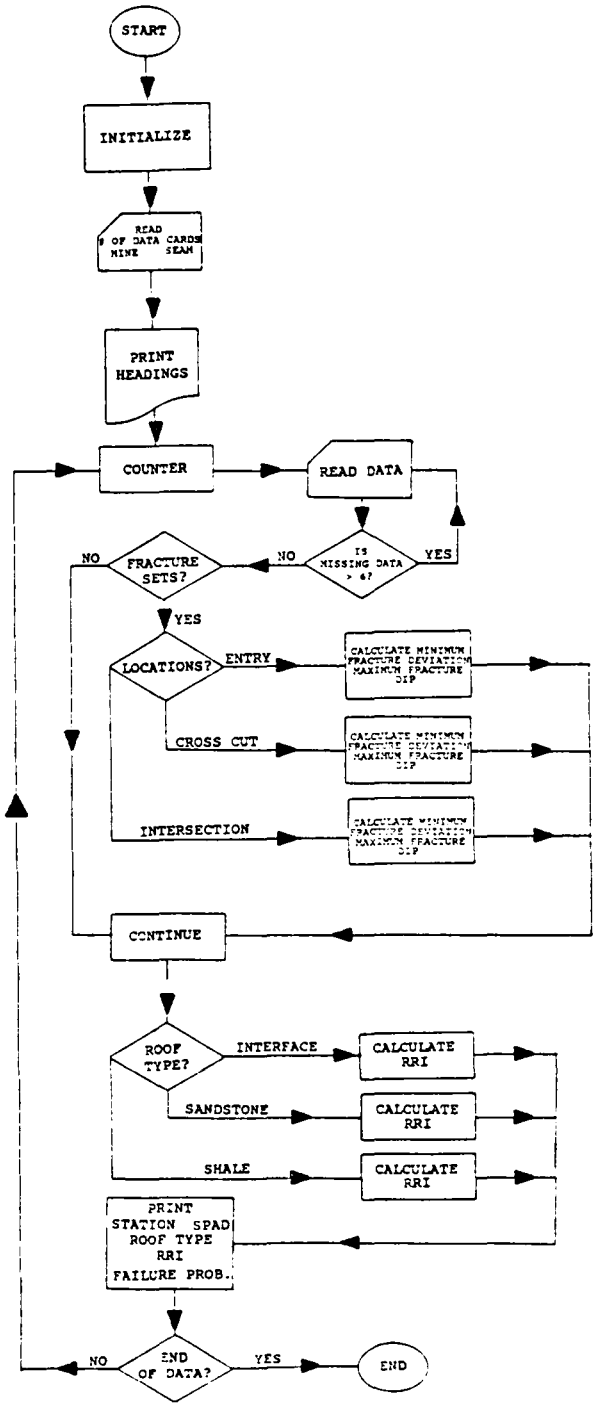

Figure 4.33: Flow chart for roof evaluation program.

from data statements; missing data is accounted for. If the number of missing variables is greater than six, a message is printed stating that there is not enough data to calculate a reasonable RRI, and the next data statement is read. The program then branches to different subroutines depending on station location within the mine. The minimum fracture deviation from entry or cross-cut trend is calculated along with the maximum fracture dip. Contol is then returned to the main program, where branching to subroutines takes place once again in order to calculate the RRI and failure probability for each roof type. The main program then outputs the data, and either returns to read another data statement or ends if all data has been read. Table 4.73 shows a sample output from the program.

Figure 4.34 is a portion of a mine map for which the failure probabilities derived from the computer program have been contoured and roof falls in that section of the mine plotted. The trend of more numerous and larger roof falls with increasing probability of failure is clear from this diagram. The larger falls are all grouped relatively close together within the 60 per cent failure probability contour; smaller falls are scattered randomly over a much larger area and tend to be found well below the 60 percent contour line.

TABLE 4.73

Sample output from computer code

MINE: SEAM: JAWBONE

STATION	SPAD	ROOFTYPE	RRI	FAILURE PROBABILITY (%)
M7	597A	Not have enough data to calculate Roof Rating Index		
M7A	658	SANDSTONE	16	71
M7B	658A	SANDSTONE	30	44
M7C	658A	SANDSTONE	27	69
M7D	799	SANDSTONE	27	69
M7E	799	SANDSTONE	28	69
M7F	799A	SANDSTONE	24	69
M7G	841	SANDSTONE	27	69
M7H	841A	SANDSTONE	27	69
M7I	841B	SANDSTONE	18	71
M7J	841C	SANDSTONE	32	44
M8	841C	SANDSTONE	28	69
M8A	878	SANDSTONE	28	69
M8B	957	SANDSTONE	24	69
M8C	957	SANDSTONE	28	69
M8D	1182	SANDSTONE	28	69
M8E	1241	SANDSTONE	25	69
M8E	1241	SANDSTONE	29	69
M8F	1321	SANDSTONE	19	71
M9	1504	SANDSTONE	19	71
M9A	1596	SANDSTONE	19	71
M9B	1606	SANDSTONE	19	71
M9C	1627	SANDSTONE	47	31
M9D	1648	SANDSTONE	70	15
M9E	1673	SANDSTONE	73	15
M9F	1697	INTERFACE	81	15
M9G	1697A	SHALE	57	28

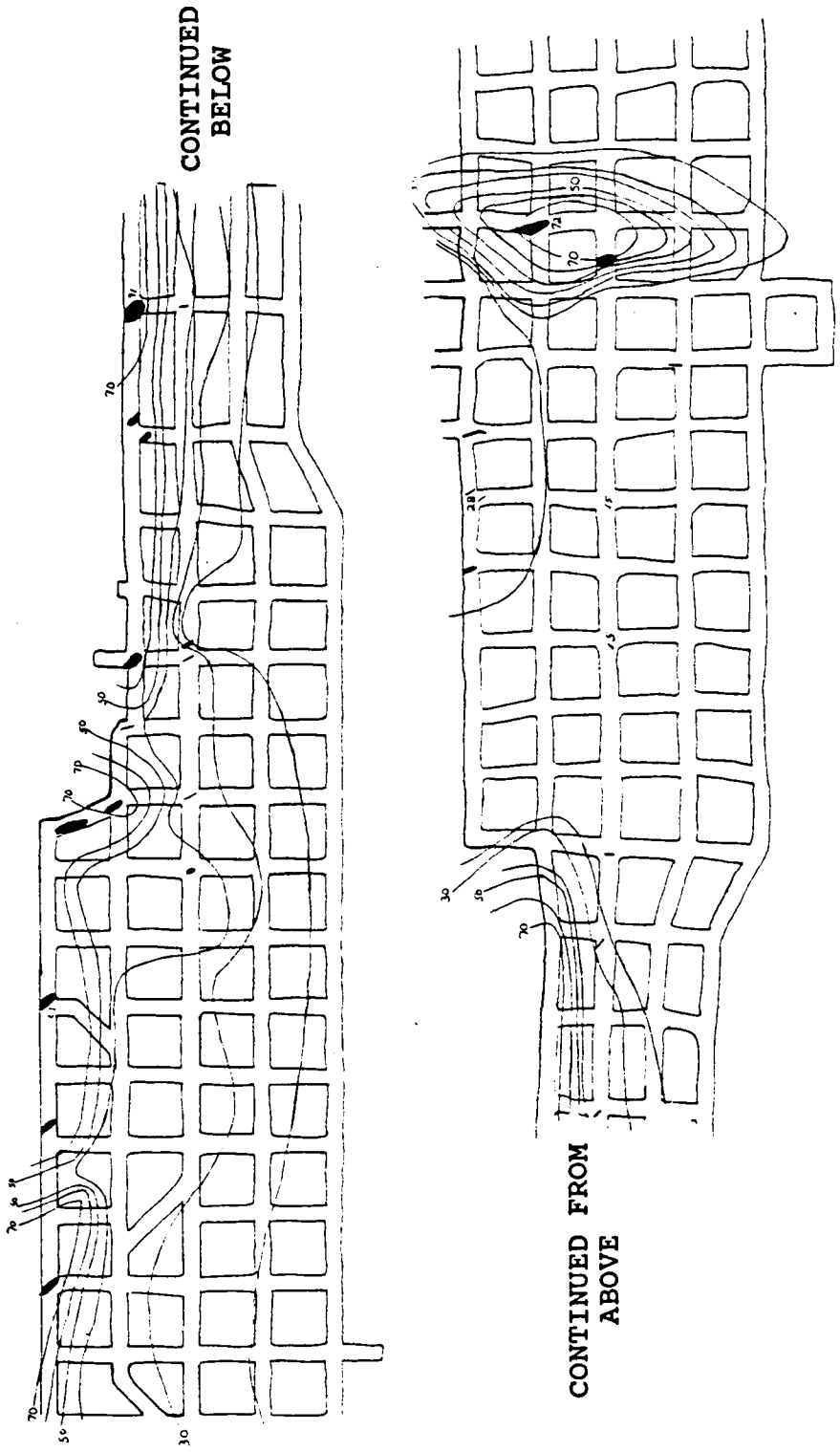

Figure 4.34: Mine map showing roof falls and contours of failure probability (%).

CHAPTER 5

RESULTS OF FINITE ELEMENT MODELING

5.1 Introduction

From statistical analysis, it appeared that the major mapped variables did not influence the stability of Interface Roof to any great degree. Rather, it seams that the behavior of this roof is determined more by its own lithologic variation than by any geomechanical characteristics such as joints, faults, etc. superimposed on it.

The finite element method was applied to two types of Interface Roof: rider seams and splay deposits. This was attempted to determine the critical distance above a seam for a rider coal or the thickness at which the interbeds of sandstone and shale might prove troublesome.

Interest was centered on the stress distributions around the openings and in the immediate roof. When stresses exceeded the strength of any of the rock material, it was taken as indicative of a roof failure.

The first analysis involved excavating the in situ conditions, mainly, to check for any failures due to excavation alone. For this analysis the immediate roof and the entire overburden was considered to composed entirely of shale. Figure 5.1 shows that no failure took place even

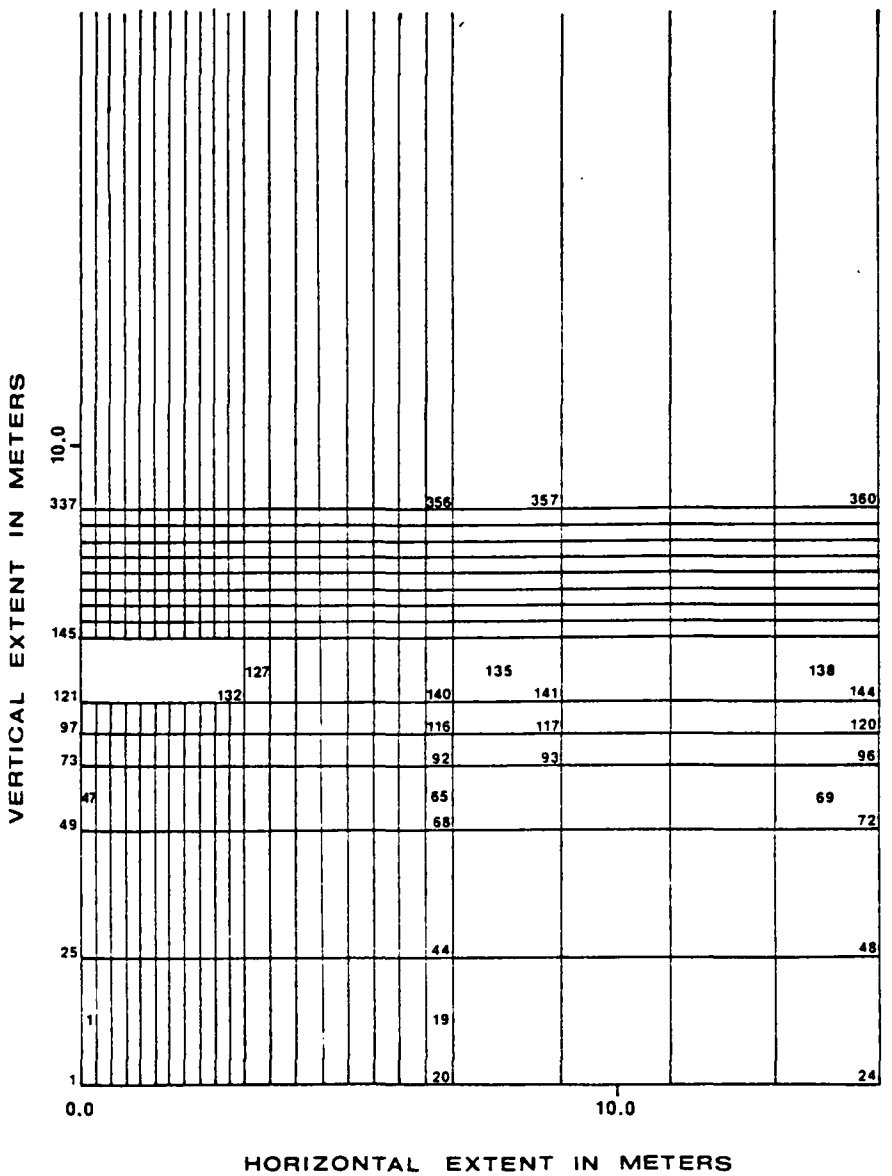

Figure 5.1: In situ analysis with mine opening excavated.

after the second phase of element removal. A further check of the program revealed that displacements around the opening were as expected, slight floor heave and roof sag.

5.2 Rider Seam Analysis

In the case of a rider seam 2.0 meters above the main seam, no failures were detected. This was also true of a rider seam 1.75 and 1.5 meters above the principal mined seam.

However, when the rider seam was placed 1.25 meters above the coal seam, tensile failure of parts of two elements of rider coal occurred (Figure 5.2). This happened only after the second iteration, or element removal, which would correspond to the last cut of the continuous miner.

With the rider seam 1.0 meter above the coal, tensile failure again occurred in the rider only after the second removal of elements. This time 2.5 elements were found to have failed (Figure 5.3). Figure 5.4 shows the failure pattern with the rider seam 0.75 meters above the coal. Again, the rider seam failed after the second iteration but 4.5 elements were affected.

When the rider seam was moved closer to the main seam, failures increased. A slight failure, 1.25 elements is noticeable in Figure 5.5 for a rider coal 0.5 meters above the main coal. For the second element removal (Figure 5.6),

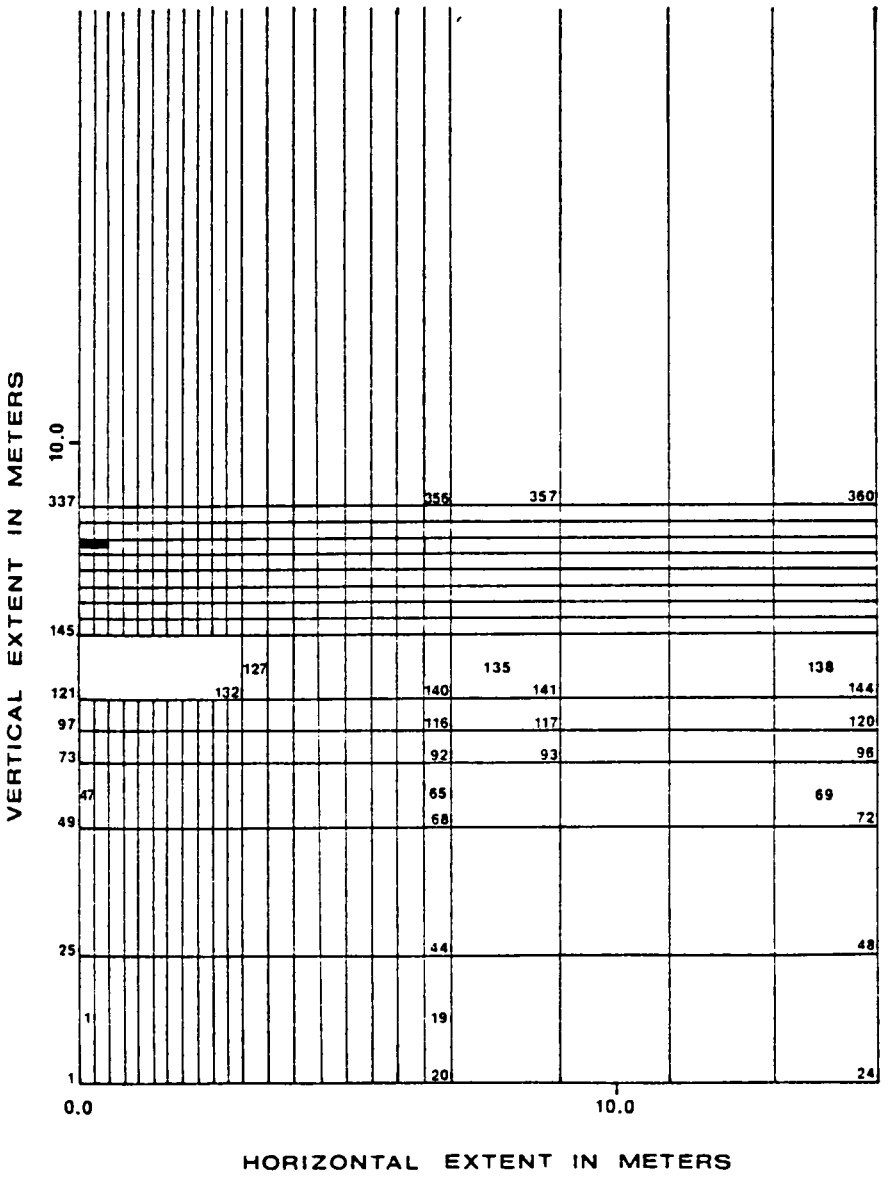

Figure 5.2: Tensile failure with rider seam 1.25 meters above the coal (2nd iteration).

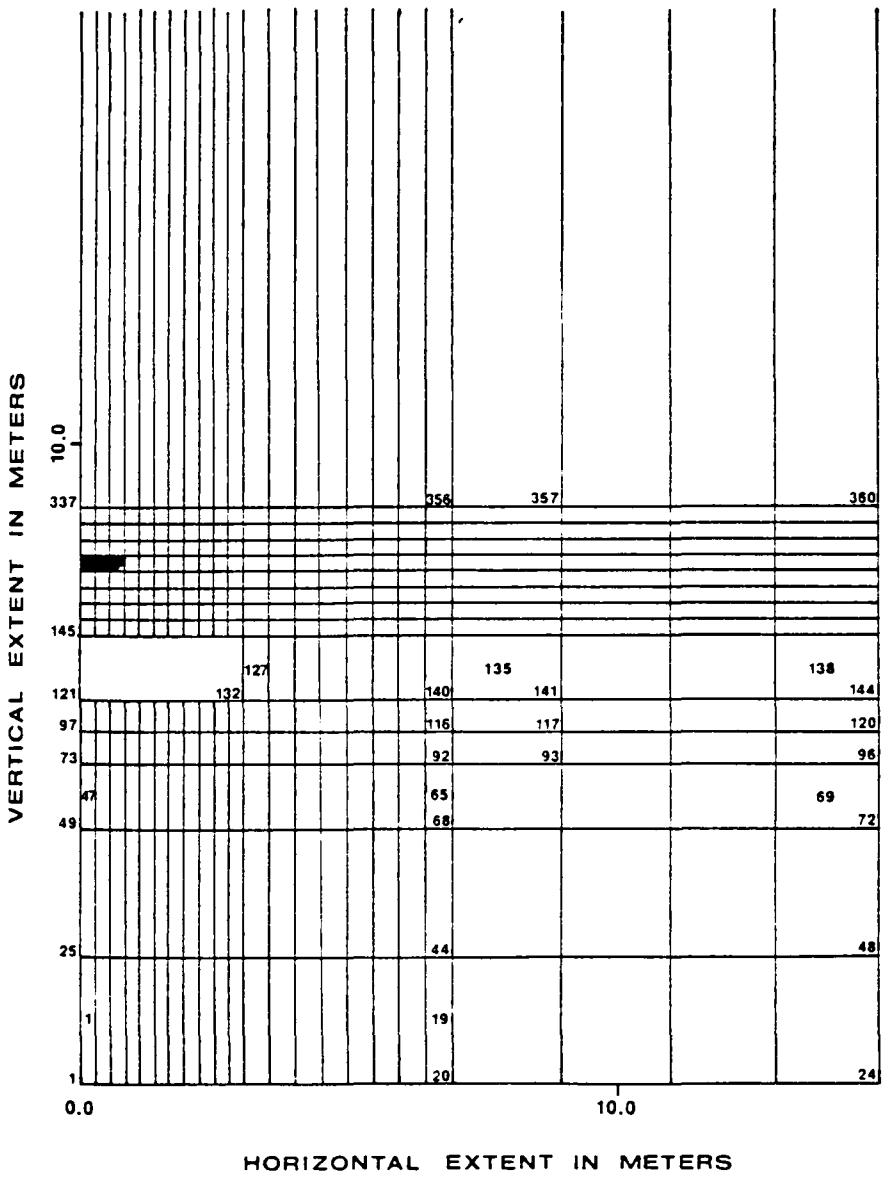

Figure 5.3: Tensile failure with rider seam 1.0 meters above the coal (2nd iteration).

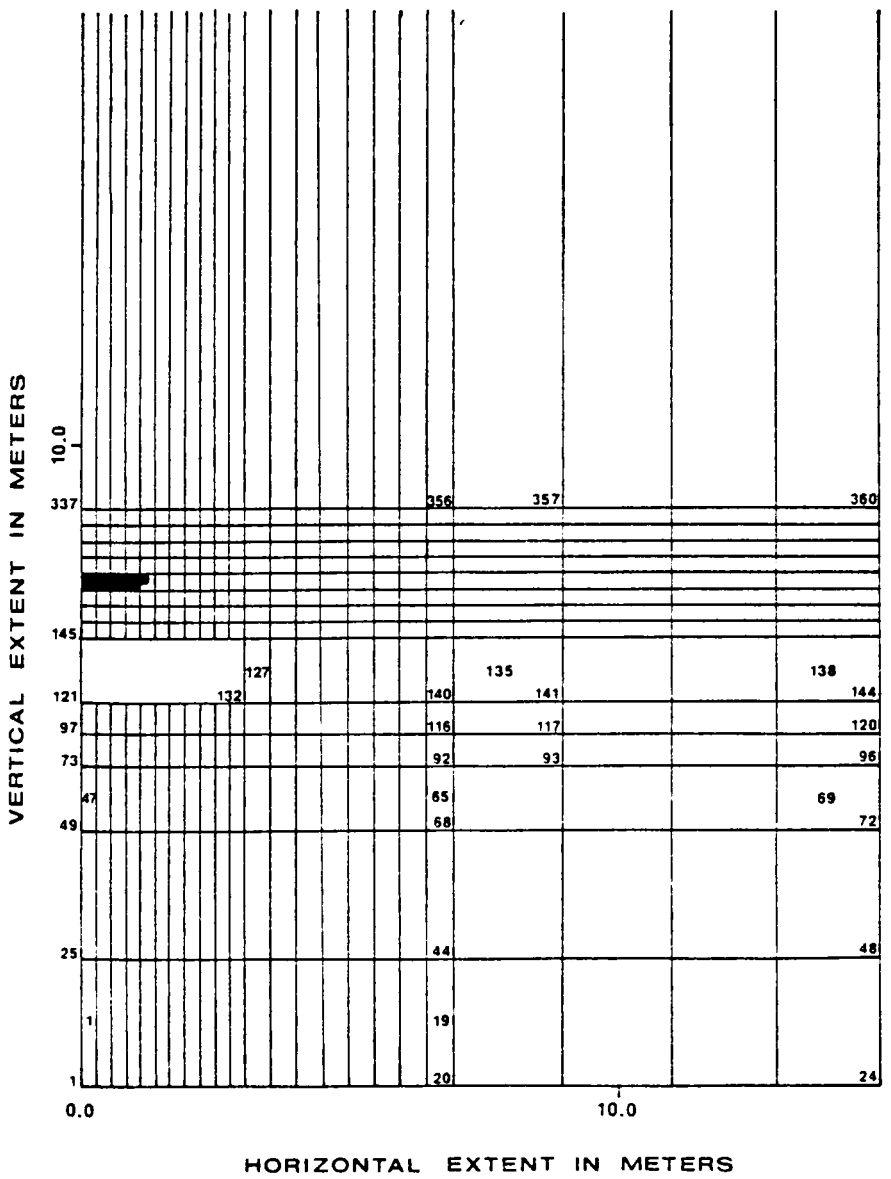

Figure 5.4: Tensile failure with rider seam 0.75 meters above the coal (2nd iteration).

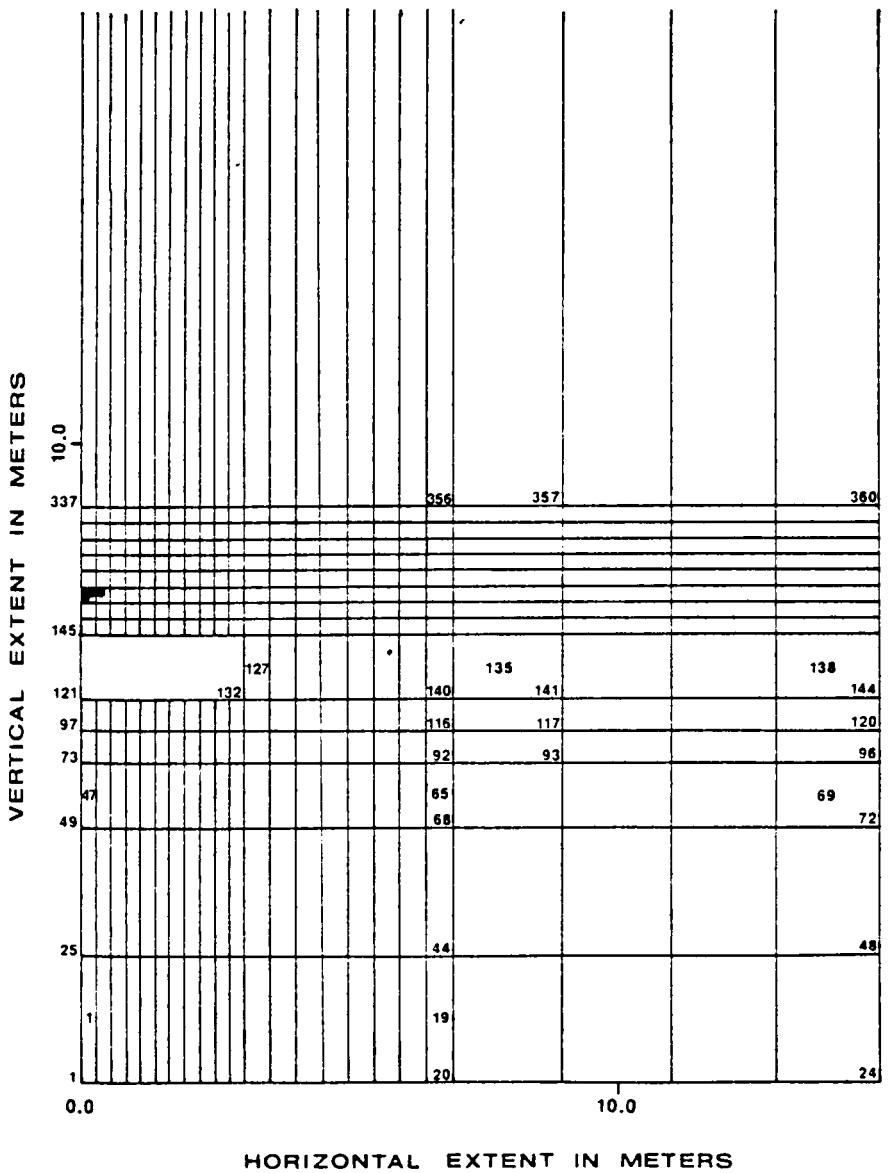

Figure 5.5: Tensile failure with rider seam 0.5 meters above the coal (1st iteration).

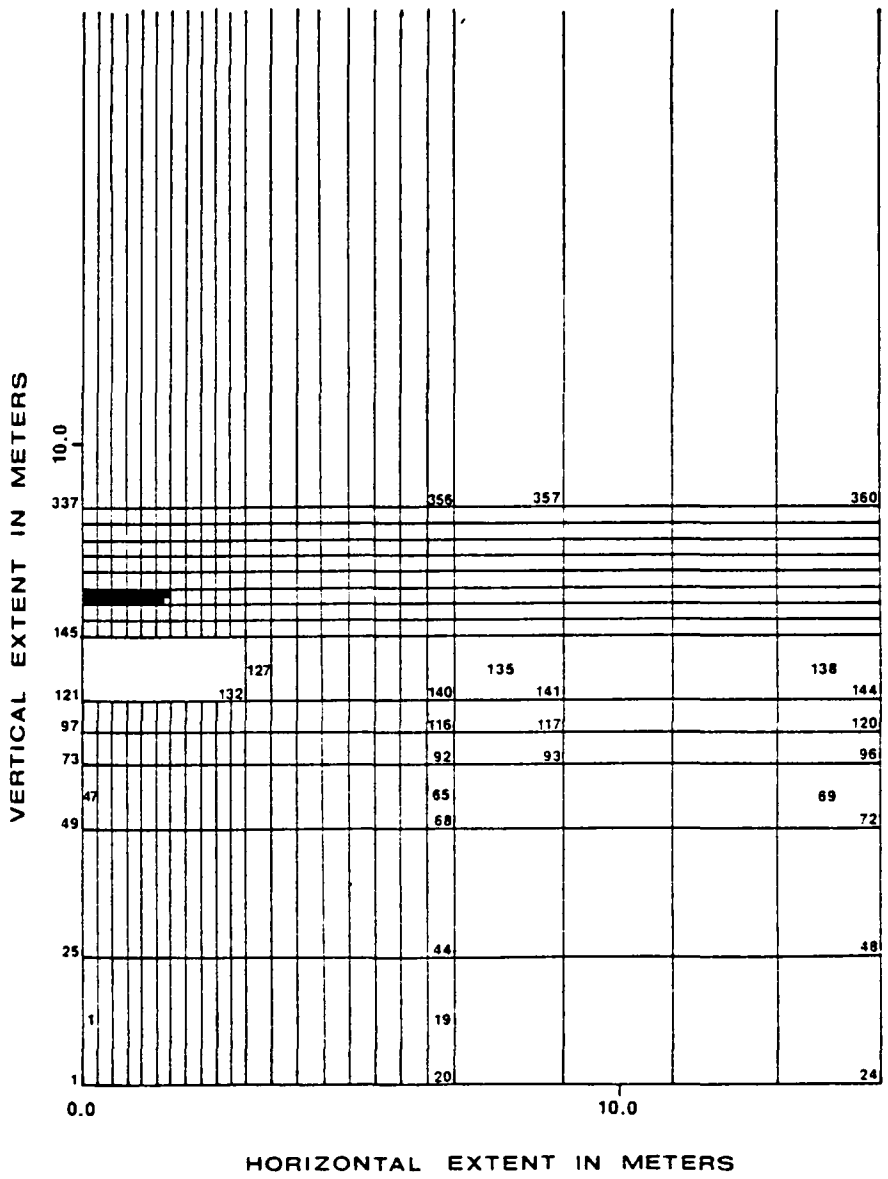

Figure 5.6: Tensile failure with rider seam 0.5 meters above the coal (2nd iteration).

a rather large, 5.75, number of elements failed in tension. Two and one-half elements failed during the first element removal when the rider seam was brought closer, 0.25 meters (Figure 5.7). For the second iteration, 7.5 elements were in the tensile failure state (Figure 5.8)

The results of the rider seam testing are tabulated in Tables 5.1 and 5.2, and in Figure 5.9.

5.3 Crevasse Splay Deposit Analysis

No failures were recorded for any of the crevasse splay deposit models. The splay deposits consisted of alternating beds of sandstone and shale beginning with one meter thick beds and ending with 0.25 meter thick beds. The engineering properties of the rocks used in this analysis were the same as those used for the rider seam analysis and which provided realistic results for that model. This would suggest that bed thickness is very critical for this roof type.

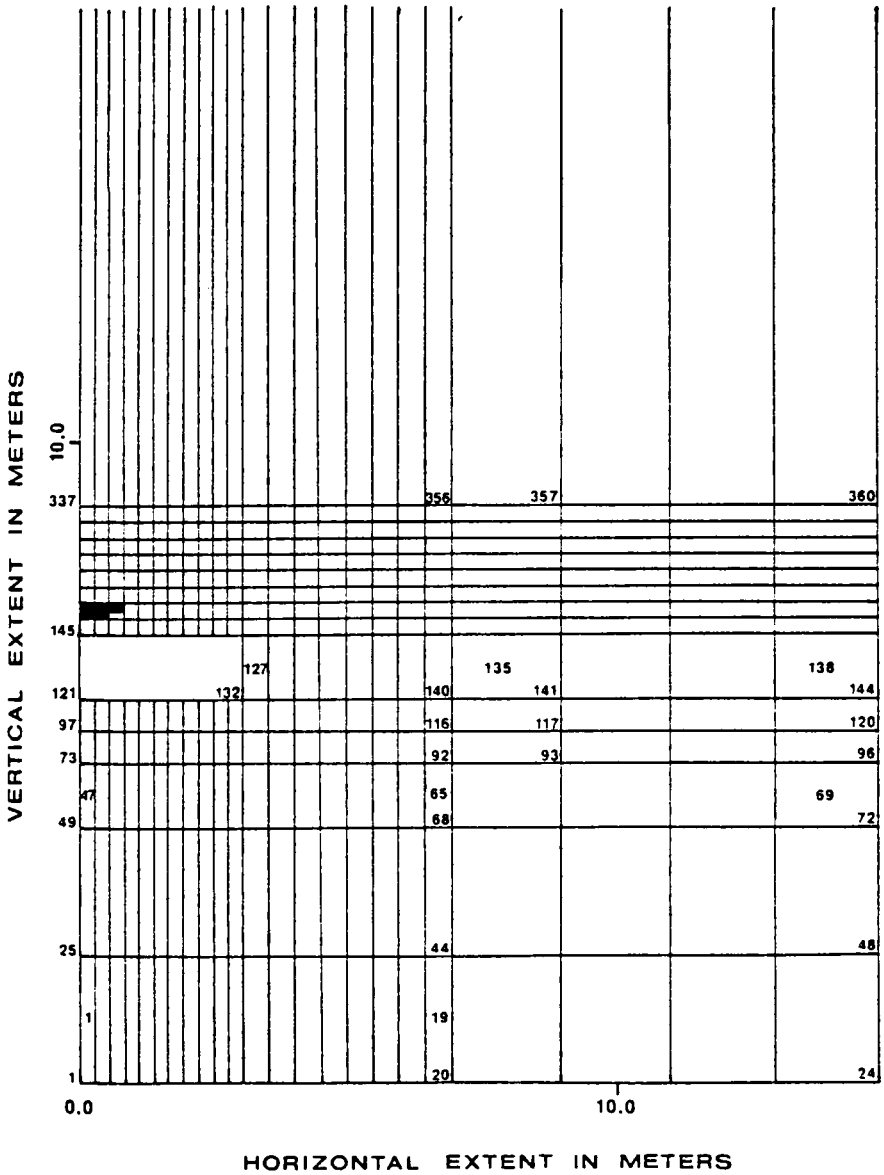

Figure 5.7: Tensile failure with rider seam 0.25 meters above the coal (1st iteration).

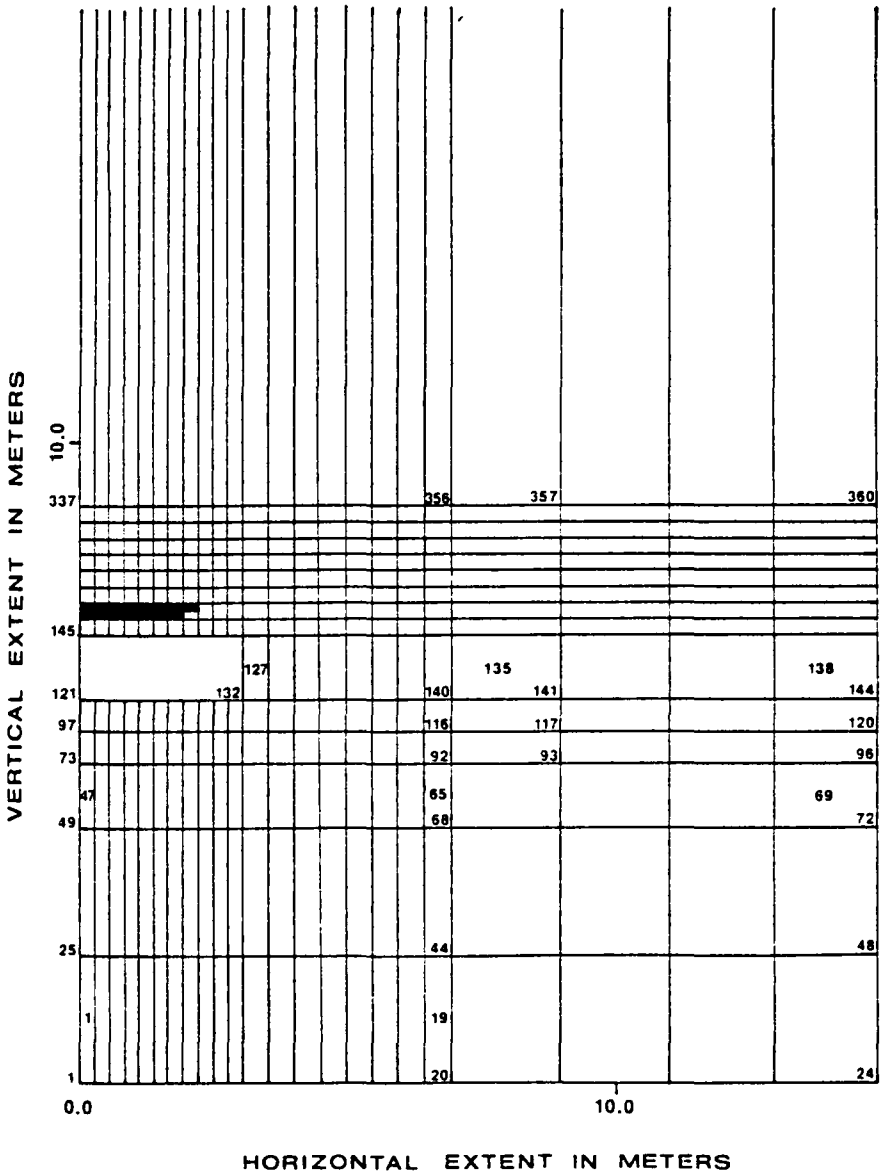

Figure 5.8: Tensile failure with rider seam 0.25 meters above the coal (2nd iteration).

TABLE 5.1

Size of tensile failure zone (1st Iteration)

(Size of Excavation 3.0 m^3) *

Height of Rider Above Coal (m)	Size of Failure Zone (m^3)
2.00	0.00
1.75	0.00
1.50	0.00
1.25	0.00
1.00	0.00
0.75	0.00
0.50	0.50
0.25	0.34

* Unit thickness and accounting for symmetry of opening

TABLE 5.2

Size of tensile failure zone (2nd Iteration)

(Size of Excavation 5.5 m^3)*

Height of Rider Above Coal (m)	Size of Failure Zone (m^3)
2.00	0.00
1.75	0.00
1.50	0.00
1.25	0.13
1.00	0.34
0.75	0.53
0.50	0.72
0.25	0.94

* Unit thickness and accounting for symmetry of opening

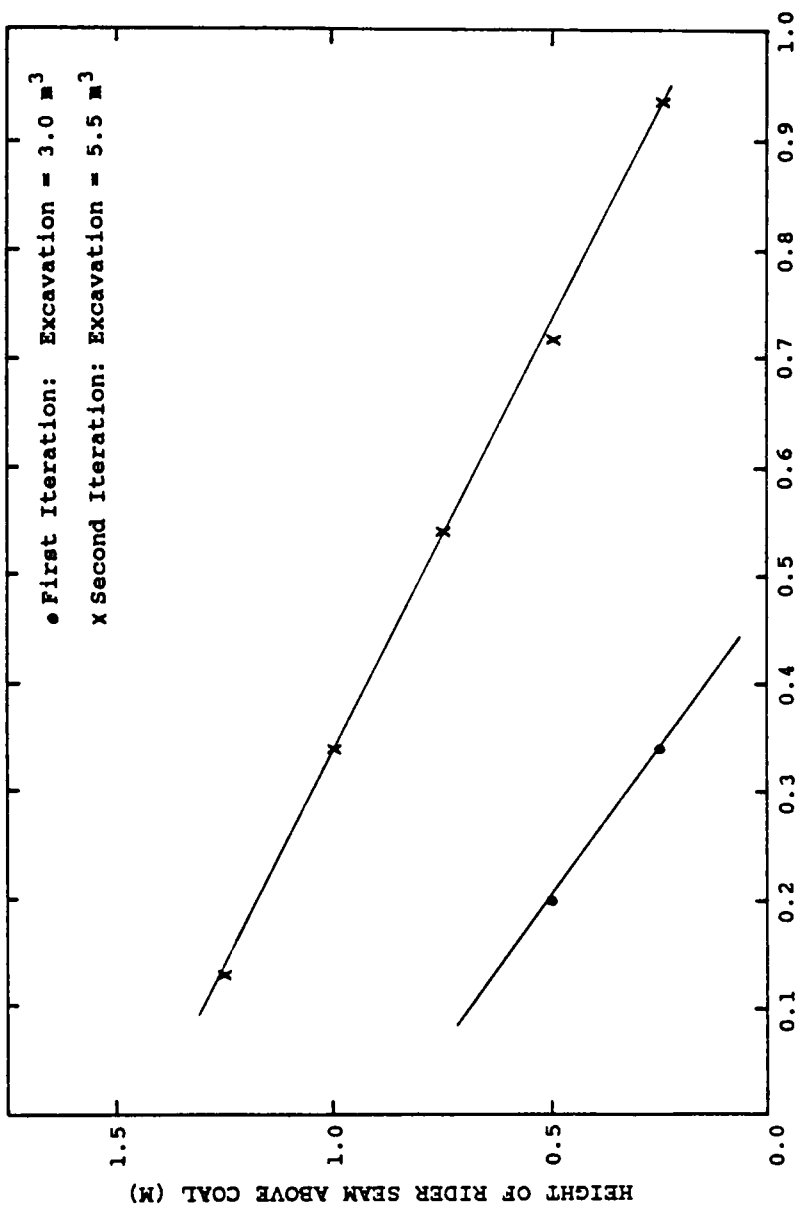

Figure 5.9: The effects of rider seam height on the size of the tensile failure zone.

CHAPTER 6

DISCUSSION

6.1 Introduction

The purpose of this research was to determine the geological and geomechanical variables common to most roof falls and to apply this information for the prediction of such falls.

The results of this study have included the development of a simplified roof classification. This classification can be used by the mining engineer, the geologist, or the miner himself to quickly categorize the type of immediate roof above the workings. Three major roof types were proposed and each was studied, either statistically or analytically.

An analysis of the roof types yielded different parameters which were found to be important in coal mine roof stability. The controlling factors in Interface Roof stability, for example, were quite different than for a Shale Roof which differed, in turn from Sandstone Roof.

This chapter discusses each roof type and the geomechanical factors which control its behavior as well as observations concerning support requirements.

6.2 Interface Roof

Interface Roof proved to be the most difficult roof type from the point of view of the statistical analysis. This was due to the fact that this roof type is actually composed of three sub-types. These are channel boundaries, interbedded sandstone and shale splay deposits, and rider coal seams. The interrelating link between the three types is the fact that their stability appears dependent on the lithologic changes within the roof and not so much on other factors, such as fractures or the presence of fossils.

Channel boundaries failed, in 17 occurrences, 65% of the time. The overriding control on roof falls in this type of roof is the polished and slickensided interface between the channel sandstone and the adjacent shale. This feature occurs due to differential compaction of the material, since the sand is much more resistant than the clay matter. Sandstone channels can usually be discovered during the exploration phase of the mine development. This allows for preparation in areas where channel boundaries are anticipated. If possible, it is best to drive main entries at the greatest possible angle to the channels. Intersections should not occur under the boundary but, rather, a larger pillar should be left to allow the cross-cut to be turned beneath a more homogeneous roof. The reason for these precautions is that channel boundaries tend to be long, somewhat linear features. If a boundary runs down the center of an entry, not

only will a fall take place due to a minimum of support, but it will be of a much greater extent. Another means of dealing with a channel boundary condition is to install angled roof bolts through the shale into the sandstone. This prevents the cantilever effect in the shale portion of the roof which is mainly responsible for falls. Many bolting machines are not capable of drilling holes at an angle so this method cannot be used in all cases. A more expedient approach would be to note the angle of the boundary and employ longer roof bolts at a short distance in the shale making sure the bolt tips are anchored in sandstone.

Splay deposits present another problem. Their instability lies in the beam-bending properties of the individual strata layers. Thin layers are much more conducive to sag and delamination than thicker layers. The increased tension in the lower rock fibers of the "beams" leads to progressive failure of each layer. Another problem with interbedded splay deposits is that if point anchor bolts are used, the possibility exists that anchorage may occur in a weak shale or siltstone layer. If all bolts are the same length and are anchored in the same strata a roof fall might be impending. For this reason, the use of point anchor bolts, unless their lengths are staggered and tension bleed-off prevented, should be avoided in splay deposit roof. Fully grouted resin bolts are preferred as these not

only make the roof beam thicker, but prevent shear stresses between layers. Entry width is another consideration in this type of roof. The wider the entry, the longer the rock beam and, hence, the greater the tensile stress built up in the rock. A reduction in entry width when splay deposits are encountered might be beneficial. Another possibility of control is the use of cribs in the center of the heading if it is not used for transportation. In areas of extremely bad top due to splay deposits, staggered cross-cuts might help to reduce the extent of falls.

The last sub-grouping of Interface Roof, rider seams, is one in which many large falls occur but, one where falls should be prevented. Where no fractures occur in the roof, rider seams fail by simple tensile failure within the seam itself followed by failure of the roof beam below. This has been shown in the preceding chapter. Rider coals can easily be seen in exploration drill cores but the task remains to determine the influence of proximity. If material properties can be determined, methods such as finite elements can be used as shown in this research. However, testing for material properties is often beyond the physical and economic capabilities of most mining operations and the presence of fractures in the roof limit analytical methods in such instances. It is suggested that, if possible, rider seams be handled in the following manner:

1. If several rider seams are within one meter of

the roof, that part of the roof should be removed during mining as it will certainly fall.

2. If a single rider seam is within three meters of the roof, it should be bolted through and the bolt anchored in solid top above.

3. If the rider seam is relatively far above the seam being mined, fully-grouted resin bolts, as long as possible should be used.

4. If fractures are present, their dip angle should be noted and the fractures bolted through. Again, if the the rider is close, it should also be bolted through. Steeply dipping fractures tend to be more hazardous because they are more likely to extend all the way up to the rider seam above the entry. If possible a mixture of angle bolts and vertically installed bolts should be used to build a continuous roof beam.

Another approach is based on the results of the finite element analysis conducted in the previous chapter. Figure 5.9 shows that the narrower the opening, the closer the rider seam can be to the seam being mined. If the roof is otherwise unfractured, a simple reduction in entry width in that area of the mine where the rider seam is in close proximity, will prevent tensile failure in the roof.

6.3 Sandstone Roof

The statistical analysis of the Sandstone Roof produced meaningful results. The Roof Rating Index appears to do a remarkable job in predicting the probabilities of failure. Some remarks concerning this roof type are in order, however. Location plays a large role in Sandstone Roof stability. Four-way intersections are the most treacherous. The

brittleness of the sandstone does not lend itself well to spanning wide areas such as found in intersections. Rather then bend, the sandstone beds are more prone to break.

Faulted coal is not a good indicator of bad top in Sandstone Roof. On the contrary, it is more likely to be associated with good top. This may be because faulted coal is often found beneath massive, unfractured sandstone which has crushed the pillars. The problem, in this case, may lie in pillar bursts if stresses conveyed by the sandstone roof are excessive.

Fossiliferous beds within the sandstone can cause roof falls. These bedding planes act in much the same way as a rider coal close to the main seam; they fail easily in tension. Beds of fossils or carbonaceous beds can usually be seen in drill core and adequate preparation must be taken before mining these areas.

Slickensides and roof fracture type were not associated with bad roof conditions in Sandstone Roof. Part of the reason for this is that Sandstone Roof is rarely faulted. Fractures appearing within this roof type are usually joints, therefore, care must be taken when interpreting statistical results. Fracture deviation is also not a factor. This leads one to believe that there are more pronounced considerations than fractures in Sandstone Roof. Fracture dip and, especially, fracture density, however,

play a major role. When fracture angles are high, roof falls tend to be very large and an increase in fracture density leads to an increase in fall probability. These factors should be taken into consideration when mining beneath Sandstone Roof. These properties can be determined either from drill core, underground, or from outcrops.

Due to its brittle nature, roof falls in Sandstone Roof tend to be sudden, violent events. Roof bolts are often sheared in half with no warning of failure. The best means of support in areas where hazardous conditions exist is simply to supply supplementary support in the form of cribs or timbers where possible. This will supply support over a greater area of the roof and will prevent the rock from falling as suddenly as if no cribs were present.

6.4 Shale Roof

The parameters associated with roof falls in Shale Roof are several. Location is again important with four-way intersections being the worst. Faulting in the coal is associated with poor roof conditions. Faults which ramp up through the coal and along the roof often go up into the roof in close proximity.

Surprisingly, fossiliferous beds do not contribute to roof falls. Fossils are often found in Shale Roof and the possible explanation for such behavior may be due to the cohesive nature of the clay matrix which makes up the silt-

stone and shale of this roof type. The bonding forces are too great to be loosened to a large degree by fossils.

Fractures in the roof play, by far, the largest role in Shale Roof stability. Fracture type is important with dip-slip faults being the most conducive to roof failure. Entry trend compared with the local fracture trend is important also. Where local fracture trends are known, the section of the mine should be laid-out according to this information so that entries intersect fractures at favourable angles. Fracture dip and density also play a strong role in causing roof falls in this roof type. The angle of dip should be noted and, if possible, bolts should intersect the fractures at the greatest obtainable angle. Otherwise, longer bolts should be used where fracture angles are great. Areas that have high fracture densities must be supported with cribs or wooden or metal straps. If not, material will fall out from between the bolts and, therefore, bolting will not accomplish its purpose. Where fracture densities are extremely high or the roof material is susceptible to wetting and drying, consideration should be given to using wire reinforced grout in the main headings to prevent recurrent problems. Figure 6.1 shows a fall in Shale Roof in which high-angle, slickensided fractures paralleled the entry. The result was an extensive and costly fall.

Figure 6.1: Roof fall caused by slickensided, high angle fractures (photograph by T. M. Gathright, II).

6.5 Summary

Each roof type is most susceptible to certain geomechanical variables as far as roof falls are concerned. It is possible to assess beforehand potential trouble areas and attempt to provide appropriate support. Each sub-type of Interface Roof must be dealt with separately, but Sandstone and Shale Roof have parameters which can be diagnosed from underground or above ground mapping and exploration. Steps can then be taken to remedy any bad situations.

The recommendations suggested above are based on the results of the statistical and finite element analysis conducted for this research and, on observation of the underground mining process.

CHAPTER 7

CONCLUSIONS AND RECOMMENDATIONS

7.1 Conclusions

The geologic environment in which coal mines exist is extremely complex and variable. Unknown tectonic forces have been superimposed on a highly complex stratigraphy and lithologic variations are almost limitless. With this in mind, the accurate prediction of coal mine roof behavior is a difficult and complex task. However, the use of a statistical and probabilistic approach allows for some latitude while still delimiting certain conditions which may be considered hazardous.

The major conclusion of this research is that, even with such immense variation, certain categories of coal mine roof are discernible. Each of these categories is controlled by distinct and often different geomechanical variables as far as stability is concerned. It is statistically possible to determine, to a large extent, which parameters are important, and to what degree, for each roof type. Once this has been accomplished a probabilistic approach can be taken, and the probability of a roof failure can be ascertained.

This study has outlined three major roof types: Interface Roof, Sandstone Roof, and Shale Roof. It has determined which geomechanical variables are responsible or, at least, associated with roof falls in the coal fields of

southwestern Virginia, most notably within the Pine Mountain thrust plate. It has also modeled, using the finite element method, a portion of the roof types which were found.

The use of numerical modeling for coal mine stability problems is still in its infancy. Because of the complicated nature of the geological system, even highly sophisticated models such as the finite element method must resort to gross simplifications. This research has found that statistical methods yield much more useable information as far as design guidelines are concerned. However, the finite element method can still indicate trends and probable failure modes within the mine roof. Furthermore, it could provide a very important tool for parametric investigations.

The end result is that coal mine roof failures can be predicted within certain degrees of confidence, thus allowing steps to be taken to either prevent falls or at least ameliorate the effects of such failures. Emphasis should not be placed only on pre-mining indicators. The careful updating of the data during mining will allow for an even more accurate characterization of potential instability problems so that, with refinement, the margin of error can be decreased still further.

7.2 Recommendations

Although this research has contributed one approach to the problem of strata control in coal mines, much work

still needs to be accomplished. The following suggestions are, therefore, submitted:

1. The data base should be increased as much as possible. Four mines are not enough. Data should be developed from as many mines in the Pine Mountain plate as possible, and the study then expanded to include Buchanan County on the northeast side of the Russell Fork fault.

2. Emphasis should be on the success of different support methods used for each roof type. If possible, sections of some mines could be used as test areas where a known roof type would be supported by various methods.

3. Interface Roof should be the subject of a study. Probabilities of failure associated with heights of rider seams and thickness of splay deposits should be determined. The channel boundary problem should be examined more extensively.

4. Additional variables, e.g., coal cleat orientation, overburden stresses, weathering, and the effects of lineaments may be evaluated and incorporated into the Roof Rating Index.

5. A computer program should be implemented in which the results of this study are contained. It should be made available to the industry and should allow the input of local mine data so that the data base can be refined and improved upon for a given location.

6. Finally, and most importantly, the results of this study should be back predicted for existing areas. Drill core examination and underground and above-ground mapping should be conducted in order to determine the Roof Rating Index for selected areas of mines. The failure rates should then be compared with the failure probabilities as predicted by the Index. When the Index has been sufficiently refined, prediction during the exploration phase should be attempted.

REFERENCES

Adler, L., and Sun, M., 1976, Ground control in bedded formations: Bull. 28, Research Division, Virginia Polytechnic Institute and State University, 266 pp.

Aggson, J. R., 1978, Coal mine floor heave in the Beckley Coalbed, an analysis: USBM RI 8274, 32 pp.

American Geological Institute, 1974, Glossary of Geology: M. Gary, R. McAfee, Jr., and C. L. Wolf, eds., Amer. Geol. Inst., Wash., D.C., 805 pp.

Ashley, D. B., Veneziano, D., Einstein, H. H., and Chan, M. H., 1981, Geological prediction and updating in tunneling--a probabilistic approach: Proc. 22nd U.S. Symposium on Rock Mech., June 29-July 2, 1981, Mass. Inst. Tech., Cambridge, Mass., p. 361-366.

Ashley, G. H., and Glenn, L. C., 1906, Geology and mineral resources of part of the Cumberland Gap coal field, Kentucky: U. S. Geol. Survey Prof. Paper 49, 239 pp.

Aggson, J. R., 1980, Design of room and pillar mining systems: Proc. 1st Conf. on Ground Control Problems in the Ill. Coal Basin, Y.P. Chugh and A. Van Besien, eds., South. Ill. Univ., June 1980, p. 44-52.

Barton, N. 1976, Recent experiences with the Q-system of tunnel support design: Proc. of the Symp. on Exploration for Rock Engineering, Johannesburg, Nov. 1976, p. 107-117.

Barton, N., Lien, R. and Lunde, J., 1974, Engineering classification of rock masses for the design of tunnel support: Rock Mech., v. 6, p. 189-236.

Beer, G. and Meek, J. L., 1982, Design curves for roofs and hanging-walls in bedded rock based on 'voussoir' beam and plate solutions: Inst. Min. and Metal., Trans., Sec. A, v. 91, p. A18-A22.

Bieniawski, Z. T., 1980, Current possibilities for rock mass classifications as design aids in mining: Preprint No. 80-349, SME-AIME Fall Meeting, Minneapolis, Minn., Oct 22-24.

Blevins, C. T., 1982, Coping with high lateral stresses in an underground Illinois coal mine: Proc. 2nd Conf. on

Ground Control in Mining, S. S. Peng and J. H. Delley, eds., West Va. Univ., July 19-21, 1982, Morgantown, W. Va., p. 137-141.

Boyer, R. F. 1964, Coal mine disasters: frequency by month: Science, v. 144, p. 1447-1448.

Burggraf, C., 1981, Roof control at Republic's Kitt mine: Min. Cong. Jour., Dec. 1981, p. 15-17.

Butts, Charles, 1927, Fensters in the Cumberland overthrust block in Southwestern Virginia: Virginia Geol. Survey Bull. 28, p. 1-12.

Campbell, M. R., 1893, Geology of the Big Stone Gap coal field of Virginia and Kentucky: U.S. Geol. Surv. Bull. 111, 106 pp.

Caudle, R. D., 1973, Mine roof stability: in Ground Control Aspects of Coal Mine Design, USBM IC 8630, p. 79-85.

Chenevert, M. E., 1969, Shale hydration mechanics: Proc. 4th Symp. on Drilling and Rock Mech., Austin, Tex., SPE 2401, Jan. 14-15, 1969, p. 201-212.

Christian, J. T., and Desai, C. S., 1977, Constitutive laws for geologic media: in C. S. Desai and J. T. Christian, eds., Numerical Methods in Geotechnical Engineering, McGraw-Hill Book Co., N. Y., 783 pp.

Chugh, Y. P., and Missavage, R. A., 1981, Effects of moisture on strata control in coal mines: Eng. Geol., 17: 241-255.

Colback, P. S. B. and Wild, B. L., 1965, The influence of moisture content of the compressive strength of rocks: Proc. 3rd Canadian Symp. on Rock Mech., Toronto, Canada, Jan. 15-16, 1965, p. 65-84.

Cox, R. M., 1974, The correlation of mine roof failure with the time elapse before support installation: Final Report USBM Contract No. H111413, Univ. of Alabama, NTIS PB-262, 478pp.

Cummings, R. A., Singh, M. M., and Moebs, N. N., 1983, Effect of atmospheric moisture on the deterioration of coal mine roof shales: Min. Eng., v. 35, n. 3, p. 243-245.

Damberger, H. H., Nelson, W. J., and Krausse, H. F., 1980, Effect of geology on roof stability in room-and-pillar

mines in the Herrin (No. 6) coal of Illinois: Proc. 1st Conf. on Ground Control Problems in the Ill. Coal Basin, Y. P. Chugh and A. Van Besien, eds., Southern Ill. Univ., June 1980, p. 14-32.

Demaris, P.J., Bauer, R. A., Cahill, R. A., and Damberger, H. H., 1983, Geologic investigation of roof and floor strata: longwall demonstration, Old Ben Mine No. 24. Prediction of coal balls in the Herrin coal: USDOE Contract No. FG01-78ET12177, 69 pp.

Denkhaus, H. G., 1964, Critical review of strata movement theories and their application to practical problems: Jour. S. Afr. Inst. Min. and Metall., March, p. 310-332.

Desai, C. S., 1979, Elementary Finite Element Method, Prentice-Hall, Inc., Englewood Cliffs, NJ, 434 pp.

Desai, C. S., and Abel, J. F., 1972, Introduction to the Finite Element Method, Van Nostran Reinhold Co., NY.

Dimick, D. and Barnum, B., 1978, Remote sensing at Southern Utah Fuel: Proc. 9th Ann. Inst. on Coal Mining Health, Safety and Research, Virginia Polytechnic Inst. and State Univ., Blacksburg, Va., p. 191-208.

Dinsdale, J. R., 1935, Ground pressure and pressure profiles around mining excavation: Colliery Eng., v. 12, p. 406-409.

Drucker, D. C., and Prager, W., 1952, Soil mechanics and plastic analysis or limit design: Q. Appl. Math., v. 10, n. 2, p. 157-165.

Ealy, D. L., Mazurek, R. E., 1982, Instability forecasts aid in reducing roof fall rates at the Beckley Mine: Min. Eng., Jan. 1982, p. 63-67.

Ealy, E. L., Mazurek, R. E., and Langrand, E. L., 1979, A geological approach for predicting unstable roof and floor conditions in advance of mining: Min. Cong. Jour., March 1979, p. 17-22.

Eby, J. B., 1923, The geology and mineral resources of Wise County and the coal-bearing portion of Scott County, Virginia: Virginia Geol. Surv. Bull. 24, 617 pp.

Elder, C. H., Jeran, P. W., and Keck, D. A., 1974, Geologic structure analysis using radar imagery of the coal

mining area of Buchanan County, Va.: USBM RI 7869, 29 pp.

Ellenberger, J. L., 1981, Hazard prediction model development: the multiple overlay technique: Preprint No. 81-16, SME-AIME, For presentation at the AIME Annual Meeting Chicago, Ill. Feb. 22-26, 1981, 6 pp.

Englund, K. J., 1964, Straigraphy of the Lee Formation in the Cumberland Mountains of Southeastern Kentucky: U. S. Geol. Survey Prof. Paper 501-B, p. B30-B38.

_____. 1979, The Mississippian and Pennsylvanian (Carboniferous) Systems in the United States--Virginia: U.S. Geol. Surv. Prof. Paper 1110-C, p. C1-C21.

Englund, K. J., and DeLaney, A. O., 1966, Intertonguing relations of the Lee Formation in southwestern Virginia: U.S. Geol. Survey Prof. Paper 550-D, D47-D52.

Fairhurst, C. and Singh, B., 1974, Roofbolting in horizontally laminated rock: Eng. Min. Jour., February, p. 80-90.

Ferm, J. C., 1974, Carboniferous environmental models in eastern United States and their significance: Geol. Soc. Amer., Spec. Pap. 148, p. 79-95.

Ferm, J. C., Melton, R. A., Cummins, G. D., Mather, D., McKenna, L., Miur, C., and Norris, G. E., 1978, A study of roof falls in underground mines on the Pocahontas #3 Seam, Southern West Virginia: USBM Minerals Health and Safety Technology, Contract Number H0230028, 81 pp.

Froelich, A. J., 1973, Preliminary report of the oil and gas possibilities between Pine and Cumberland Mountains, southeastern Kentucky: Kentucky Geol. Survey. X, Rept. Invest. 14, 12 pp.

Gathright, T. M., II, 1981, Lineament and fracture trace analysis and its application to oil exploration in Lee County, Virginia: Virginia Division of Mineral Resources Publication 28, 40 pp.

Giles, A. W., 1921, The geology and coal resources of Dickenson County, Virginia: Virginia Geol. Survey Bull. 21, 224 pp.

_____. 1925, The geology and coal resources of the coal-bearing portion of Lee County, Virginia: Virginia Geol.

Survey Bull. 26, p. 1-177.

Glenn, L. C., 1925, The northern Tennessee coal field: Tennessee Div. Geol. Bull. 33-B, 478 pp.

Gregory, L. A., 1981, Relationship of lineaments to roof falls in Macalpin--East Gulf Mines, East Gulf, West Virginia: Unpublished Masters Thesis, Univ. South Carolina, 49 pp.

Grizzle, J. E., Starmer, C. F., and Koch, G. G., 1969, Analysis of categorical data by linear models: Biometrics, v. 25, p. 489-504.

Hackell, P., 1962, Rock mechanics and mining engineering: Mine and Quarry Eng., v. 28, n. 5, p. 215-219.

Harnsberger, T. K., 1919, The geology and coal resources of the coal-bearing portion of Tazewell County, Virginia: Virginia Geol. Survery Bull. 19, 195 pp.

Harris, L. D., 1965, The Clinchport thrust fault--a major structural element of the southern Appalachian mountains: U.S. Geol. Surv. Prof. Paper 525-B, p. B49-B53.

_____. 1967, Geology of the L. S. Bales well, Lee County, Virginia--a Cambrian and Ordovician test: in Proceedings of the technical sessions Kentucky Oil and Gas Association 29th Annual Meeting, June 3-4, 1965: Kentucky Geol. Surv. Ser. X Special Paper 14, p. 50-55.

_____. 1970, Details of thin-skinned tectonics in parts of the Valley and Ridge and Cumberland Plateau provinces of the southern Appalachians: in G. W. Fisher, F. J. Pettijohn, J. C. Reed, Jr., and K. N. Weaver, eds., Studies of Appalachian Geology: Central and Southern (Cloos Volume), p. 161-173.

Harris, L. D. and Milici, R. C., 1977, Characteristics of thin-skinned style of deformation in the southern Appalachians and potential hydrocarbon traps: U.S. Geol. Survey Prof. Paper 1018, 40 pp.

Haynes, C. D., 1975, Effects of temperature and humidity variations on coal mine roof stability: Proc. Symp. on Underground Mining, Louisville, Ky., Oct. 21-23, 1975, publ. by National Coal Assoc., Wash., D.C., v. 2, p. 120-126.

Headlee, A. J. W., 1944, Fracture zones in mine strata: Min. Cong. Jour., v. 30, p. 57-60.

Herget, G., 1982, TV borehole inspection and vacuum testing of roof strata, Proc., 2nd Conf. on Ground Control in Mining, S. S. Peng and J. H. Kelley, eds., July 19-21, 1982, Morgantown, W.V., p. 209-213.

Hoch, M. T. and Pascoe, W., 1982, Remote sensing analysis: a disign tool for longwall mining: Proc. 2nd conf. on Ground Control in Mining, S. S. Peng and Jay H. Kelley, eds., West Virginia Univ., July 19-21, 1982, Morgantown, W. Va., p. 249-255.

Holmes, P., 1982, Relations between geology and the stability of faces and roadways in the Barnsley seam: Strata Mechanics, Proc. of the Symposium on Strata Mechanics, Newcastle upon Tyne, April 1982, p.118-122.

Horne, J. C., Ferm, J. C., Caruccio, F. T., and Baganz, B. P., 1978, Depositional models in coal exploration and mine planning in Appalachian Region: AAPG Bull. Vol. 62, no. 12, p. 2379-2411.

Hopkins, M. E., 1980, Coal geology and underground mining, Illinois coal basin: Proc., 1st Conf. on Ground Control Problems in the Illinois Coal Basin, Y. P. Chugh and A. Van Besien, eds., South Ill. Univ., June 1980, p. 1-13.

HRB-Singer, Inc., 1979, Pre-mining identification of hazards associated with coal mine roof measures: USBM OFR 167-81, 205 pp.

Hubbert, M. K., and Rubey, W. W., 1959, Role of fluid pore pressure in mechanics of owerthrust faulting; pt. 1, Mechanics of fluid-filled porous solids and its application to overthrust faulting: Geol. Soc, America Bull., v. 70, p. 115-166.

Hustrulid, W. A., 1976, A review of coal pillar strength formulas: Rock Mech. v. 8, p. 115-145.

Hylbert, D. K., 1978, The classification, evaluation, and projection of coal mine roof rocks in advance of mining: Min. Eng., Dec. 1978, p. 1667-1676.

_____, 1980, Delineation of geologic roof hazards in selected coal beds in eastern Kentucky with LANDSAT imagery studies in eastern Kentucky and the Dunkard Basin: BuMines OFR 166-81, 100 pp.

Iannacchione, A. T., Ulery, J. P., Hyman, D. M., and Chase, F. E., 1981, Geologic factors in predicting coal mine roof-rock stability in the Upper Kittanning Coalbed,

Somerset County, Pa.: USBM RI 8575, 41 pp.

Jaeger, J. C., and Cook, N. G. W., 1979, Fundametals of Rock Mechanics: 3rd Ed., Methuen & Co., Ltd., London, 593 pp.

Jansky, J. J. and McCabe, K. W., 1979, Evaluation of remote sensing techniques for planning mining operations: SME-AIME Mini-Symposium Series No. 79-07, Underground Coal Mine Design and Planning, New Orleans, La., Feb. 1979, p 39-45.

Jeran, P. W., and Jansky, J. H., 1983, A guide to geologic features in coal mines in the northern Appalachian coal basin: USBM IC 8918, 16 pp.

Jillson, W. R., 1919, The Kendrick Shale: a new calcareous fossil horizon in the coal measures of eastern Kentucky: Kentucky Dept. Geology and Forestry ser. V, Mineral and Forest Resources of Kentucky, V. 1, n. 2, p. 96-104.

John, K. W., 1981, A compromise approach to tunnel design: Proc. 22nd U.S. Symp. on Rock Mech., Mass. Inst. Tech., Cambridge, Mass., June 29-July 2, 1981, p.313-321.

Johnston, J. E., Miller, R. L., and Englund, K. J., 1975, Applications of remote sensing to structural interpretations in the southern Appalachians: Jour. Research, U. S. Geol. Surv., V. 3, n. 3, p. 285-293.

Jumikis, A. R., 1979, Rock Mechanics: Trans Tech Publications, Rockport, MA, 356 pp.

Kane, W. F., 1981, Direct shear behavior of rock joints in a granite gneiss: Unpublished Masters Thesis, Virginia Polytechnic Inst. and State Univ., Blacksburg, Va., 141 pp.

Karabin, G. J., Jr. and Debevec, W. J., 1976, Comparative evaluation of conventional and resin bolting systems: U.S. Mine Safety and Health Administration, IR 1033, 22 pp.

Karabin, G. J., Jr., Cybulski, J. A., and Kramer, J. M., 1982, The formation and effects of transient abutment stress during nonuniform face advance: Proc. 2nd Conf. on Ground Control in Mining, S. S. Peng and J. H. Kelley, eds., West Virginia Univ., July 19-21, Morgantown, W. Va., p. 233-240.

Kester, W. M., and Chugh, Y. P., 1980, Premining investigations and their use in planning ground control in the Illinois basin coal mines: Proc. 1st Conf. on Ground Control Problems in the Ill. Basin, Y. P. Chugh and A. Van Besien, eds., South. Ill. Univ., June 1980, p. 33-43.

Kidybinski, A., 1982, Critical roof span approach to selection of proper coal mining system: Proc. 2nd Conf. on Ground Control in Mining, S. S. Peng and J. H. Kelley, eds., West Va. Univ., July 19-21, Morgantown, W. Va., p. 175-182.

Krause, H. F. and Damberger, H. H., in press, Clay-dike faults and associated structures in coal-bearing strata--deformation during diagenesis: Compte Rendu, Ninth Int. Cong. of Carboniferous Geology and Stratigraphy.

Krausse, H. F., Damberger, H. H., Nelson, W. J., Hunt, L. R., Ledvina, C. T., Treworgy, G. G., and White, W. A., 1979, Roof strata of the Herrin (No. 6) Coal and associated rock in Illinois--summary report: Illinois Mineral Notes 72, Illinois Geological Survey, 54 p.

Kuppusamy, T., 1984, Unpublished finite element code, Virginia Polytechnic Institute and State University, Blacksburg, VA.

Lehr, E., 1935, Modellversuche an Balken auf elastischer Unterlage zur Klarung der Spannungsverteilung im Hangenden von Abbauortern: VDI-Forschungsheft 372, VDI-Verlag, Berlin.

Lightner, J. G., 1979, Improved numerical procedures for soil-structure interaction including simulation of construction sequences: Unpublished Master Thesis, Virginia Polytechnic Institute and State University, Blacksburg, VA, 141 pp.

Mahtab, M. A., 1973, Influence of natural jointing on coal mine stability and on the preferred direction of mine layout: Ground Control Aspects of Coal Mine Design, Proc. USBM Tech. Trans. Sem., Lexington, Ky., p. 70-78.

McCabe K. W., 1981, Remote sensing in the coal mining industry--an update: Proc. 11th Ann. Inst. on Coal Mining Health, Safety, and Research, M. Karmis, J. A. Lamonica, J. L. Patrick, and J. R. Lucas, eds., Virginia Polytech. Inst. and State Univ., Blacksburg, Va., August 26-28, p. 115-127.

McCulloch, C. M., Deul, M., and Jeran, P. W., 1974, Cleat in bituminous coalbeds: USBM RI 7910, 25 pp.

McCulloch, C. M., Jeran, P. W., and Sullivan, C. D., 1975, Geologic investigations of underground coal mining problems: USBM RI 8022, 30 pp.

McDonough, J. T., 1976, Site evaluation for cavability and undergrond support design at the Climax mine: Monograph 1 on Rock Mech. Applications in Mining, 17th Symp. on Rock Mech., W. S. Brown, S. J. Green, and W. A. Hustrilid, eds., p. 112-126.

Milici, R. C., 1970, The Allegheny structural front in Tennessee and its regional tectonic implications: Amer. Jour. Sci., v. 268, p. 127-141.

Milici, R. C., Gathright, T. M., II, Miller, B. W., and Gwin, M. R., 1982a, Geologic factors related to coal mine roof falls in Wise County, Virginia: Report prepared for Appalachian Regional Commission, Contract No. CO-7232-80-I-302-0206, 103 pp.

Milici, R. C., Gathright, T. M., II, Miller, B. W., Gwin, M. R., and Stanley, C. B., 1982b, Geologic features related to coal mine roof falls in southwestern Virginia: Proc. 13th Ann. Inst. on Coal Mining Health, Safety and Research, Virginia Polytechnic Inst. and State Univ., Blacksburg, Virginia, p. 209-220.

Miller, M. S., 1974, Stratigraphy and coal beds of Upper Mississippian and Lower Pennsylvanian rocks in southwestern Virginia: Virginia Div. Min. Resources Bull. 84, 211 pp.

Miller. R. L., 1969, Pennsylvanian formations of southwest Virginia: U. S. Geol. Survey Bull. 1280, 62 pp.

_____. 1973 Where and why of Pine Mountain and other major fault planes, Virginia, Kentucky, Tennessee: Am. Jour. Sci., Cooper Volume, p. 353-371.

Moebs, N. N., 1973, Geologic guidelines in coal mine design: Ground Control Aspects of Coal Mine Design, Proc. Bureau of Mines Technology Transfer Seminar: Lexington, Ky., March 6, 1973, USBM IC 8630, p. 63-69.

_____. 1977, Roof rock structure and related roof support problems in the Pittsburgh coalbed of southwestern Pennsylvania: USBM RI 8230, 30 pp.

_____. 1981, The geologic character of some coal wants at the Westland Mine in southwestern Pennsylvania: USBM RI 8555, 25 pp.

Moebs, N. N. and Ellenberger, J. E., 1980, Hazardous roof structures in Appalachian coal mines: Unpublished Report, U.S. Bureau of Mines, 7 pp.

_____. 1982, Geologic structures in coal mine roof: USBM RI 8620, 16 pp.

Moebs, N. N., and Ferm, J. C., 1982, The relation of geology to mine roof conditions in the Pocahontas No. 3 coalbed, USBM IC 8864, 8 pp.

Moelle, K. H. R., 1972, On structural analyses of oriented bore cores from the West Wallsend No. 2 colliery holding, Proc. Aus. I. M. M. Conference, Newcastle, N.S.W., May-June 1972, p. 43-49.

Moody, J. D. and Hill, M. J., 1956, Wrench-fault tectonics: Bull. Geol. Soc. America, v. 67, p. 1207-1246.

Morgan, T. A., 1973, Coal mine roof problems: Proc. USBM Tech. Trans. Sem., Lex., KY, March 6, 1973, USBM IC 8630, p. 56-62.

Morgan, T. A., Fisher, W. G., and Sturgis, W. J., 1965, Distribution of stress in the Westvaco Trona Mine, Westvaco, Wyo.: USBM RI 6675, 58 pp.

Morley, A., 1948, Theory of Structures: Longmans, Green, and Co.

Morse, W. C., 1931, Pennsylvanian invertebrate fauna: Kentucky Geol. Surv., Ser. 6, v. 36, 293-348.

Mullenex, R. H. and Miller, M. S., 1981, Use of depositional models and stratigraphic mapping techniques to determine new coal reserve potentials in the Appalachian region: SME Preprint 81-17, AIME Annual Meeting, Chicago, IL., Feb. 1981, 5 pp.

Nelson, R. A., 1979, Natural fracture systems: description and classification: Jour. American Assoc. Pet. Geol., v. 63, n. 12, p. 2214-2221.

_____. 1981, Faults and their effect on coal mining in Illinois: Illinois State Geol. Surv., Circular 523, 40 pp.

Nelson, R. A., and Nance, R. B., 1980, Geologic mapping of roof condtions, Crown II mine, Macoupin County, Illinois: SME-AIME Preprint No. 80-308, For Presentation Fall Meeting Minneapolis, Minn., Oct. 22-24, 1980, 9 pp.

Oberlick, G. J., 1978, Remote sensing at Marrowbone Development Company: Proc. 9th Ann. Inst. on Coal Mining Health, Safety, and Research, W. E. Foreman, ed., Virginia Polytech. Inst. and State Univ., Blacksburg, VA., Aug. 1978, p. 163-189.

Obert, L. and Duvall, W. I., 1967, Rock Mechanics and the Design of Structures in Rock: Wiley, New York, 626 pp.

Obert, L., Duvall, W. I., and Merrill, R. H., 1960, Design of underground openings in competent rock: USBM Bull. 587, 36 pp.

Ott, L., 1977, An Introduction to Statisical Methods and Data Analysis: Wadsworth Publ. Co., Belmont, CA., 730 pp.

Overbey, W. K., Jr., Komar, C. A., and Pasini J., III, 1973, Predicting probable roof fall areas in advance of mining by geological analysis: USBM Health and Safety Research Program, Technical Progress Report--70, May 1973, 17 pp.

Panek, L. A., 1956, Principles of reinforcing bedded mine roof with bolts: USBM RI 5156, 25 pp.

_____. 1962, The effect of suspension in bolting bedded mine roof: USBM RI 6138, 59 pp.

Parker, J., 1966, How moisture affects mine openings: Eng. and Min. Jour., v. 167, n. 11, p. 95-97.

Parsons, R. C. and Dahl, H. D., 1971, A study of the causes of roof instability in the Pittsburgh coal seam: Proc. 7th Canadian Symp. Rock Mech., Mar. 25-27, 1971, Alberta, Canada, 14 pp.

Patrick, W. C., and Aughenbaugh, N. B., 1979, Classification of roof falls in coal mines: Min. Eng., March 1979, p. 279-283.

Peng, S. S., 1978, Coal Mine Ground Control: John Wiley & Sons, New York, 450 pp.

_____. 1980, Roof falls in underground coal mines:

Technical Report No. TR 80-4, West Virginia Univ., 42 pp.

Pothini, B. R., Thaler, J. H., and Finlay, W. L., 1976, Rock mechanics considerations in mine design for a deep, bedded deposit under the influence of residual tectonic forces: Monograph 1 on Rock Mechanics Applications in Mining, 17th Symp. on Rock Mech., W. S. Brown, S. J. Green, and W. A. Hustralid, eds., p. 46-52.

Price, N. J., 1966, Fault and Joint Development in Brittle and Semi-brittle Rock: Pergamon Press, Elmsford, N.Y., 176 pp.

Price, P. H., 1931, The Appalachian structural front: Jour. Geol., v. 39, pp. 24-44.

Protod'iakonov, M. M., 1964, Evaluating the jointedness and strength of rock in the mass: Rept. for the Seminar on Questions in the Investigation of the Mechanical Properties of Rock in the Mass, Moscow, 32 pp.

Radcliffe, D. E. and Stateham, R. M., 1978, Effects of time between exposure and support on mine roof stability, Bear Coal Mine, Somerset, CO: USBM RI 8298, 13 pp.

Reddy, J. N., 1984, An Introduction to the Finite Element Method, McGraw-Hill, Inc. 495 pp.

Rich, J. L., 1934, Mechanics of low-angle overthrust faulting as illustrated by Cumberland thrust block, Virginia, Kentucky, and Tennessee: Am. Assoc. Petroleum Geologists Bull., v. 18, p. 1584-1596.

Rinkenberger, R. K., 1978, Operational application of remote sensing technology for predicting mine ground hazard areas: Proc. 9th Ann. Inst. on Coal Mining Health, Safety, and Research, Virginia Polytechnic Inst. and State Univ., Blacksburg, VA., p. 225-243.

Rodgers, J., 1964, Basement and no-basement hypotheses in the Jura and the Appalachian Valley and Ridge: in W. D. Lowry, ed., Tectonics of the southern Appalachians: Virginia Polytechnic Inst. Dept. Geol. Sci. Mem. 1, p. 71-80.

Safford, J. M., 1869, Geology of Tennessee: S. C. Mercer, Printer to the State, Nashville.

Schoemaker, R. P., 1949, A review of rock pressure problems: Trans. AIME, v. 181, p. 334-351.

Seegmiller, B. L., 1982, Geotechnical and stability requirements for future coal mines: Proc. 1st Int. Conf. on Stability in Underground Mining, C. O. Brawner, ed., August 16-18, 1982, Vancouver, B.C., p. 223-244.

Shepherd, J. and Burston, R. J., 1977, Maps of faulting and roof failure at Aberdare East Colliery, Cessnock, N.S.W: Investigation Report 122, CSIRO Minerals Research Laboratories, 6 pp.

Shepherd, J. and Fisher, N. I., 1978, Faults and their effect on coal mine roof failure and mining rate: a case study in a New South Wales colliery: Min. Eng., Sept. 1978, p. 1325-1334.

Stateham, R. M. and Radcliffe, D. E., 1978, Humidity: a cyclic effect in coal mine roof stability: USBM RI 8291, 19 pp.

Statistical Analysis System, 1982a, SAS User's Guide: Basics: SAS Institute Inc., Cary, NC, 923 pp.

Statistical Analysis System, 1982b, SAS User's Guide: Statistics: SAS Institute Inc., Cary, NC, 584 pp.

Stearns, R. G., 1954, The Cumberland Plateau overthrust and geology of the Crab Orchard Mountains area, Tennessee: Tennessee Div. Geol. Bull. 60, 47 pp.

_____. 1955, Low angle overthrusting in the central Cumberland Plateau, Tennessee: Bull. Geol. Soc. America, v. 66, p. 615-628.

Stefanko, R. and Delacruz, R. V., 1964, Mechanisms of load loss in roof bolts: Proc. 6th Symp. Rock Mech., Univ. Mo.--Rolla, October, p. 293-309.

Stritzel, D. L., 1980, Observations in mines which are indicative of ground control problems in the Illinois basin: Proc. 1st Conf. on Ground Control Problems in the Ill. Coal Basin, Y. P. Chugh and A. Van Besien, eds., South. Ill. Univ., June 1980, p. 53-58.

Tennant, J. M., 1982, Methods used to monitor roof geology and entry supports: Proc. 2nd Conf. on Ground Control in Mining, S. S. Peng and J. H. Kelley, eds., July 19-21, 1982, Morgantown, W.V., p. 118-122.

Wentworth, C. K., 1921, Russell Fork fault of southwest Virginia: Jour. Geol., v. 29, p. 351-369.

_____. 1922, The geology and coal resources of Russell County, Virginia: Virginia Geol. Surv. Bull. 22, 179 pp.

Wier, C. E., 1969, Factors affecting coal mine roof rock in Sullivan County, Indiana: Proc. Indiana Acad. Sci. for 1969, Indianapolis, IN., v. 79, p. 263-269.

Wilson, E. L., 1965, Structural analysis of axisymmetric solids: AIAA Jour., n. 12, p. 2269-2274.

Zienkiewicz, O. C., 1977, The Finite Element Method: McGraw-Hill, Inc., NY, 787.

The vita has been removed from the scanned document

GEOLOGIC AND GEOTECHNICAL CONTROLS ON THE STABILITY OF COAL MINE ENTRIES

by

William Francis Kane

Committee Chairman: Michael Karmis

Mining Engineering

(ABSTRACT)

Roof and rib failures in underground coal mines are one of the major problems facing the industry today. In addition to safety considerations, the resulting economic impact of such failures is staggering. Uncovering and replacing buried and damaged equipment and clearing entries can account for a large expenditure in lost man-hours and machinery. Yet, because of the complex nature of their formation, geological variability, and structural characteristics, coal mine roof strata are one of the least controllable of all mine design parameters. This is especially true along the leading (southeastern) edge of the Appalachian coalfields where considerable faulting and movement has contributed to hazardous coal mining roof conditions.

For this research, a detailed study of several mines, in the southern Appalachian coalfields, was undertaken to determine the most prominent geomechanical factors affecting roof stability and to evaluate their influence in promoting unstable ground conditions. in order to accomplish this

task, the major geological and geomechanical features found to be detrimental to coal mine roof within the Appalachian basin were identified and mapped in four Virginia mines.

Statistical processing by chi-square and linear regression analysis as well as analytical analysis by the finite element method were used to determine the influence of geology, mine-layout, and support methods on roof stability. It was found that some easily determined parameters can be successfully used to predict potentially unstable areas. A simplified roof classification system was developed based on the geomechanical parameters, which can be used to assess the stability of a particular roof type. A Roof Rating Index was also devised capable of expressing the probability of a failure under a given set of geomechanical conditions.